Peripheral and central effects of botulinum toxin type A in the rat motor nervous system

Šoštarić Mužić, Petra

Doctoral thesis / Disertacija

2024

Degree Grantor / Ustanova koja je dodijelila akademski / stručni stupanj: **University of Zagreb, School of Medicine / Sveučilište u Zagrebu, Medicinski fakultet**

Permanent link / Trajna poveznica: https://urn.nsk.hr/urn:nbn:hr:105:216406

Rights / Prava: In copyright/Zaštićeno autorskim pravom.

Download date / Datum preuzimanja: **2024-11-26**

UNIVERSITY OF ZAGREB
SCHOOL OF MEDICINE

Petra Šoštarić Mužić

Peripheral and central effects of botulinum toxin type A in the rat motor nervous system

DISSERTATION

Zagreb, 2024

UNIVERSITY OF ZAGREB
SCHOOL OF MEDICINE

Petra Šoštarić Mužić

Peripheral and central effects of botulinum toxin type A in the rat motor nervous system

DISSERTATION

Zagreb, 2024

This PhD thesis was made at the Department of Pharmacology, University of Zagreb School of Medicine. Majority of the experiments performed for this dissertation were done at the Laboratory of Molecular Neuropharmacology, Department of Pharmacology, University of Zagreb School of Medicine. In vitro experiments and western blot analysis were performed at Neurotoxins, Neurodegeneration and Regeneration Lab, Department of Biomedical Sciences, University of Padova (under supervision of Assist. Prof. Marco Pirazzini).

Mentor 1: Dr.sc. Ivica Matak, mag.mol.biol., PhD
Department of Pharmacology, School of Medicine, University of Zagreb, Croatia

Mentor 2: Assistant professor Marco Pirazzini, PhD
Department of Biomedical Sciences, University of Padua, Italy

I wish to thank my mentor Dr.sc. Ivica Matak for giving me a chance to begin my scientific journey and my co-mentor assist.prof. Marco Pirazzini for hosting me in his lab in Padua. I wish to thank both mentors for their support and understanding during the writing of this dissertation.

I would like to express my gratitude to the rest of the Department of Pharmacology; it takes a village to raise a PhD student, and each and every one of you has contributed in some way with your support, advice, and help to bring this dissertation to light, especially the party who will be remembered as Room 308.

Special thanks to my colleagues in the laboratory in Padua who also contributed to my scientific path and, if nothing else, taught me to say allora, dimmi, and pubblica.

Lastly, I would like to extend my heartfelt thanks to my husband for his support during this journey, which at times seemed like it would never end. I would also like to dedicate a sentence to my dog Medo, who faithfully stayed by my laptop during the long nights of writing.

All of you shared with me the laughter and stress, the beautiful and the less beautiful side of the research life, and for that, I thank you.

And lastly, never be afraid to wonder what is behind the big, old, dusty curtain.

…See, in these silences in which things
yield and almost betray
their ultimate secrets,
at times, one half expects
to discover an error in Nature,
the still point of reality, the missing link that holds not,
the thread to untangle that finally gets us
right at a truth of some kind.
Our glance fumbles all around,
the mind seeks, makes harmonies, falls apart…
…Yet the illusion wanes, and in time we return
to our noisy cities where the blue shows
only in fragments…
Eugenio Montale, "The Lemon Trees", from the collection "Cuttlefish bones", 1925

CONTENT:

List of abbreviations

ATP, adenosine triphosphate

BBB, Basso Beattie Bresnahan locomotor scale

BoNT-A, botulinum toxin type A

ChAT, choline acetyltransferase

CNS, central nervous system

DAS, digit abduction score

EMG, electromyography

GABA, γ-aminobutyric acid

H_C, C-terminal heavy chain domain of botulinum toxin

H_N, N-terminal heavy chain domain of botulinum toxin

i.m., intramuscular

i.n., intraneural

INN, international nonproprietary name

i.p., intraperitoneal

i.t., intrathecal

kDa, kilodalton (Mr=1000)

LC, light chain domain of botulinum toxin

LD50, lethal dose 50

MAP-2, microtubule-associated protein 2

NMJ, neuromuscular junction

PSG, protein-sialoganglioside

Syt, synaptotagmin

SNAP-25, synaptosomal-associated protein of 25 kDa

SNARE, soluble N-ethylmaleimide-sensitive factor attachment protein receptor

SV2, synaptic vesicle protein 2

TeNT, tetanus toxin

TrxR-Trx, thioredoxin reductase-thioredoxin system

VAMP, vesicle-associated membrane protein

1. INTRODUCTION AND BACKGROUND OF PROPOSED RESEARCH

Botulinum toxin type A (BoNT-A) is an extremely potent presynaptic neurotoxin derived from bacterium *Clostridium botulinum*. It primarily acts on the presynaptic part of neuromuscular junction where the toxin cleaves one of the soluble N-ethylmaleimide-sensitive factor attachment protein receptor (SNARE) proteins responsible for neurotransmitter exocytosis. This results in silencing of the synapse with consequent denervation accompanied by muscle paralysis and atrophy (1). Despite its potency (human lethal dose) is around 1 ng/kg when injected intramuscularly (i.m.) (2,3), it is widely regarded as a safe therapeutic and the first-choice treatment of several neurological disorders characterized by sustained or intermittent focal muscular hyperactivity. Since its first approved indication (4), BoNT-A has become a preferred treatment for many forms of spasticity (5). The i.m. BoNT-A injections have been shown to effectively relax and normalize the activity of abnormally contracting muscles, demonstrating to be a well-tolerated treatment in a variety of movement disorders and other neurological and non-neurological disorders, benefiting patients' quality of life. BoNT-A injections are accompanied by minimal local and a lack of systemic adverse effects, provided that appropriate model of application and dosage is employed (6).

The efficacy and safety of BoNT-A has mostly been attributed to its local neuroparalytic effects in injected muscles. However, the duration and intensity of neuromuscular paralysis (as the only presumed mechanism of action) does not always correlate to duration of its antispastic or anti-dystonic action. Clinical reports indicate that the beneficial effects of the toxin treatment may extend beyond the period of peripheral muscle weakness, while some patients may find the therapeutic duration unsatisfactory, demanding earlier reinjections, even when local neuromuscular action persists (7–9). Recent preclinical findings proposed the existence of BoNT-A axonal transport and central transcytosis in the motor and sensory system (8,10–12). In our laboratory, other clostridial neurotoxin was used to develop an experimental model of muscle hypertonia in rats: the tetanus neurotoxin (TeNT). TeNT-evoked muscle local spasticity proved to be a good experimental model to characterize the antispastic action of BoNT-A and to examine its possible central effects on abnormal muscle tone (13).

With the chronic use of BoNT-A and expanding list of indications in neuromuscular disorders, there is a need to examine and characterize all relevant sites of BoNT-A action on spinal circuits involved in motor processing. While the role of central BoNT-A action in the sensory system

was shown to rely on the toxin's central actions, up to now possible functional role of BoNT-A central action in the motor system remained to be examined. In this PhD thesis, we aimed to characterise BoNT-A action on normal and spastic muscles by examining its activity at peripheral motor terminals, and, following retrograde axonal transport and central transcytosis, on spinal premotor synapses.

1.1. General aspects of clostridial neurotoxins

Botulinum and tetanus toxins are homologous clostridial neurotoxins derived from a common ancestral gene and one of the most potent toxins known to man. Both are produced by anaerobic gram positive bacteria from genus *Clostridium*. Botulinum toxin type A and other serotypes are produced as exotoxins by few species of sporogenous rod-shaped bacteria belonging to Clostridium genus in anaerobic conditions such as *C. botulinum, C. baratii, C. butyricum, C. argentinense* (14). These toxins, classified into eight recognized serotypes (A-G and X), induce botulism in both humans and animals. Today we know of a growing number of subtypes, chimeric toxins, BoNT-like toxins and homologs, thanks to recent advancement in microbial genomes sequencing (15–18). There is also a report of two non-neurotoxigenic *Clostridium subterminale* strains with BoNT-B genes containing a premature stop codon that prevents the expression of BoNT-B, known as silent B genes (19). Interestingly, the original nomenclature placed a bacteria that was firstly named as *Bacillus botulinum* and held as only one spore forming-organism causing botulism, and not a diverse palette (as we know today). This was later changed when the aerobic *Bacillus* genus was separated from the anaerobic *Clostridium* genus (20), and the change was proposed by Ida Bengston (1923) (21).

Botulism is acute neuroparalytic disease of humans and animals, which usually presents with symptoms of muscle weakness and flaccid paralysis affecting bulbar and ocular musculature, but in severe cases it can present with weakness of the neck, limbs, torso and generalized paralysis, extending ultimately to paralysis of respiratory muscles and potentially fatal respiratory failure. The effects are caused by blockage of acetylcholine exocytosis. This results in silencing of the synapse with consequent denervation accompanied by muscle paralysis and atrophy (1).

We can distinguish between different forms of botulism which depend on types of BoNT serotype, the route of entrance of the toxin into the organism and the mode of its distribution

2

into the bloodstream. Animals and humans differ in susceptibility to different serotypes. Botulism in humans is mostly caused by serotype A, B, E and, rarely, F, while type C and D mainly cause disease in animals. The times of onset, duration of action, symptoms and clinical progression of botulism can differ according to the serotype of BoNT and the type of botulism, with serotype A causing a more severe and prolonged disease.

Foodborne botulism is the most frequent type of botulism caused by ingestion of pre-formed BoNT complexes in the spoiled food (1,22) first described by Justinus Kerner in his very detailed paper from 1820 (23) where he described nearly all major symptoms of botulinum toxin intoxication that we recognize today. During that time, smoking of the sausages was done in very poor hygienic conditions, which led to outbreaks of smoked sausage-related poisoning. The suspected causative toxin was named the sausage toxin (derived from *botulu*s= lat. sausage (21,24). Today, consuming the food contaminated with toxins remains, still, the predominant cause of botulism poisoning, particularly through improperly sterilized homemade preserved foods of various types (17).

Inhalation botulism occurs due to inhalation of the toxin, after which the toxin enters the bloodstream. This can happen due to exposure during industrial production. This route of the intoxication was widely discussed during World War II (WWII) when botulinum toxin was investigated as a potential inhalational biochemical weapon (2,25).

Iatrogenic botulism can happen due to misused and incorrect dosage of therapeutically used BoNT. Unregulated dosage in off-label use of BoNT, high doses used for cosmetic purposes, or illegal BoNT-A preparation are just some of the causes of iatrogenic botulism (26,27). Recent outbreak of iatrogenic botulism in Europe included 5 different countries (Germany, Austria, France, Switzerland and Turkiye) after intragastric BoNT injections for the treatment of obesity at two private hospitals-one in Istanbul and one in Izmir. The patients were administered doses ranging from 1000 to 2500 units of BoNT (28).

Infant botulism can affects children younger than 12 months after ingestion of the *C. botulinum* spores (from soil, agricultural product or honey) after which the spores proliferate into viable bacteria inside the gastrointestinal tract, and generate the toxin inside the body (29). Similarly to children, intestinal toxemia botulism targets adults, with *C. botulinum* colonizing the intestinal tract and producing the toxin, similar to infant botulism. The intestinal tract of the healthy adult does not normally support the spore germination and toxin production, however

it can occur when the microbiota of the gastrointestinal tract is compromised or altered by abdominal surgical procedures or antibiotic therapy (30).

Wound botulism can be caused by unhygienic subcutaneous or subdermal injections of a particular type of heroin (black tar heroin), when wounds are contaminated with *C. botulinum* and toxin is transmitted to systemic bloodstream (31).
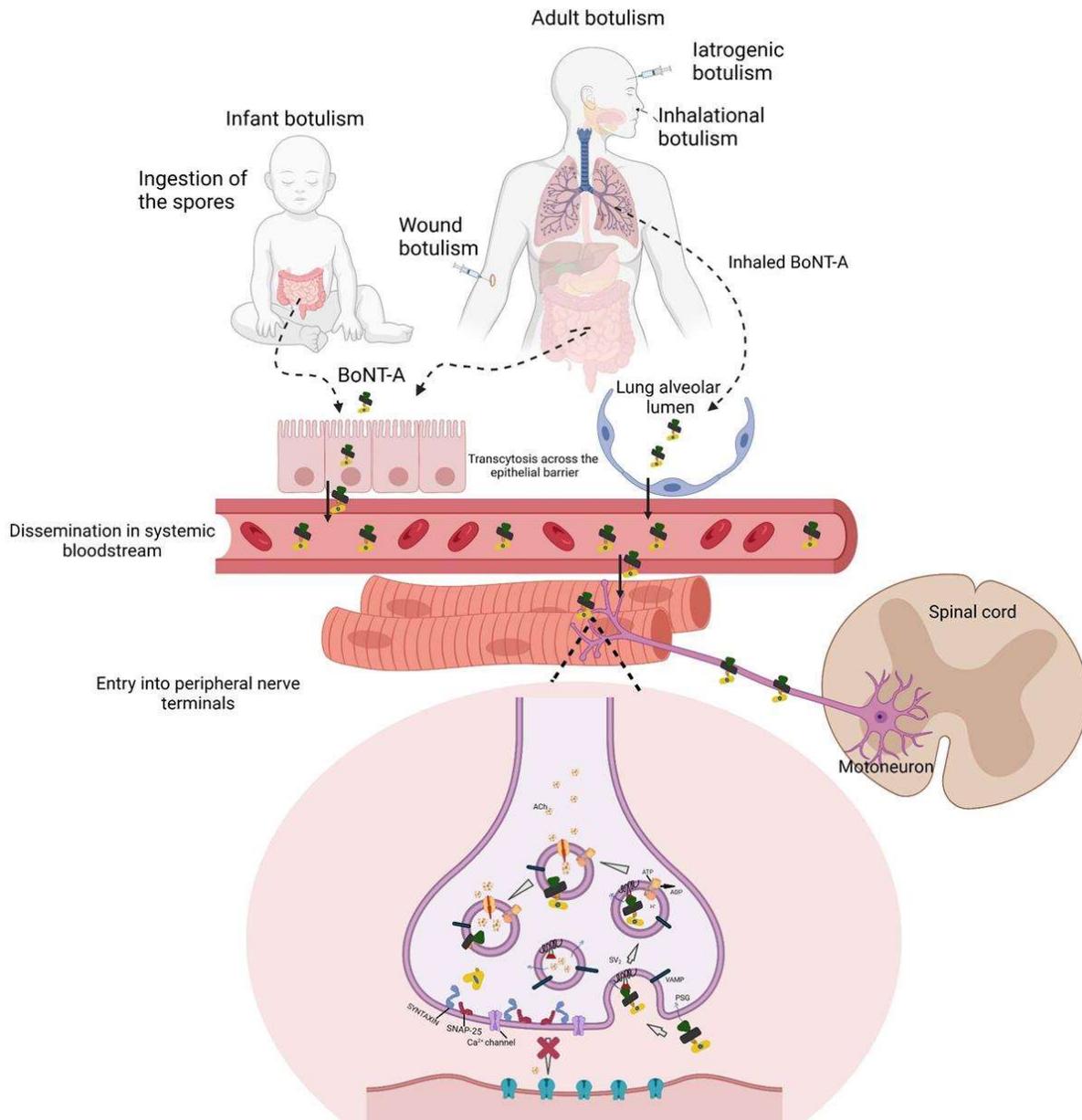
Figure 1. Routes and entry pathways of BoNT-A. *The two primary routes of BoNT-A entry and the types of botulism associated with them are as follows: foodborne botulism, which occurs in adults through the consumption of BoNT-contaminated foods, and infant botulism, resulting from the ingestion of spores present in foods such as honey, which then proliferate*

4

into neurotoxigenic clostridia within the gastrointestinal tract. Other forms of botulism, distinguished by the route of BoNT entry, include wound botulism, inhalation botulism, and iatrogenic botulism, as previously explained. When ingested or inhaled, the BoNT-A complex navigates through the intestinal lumen or lung alveoli, traversing epithelial layers via transcytosis before entering the bloodstream. Subsequently, the toxin is systematically distributed into the extracellular fluid of peripheral tissues, including muscles. BoNT-A molecules, whether distributed systemically or injected i.m., then target neuromuscular junctions, resulting in muscle paralysis. While circulating BoNT-A cannot breach the blood-brain barrier, a portion is transported retrogradely within peripheral nerves toward the central nervous system (CNS). Advantageous pharmacokinetic properties enabling BoNT-A potent toxicity are the ability to survive various proteolytic conditions within the gastrointestinal tract and transverse the epithelial layer to enter the bloodstream, with long enough half-life to survive the transport and reach the neuronal terminals and specific intracellular cytosolic protein targets. The figure was created with Biorender.com, (accessed on 19-03-2024) according to Rossetto et al. (31).

Tetanus neurotoxin is derived from *Clostridium tetani*, a gram-positive anaerobic spore forming bacilli. This species posesses much less diversity in serotypes and toxins production when compared to botulinum toxin bacteria. The *C. tetani* spores are widely distributed in soil, water, gastrointestinal tract of the animals and some humans and are extremely stable, surviving high temperatures (but most of them will be killed when boiling for more than 15 minutes) (32). Tetanus toxin is the causative agent of tetanus, which is known to humans for more than 3000 years, and it was first described in ancient Egypt. The Edwin Smith papyrus discussed a case of a tetanus after cranial trauma around 1550 BC referring to physicians of that time, "do not treat the ailment" (33). Today in a modern world, tetanus is almost a forgotten disease, rare in urban environments due to prophylactic guidelines of vaccination and availability of tetanus toxoid and tetanus immune globulin (TIG), which are needed in circumstances where the patient's vaccination history is not reliable. However, in Africa and southeast Asia tetanus remains a major health problem (32).

Tetanus is presented by four different clinical presentations: neonatal, generalised, localised and cephalic. Usually, the bacterium enters via puncture wounds or through wounds characterized with deep tissue injury, sometimes during surgical procedures, rarely following insect bites or intravenous drug use (34).

Neonatal tetanus usually occurs after delivery within 28 days from birth, when the birth take place in presence of unsanitary conditions or when unsanitary surgical instruments are used to cut the umbilical cord, combined with inadequate maternal vaccination and poor perinatal hygiene (35). Cases of neonatal tetanus are characterized by stiffness or spasms that gradually progress and are followed by inability of the infant to breastfeed and cry after the 3rd day of life (WHO-recommended surveillance standard of neonatal tetanus).

Localised tetanus can develop after low doses of toxin or it can be an early trait of generalized tetanus. This type of tetanus typically affects the area associated with toxin entry or regional muscles. *Generalised tetanus* occurs more commonly than the localised one, with all muscle groups affected. It is characterised by stiffness which progresses to prolonged and painful muscle spasms, and, in severe cases, paralysis of respiratory muscles which leads to respiratory distress and potential death. *Cephalic tetanus* is a very rare yet dangerous form of tetanus that can develop from craniofacial wounds, or colonization of mouth gingivae with *C. tetani* spores. The peculiar part of cephalic tetanus is its early phase symptoms which corresponds to the effect of botulinum toxin, with flaccid cranial nerve palsy which precedes or accompanies lockjaw and later progress to generalised tetanus.

1.2. History of botulinum toxin type A in medicine

Botulism as a disease has been present throughout human history, but we have only a few historical sources on food poisoning before the 19th century. In medieval times Emperor Leo VI of Byzantium (886-911 century) forbade the making and consumption of blood sausages prepared in the pig stomach (21). There may have been numerous cases but historic people did not connect the foodborne infections with paralytic diseases. For example, there is a series of intoxication cases in old medical literature which are reported as Atropa belladonna intoxication, but are followed with fatal muscle paralysis, which cannot be attributed to atropine intoxication (24). First accurate description dates back to the beginning of the 19th century, when the German physician and poet Justinus Kerner associated repeated outbreaks of muscle

paralysis followed after the consumption of poisoned sausages. Kerner conducted a series of experiments both on animals and even on himself. He placed a piece of spoiled sausage on the tip of his tongue and noticed an exceptional dryness of the mouth. He determined that this toxin affects the autonomous and motor system. He was the first to proposed botulinum toxin possible therapeutic use in treating hyperactive disorders of the autonomic nervous system, as well as hyperkinetic movement disorders, such as the involuntary movement of chorea, due to the toxin's effect of inducing muscle weakness (21). Interestingly, during the World War II all parties were interested into research and purification of botulinum toxin as a biochemical weapon, but also to develop protective measures if their soldiers encounter this potent and deadly toxin (2,25). James Lamanna and Richard Duff working at Fort Detrick, Maryland, a US Army facility, discovered a technique to crystalize and concentrate botulinum toxin, which led to purification and later production of a great amount of toxin by Edward Schantz in 1946. The breaking point was the discovery of mechanisms behind paralytic effect in 1949 (36) and the experiment with botulinum toxin A into the hind limb of chicken's embryo which showed that the toxin can cause a dose-dependent muscle weakness (37). Inspired by the embryo experiment, Allan Scott, MD, ophthalmologist got an idea to use botulinum toxin in the case of strabismus. He conducted a series of experiments after borrowing the toxin from Schantz, first injecting the ocular muscles of monkeys which suffered from strabismus. Later he did a series of experiments on human patients showing that botulinum toxin in small amounts and injected in appropriate muscle can be a safe and successfully therapeutic for strabismus, weakening the hyperactive ocular muscles (38). In 1989, FDA approved the botulinum toxin type A for the first medical indication, strabismus. BoNT-A approval for strabismus led to approval of BoNT-A for blepharospasm and hemifacial spasm that same year, 1989. From 1989 to present, FDA approved several other indications for BoNT-A use such as facial wrinkles, frown lines, cervical dystonia, chronic migraine, bladder dysfunction, upper and lower limb spasticity and axillary sweating (39). Currently, BoNT-A stands out as one of the most frequently utilized therapeutic proteins manufactured by more than 20 producers globally (40). The potency units, derived from mouse intraperitoneal LD50, are unique to each commercial BoNT preparation and, therefore, not interchangeable or translatable between products. As a result, BoNT preparations from different manufacturers possess distinct generic designations. In Europe, the European Medicines Agency (EMA) adopts international nonproprietary names (INN) for regulatory purposes (41). Conversely, the United States Food and Drug Administration (FDA) employs United States Adopted Names (USAN) (42) for similar regulatory functions.

Table 1. European Medicines Agency (EMA) and United States Food and Drug Administration (FDA) approved indications and brands of botulinum toxin.

Botulinum toxin (INN; USAN; brand name)	Produced by:	Indication
Clostridium botulinum type A neurotoxin complex; onabotulinumtoxinA; (Botox and Botox cosmetic)	Allergan Inc	Strabismus
		Blepharospasm
		Cervical dystonia
		Glabellar lines
		Axillary hyperhidrosis
		Adult upper limb spasticity
		Chronic migraine
		Urinary incontinence due to detrusor overactivity
		Overactive bladder
		Lateral canthal lines
		Adult lower limb spasticity
		Pediatric upper limb spasticity
		Forehead lines
botulinum toxin type B; RimabotulinumtoxinB; (Myobloc/Neurobloc)	Solstice Neurosciences, LLC	Cervical dystonia
Clostridium botulinum neurotoxin type A; IncobotulinumtoxinA; (Xeomin)	Merz Pharma GmbH & Co KGaA	Cervical dystonia
		Blepharospasm
		Cervical dystonia
		Glabellar lines

		Adult upper limb spasticity
		Sialorrhea
clostridium botulinum type A toxin-haemagglutinin complex; Abobotulinum toxin A; (Dysport)	Ipsen Biopharm Limited	Cervical dystonia
		Glabellar lines
		Adult upper limb spasticity
		Pediatric lower limb spasticity
		Adult lower limb spasticity

Despite the widespread therapeutic use of BoNTs in human medicine, its potential in veterinary medicine largely remains uncharted and unexplored, primarily due to the absence of licensing for veterinary use of BoNT products. There are a few small controlled clinical trials that showed the efficacy of BoNT-A in the treatment of pain in dogs (43–45) and a few case series showing the use of BoNT-A in the treatment of lower esophageal sphincter achalasia-like syndrome, urinary incontinence, prostatic hypertrophy in dogs and stringhalt in horses (46–49), which potentially opens a therapeutic market for BoNT-A in veterinary medicine.

1.3. The structural and functional elements underlying the mechanism of BoNT-A action

1.3.1. Structure of BoNT-A complex

The molecular complex of BoNT-A, released from *C. botulinum* as an exotoxin, contains a neurotoxin part (150 kDa) formed by a catalytic domain, translocation domain, and binding domain. Together with non-toxic accessory proteins (750 kDa) the neurotoxin forms a large 900 kDa high-molecular-weight molecule called the progenitor toxin complex (PTC). Within the complex, auxiliary proteins composed of hemagglutinins and non-hemagglutinins serve to protect the toxin from proteases in the gastrointestinal tract and facilitate its absorption in the intestines (31).

The neurotoxin architecture comprises a heavy chain (H, 100 kDa size) and a light chain (L, or LC, 50 kDa) connected by a disulfide bond. These chains are organized into three functionally divided 50 kDa domains: the L, H_N (the N-terminal part of the H), and H_C (the C-terminal part of the H). The catalytic L domain contains a Zn^{2+}-metalloprotease responsible for cleaving

specific SNARE proteins, in particular synaptosomal-associated protein of 25 kDa (SNAP-25) in the case of BoNT-A, which prevents neurotransmitter exocytosis from the presynaptic terminal. The H_N domain facilitates the translocation of the light chain from intraneural vesicles into the cytosol (50), while the H_C domain serves as the binding part, recognizing presynaptic acceptors at neuronal terminals and enabling toxin endocytosis. Together, all BoNT serotypes, along with TeNT, share a homologous structure of 150 kDa, which functions as a nanomachine delivering the toxic light chain into the nerve terminal.
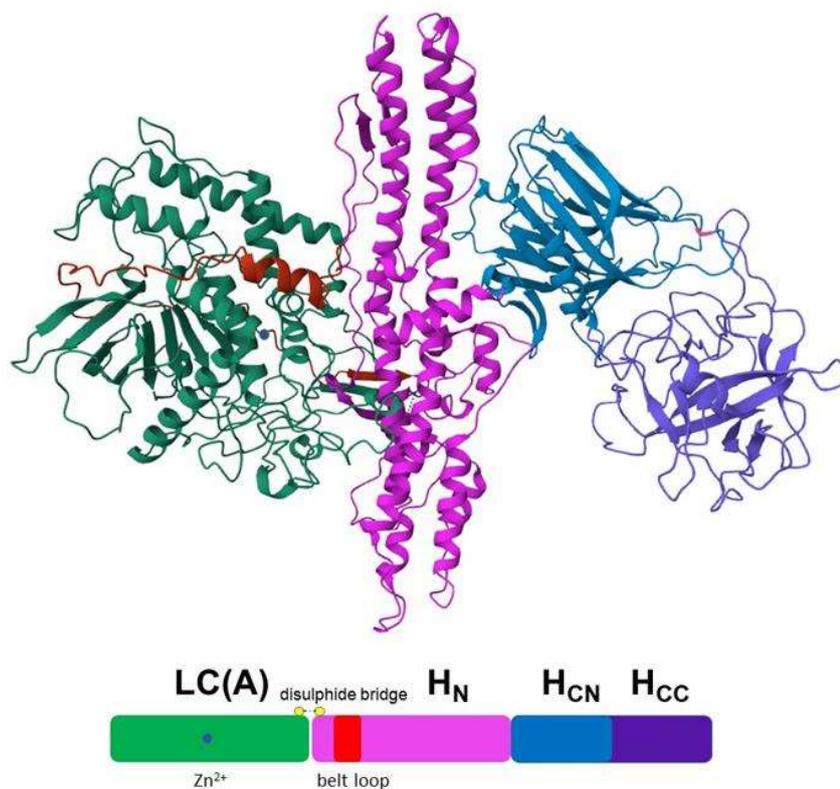
Figure 2. BoNT-A complex. *The crystal structure of botulinum neurotoxin A1 (BoNT-A1). The 150 kDa neurotoxin molecule is composed of a 50 kDa heavy chain which is made of two subdomains C-terminal part of C- domain (H_{CC}- purple part), and the N-terminal part of C-domain (H_{CN}-blue part). The next part is a pink-colored, 50 kDa HN domain, which includes a belt loop and a disulfide bridge that connects to a 50 kDa light chain (LC) in green, encompassing a metalloproteolytic Zn2+ showed as a blue dot. The H_{CC} domain binds specifically to nerve terminals, the H_N domain translocate the L chain into the nerve terminal cytosol, and the L chain acts as a metalloprotease, cleaving and inactivating specific SNARE*

proteins involved in neurotransmitter release, ultimately causing nerve paralysis. The short "belt" loop subdomain of the H_N domain (depicted in red) surrounds the L chain. Protein Data Bank (PDB) accessions https://www.rcsb.org/structure/3BTA.

1.3.2. Mechanism of BoNT-A action

The BoNT-A enters inside neurons solely as its 150 kDa neurotoxic component. The H_C subunit plays a crucial role in both binding to and internalizing into neurons. It accomplishes this by binding to specific dual protein-sialoganglioside (PSG) acceptors on the synaptic plasma membrane's outer surface. The PSG oligosaccharide domain extends far from the surface of the membrane itself and is abundantly distributed on the membrane, enabling easy binding of the BoNT dipole molecule as it diffuses through the extracellular space (31).

In addition to low-affinity binding to PSG, BoNTs binds to high affinity membrane protein acceptors, synaptic vesicle protein (SV2) and synaptotagmin (Syt), which unlike PSG are not outwardly displayed on the nerve terminal surface, rendering them inaccessible to BoNT. Recently it was discovered that for efficient vesicular entry BoNT-A binds to the tripartite PSG-Syt1-SV2 complex (51). However, they become accessible only after the fusion of the synaptic vesicle with the presynaptic membrane, causing the synaptic vesicle to enter the extracellular environment. SV2 is present in three isoforms (SV2A-C) within neurons. BoNT-A can utilize any of these SV2 isoforms to facilitate its binding and endocytic entry into neurons, with SV2C exhibiting the highest affinity (52). Interestingly, BoNT-A binding to glycosylated part of SV2C is important for display of BoNT-A toxicity on NMJ (53,54) as N-glycans vary between tissues and cultured cells. These variations could have a potential clinical relevance, as patterns of glycosylation differ also inter- and intraspecifically, as in the well-known case of the ABO blood groups. This could provide a simple explanation for the variable sensitivity of different patients to BoNT-A injection, which is often observed in clinical settings. By binding to the aforementioned proteins, BoNT rapidly enters the synaptic vesicle. The number of BoNT molecules correlates with the number of SV2 molecules in the synaptic vesicle membrane. The rate at which BoNT enters the synaptic vesicle is equal to the rate of synaptic vesicle endocytosis and the rate of paralysis of the mouse phrenic nerve hemidiaphragm, which serves as a standard neuromuscular junction (NMJ) for testing the potency of BoNT (55). In order to reach the targeted snare proteins, the L chain must be released from the synaptic vesicle into the cytosol. The main factor contributing to the translocation of the L chain is the pH gradient across the synaptic vesicle membrane driven by vesicular ATPase proton pump, which

facilitates the entry of neurotransmitters into synaptic vesicles together with H+ ions after exocytosis. It has long been known that BoNTs form low-conductance ion channels in flat lipid bilayers at low pH. The acidic environment leads to a conformational change in the H_N domain, preventing it from penetrating the lipid bilayer of the synaptic vesicle membrane. When the pH decreases on the *cis* side of the membrane (the side facing the lumen of the synaptic vesicle), it motivates the L chain to cross to the other side. The L chain must unfold to pass through the channel. To move the L chain to the trans side of the membrane (the cytosolic side), the disulfide bond must be cleaved, allowing the L chain to pass into the cytosol (56). If the cleavage of the disulfide bond were to happen earlier, it would prevent the translocation of the L chain. The redox system NADPH–thioredoxin Reductase (TrxR)–thioredoxin (Trx) was found to have a major role in releasing the L chain into the neuronal cytosol. The tertiary fold of Trx is similar to that of ancestral chaperonins, so it is also possible that Trx functions as a chaperonin for L-chain translocation. Changes in the structure of BoNT-A are accompanied by simultaneous changes in the structure and organization of membrane lipids. Upon translocation into the cytosol, the LC polypeptide undergoes a refolding process and transforms into a $Zn2+$-dependent metalloproteolytic enzyme. This enzyme, known as LC metalloprotease, cleaves a single peptide bond located 9 amino acids away from the C-terminal end of the membrane-bound synaptic protein called synaptosomal-associated protein of 25 kDa (SNAP-25) (57). SNAP-25 is a membrane protein consisting of 206 amino acids, anchored to the cytosolic side of the presynaptic plasma membrane. Together with its binding partners, the membrane-associated protein syntaxin, and the vesicle-associated membrane protein (VAMP)/synaptobrevin, SNAP-25 forms complexes that mediate synaptic vesicle fusion with the presynaptic plasma membrane. This heterotrimeric complex, essential for Ca^{2+}-dependent synaptic vesicular release of neurotransmitters, is referred to as SNARE complex (50) mentioned earlier.

Certain serotypes of BoNT achieve their metalloprotease activity by cleaving different SNARE proteins. For example, BoNT-A selectively targets SNAP-25, while BoNT-C has an affinity for both SNAP-25 and syntaxin. BoNT-B, BoNT-D, BoNT-F, BoNT-G, and TeNT selectively cleave VAMP. The fact that inactivation of any of these three proteins leads to unsuccessful exocytosis demonstrates the importance of these proteins for the normal function of neurotransmitter exocytosis. The silencing effect of BoNT-A on synapses is reversible as it does not kill the intoxicated neurons. Patients who experience respiratory paralysis can recover, and death can be prevented with mechanical ventilation. Numerous factors contribute to the

longevity of BoNT within neurons, including the sensitivity of the neurons, the species affected, and the neurotoxin's susceptibility to intracellular protein degradation mechanisms. In humans, the duration of paralysis varies widely, ranging from around two weeks for BoNT-E1 to approximately three to four months for BoNT-A1 (31,58). Nevertheless, while BoNTs do not induce axonal degeneration at levels associated with botulism, observable reversible muscle atrophy occurs. The duration of paralysis is primarily influenced by the longevity of the metalloprotease within the nerve terminal cytosol, although it is not the sole contributing factor (59–61), with BoNT-A having the longest duration period. Furthermore, the duration of paralysis varies based on the type of neurons involved, as paralysis impacting autonomic nerve terminals tends to endure longer than paralysis affecting the NMJ (62). Understanding the duration of action also sheds light on the mechanisms involved in the inactivation and turnover of SNARE proteins within nerve terminals (60,63), as well as the formation of the SNARE complex (59). Furthermore, the persistence of BoNT activity is crucial for their therapeutic use, as toxins with longer durations of action necessitate fewer injections of lower doses.
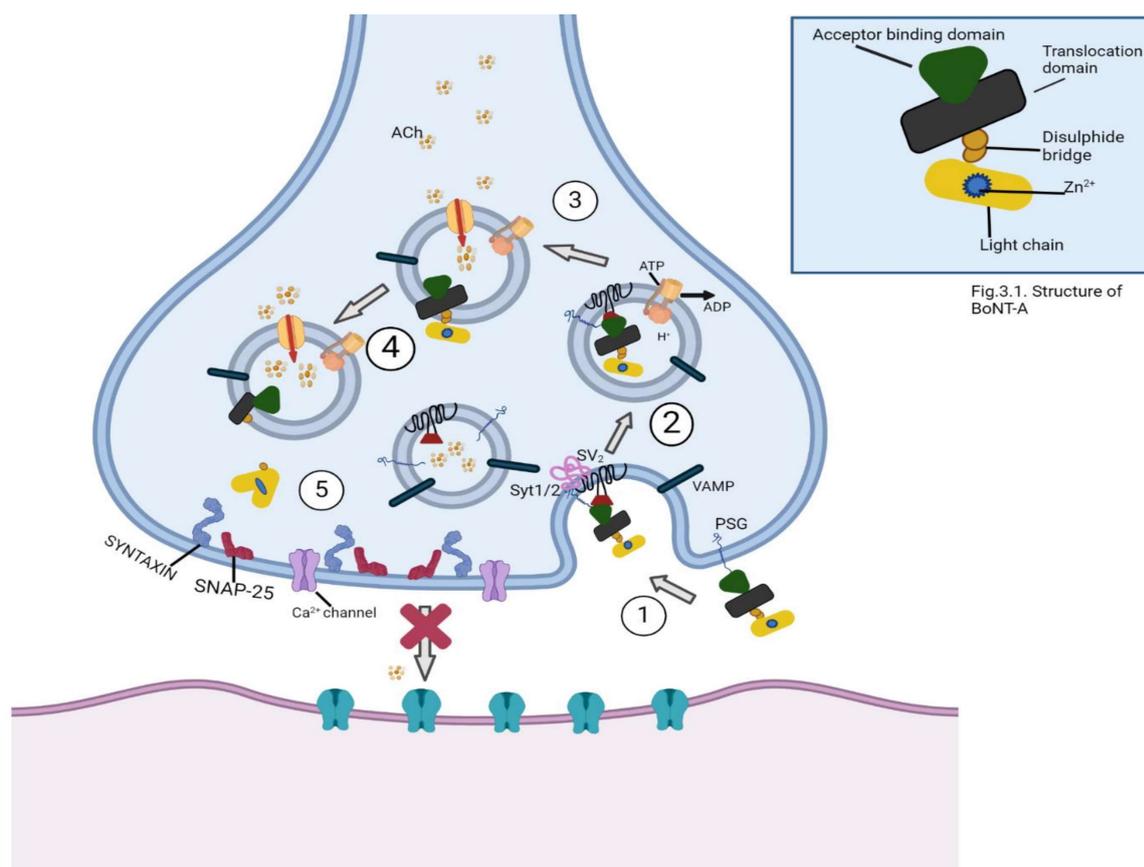
Figure 3. The mechanism of synaptic BoNT-A action. *The mechanism of BoNT-A action consists of 5 steps. The first step (1) involves the binding of the neurotoxin HC-C domain (depicted in green) to a polysialoganglioside (PSG) located on the presynaptic membrane.*

Binding to PSG subsequently enables attachment to the glycosylated portion of the SV2 receptor (N-glycan part marked in red) which is already in a tripartite PSG-Syt1-SV2 complex, which enables vesicular internalization. Subsequently, during step two (2), BoNT-A gets internalized into synaptic vesicles (SVs) which is facilitated by synaptic membrane recycling. This process is driven by the v-ATPase pump, which induces acidification of the vesicle and protonation of BoNT. Step three (3) demonstrates the pH-driven accumulation of the neurotransmitter ACh via the vesicular neurotransmitter transporter, alongside membrane translocation of the L chain into the cytosol. The translocation domain assists in this process, although its mechanism remains unidentified. In step four (4), the release of the L chain (depicted as a light yellow particle with a blue dot representing an active Zn2+ atom) occurs through the separation of a disulfide bond, which is activated by the endogenous thioredoxin reductase-thioredoxin system (TrxR-Trx). Following this, in step five (5), within the cytosol, the metalloprotease activity of the L-chain triggers proteolytic cleavage of one of the three SNARE proteins. These SNARE proteins constitute the heterotrimer complex (SNARE complex), which is crucial for membrane fusion events leading to synaptic vesicle exocytosis. Figure made according to Šoštarić et al. (64); in Biorender.com; accessed on 19-3-2024).

1.3.3. Sibling neurotoxins: similarity of BoNT-A and TeNT mechanisms of action

The genes responsible for various BoNT serotypes and TeNT, a toxin originating from *Clostridium tetani* that triggers tetanus, originate from a shared ancestral gene. Tetanus neurotoxin is translated as a single polypeptide chain of 150 kDa (65). It is the sole causative agent of tetanus, which is characterized by generalized sustained or intermittent muscle spasms, and may be fatal if respiratory muscles are affected. Similar to BoNTs it consists of light (L, 50 kDa) and heavy chain (H, 100 kDa) linked by a single disulfide bond, which is essential for neurotoxicity (66), but distinct from BoNTs it does not contain auxillary proteins.

Both TeNT and BoNTs, targeting specific presynaptic nerve terminals, operate through a similar mechanism closely tied to their modular structure. This mechanism encompasses five main steps: (1) binding to the presynaptic membrane, (2) internalization within synaptic vesicles through endocytosis, (3) translocation of the L domain across the membrane to the cytosol, facilitated by the H_N domain, (4) reduction of the interchain disulfide bond, activating the L metalloprotease domain, and (5) selective cleavage of one or more of the three SNARE proteins, resulting in the blockade of neurotransmitter release. Both TeNT and BoNT are both dipole molecules that bind with its H_{CC} domain to the presynaptic plasma membrane via

interaction with negatively charged polysialoganglioside (PSGs) which are abundantly present in nerve terminals (67–69). PSG-bound TeNT and BoNT-A are ready to bind their other receptor, SV2 (70), following the internalisation inside the lumen of synaptic vesicule (55,71,72). For a considerable period, the identity of the protein receptor facilitating the retroaxonal transport of TeNT remained unknown. Early observations indicated that TeNT enters a subset of endocytic vesicles known as signaling endosomes. These vesicles coordinate clathrin-mediated endocytosis and the sequential actions of Rab5 and Rab7 GTPases, orchestrating the transmission of neurotrophic signals from the peripheral nerve terminals to the soma of peripheral neurons (73). Nidogen-1 and nidogen-2 are also responsible for directing TeNT into signaling endosomes (74–78). Similar evidence supporting BoNT-A migration by retrograde axonal transport and transcytosis to different parts of central nervous system have been indicated by neuroparalytic action and cleaved SNAP-25 (8–10,79–84). Truncated SNAP-25 has been identified in various regions subsequent to the peripheral administration of BoNT-A1 in different animal models: (i) within the facial nucleus and trigeminal nucleus caudalis of rats (11,79,81), (ii) in the ventral horns of the spinal cord following hind-limb injection in rats (83), and (iii) in the dorsal horn after peripheral subcutaneous or i.m. injections in rats (83). Noteworthy is the observation that SNAP-25 cleavage extends to neurons situated up to two synapses away from the initially targeted neuron, indicating the toxin's capability to undergo successive cycles of neuronal entry, axonal transport, and transcytosis (82,84). Evidence suggests that BoNT-A1 is co-transported with TeNT in cultured motor neurons in vitro, indicating that BoNT-A may utilize non-acidic carriers similar to TeNT (84). One possible explanation is that at the level of NMJ, BoNT-A enters different synaptic vesicles pools, and some of these vesicles are non-recycling (55,71). Next step in neurotoxins trafficking is membrane translocation inside synaptic vesicles. Luminal pH is acidified by the vesicular ATPase proton pump which exploits TeNT and BoNTs to translocate their L chain into the cytosol, due to low-pH-induced conformational change of the toxin molecule (more detailed explained in previous chapter). When released in the cytosol of the neuronal terminal, L chain of TeNT cleaves VAMP, an integral protein of the SV membrane, while BoNT-A cleaves SNAP-25, protein present on cytosolic surface of the presynaptic membrane. Both VAMP and SNAP-25 are part of the SNARE complex, a core of the membrane fusion nanomachine allowing the release of the neurotransmitter in the synaptic cleft (85). The divergence in the effects of TeNT and BoNT-A stems from their selective targeting of different neuron types. While both neurotoxins induce neuroparalysis via the cleavage of SNARE proteins, TeNT induces spastic paralysis, whereas BoNT-A induces flaccid paralysis. TeNT primarily targets

inhibitory interneurons within the ventral horn of the spinal cord (Ia inhibitory neurons and Renshaw cells, but also other types of interneurons (86), disrupting the balance between inhibitory and excitatory signals and resulting in hyperexcitability of motor neurons and subsequent spasticity (87,88). In contrast, in the motor system BoNT-A predominantly targets peripheral motor terminals leading to the blockade of acetylcholine release and subsequent muscle weakness characteristic of flaccid paralysis, with possible selectivity for excitatory cholinergic interneurons in the spinal cord's ventral horn (potentially C-boutons of V0c interneurons (10) after its axonal transport .
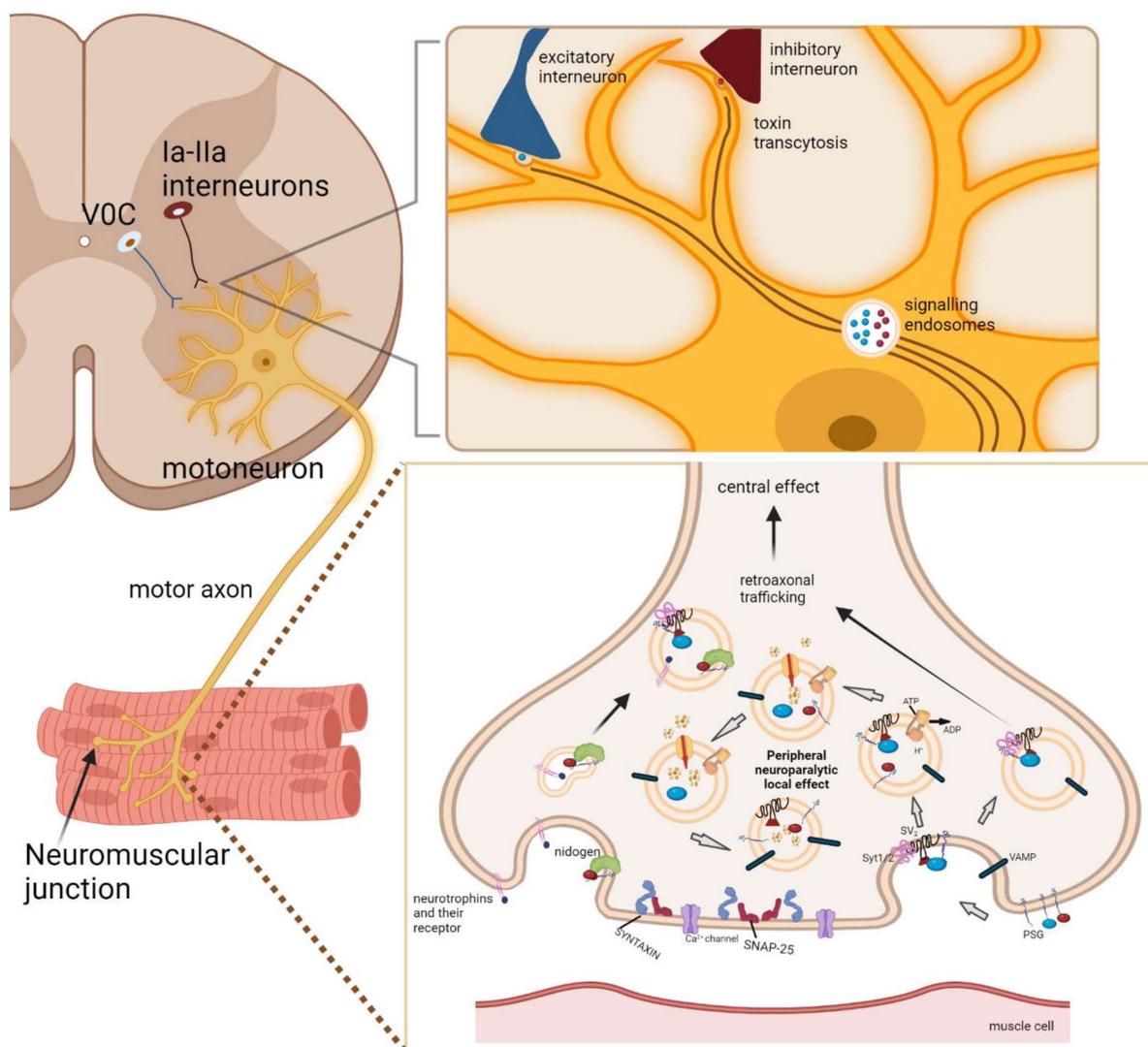
Figure 4. Schematic representation of BoNT-A and TeNT mechanisms of action (according to Pirazzini et al. (89)). *Initially, both toxins primarily bind to peripheral motor terminals, with TeNT preferentially binding to motor while BoNTs selectively target both motor and autonomic cholinergic nerves. BoNTs bind to the PSG-synaptotagmin-SV2C complex, as*

explained in more detail in the previous chapter, and undergo endocytosis into recycled synaptic vesicles. From acidified vesiclesBoNT, may undergo translocation into the cytosol of peripheral nerve terminals, leading to the cleavage of SNAP-25, or enter non-acidic vesicles followed by retroaxonal transport. Similarly, TeNT binds to PSG and nidogen, which may be similar to BoNT form complexes with synaptotagmin. These complexes undergo endocytosis and are then retroaxonally transported to central synapses. Furthermore, both TeNT and BoNTs exhibit central neuroparalysis, due to their release into spinal cord interstitial extracellular fluid followed by preferential interaction with either inhibitory (TeNT) or excitatory synapses (BoNT-A).

1.4. BoNT-A and movement disorders

1.4.1 Review of BoNT-A clinical use in spasticity and dystonias

The clinical effectiveness and safety of BoNT-A rely on its ability to induce temporary and reversible synaptic silencing. In 1977, Allan Scott was the first to publish the results of strabismus therapy using small doses of botulinum toxin precisely injected into the orbicularis muscle. The results demonstrated that injecting botulinum toxin in small doses effectively alleviates overtly active muscles. In 1981, botulinum was injected for the first time for blepharospasm by Jankovic and its efficacy was subsequently confirmed in smaller placebo-controlled studies (90) and larger multicentric studies (91). Its efficacy in spasmodic torticollis, the most common type of dystonia, was reported by Tsui et al., (92). In 1989, BoNT-A was approved by U.S. Food and Drug Administration (FDA) for the treatment of strabismus, blepharospasm, and hemifacial spasm. Afterwards it was slowly introduced for treatment of other movement disorders, including tremors, tics, myoclonus, and spasticity.

Dystonia is defined as "sustained or intermittent muscle contractions causing abnormal, often repetitive, movements, postures, or both" (93,94) and it is classified as focal (affecting only one part of the body), segmental (nearby regions are affected) and generalized (multiple areas of the body are affected). Focal dystonias like blepharospasm, spastic dysphonia and cervical dystonia (torticollis) are indications where BoNT-A treatment is a gold standard therapy, but the whole action behind its effect on dystonia is not completely understood (95,94), especially since the loss of inhibition is a dominant driving force of uncontrolled movement (94,97–103). Treatment of focal dystonia is still symptomatic due to yet unresolved pathophysiological causes affecting many levels of the CNS, and BoNT-A therapy is a golden standard for both focal and segmental dystonia with botulinum toxin injections in the affected muscles, agreed

by most guidelines. Generalized or axial dystonia affecting larger regions of the body can be managed with oral or intrathecal antispasmodics like baclofen and tizanidine, with limited efficacy and more numerous side effects such as drowsiness, dizziness, fatigue and nausea. High complication rates from surgical procedures and possible infection and pump malfunction makes intrathecal baclofen a second-line agent in dystonia treatment. Furthermore, gradual discontinuation of baclofen treatment is advised due to possible development of withdrawal syndrome, if abruptly discontinued (104,105). Possible treatments include also benzodiazepines and most commonly used are clonazepam and diazepam. However, similar to baclofen they can induce different side effects including sedation and depression and similar to baclofen, abrupt discontinuation can lead to withdrawal syndrome (105). Several clinical trials that indicated beneficial efficacy for botulinum toxin treatment in focal dystonia, resulted in both BoNT-A and BoNT-B being approved by FDA and European Medicine Agency (EMA). When injected to the target muscle, botulinum toxin is swiftly absorbed into the presynaptic nerve terminals. Its paralytic effect is initiated by inhibiting the release of acetylcholine, effectively obstructing neuromuscular transmission which causes reversible muscle weakening lasting for 12-14 weeks. In a study comparing the effects of different dosing regimens, Ranoux et al., (106) observed that the duration of effect was notably longer with the abobotulinumtoxinA regimen compared to the onabotulinumtoxinA regimen (mean durations of 114 days and 89.3 days, respectively). However, the prolonged clinical efficacy associated with abobotulinumtoxinA was accompanied by a higher incidence of adverse events (36.0% for abobotulinumtoxinA versus 17.6% for onabotulinumtoxinA). This difference might have occurred due to a dose conversion ratio between the two pharmaceutical preparations, resulting in higher dose of active protease delivered in patients treated with abobotulinumtoxinA.

Meanwhile, Jochim et al. (107) conducted an analysis on the long-term efficacy and safety of onabotulinumtoxinA and abobotulinumtoxinA treatments in patients with cervical dystonia. Their study, comprising 2,592 onabotulinumtoxinA treatment sessions in 135 patients and 6,660 abobotulinumtoxinA treatment sessions in 209 patients, revealed stable mean doses and injection intervals for both formulations. This suggests that the therapy remains safe and effective even with prolonged treatment durations. Regarding the prolonged impact of botulinum toxin on individuals with cervical dystonia, numerous investigations (108–113) have highlighted its enduring efficacy. Notably, the study with the longest follow-up period revealed that the sustained effectiveness of BoNT repeated treatments may last for more than two decades (114).

Therapeutic response to BoNT can be variable, and the lack of efficacy from BoNT-A treatment can be due to several factors, such as inadequate dosage, inappropriate muscle selection and targeting resulting from the absence of EMG/ultrasound guidance, changes in the pattern of dystonic muscle contractions, or the development of neutralizing antibodies.

Older pharmaceutical toxin preparations that contained a higher fraction of inactive protein (up to 5 x more proteins for equivalent potency compared to novel preparation) were associated with dose-dependent emergence of neutralizing antibodies (90,115). Increased dosage per session and more frequent injections are correlated with a heightened likelihood of developing neutralizing antibodies, thereby discouraging the use of booster injections (116).

Dystonic patients may suffer from dystonic tremors affecting the head and neck which manifest in patients diagnosed with cervical dystonia (CD), while those experiencing spasmodic dysphonia might exhibit tremors in their voice. Similarly, individuals with focal dystonia in the upper extremities, such as organic writer's cramp or musician's dystonia, may present with dystonic hand tremors, along with other task-specific tremors. BoNT was shown to be a successful treatment for dystonic tremors (117–119) however its use in these conditions is off-label, as it is not yet approved for tremor indications.

In addition to the motor deficits evident as intermittent muscular hyperactivity, patients with focal dystonia commonly experience non-motor symptoms, with pain being a prevalent issue. Up to 88,9% of patients report pain at some point during the course of the disease (120). Pain frequently drives patients with cervical dystonia to seek medical intervention (121).

Despite comprehensive understanding of the mechanisms underlying muscle relaxation, the analgesic effects of BoNTs are still not fully understood (122). There have been several possible hypotheses behind BoNT antinociceptive effect in dystonia: i) inhibition of acetylcholine release which leads to decreased muscle tone and volume followed by decompression of nerve fibers; ii) improved muscle metabolism and increased oxygenation which eliminates sensitisation (122); iii) changes in the CNS manifested as lower cortical representation of the injected muscle due to reduced activity of afferent neurons (7); iv) decreasing of central desensitisation by direct toxin action in the CNS due to retrograde axonal transport and indirect by decreased neurotransmitter release from peripheral nerve terminals (123,11). Indicatively, pain-relieving effect may occur earlier than the beneficial motor effect, and at lower doses, which is in line with independent antinociceptive effect not related to relief of muscle

hyperkinesia by the toxin (124). However, there are little studies investigating direct antinociceptive mechanisms of BoNT in dystonic patients, and mechanism discussed above are derived mainly from preclinical pain studies related to inflammatory or neuropathic pain.

Spasticity is only one of the possible manifestations of the upper motor neuron (UMN) syndrome, arising from a variety of neurological conditions. It is characterized by hyperexcitable tonic stretch reflexes manifesting as increased tone, clonus, spasms, co-contractions, and central paresis (125,126). It is usually involving a lesion located proximally in relation to lower motor neurons, thus associated with the pyramidal tract connecting the cortex with spinal cord. Contractures and pain are two major complications of spasticity (127), leading to reduced range of passive joint motion and greatly impacting quality of patients' life. Additional complications can be present depending on the underlying aetiology, such as ataxia, apraxia and bradykinesia. Aetiology can vary greatly, with stroke, multiple sclerosis and cerebral palsy being the most frequent causes of spasticity. Spasticity classification is determined based on the affected body region, according to which we can distinguish upper limb spasticity, lower limb spasticity, hemispasticity, paraspasticity and tetraspasticity. It manifests in approximately 80% of individuals diagnosed with multiple sclerosis (128) and in 65–78% of those who have experienced spinal cord injuries (129) (130). In stroke survivors it has an incidence of 38% (131). Yet, spasticity affects 97% of chronic stroke survivors that experience moderate to severe motor impairments (129).

Unlike dystonia where treatment options are limited, spasticity offers a range of alternatives beyond BoNT-A. These include physical modalities, oral medications, chemodenervation using phenol or alcohol, intrathecal baclofen therapy, and surgical interventions (132). Nevertheless, the widespread adoption of BoNT-A-induced synaptic silencing has established itself as a prominent treatment for spasticity. After i.m. injections of BoNT-A, clinical effects manifest several days later and last for about 3 months. After this period, the neuromuscular junction neurotransmission is restored and spasticity reoccurs.

Typically, patients necessitate recurrent BoNT injections every 3 to 4 months, as indicated by studies conducted by Moeini-Naghani et al. (133) and Simpson et al. (134). Yet, a survey conducted among treating physicians and patients revealed that most individuals favor more frequent injections to attain improved clinical outcomes, according to findings by Bensmail et al. (135).

A recent meta-analysis study encompassing 40 trials conducted by Andringa et al. (136) demonstrated compelling evidence regarding the efficacy of BoNT in reducing resistance to passive movement and enhancing self-care abilities, as assessed by the (modified) Ashworth scale. Furthermore, improvements in self-care ability for the affected side were observed post-intervention and during follow-up. Notably, robust evidence indicated no significant impact on "arm-hand capacity" during follow-up. BoNT was found to significantly alleviate "involuntary movements," "spasticity-related pain," and "carer burden," while also enhancing "passive range of motion." However, there was a lack of evidence supporting improvements in "arm and hand use" post-intervention.

Currently employed doses in clinical practice, as recommended by consensus statements (137), tend to exceed those administered in published randomized controlled trials. Two exhaustive analyses have determined that elevated doses of BoNT-A show promise in effectively alleviating spasticity in both the upper and lower limbs following stroke, while exhibiting minimal adverse effects (138,139). Increasing the volume of BoNT-A solution injected is believed to enhance its therapeutic effects by facilitating the toxin's ability to reach a greater number of motor endplates. Certain studies have revealed that administering BoNT injections with a higher volume or targeting the endplate yields a more pronounced neuromuscular blockade, leading to greater reductions in spasticity and co-contraction compared to injections with a lower volume or those not specifically targeting the endplate (140). Other techniques aimed at enhancing toxin efficacy include guided injection methods such as monitoring the EMG activity, identifying motor points using electrical stimulation (ES), or visualizing target sites with sonography. While the superiority of one guidance technique over another remains to be established, studies consistently demonstrate that EMG, ES, or sonography-guided injections are superior to anatomical localization through muscle palpation (141–143).

Several studies have indicated that initiating treatment as early as 3–6 months after disease onset effectively addresses muscle hypertonia and reduces the risk of subsequent complications, such as contracture development (144,145). Many studies examining the use of botulinum toxin for spasticity typically encompass only a limited number of injection cycles. However, a small number of studies have reported both safety and sustained efficacy for up to five injection cycles spanning several years (146–149).

Time of onset and duration of BoNT-A effectiveness in different movement disorders is variable and dependent on various factors, one of which is age of the patient. Older patients are consistently showing faster achievement of beneficial effects from BoNT-A treatment, which could be explained by muscular changes in aging (150). Despite being one of the most potent toxins, BoNT is remarkably safe when administered by experienced and skilled clinicians, even over extended periods spanning years or decades (111). It is believed that adverse effects, such as weakness, arise from local impacts and the diffusion of the toxin into adjacent muscles (4). However, use of BoNT in elderly patients should be cautious when injecting in neck muscles due to possible pre-existing cervical spine instability and underlying cervical musculature weakness (151). Systemic adverse effects occur rarely, but it is possible for allergic reactions, generalized weakness or flu-like symptoms to occur. Variable percentage of patients (1.7-20%) reported flu-like symptoms 24 hours post BoNT-A treatment (152), which could be linked to the generation of certain interleukins, notably the chemokine interferon-γ inducible protein 10 kDa (CXCL10) (153). While concerns about the antigenicity of BoNT were significant in the past, leading to recommendations against injections more frequently than every 3 months, the frequency of immunogenicity, or the development of blocking antibodies has substantially decreased (108,154). Instances of primary nonresponders, who show no effect after BoNT administration, are exceedingly rare and may be attributed to prior vaccination against BoNT or subclinical BoNT exposure. Secondary nonresponders, on the other hand, may stop responding to repeat injections due to antibodies targeting functionally relevant BoNT epitopes or its binding portion, hindering the BoNT complex from entering the presynaptic terminal. Decreased concerns about secondary unresponsiveness are prompting studies suggesting that more frequent injections (less than every 12 weeks) or higher doses might be safer and can enhance patient satisfaction (155,156).

1.4.2. Insight from in vitro studies and in vivo models

Neurophysiological exploration across human studies consistently demonstrates the efficacy of botulinum toxin in alleviating both disorders; i) dystonic motor symptoms and ii) increased muscle tone present in spasticity. It is currently believed that its positive impacts on motor disorders primarily stem from its ability to cause local chemodenervation of the nerves in both the muscles and sensory organs, resulting in the indirect restoration of spinal reflexes and the improvement of central movement processing (157). One of the key attributes that

makes BoNT-A a remarkable therapeutic option and what distinguishes it from other available medications, such as baclofen, is its extended duration of action.

Primary fetal mouse spinal cord cultures and in vivo experiments both on adult C57BL/6N mice and Sprague Dawley rats showed that extended duration of BoNT- A effects can be attributed to sustained catalytic activity of the protease within nerve terminals (158–160). Preparation of cerebellar granule neurons from rats and in vivo experiment in mice showed slow replacement of BoNT-A cleaved SNAP-25 from neurons (158,159). This truncated SNAP-25 interferes with neuroexocytosis by acting as a dominant-negative factor (158–160).Aside from long duration of action, reversible synaptic silencing of nerve terminals is another key feature of BoNT-A as a therapeutic. In vivo experiments indicate that intoxication of peripheral nerve endings with BoNT-A is fully reversible and does not lead to degeneration of the terminal (161).

In vivo recordings in mouse sternomastoid muscle after a single i.m. injection of BoNT-A showed that toxin's prevention of exocytosis initiates significant synaptic remodeling in motoneurons, characterized by extensive sprouting and the formation of new synapses (161).This sprouting network plays a crucial role in restoring functional communication between motoneurons and muscle fibers (158,161).Importantly, these sprouts are eliminated once the original parent terminal regains its ability to release neurotransmitters (159,161). Both in vitro spinal cord cultures and in vivo experiments demonstrate that nerve stimulation accelerates the onset of BoNT-A poisoning (162,52), indicating a preference for uptake by hyperactive nerve terminals, which may play a role in its antispastic activity. However, it is questionable whether increased nerve activity also correlates with better or longer-lasting efficacy in movement disorders (163).

When injected by experienced clinicians, BoNT-A is a safe and effective remedy for overspastic and dystonic muscles, however, adverse effects are possible in both injected and non-injected muscles. Furthermore, some of the most frequent adverse events include dysphagia, muscular weakness, blurried vision, dry mouth and diplopia. In New Zealand White rabbits, Fortuna et al. (164) found changes in BoNT-A injected muscles, present even 6 months post injections. Muscles were atrophic, with fat build up in the place of the previous muscles and the animals showed less strength in affected muscles with reduced muscle mass. Non-recovering atrophy was also present in our research results, even when animals recovered from motor deficits caused by peripheral synaptic silencing (Šoštarić et al., 2022, Appendix I). In rats with spinal cord injury, pathological characteristics of calf and motor functions were analysed after BoNT-

A injection and showed increased pathological changes with reduced weight of the injected and adjacent muscles and change of myosin heavy chain after BoNT-A i.m. injections. Moreover, the presence of evidence demonstrating a transition in muscle fiber phenotype, as indicated by heightened expression of slow myosin heavy chain in muscles subjected to BoNT-A treatment (165–167), may hold significant implications for the therapeutic management of spastic muscles. Such muscles exhibit distinct and time-dependent alterations in their contractile properties (168,169). Furthermore, histological studies in rats has demonstrated that higher volumes of BoNT-A increases muscle paralysis (170). Moreover, experiments in rabbits showed that application of more diluted BoNT preparations, whether combined with electrical stimulation or not, led to increased paralysis of the gastrocnemius muscle. Histological examinations revealed that muscles treated with the more diluted BoNT preparation alongside electrical stimulation exhibited pronounced muscle atrophy, variability in fiber size, and clustering of type 1 fibers.

1.4.3. TeNT induced muscle spasticity as a model for experimental hypertonia

In animals, especially rodents, considerable differences exist regarding the severity of central nervous system injury and subsequent motor function. Rodents can endure substantial brain trauma, and yet show mild or even no motor deficits. Despite this, animal models with severe brain injuries but minimal motor dysfunction remain valuable for studying various aspects of brain injury and potential treatments. However, to delve into the origins of motor dysfunction, including spasticity and hyperreflexia, it becomes crucial to utilize animal models where these outcomes are clearly measurable. For example, when it comes to cerebral palsy, only two models describe motor function deficits (171) out of 13 different hypoxia-ischemia models or inflammation based models of developmental injury.Other models include unilateral damage to motor cortex (172,173) or motor restriction by physical imobilisation (174,175). Mouse genetic models with glycine receptor mutations cause loss of large spinal motoneurons (176). Symptomatic models of dystonia can be obtained in different species and induced by pharmacological manipulations or after targeted gene alterations (177) with identified basal ganglia abnormalities, including alterations in striatal GABAergic and dopaminergic transmission. While the aetiology of muscular hyperactivity differs between hyperkinetic movement disorders and spasticity, both conditions are linked to impaired inhibitory control of lower motor neurons (99,184). Matak (13), showed that local small doses of TeNT could be successfully employed as a model for reversible experimental hypertonia. Furthermore, baclofen as a drug often used in spasticity treatment is effective in alleviating the TeNT-evoked

local muscular spasm (13) which supports previous observations of common medication effectiveness for muscle hypertonia in dystonia, spasticity and tetanus (184,185). When injected with small doses of TeNT (1.5 ng) in gastrocnemius muscle, animals develop muscle contractions, characterized by prolonged stiffness in the hind paw with a sustained extension and resistance to passive flexion of the ankle. Described muscle spasm reaches its full development on day 7 post TeNT injections and animals' gradual recovery can be easily followed by behavioural assessment of spasm intensity (13). Positive aspects of TeNT as an effective model for observing motor disorders at the spinal cord level are exclusive motor deficits, reversible effect and possible precise targeting of spinal level impairments. TeNT-evoked local spastic paralysis could be employed to induce the motor neuron disinhibition and exaggerated excitatory drive, however, the localized muscle spasms induced by TeNT do not encompass the entire complexity of clinical disorders. When used as a model of naturally occurring spasticity, its use may be limited only to certain aspects, such as the disinhibition of local spinal interneurons (13). Models such as rats with spinal cord injuries and hereditary spastic mice face drawbacks, including permanent damage of widespread brain or spinal regions affecting multiple muscle groups, thus limiting the possible assessment of low dose locally administered intramuscular BoNT-A (see Table 2). However, administering local small doses of TeNT leads to lasting yet reversible focal spasticity, with measurable changes in its severity and animal recovery. Additionally, its reversibility allows for monitoring the long-term effects of botulinum toxin, and reducing the number of animals required in experiments. Furthermore, precise injections of TeNT into the muscle induce spinal disinhibition of motoneurons innervating the targeted area, a feat that is scarcely achieved by other models.

Table 2: Summary of possible in vivo models resembling spasticity or dystonia vs. model of TeNT evoked experimental hypertonia

Literature data			
Motor disorders	In vivo model	Treatment	Disadvantages due to extent of CNS damage
Cerebral palsy (171)	Hypoxia- ischemia models	Chronic unilateral carotid occlusion followed by hypoxia	Loss of oligodendrocytes; Cerebral infarct: subventricular layer and corpus callosum; hippocampal atrophy.
		Transient bilateral carotid ligation	White matter injury, loss of oligodendrocyte; activated glia
		Chronic bilateral carotid occlusion with and without hypoxia	White matter injury in corpus callosum, activated glia, elevated inflammatory mediators
Other developmental injuries characterized with spasticity (172-176)	Cortical silencing	Chronic GABA agonist delivery to motor or sensorimotor cortex	Loss of spinal cholinergic interneurons; increased vascularization of silenced cortex
	Unilateral damage to motor cortex	Unilateral ablation of motor cortex	Complete excision of motor cortex. Preservation of more afferent synapses in ventral horn, loss of spinal interneurons
	Motor restriction by physical immobilization	Bounding together both hind limbs with paper tape	Impaired development of corticospinal tract projections in spinal cord; smaller size of spinal motoneurons
	Spinal cord injury	Contusion/compression	Permanent damage of nerves/non recovering lesions/loss of innervation/ loss of motor and sensory function
	Genetic models	glycine receptor mutations	Loss of large spinal motoneurons
Dystonia symptomatic models (177)	Genetic models caused by different mutations		Paroxysmal generalized dystonia; focal limb dystonia (limited to small cerebellar portion) with alterations in striatal GABAergic and dopaminergic transmission.
PhD Thesis			
Focal spasticity	In vivo model	Treatment	Advantages
	Experimental hypertonia induced by i.m. TeNT injections (13)	i.m. TeNT	Reversible effect (duration:3-4 weeks); exclusive motor deficits, and possible precise targeting of spinal level impairments, characterized with measurable changes
Novelty			
Reversible focal muscle hypertonia resembling impaired inhibitory control of lower motor neurons similar to both, dystonia and spasticity			

CNS, central nervous system; GABA, γ-amino butyric acid; TeNT, tetanus toxin

1.4. 4. Behind the curtain: peripheral theory of BoNT-A action favoring exclusive peripheral sites of its action as a therapeutic

According to a long-standing theory, the BoNT-A effect on spastic muscle arises solely due to its peripheral cleavage of SNAP25 at the cholinergic peripheral motor terminals, where its blockage of acetylcholine cause local weakness and relaxation of extrafusal muscle fibers in the injected muscle. In 1971, Drachman (180) proposed BoNT-A as an "ideal nerve blocking agent," with known mechanism of action and specificity in solely targeting cholinergic transmission, reversibility without causing permanent impairment to nerve or muscle function or structure, ability to universally block motor neuron terminals of striated skeletal muscle, ease of use with simple injection into desired muscle regions, safety when utilized with appropriate precautions, and apparent lack of systemic or central nervous system effects (181). Furthermore, first series of BoNT-A utilization as therapeutic (38,182,183), outlined the principles and characteristics of botulinum toxin, based on research involving monkeys and humans which supported the Drachman's theory of inducing solely local muscular blockage of neuroexocytosis.

However, Giladi (184), proposed physiological changes at the level of the central nervous system as a mode of action on afferent pathways after i.m. BoNT-A injection, similar or equivalent to "sensory trick" in dystonia. Changes of the activity of mesencephalic nucleus neurons after very high BoNT-A dose injection into the massetter, as well as the histological evidence of fiber atrophy in both extrafusal and intrafusal muscle fibers, suggested possible direct effect of BoNT-A on gamma motoneuron of muscle spindle in a rat deep masseter muscle and biceps femoris (185,186). These two studies were further interpreted as main arguments for a theory that BoNT-A causing relief in dystonia can be due to its action on muscle tone reflex by affecting intrafusal muscle fibres. However, it has to be pointed out that the mentioned study employed very high, non-physiological doses of BoNT-A and a very short term latency between the BoNT-A application and electrophysiological measurement, questioning its clinical relevance (185). The study of Rosales et al. could not distinguish whether the degenerative changes of intrafusal fibers are an indirect consequence of its action at extrafusal terminals (186). Similarly uncharacterized arguments were based on observations from patients with essential tremor and dystonia, which exhibit reduced presynaptic inhibition of Ia terminals between flexor and extensor forearm muscles (187,188). Their presynaptic inhibition was restored after BoNT-A injection in the wrist flexor of these patients (188). However, these observations did not examine the causal involvement of the toxin's action at intrafusal terminals

in the observed toxin's beneficial actions on restoration of presynaptic inhibition. Nevertheless, Gracies (189) highlighted the encapsulation of muscle spindles, raising doubts about the potential for the large BoNT-A molecule to penetrate them. Considering the existing data, uncertainties arise regarding whether BoNT-A directly affects the γ-motor neurons, or if the observed outcomes are instead an indirect result of the blockade of α-motor neuron activity (189).

1.4.5. Summarized clinical evidence for BoNT-A action beyond neuromuscular junctions and muscle spindles

Clinical observations not explainable by theory of exclusively peripheral BoNT-A action include long or short lag period between BoNT-A injections and clinical improvement. Within a few hours following intramuscular injections of BoNT-A, there is an observable alteration in synaptic exocytosis. This manifests as a reduction in the frequency of spontaneous neurotransmitter release from presynaptic nerve terminals, specifically leading to a decrease in the frequency of miniature endplate potentials (MEPPs) (190,191). Decreased action of neuromuscular junctions is visible after 2 days post BoNT-A injections, with a maximal effect 21 days post BoNT-A (192). But clinical improvement can be seen sometimes in a merit of hours and days, and in some cases of torticollis, they require longer latency periods e.g. 6 weeks (193). It appears that BoNT exert its beneficial effects in two phases of clinical response. First phase take place in a period within few days post injections and late response, seems to take from 1 to 6 weeks post BoNT-A. This late beneficial response is hard to explain by only peripheral synaptic silencing, and it is suggesting an additional mechanism of action in exertion of therapeutic BoNT-A effect. Non-injected, distant muscles from injection site may also be affected after local muscle injection (194,201). BoNT-A injection around the eyes for treatment of Meige's syndrome can decrease lower facial involuntary movements (94), possibly due to plastic changes and central BoNT-A action. However, a local diffusion or systemic distribution of injected toxin may also occur, causing well known local side effects (e.g. difficulty in swallowing after BoNT-A injection into cervical muscles), and subclinical electromyographic changes in distant muscles characterized by jitter (variation of the time interval between the two action potentials of a given motor unit (naći reference) due to systemic distribution of BoNT-A. Moreover, a whole-body relaxation was present after BoNT-A injection in one leg in a child patient with dystonic cerebral palsy, possibly due to overtly high total dose (196).

One of the primary beneficial effects of applying BoNT for spasticity and dystonia is inducing muscle weakness, which reduces the severity of muscular spasms. However, BoNT-A also shows a true antispastic effect, not decreasing only severity but also the frequency of muscular spasms, as shown in patients with blepharospasm and torticollis (90,197–199), which also suggest a BoNT-A effect beyond simple paralysis of neuromuscular junction. There is currently an absence of connection between the actual peripheral muscle weakness and the clinical improvement, which could also be explained by the uncharacterized central action of the toxin. For example, patients with existing muscle weakness complain about persistent muscle spasms in the treated muscle, along with subsequent discomfort, which persist alongside remaining weakness, thus, in demand of shorter interval between the treatments despite significant residual blockage of NMJs (192). On the contrary, patients may experience beneficial effects months after the present muscle weakness disappears (188,200) meaning that BoNT-A effects persist much longer then its peripheral neuroparalytic action. Mazzocchio et al., (201), reported beneficial antispastic effect of BoNT-A in spite of the reduced presence of NMJ blockage. Furthermore, there is evidence indicating an enhancement of function in muscles that act as antagonists to the injected muscle (202,203).

As mentioned before, discomfort and pain are usually the main cause of seeking clinical intervention in patients with dystonia (204). High proportion of patients feel alleviation of cervical tension and tenderness after BoNT-A treatment (193,94). Similar discomfort alleviation is present also in patient with blepharospasm, as reduced burning and itching of the eyes after BoNT-A injection (205). Moreover, BoNT-A has showed as effective remedy in decreasing sensory symptoms of central origin such as sensory component of tics (206) and the inner restlessness in a patient with tardive akathisia (207).

Cortical effects following peripheral BoNTs treatment in humans were demonstrated in many functional studies using neurophysiological techniques. Naumann and Reiners suggested that BoNT injections can modify the afferent input coming from the injected muscles and modulate the abnormal central motor pattern involved in focal dystonia, by the study of long-latency reflexes (LLRs) in control and BoNT-A treated patients (208). Afferent peripheral inputs on the cortex were studied by Kanovsky et al. by recording the somatosensory evoked potentials (SEPs) evoked by electrical stimulation of peripheral nerve trunks (209). The precentral component of SEP appears to mirror the activation of a functional loop involving the cortico-subcortical-cortical circuit, which includes the basal ganglia, premotor, and supplementary

motor areas. Consequently, the authors proposed that their observations might indicate alterations in precentral cortex excitability resulting from the modulation of spindle afferent input induced by BoNT. Similar results were obtained in BoNT-A treated patients suffering from hemiplegic cerebral palsy with spasticity (210). This SEP improvement after BoNT injection has been recently confirmed in a study performed in children with spastic diplegic cerebral palsy (211). Changes in cortical organisation of different areas after BoNT injections has also been reported (212). The alterations observed in the primary motor cortex of individuals with dystonia could potentially result from abnormal sensory inputs, which BoNT-A injections may temporarily influence.The same research team illustrated a reversible restructuring of the hand motor cortical map following BoNT-A injections in patients with cervical dystonia (213) and primary writing tremor (214). By employing paired-pulse transcranial magnetic stimulation (TMS) protocols, researchers noted changes in intra-cortical inhibitory mechanisms subsequent to BoNT injections among patients experiencing upper limb dystonia (215,216). Potential changes in cortical activation patterns induced by BoNT-A activation were investigated by positron emission tomography (PET), which showed heightened activity in striatum and non-primary motor areas in dystonia and during voluntary movements, alongside decreased activity in the primary motor cortex (217).

In a study involving individuals with hemiplegia and chronic distal arm spasticity following an ischemic stroke impacting the motor cortex (218), a notable correlation emerged between clinical improvement and a reduction in activation within the posterior cingulate/precuneus region following BoNT treatment. The authors propose that changes in cortical reorganization following BoNT treatment might result in a more targeted activation of regions affected by stroke, potentially leading to a reduction in the activation of previously hyperactivated areas, such as this associative region which typically shows increased activation after a motor stroke.

Nevrly et al. (219) described a notable rise in fMRI activation in response to finger movement across various brain regions, encompassing both bilateral (primary and secondary somatosensory cortex, superior and inferior parietal lobule, supplementary motor and premotor cortex, anterior cingulate cortex) and contralateral (primary motor cortex) areas . Additionally, ipsilateral activation was observed in the thalamus, insula, and putamen. Changes in cerebellar activation after spasticity treatment with BoNT-A were also observed by Chang et al. and Hok et al., which presented evidence supporting the modulation of cerebello-cortical connectivity in cervical dystonia patients undergoing treatment with BoNT-A (220, 221). Furthermore,

findings from these and additional studies (222,9) suggest that the central effects triggered by peripheral BoNT-A injection go beyond merely impacting the cortical and subcortical representations associated with the treated muscles; they also extend to circuits involved in controlling other areas of the body affected by the treatment.

It is suggested that sustained clinical benefits from long-term BoNT-A treatment may impact plastic changes in motor cortex output following the reorganization of the entire synaptic circuitry. Alteration in cortical plasticity after BoNT-A treatment in patients with cervical dystonia has been reported previously (223). One month after BoNT-A injections into neck muscles, the heightened typical dystonic response to paired associative stimulation in hand muscles was alleviated. This reduction correlated with improvements in cervical dystonia posture and pain, indicating that alterations in cortical hand area plasticity likely stem from changes in afferent input at distant sites of BoNT-A injection. These findings also imply an added cortical effect of BoNT. In contrast to these observed plastic changes in adults, there is no indication of plastic brain changes following BoNT treatment in children (224).

1.5. Central effects of BoNT-A

1.5.1. Insights from models evidencing BoNT-A direct central interaction with sensory and motor systems

BoNT-A interaction with sensory and motor systems has been found to involve spinal cord and brainstem circuitry, and cleaved SNAP-25 was identified in the motor regions adjacent to the primary motor neurons, as reported by Antonucci et al., Restani et al., Matak et al., and Koizumi et al. (79,83,225,226). Rosales et al. and Giladi strongly emphasized the beneficial effects of BoNT-A solely on the levels of extrafusal and intrafusal muscles, indirectly leading to central reorganization (as explained in 1.4.4.) known in dystonia as "sensory trick" (227,184). Other experiments suggested possible effect of i.m. BoNT-A on intraspinal recurrent inhibition (Renshaw inhibition). Morphological and physiological investigations in rats have yielded evidence indicating a decrease in motoneuron input to Renshaw cells following peripheral injection of BoNT-A (228–167).

Nevertheless, a study involving cats demonstrated that i.m. administration of BoNT-A had no discernible impact on the discharge pattern of individual Renshaw cells (230). A separate study revealed a reduction in recurrent inhibitory activity subsequent to muscle injection of BoNT-A, leading to heightened excitability of motoneurons (231). The observed outcomes were linked

to the influence of BoNT-A on the inhibitory synapse between Renshaw cells and α-motoneurons (231). Investigations involving individuals with lower limb spasticity similarly suggest a decline in recurrent inhibition strength following i.m. administration of BoNT-A (201). Functionally, spinal motoneurons in cats treated with BoNT-A injections into the medial gastrocnemius muscle display variations in rheobase current, input resistance, time constant, and duration of the after-hyperpolarization (232). Metabolic changes have been observed in rat hypoglossal motoneurons after i.m. BoNT-A (233). Disruption of synaptic transmission leads to alterations in the expression of multiple genes in spinal motoneurons (234). Moreover, notable decreases in the density of gephyrin, a protein responsible for clustering glycine receptors, on the membrane of abducens motoneurons in cats have been documented following injection of BoNT-A into their respective target muscle (235). Multiple research endeavors conducted by Delgado-Garcia's team (235) have illustrated alterations in abducens motoneurons that are contingent on the dosage of BoNT-A administered into the lateral rectus muscle of cats. Pastor et al. showed that sevelar days after i.m. BoNT-A excitatory and inhibitory synaptic transmission to abducens motoneurons is strongly affected (237). Furthermore, motoneurons exhibit alterations in their firing patterns, exemplified by the emergence of a notably reduced discharge rate (235). These modifications coincide with ultrastructural changes, including synaptic stripping observed at the level of motoneuron cell bodies (248). It is important to highlight that thes alteration were found to be dose-dependent (236,235). At the spinal level, the inhibition of motoneuronal functionality, with reflex inhibition and suppression of input from afferent fibers, results in various effects on CNS (201). Marchand-Pauvert et al. reported reduction in spinal inhibition in patients affected by spastic leg paresis, developed after ischemia, hemorrhage or head injury (238). After BoNT-A injection into the triceps surae muscle, they observed a decrease in the inhibition of the vastus H-reflex by the posterior tibial nerve. They hypothesized that this reduction in spinal inhibition might stem from alterations in the recurrent inhibitory pathway. The decline in recurrent inhibition, attributed to peripherally administered BoNT-A, seems to result from axonal transport and the blockade of the cholinergic synapse between motoneuron recurrent collaterals and Renshaw cells. Similar results related to reciprocal inhibition of distant muscles were obtained by Aymard et al. (239).

1.5.2. Peripherally injected BoNT-A is axonally transported to spinal cord similar to TeNT

For BoNT-A to reach synapses located at a distance, it must first be loaded onto organelles moving retrogradely, evade degradation within the cell soma, be released at postsynaptic sites, undergo another round of uptake, and ultimately be released into the cytosol to exert its proteolytic effects, which is very similar to TeNT retrograde axonal transport, which was in detailed explained earlier (1.3.3.).

Using animal model, retrograde transport of BoNT-A was showed long ago. I125 labeled botulinum toxin was transported to the motoneurons in the spinal cord of the rat (240,241). Early research of BoNT-A postulated presence of changes at the level of alpha moto neuron after toxin application (235).

In compartmentalized motor neuron cultures, Restani et al. (82) demonstrated that the Hc domain of both TeNT and BoNT-A is transported via the same class of axonal organelles. These organelles were also observed to contain the neurotrophin receptor p75 (82), which is transported within axons via microtubules (242). The importance of microtubule-dependent transport for BoNT-A was confirmed also by in vivo studies. Administration of colchicine, which is a microtubule-depolymerizing agent, inhibits the distant effects of BoNT-A (79,83,84). Another important point is that vesicles carring BoNT-A retrogradely to neuron soma does not undergo acidification (82,243). This process is crucial for trapping the neurotoxin within the vesicle's interior, preventing the L chain from translocating into the cytosol, and maintaining the toxin's integrity during its traffic. The discovery that TeNT and BoNT share the same axonal carriers might not be entirely unexpected. Schmieng et al. (242) demonstrated that distinct ligands can employ shared axonal carriers within motor axons, and be sorted to different destinations within the cell body. TeNT and neurotrophins, such as brain-derived neurotrophic factor (BDNF), are specifically targeted to the dendritic compartment of motoneurons. Subsequently, they are transported via transcytosis to afferent synapses (244), highlighting a distinct localization pattern. However, transcytosis is a highly specific process and, after toxin's transport to cell body, TeNT is specifically entering in the cytosol of inhibitory neuron terminals. Similar process has been observed with BoNT-A following retrograde transport in the rat visual system (79,245). Following injections into the optic tectum, catalytically active BoNT-A undergoes retrograde transport along ganglion cell fibers. It then

cleaves its target, SNAP-25, within cholinergic amacrine cells that interact with retinal ganglion cells. These ganglion cells' axons were initially exposed to the neurotoxin in the tectum (79). This shows the core of transcytosis specificity discussed before, as Restani et al., (82) displayed that only particular types of retinal terminals contain cleaved SNAP-25. Moreover, it was also showed that BoNT-A preferentially target excitatory glutamatergic synapses in hippocampal neurons (246). It is also possible that BoNT-A, following retrograde transport to motoneuronal soma, might target the axonal collateral synapse impinging onto the inhibitory Renshaw cells by anterograde transport from the soma. Immunohistochemical analyses have shown co-localization of the cholinergic marker choline acetyltransferase and BoNT-A-truncated SNAP-25 in the spinal cord following i.m. administration of the neurotoxin (83). The axonal transport of BoNT-A has been observed to extend propagation to two synapses away from the injection site. This provides evidence that BoNT-A undergoes specific transcytosis while retaining its enzymatic activity (10,245).

Furthermore, BoNT-A anterograde trafficking was also demonstrated in vitro studies on central neurons employing microfluidic devices (247). Koizumi et al. 2014 detected axonal retrograde transport of BoNT-A, observing cl-SNAP-25 presence in both ipsilateral and contralateral ventral and dorsal horns in a rat model after very high i.m. peripheral BoNT-A dose (50 U/kg). This occurred after ipsilateral injection in gastrocnemius muscle of two distinct subtypes of BoNT-A, specifically A1 and A2. Serotype A1 was found to be much more effective than serotype A2 in the transport (either axonal + trans-synaptic or systemic) to the contralateral ventral horn of the spinal cord.

Retrograde axonal transport of BoNT-A showed as significant mode of action for antinociceptive effects of BoNT-A. Retrograde transport of BoNT-A in sensory neurons to dorsal horn of spinal cord was showed after injection in the hindpaw of the rat (248). Matak and Lacković demonstrated in a series of experiments that central antinociceptive effect of BoNT-A alleviates pain in different animal models (249–251). Findings were also followed by determination of cleaved SNAP-25 in central areas (medullary dorsal horn of trigeminal nucleus caudalis; spinal cord) after peripheral BoNT-A administration, respectively (83, 81).

2. HYPOTHESIS

The intensity and duration of the beneficial effect of i.m. administered botulinum toxin in experimental local spasticity in the rat, in addition to action at the level of muscle nerve endings, also depends on its direct action at the level of central motor region.

3. AIMS OF THE RESEARCH

General aim:

To examine the role of the central action of intramuscularly injected botulinum toxin type A in gastrocnemius muscle, on the incidence and duration of peripheral flaccid paralysis in a rat, and the duration of antispastic beneficial effect in a model of local muscle spasm, evoked by i.m. application of tetanus toxin (TeNT).

Specific aims:

1. Histological and immunohistochemical characterisation of the sites and course of botulinum toxin type A action at the muscle level in the extrafusal and intrafusal nerve endings of motor neurons.
2. Immunohistochemical characterization of the effect of botulinum toxin type A at the level of secondary spinal cord synapses.
3. Behavioral and electrophysiological characterization of the effects of botulinum toxin type A on motor behavioral and electromyographic parameters in non-spastic animals and animals with TeNT-evoked local muscle spasticity.

4.   MATERIALS AND METHODS

4.1.   Animals and treatments

4.1.1.   Animals

Adult male Wistar Han rats (University of Zagreb School of Medicine, Croatia), 3-6 months old and weighing around 300 g at the beginning of the experiment, were used. Three rats per home cage were kept under a 12-hour light/ dark cycle and supplied with cardboard play tunnel enrichment. Access to food and water was *ad libitum*. All procedures involving animals and animal care were carried out following the European Union Directive (2010/63/EU), the ARRIVE guidelines 2.0: Updated guidelines for reporting animal research (252) and approved by the institutional review board (University of Zagreb School of Medicine) and Croatian Ministry of Agriculture ethical committees (permit no. EP 229/2019) in accordance with the current Croatian Act (The Animal Protection Act (NN 102/17) and the Ordinance on the protection of animals used for scientific purposes (OG 55/13 with amendments 39/17 and 116/19).

To ensure consistency in parameters susceptible to variations such as weight and dosing, only the male rats were used for the experiments, as these parameters can be affected by differences in sexual dimorphism, e.g. muscle size, overall body weight and nerve length. This approach aimed to minimize possible systemic effects of injected BoNT-A due to the uneven ratio of injected dosage and weight.

4.1.2.   BoNT-A injections

For i.m. injections of BoNT-A (INN: Clostridium botulinum type A neurotoxin complex, Allergan Inc., Irvine, CA, USA), different doses were employed: 1, 2, or 5 international units per kg (U/kg), with each unit consisting of 48 pg of 900 kDa toxin complex. Animals were briefly anesthetized with isoflurane (Forane, Abbott Laboratories, Abbott Park, IL, USA), using 5% for induction and 1–1.5% for maintenance with a gas anesthesia system for small animals (Ugo Basile, Varese, Italy). BoNT-A was injected into the right gastrocnemius in a volume of 20 µL, divided into the lateral and medial belly of the gastrocnemius muscle (10 µL each). A 50 µL Hamilton syringe was used for i.m. (i.m.) injections, as previously described in (13) and Šoštarić et al., 2022; Appendix I.

For intraneural injections of BoNT-A into the sciatic nerve, animals were deeply anesthetized with an intraperitoneal (i.p.) mixture of ketamine (Ketamidor® 10%, Richter Pharma AG, Wels, Austria; 70 mg/kg i.p.) and xylazine (Xylased® Bio, Bioveta, Ivanovice na Hané, Czech Republic; 7 mg/kg i.p.). Fur was trimmed at the location of the right thigh and sanitized with 70% ethanol. An incision was made at the lateral mid-femoral level, followed by blunt dissection of the thigh muscles and exposure of the sciatic nerve. A Hamilton syringe needle (0-10 μl) (Cat. No. #701, Hamilton, Bonadouz, Switzerland) was used for BoNT-A injection into the nerve trunk, as previously described (249). The needle penetrated the epineurium, and, following the 1 cm advancement along the nerve, the 2 μl volume of BoNT-A (2 U) was carefully injected into the trunk to evoke visible bulging of the nerve. To allow for BoNT-A diffusion the needle was kept inside the nerve in the same place for 3 minutes, and then slowly withdrawn. Then, the nerve was retracted back to its natural position (Šoštarić et al., 2024; Appendix II), and the same procedure was performed at the contralateral leg.

4.1.3. BoNT-A neutralizing antitoxin injection

Twenty-four hours post-BoNT-A injections, rats were administered intrathecally (i.t) or i.m. BoNT-A-neutralizing equine antitoxin (National Institute for Biological Standards and Control, NIBSC code 14/174, Potters Bar, United Kingdom) or horse serum (Gibco, ThermoFisher Scientific, Waltham, MA, USA) as a control treatment. For i.t. injections of BoNT-A neutralizing antitoxin, animals were anesthetized with isoflurane (5% induction, 2% maintenance), as previously explained for BoNT-A i.m. injections. The i.t. injection into the spinal canal was performed at the level of the cauda equina in a total volume of 10 μl per animal (5 μl of antiserum or horse serum diluted in 5 μl of saline) and inserted by a 28G x ½" tip of a 0.5 ml tuberculin syringe between lumbar vertebrae (L4-L6) (13), (Šoštarić et al., 2022; Appendix I, Šoštarić et al., 2024; Appendix II). Successful entering and injection of the lumbar spinal canal was confirmed by brief and sudden movement of hindlimb or tail of the injected animal. On the right picture (B) rat was injected with BoNT-A neutralizing antitoxin, or horse serum administered as a control treatment. A small incision of the skin was made at the lumbar part of the rats back to expose midline junction of the paraspinal muscles and tuberculin syringe needle was administered between the L4-L6 lumbar vertebrae into the spinal canal at the level of cauda equina. After observation of brief tail or hindlimb movement, antitoxin was slowly injected into the lumbar space, and the needle was retracted 10-15 seconds afterwards.
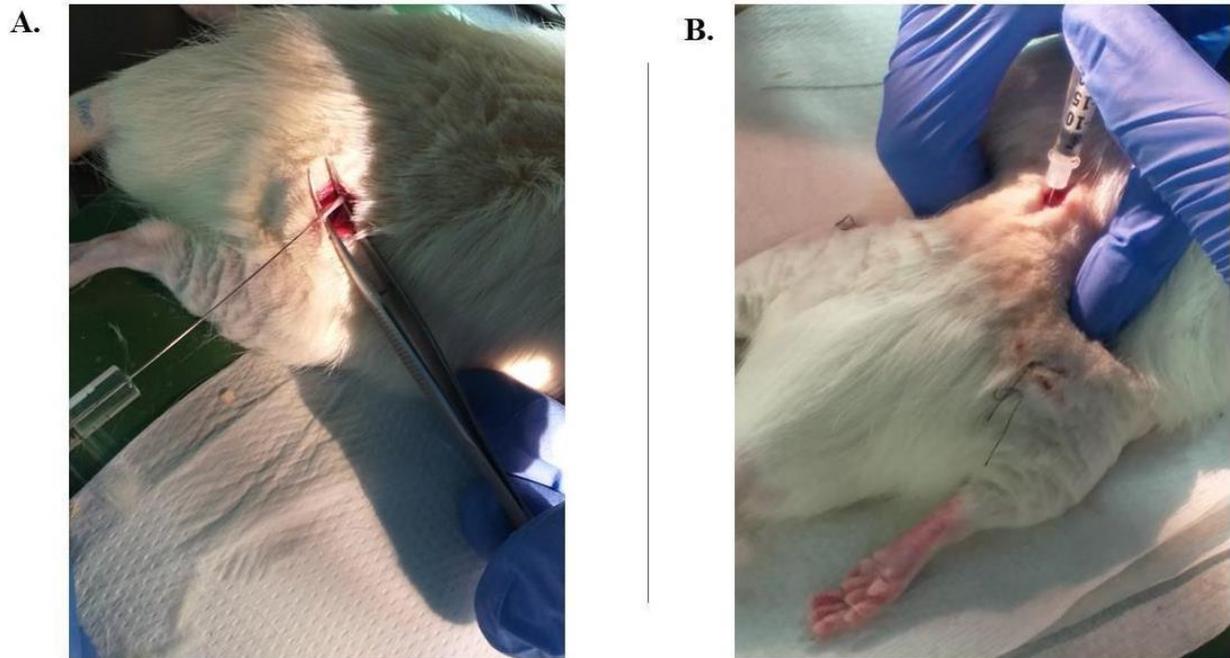
Figure 5. The process of intraneural injection into the sciatic nerve (left) and intrathecal injection into the lumbar part of the spinal cord (right).

4.1.4. α-latrotoxin injection

For α-latrotoxin injections, animals were anesthetized with isoflurane as previously explained. α-Latrotoxin (Alomone; Jerusalem, Israel) was diluted in saline vehicle and injected into the gastrocnemius muscle of the right hindlimb, either one day before BoNT-A i.m. injections or 3 days post BoNT-A. Latrotoxin was injected in the dose of 4 µg per 20 µl, divided equally to 4 injection sites inside the 4 quadrants of the lateral and medial belly of the gastrocnemius muscle (5 µl each).

4.1.5. TeNT injection

For injections of tetanus neurotoxin (TeNT, Sigma, St. Louis,MO, USA) into the gastrocnemius muscle of right hindlimb, animals were anesthetized with isoflurane (13), (Šoštarić et al., 2022; Appendix I, Šoštarić et al., 2024; Appendix II). TeNT (1.5 ng) was diluted in saline vehicle containing 2% bovine serum albumin (BSA) and injected as a total of 10 µl, divided into lateral and medial bellies of the right gastrocnemius (5 µl each site). The dose was chosen based on the previous experiments employing non-systemic toxin doses (13,253).

For TeNT injections in the whisker pad, animals were anesthetized with isoflurane, and a syringe was used to employ 10 µl of diluted TeNT (50 pg in 0.9% NaCl 0.2% gelatin), as previously described (Fabris et al., 2023; Appendix IV).

Figure 6. Injection into a whisker pad of the rat. *Rat was briefly anesthetized with isoflurane (5% induction) and injected with a syringe into a right whisker pad. Ten µl of tetanus toxin (TeNT), was slowly injected in the WP, while using forceps to pinch and stabilizethe skin surface for injection.*

4.1.6. Pharmacological *in vivo* treatments

In the first experiment, we assessed the dose response of early and late BoNT-A antispastic action. The animals were assigned randomly to 5 experimental groups (N=8/group) and administered i.m. tetanus neurotoxin (1.5 ng) into the gastrocnemius muscle to evoke spastic paralysis of the right lower hindlimb as a control treatment animals received saline vehicle containing 2% BSA i.m. into the right gastrocnemius. Once spasticity developed, and

peaked on day 7 post TeNT injections, animals were injected i.m. with different doses of BoNT-A (1, 2 and 5 U/kg) in the gastrocnemius, of the spastic hindlimb, or with saline. Motor behaviour tests were performed before treatments, on days 3 and 7 post TeNT, and after BoNT-A injections on day 8 and 10 post TeNT (equivalent to days 1 and 3 post BoNT-A injections). Subsequent measurements were taken weekly until day 56 post-TeNT/49 post-BoNT-A. After the animals recovered from flaccid paralysis post BoNT-A injections, we re-injected animals with TeNT (1.5. ng) in the right gastrocnemius, to assess late BoNT-A antispastic effects. Measurements were then repeated on days 3, 7, 12, and 19 post-second TeNT injection (equivalent to days 52, 56, 61, and 68 post-BoNT-A) (Figure 7).

Figure 7. The time course and schematic representation of experimental treatments. *Intramuscular (i.m.) tetanus neurotoxin (TeNT) and i.m. botulinum toxin type A (BoNT-A) and motoric test in rats were performed. The numbers above the timeline indicate experimental days following the i.m. TeNT and BoNT-A treatment. BBB-Basso Beattie Bresnahan locomotor scale; DAS-digit abduction score. The figure was created with Biorender.com (accessed on 24/02/2024).*

In a separate experiment, we assessed the role on central action and transcytosis of i.m.ly administered BoNT-A and its late antispastic activity. Animals (N = 6/group) were injected with BoNT-A (5 U/kg) or with saline (control treatments), in the gastrocnemius to evoke flaccid paralysis and muscle weakness of the right hindlimb. The next day (24 hours post BoNT-A i.m. injections), animals were injected with BoNT-A neutralizing antitoxin (10 i.u.) in the lumbar part of the spinal cord, to prevent possible central transcytosis of BoNT-A (figure x). On day 50 post BoNT-A injections, animals were re-injected in the right gastrocnemius with TeNT (1.5 ng) to evoke local spasticity, and motor measurements to assess late antispastic activity of BoNT-A were performed on day 3,7,12 and 19 post TeNT injection (equivalent to days 53, 57, 62 and 69 post-BoNT-A).

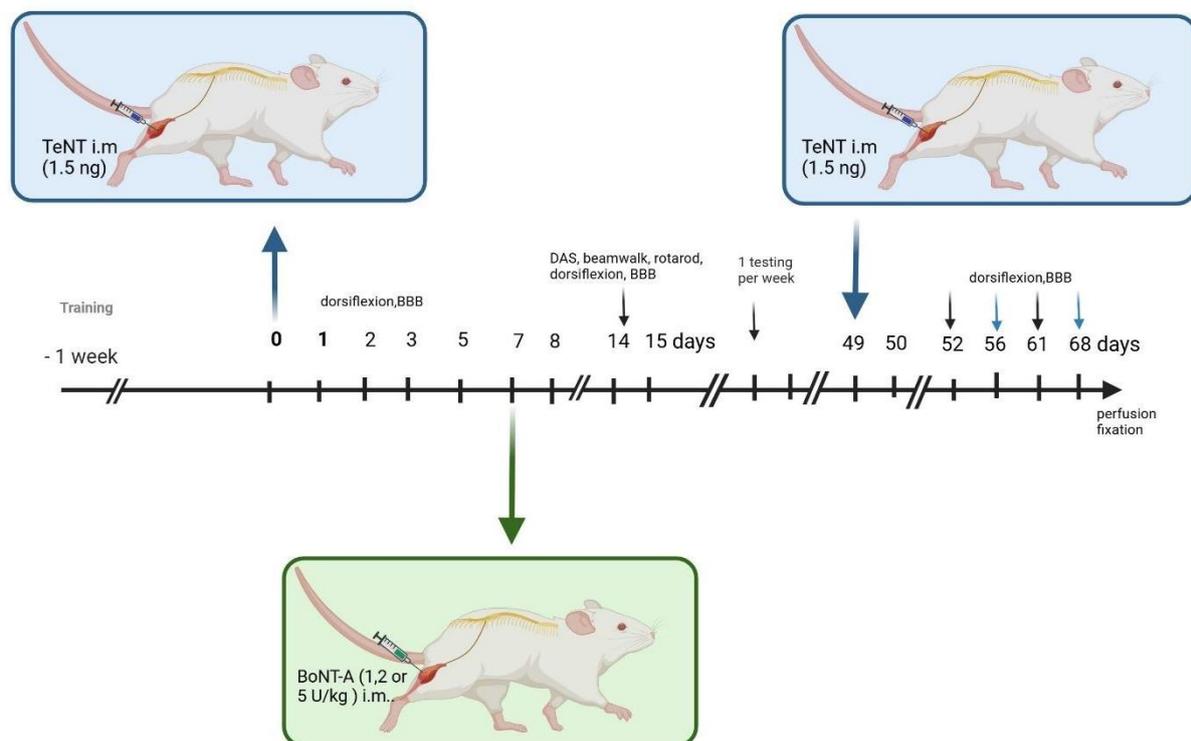**Figure 8. The time course and schematic representation of experimental treatments.**
Intramuscular (i.m.) botulinum toxin type A (BoNT-A), BoNT-A neutralizing antitoxin injected intrathecally (i.t.) in the lumbar part of cauda equina and i.m. tetanus neurotoxin (TeNT) in the

right gastrocnemius were performed. The numbers above the lines indicate days following stated treatments. BBB- Basso Beattie Bresnahan locomotor scale. The figure was created with Biorender.com (accessed on 24/02/2024).

In another experiment, we assessed BoNT-A action on normal muscle tone and function and its long-term antispastic effects. Animals were assigned randomly to different experimental groups (N=6-8/group) using block randomization. BoNT-A (2 U/kg) was injected in the sciatic nerve of both hindlimbs to induce muscle weakness of the lower leg. Next day, after 24 hours, BoNT-A neutralizing antitoxin (5.i.u./10 μL; or 50 % saline-diluted horse serum serving as control) was injected into the lumbar part of the spinal canal to prevent central action of BoNT-A mediated by spinal transcytosis. To assess BoNT-A action on normal muscle tone and motoric function, motor measurements were performed before treatment, and after treatment every seven days until animals fully recovered. On day 62 post BoNT-A, animals were re-injected unilaterally with TeNT (1.5 ng) in the gastrocnemius muscle to evoke local spasticity of right hindlimb. Long-term antispastic effects of BoNT-A were assessed with different motoric and behaviour tests on day 3, 7, 12 and 15 post TeNT injection (equivalent to 65, 69, 75 and 77 post BoNT-A) as evident on Figure 9.
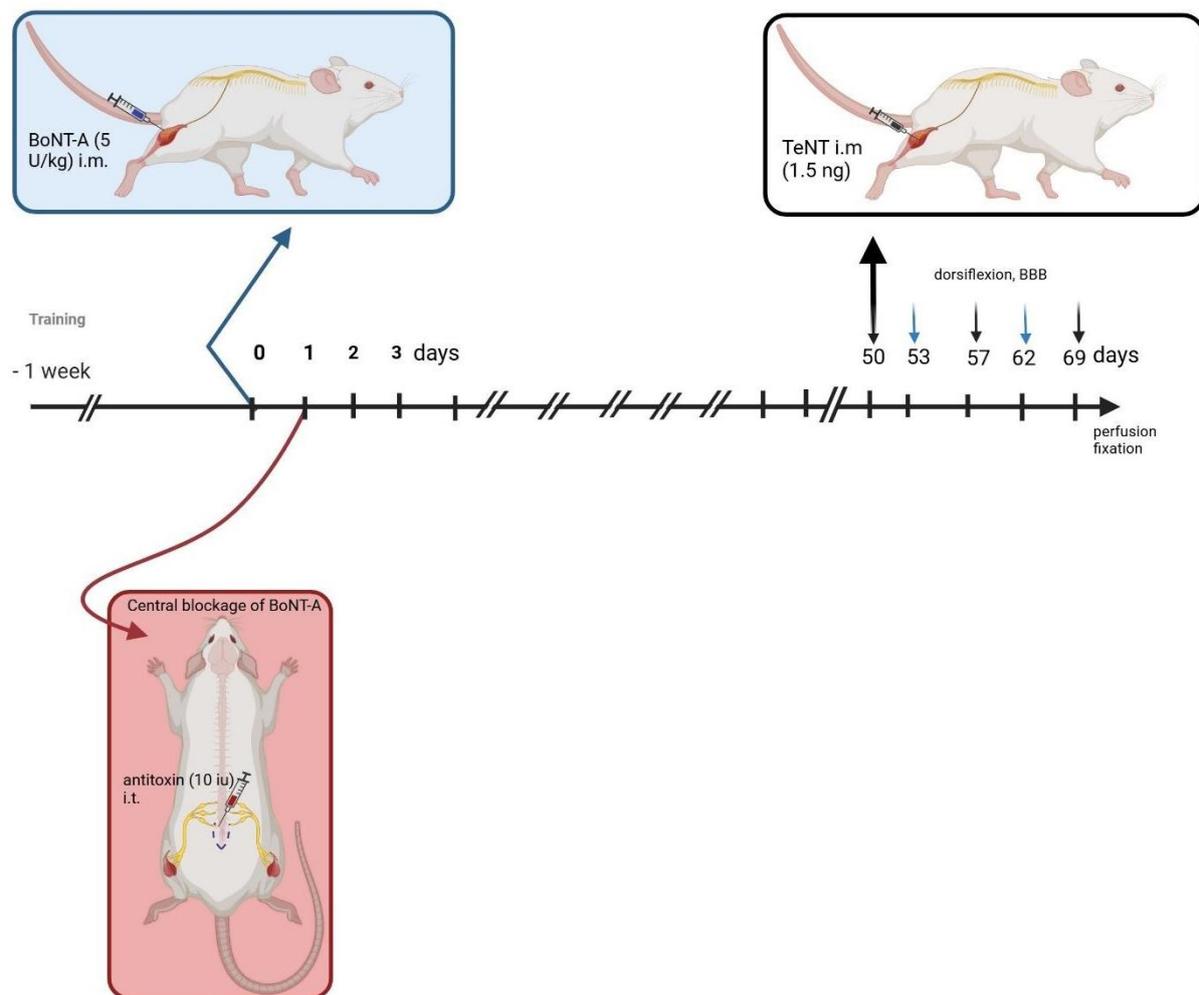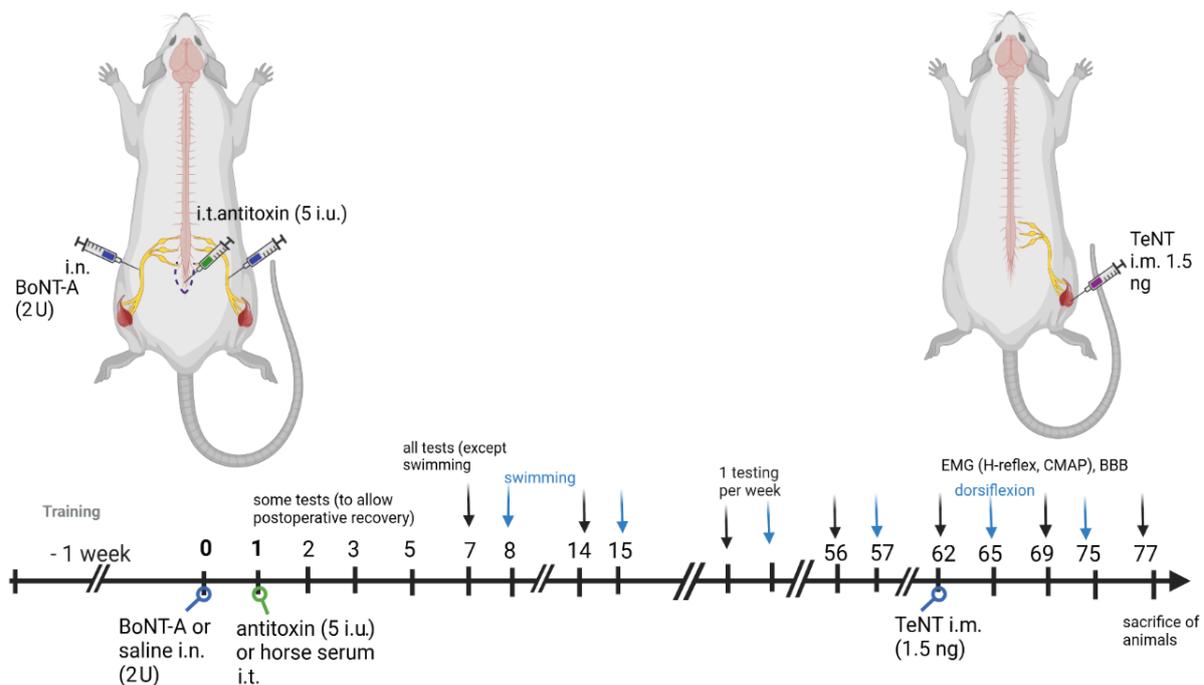
Figure 9. The time course and schematic representation of experimental treatments. *Bilateral intraneural (i.n.) botulinum toxin type A (BoNT-A), intrathecal (i.t.) BoNT-A-neutralising antitoxin and unilateral intramuscular (i.m.) tetanus toxin (TeNT), and functional behavioural motor testing in rats were performed. The numbers above the timeline indicate experimental days following the i.n. BoNT-A treatment. H-reflex; Hoffmann's monosynaptic reflex; BBB, Basso Beattie Bresnahan locomotor scale. The figure was created with Biorender.com (accessed on 22/09/2023). (Šoštarić et al., 2024; Appendix II)*

In the last experiment, we aimed to assess the relative contribution of peripheral and central effects of BoNT-A on normal and spastic muscle by employing α-latrotoxin. Animals were randomly assigned to four groups (N=6-8/group). Latrotoxin induces rapid neuromuscular junction destruction caused by calcium influx into the presynaptic nerve terminal, followed by fast axonal regeneration and motor recovery (254). In this experiment, we administered latrotoxin prior to and post BoNT-A i.m. injections to assess the action of BoNT-A on peripheral motor terminals. The gastrocnemius muscle of the right hindlimb was injected with latrotoxin (4 um) or saline (as a control treatment) one day prior to i.m. BoNT-A injections (5 U/kg), in order to destroy neuromuscular junctions and thus reduce the peripheral entry of

44

BoNT-A. To abolish already established peripheral effects of BoNT-A, latrotoxin was injected i.m. 3 days post BoNT-A injection. Motoric tests for assessing local motor function and EMG measurements were repeatedly performed to monitor motor recovery. After the animals substantially recovered on day 80, all treatment groups were reinjected into the same gastrocnemius with TeNT (1.5 ng) to induce local spastic paralysis of the right hindlimb. Recovery from spastic paralysis was assessed by ankle dorsiflexion resistance tests and monosynaptic reflex excitability (Hmax/Mmax) measurements on days 0, 7, 14, 21, and 28 post TeNT (equivalent to days 80, 87, 94, 100, and 107 post BoNT-A i.m. injection), as noted in Figure 10 (Unpublished data).
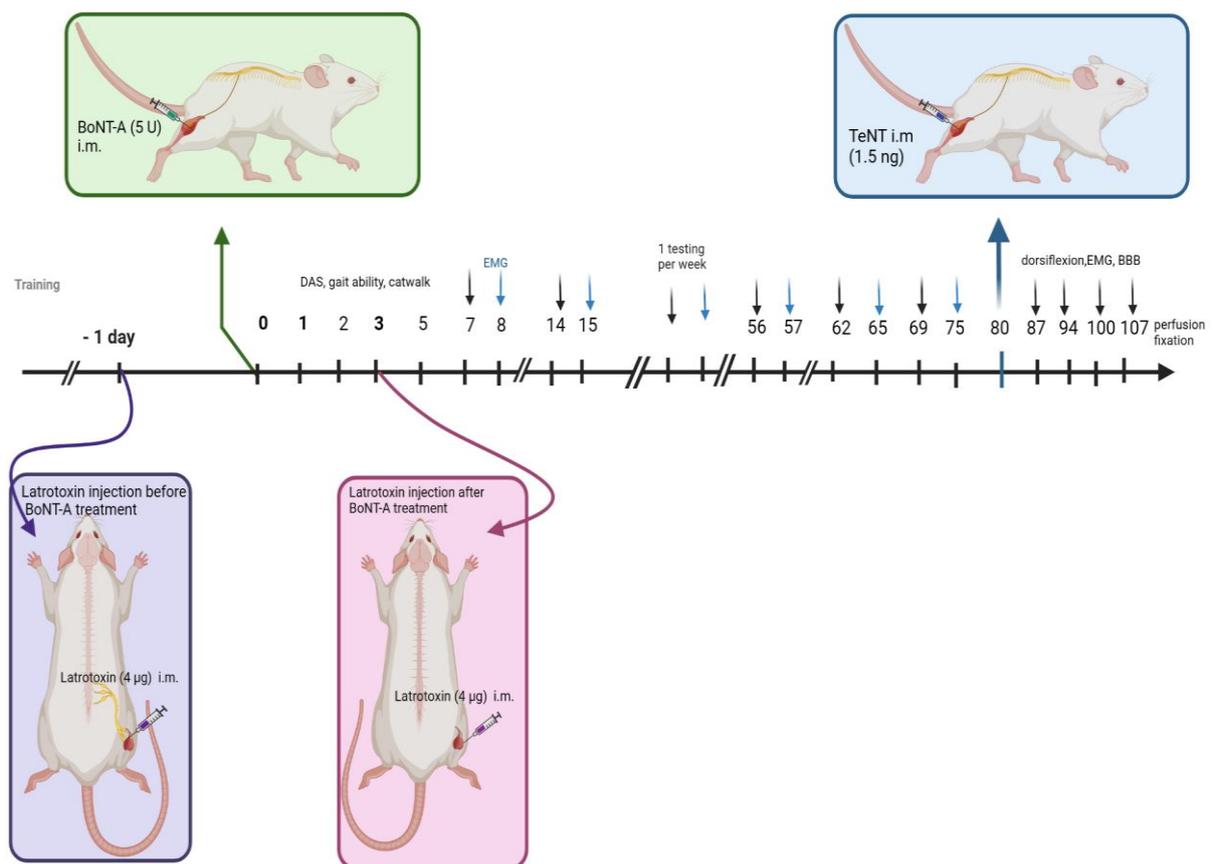
Figure 10. The time course and schematic representation of experimental treatments.

Unilateral intramuscular (i.m.) injections of latrotoxin, BoNT-A and TeNT into the right gastrocnemius, and functional motor testing in rats were performed. The numbers above the timeline indicate experimental days after named treatments. DAS- digit abduction score, EMG-electromyographic measurements; BBB- Basso Beattie Bresnahan locomotor scale. The figure was created with Biorender.com (accessed on 24/02/2024).

4.1.7. Isolation and treatment of primary culture of cerebellar granules neurons

Cerebellar granules neurons (CGN) were isolated from 4-5 days old rat pups following the procedure described by (255). Cerebellar part of the pup's brain were collected and mechanically disrupted in order to facilitate enzymatic degradation with trypsin in the presence of Deoxyribonuclease I (DNase I). Plastic well plates or cover glasses were used as a plating surface for dissociated cells, with planted densities counted as 4×10^5 or 2×10^5 cells per well. The cultures were then maintained for a minimum of 6 days at 37°C in a 5% CO_2 atmosphere in Basal Medium Eagle (BME) supplemented with 10% fetal bovine serum, 25 mM KCl, 2 mM glutamine, and 50 µg/mL gentamicin. On 18-24 h post seeding, cytosine arabinoside (10 µM) was added to the culture medium to prevent the proliferation of non-neuronal cells. Seven days after preparation, CGN cells were treated with different doses (Table 3.) of BoNT-B, BoNT-D, BoNT-G or TeNT for 12 hours in a complete culture medium.

Table 3. Toxin doses used for treatment of cerebellar granule neurons (CGN)

Treatments	TeNT	BoNT-B	BoNT-G	BoNT-D
Doses	0.05 pM	0.005 nM	5 nM	0.025 pM
	0.5 pM	0.05 nM		
	5 pM	0.5 nM		
	50 pM	5 nM		

4.2. Behavioural and neurophysiological motor assessment

4.2.1. Motor assessment of local muscle weakness and normal locomotor functions

4.2.1.1. Assessment of local muscle weakness: digit abduction score and gait ability

The local muscle weakness of the lower leg upon different types of BoNT-A injections resulted in impairment of the motor use and appearance of the hind paw toes during separation from the ground (toe spreading reflex), and its appearance and functional use during ground

contact. By unilaterally observing each hindpaw, we monitored the onset and recovery of motor function of the lower leg.

The DAS score is based on scoring system that evaluates impairment of the toe-spreading reflex, a normally occurring ability to spread toes when the animal is lifted from the ground. Scores are given based on toe abduction ranging from 0-4. Numbers are defined as follows: 0 = separation of all toes; 1 = separation of four toes; 2 = separation of three toes; 3 = separation of two toes; and 4 = no toe separation (256) (Šoštarić et al., 2022; Appendix I Šoštarić et al., 2024; Appendix II). Gait ability assessment is based on a scoring system that evaluates the appearance of the hindlimb and its use performance of gait, climbing and slope walking, with the sum of 5 individual parameters indicative of lower leg muscle weakness (257,258). The total score ranging from 0-10 was based on the sum of scores from the following parameters: 1) hindlimb abduction during suspension by the animal's tail; 2) the hind paw appearance during sitting on the ground; 3) hindlimb use during bipedal stance while leaning against the cage side; 4) hindlimb use while walking on a slope; 5) use of paw toes and hindlimb strength during climbing. To quantify the motor impairment for each parameter observed, the observations were scored using a scoring range from 0-2, where 0 stands for disabled and 2 for normal hindlimb use, as previously explained (Šoštarić et al., 2024; Appendix II). Each of the mentioned motor tests was evaluated independently by two observers unaware of the animal treatment.

4.2.1.2. *Assessment of locomotor functions: beamwalk, rotarod and swimming*

To assess the role of the locomotor function and coordination, and central spinal motor input after BoNT-A treatment, tests such as a narrow beam, rotarod and swimming were performed. *Narrow beam walking* – rats were trained to cross the 1 m long, 2.5 cm square cross-section wooden beam by walking from one side to the other, into the safety of a rectangular, wall-enclosed dark platform (25 cm × 25 cm × 25 cm, 10 cm × 10 cm entrance). Latency to cross the beam walk was measured and assessed as previously described (Šoštarić et al., 2022; Appendix I, Šoštarić et al., 2024; Appendix II) (259). Animals were pre-trained daily during the week preceding the BoNT-A treatment to cross the bar swiftly without stumbling, stopping, or falling.

Rotarod test assesses the duration of time that animals spent on a rotarod device constantly rotating at 13 r.p.m. Maximum trial duration was set at 180 seconds, and latency time was measured from the start of the rotation until the animals fell. Animals were pre trained to easily

maintain the balance for 3 minutes before the toxin treatment, as described previously (Šoštarić et al., 2022; Appendix I, Šoštarić et al., 2024; Appendix II).

In order to assess the *swimming performance,* individual rats were placed inside the circular swimming pool filled with water (180 cm diameter, water depth 30 cm, temperature 24 ˚C), and monitored with a wide-angle video camera (Basler AG, Basler, Ahrensburg, Germany) installed above. Values such as swimming mean and velocity were monitored and calculated during two trials, each lasting 120 seconds, for each animal during a single measurement session. The assessment was performed using video analysis software (Noldus Ethovision XT ver. 11.5; Noldus, Wageningen, Netherlands) monitoring the animal's body center position every 0.133 s (7.5 Hz) (Šoštarić et al., 2024; Appendix II).

4.2.1.3.   *Automated gait analysis*

The static and dynamic gait parameters were analyzed by automated gait aquisition and analysis system (GaitLab, ViewPoint, Lyon, France) that provides locomotor parameter specification based on rodent footsteps and body silhouette. Paw positions of freely walking rats were recorded using a high frame-rate infrared video camera (100 frames per second), positioned beneath a 125 cm long transparent glass runway with green LED lighting directed onto the sides of the walkway, illuminating the paw contact area upon contact with the surface. The rats entering the trial, should cross at least 80 cm of a walkway, constantly without halting or turning, and transverse towards the home cage. At least three successful trials, as explained, were recorded for each animal during one measurement session. The GaitLab software was used to analyze different dynamic (stance time, swing time, stride cycle etc.) and static gait parameters (stride length, mean intensity, paw area etc.) for each individual paw.

4.2.1.4.   *Electromyographic measurements of neuromuscular function and monosynaptic reflex*

For electromyographic measurements of neuromuscular paralysis and its recovery post BoNT-A injections, compound muscle action potential (CMAP or M-wave) was recorded from right gastrocnemius of anaesthetised animals (isoflurane:5% induction, 2 % maintenance). To assess monosynaptic Hoffman reflex (H-reflex) and its relation to BoNT-A antispastic activity post TeNT injections, gastrocnemius or whisker pad was recorded under the general anaesthesia induced and secured by i.p. injection of ketamine/xylazine mixture (70/7 mg/kg). Rats were

placed in a wooden box with the tail and hindlimbs protruding out, and the stimulating stainless steel needle electrodes (29 G, Cat. #. MLA1203, AD Instruments, Oxford, UK) were subcutaneously (s.c.) inserted over the sciatic notch and mid-thigh femur. The recording needle was placed just above the lateral belly of the gastrocnemius muscle, and together with the stimulating electrodes, connected to the two-channel extracellular amplifier (EXT-02B, NPI electronic GmbH, Germany) via two headstages. The reference electrode was s.c. inserted above the lateral ankle, and a ground electrode was s.c. injected into the thoracolumbar area of the back (see Figure 11). Analog signals obtained from the amplifier were digitized via a data acquisition unit (Micro1401-4, CED, UK) and then fed to a PC for both online visualization and offline analysis using Spike2 software version 10 (CED, Cambridge, UK). For CMAP measurements of the whisker pad (WP), rats were placed in a wooden box, with the head protruding out. Stimulating electrodes were placed s.c. near the area of the facial nerve. Recording and reference electrodes were inserted into the WP and under the skin at the nose tip, respectively, and a ground electrode was s.c. injected into the thoracolumbar area of the back, as described previously (Fabris et al., 2023; Appendix IV). The CMAP or M-wave is generated after stimulation of the sciatic nerve trunk, when orthodromic and antidromic depolarization is traveling via myelinated motor and sensory fibers. The sensory fibers primarily stimulated are Ia afferents that activate the monosynaptic reflex evoking the delayed Hoffman's or H-reflex of the muscle. The maximal peak-to-peak amplitudes of the M wave and H-reflex in mV (M_{max} and H_{max}) were measured by stimulation with increasing voltages, as previously described (Šoštarić et al., 2024; Appendix II, Fabris et al., 2023; Appendix IV) (253,260).

Figure 11. Positioning of needle electrodes for electromyographic recording in anesthetised rats. *Compound action muscle potential (CMAP) and monosynaptic Hoffman reflex (H-reflex) were recorded in the right gastrocnemius of the anaesthetized animal placed in a prone position inside a narrow wooden box, with the tail and hindlimb protruding out. Stimulating needle electrodes, (numbers 1 and 2), were subcutaneously (s.c.) placed above the hip and mid-thigh to stimulate the sciatic nerve. The recording needle (number 3) penetrated the skin and entered the lateral gastrocnemius muscle (2-3 mm deep). The reference electrode was placed s.c. at the lateral side of the tarsal joint (4), while the ground electrode was s.c. injected into the lumbar part of the back (5).*

4.2.2. Assessment of TeNT-evoked local spasm and associated locomotor deficits

4.2.2.1.   Resistance to ankle dorsiflexion

To measure the intensity of TeNT-evoked calf muscle spasticity, animals were assessed for passive ankle flexion resistance by employing a digital kitchen scale with a plastic platform attached to its surface. Plantar paw of calm hand-held animals lifted from the ground were gently pressed to the plastic platform on the kitchen scale. The dorsiflexion of TeNT-treated spastic hind-limb was performed to sligtly exceed the 90° tibiotarsal angle, after which the

pressure was slightly relieved until the tibiotarsal angle returned to 90°, and values in grams (g) were noted. The average of two measurements per session was calculated as previously described (13), (Šoštarić et al., 2022; Appendix I, Šoštarić et al., 2024; Appendix II).

4.2.2.2.   Basso Beattie Bresnahan locomotor scale

Gait locomotion and appearance of the hindlimb post TeNT treatment were evaluated by employing the modified Basso Beattie Bresnahan (BBB) locomotor scale, originally used to assess motor deficits after experimental spinal cord injuries (261). The BBB scale consists of scores ranging from 0 to 21, assigned to the animal based on the observation of various elements of motor performance as it freely walks on a flat surface. The rats were video-recorded while walking across a table to return to their home cage, as previously described (Šoštarić et al., 2022; Appendix I, Šoštarić et al., 2024; Appendix II).

4.2.3. Assessment of lower leg muscle atrophy

After BoNT-A treatment, hindlimb muscles presented with loss and thinning of the muscle tissue. These changes in lower leg width and muscle mass were used to assess muscle atrophy during the experiment. Measurements of dorsoventral and mediolateral calf diameter were performed once every week until the end of the experiment using a caliper device (Šoštarić et al., 2022; Appendix I, Šoštarić et al., 2024; Appendix II). At the end of the experiment, gastrocnemius, soleus, and tibialis anterior muscles were dissected from fixative-perfused animals of all treatments, and their weights were measured on a laboratory scale.

4.3.   Western Blot analysis of CGN to test cleaved VAMP antibody for detection of TeNT enzymatic activity

Cerebellar granule neurons were treated with the previously specified treatments (see Table 3), seven days after their preparation, for a duration of 12 hours in a complete culture medium. Cells cultured on plastic surfaces were subsequently lysed directly within the wells using Laemmli Sample Buffer (LSB) containing Hepes (10 mM), NaCl (150 mM), SDS (1%), EDTA (4 mM), along with protease and phosphatase inhibitors, supplemented with mercaptoethanol and bromophenol blue. The lysed cell samples were then collected for Western Blot analysis. They were loaded onto NuPage 4–12% Bis-Tris gels for SDS-PAGE electrophoresis in MOPS buffer (Thermo Fisher Scientific, B0001). The proteins were subsequently transferred onto Protran nitrocellulose membranes and blocked for 1 hour in PBS-

T (PBS containing 0.1% Tween 20) supplemented with 5% non-fat dried milk. Incubation with primary antibodies (intact VAMP-2 at 1:2000 dilution; Ab-VAMP77 at 1:2000 dilution) was carried out overnight at 4°C. Following washes with PBS-T, the membranes were incubated at 4°C with appropriate HRP-conjugated secondary antibodies (at 1:5000 dilution) for 90 minutes. After thorough washes, the signals were visualized using LuminataTM and detected using a Uvitec gel doc system (Uvitec, Cambridge, UK).

4.4. Immunohistochemical localisation of BoNT-A and TeNT enzymatic action

At the end of each behavioural experiment, animals were deeply anaesthetized by i.p. injection of ketamine/xylazine mixture (100/10 mg/kg) and sacrificed by transcardial perfusion with physiological saline, followed by fixative (4% paraformaldehyde in phosphate-buffered saline (PBS) fixative). The spinal cord and hindlimbs muscles were dissected and placed in a post-fixing solution containing 15% sucrose in the fixative solution overnight. The next day the solution was changed, and tissues were further kept in 30% sucrose PBS solution. When they sank, the tissues were moved from the solution, dried on a paper towel to remove the sucrose solution, and stored in an ultra-freezer at -80 °C. Free-floating immunohistochemistry was performed for spinal cord slices previously cut on a cryostat (35 μm thick), while muscles were cut at 20 μm and immediately transferred to glass adhesion slides (Super Frost Plus Gold, Thermo Scientific, Waltham, USA), kept at -20 °C.

4.4.1. BoNT-A enzymatic activity in peripheral motor terminals

To characterize the enzymatic activity of BoNT-A in peripheral motor terminals, immunohistochemical detection of cleaved SNAP 25 was performed on gastrocnemius muscle tissue slices (20 μm thickness), transferred to adhesion slides. The slides with muscles were washed in PBS three times for 5 minutes each and followed by 1-hour blockage of unspecific signals with 10% normal goat serum (NGS) diluted in PBS with 0.25% Triton X-100 (PBST). Next, a primary non-affinity purified rabbit polyclonal antibody recognizing the BoNT-A-cleaved SNAP-25 fragment (SNAP-25197; National Institute for Biological Standards and Control, Potters Bar, UK), validated in previous studies (262,263), was diluted at a ratio of 1:4000 in 1% NGS and PBST and left to incubate overnight at room temperature. The following day, slides were washed with PBS three times for 5 minutes each and incubated with anti-rabbit Alexa Fluor 555 secondary antibody at a ratio of 1:400 (Cell Signaling Technology, Danvers,

USA) for 2 hours at room temperature. After incubation, slides were again washed, dried, and coverslipped with a mounting agent. Images of immunohistochemical staining were taken at 40x magnification by a fluorescent Olympus BX-51 microscope coupled to a DP-70 digital camera, and CellSens Dimension visualization and quantification software (Olympus, Tokyo, Japan) (Šoštarić et al., 2022; Appendix I, Šoštarić et al., 2024; Appendix II). Semi-quantification of the cleaved SNAP-25 was performed as previously described (Šoštarić et al., 2022; Appendix I) (264) and enclosed in figure in Šoštarić et al., 2022; Appendix I, Šoštarić et al., 2024; Appendix II. In muscle slices from each animal, four visual fields from four different slices were selected and assessed on a scale of 0 to 4, based on the appearance and profusion of NMJs, nerve terminals, and axons positive for cleaved-SNAP25 (Šoštarić et al., 2022; Appendix I, Šoštarić et al., 2024; Appendix II).
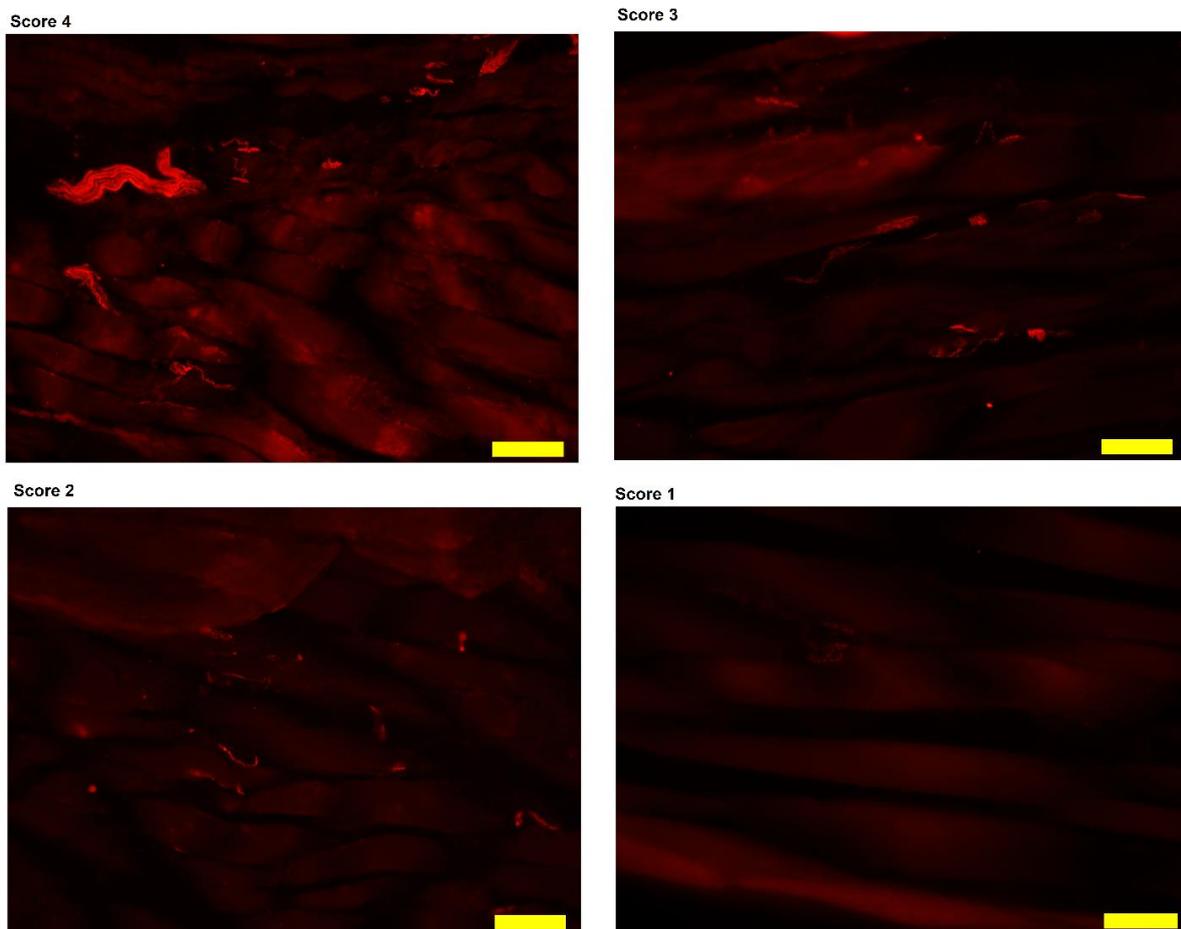

Figure 12: Representative images for scoring system for presence of cleaved SNAP-25 in neuromuscular junctions (NMJs) and axons. *The immunohistochemical scoring system was adopted from* (264)*, with representative images from Šoštarić et al., 2024; Appendix II. A score of 4 indicates strong staining observed in numerous NMJs, terminals, and intramuscular nerves*

(with the number of axons equal to or greater than 10). A score of 3 signifies strong staining observed in multiple NMJs and nerve terminals. A score of 2 indicates moderate staining observed in numerous NMJs. A score of 1 is assigned when only a few or weak NMJ staining is observed. A score of 0 is given when there is no staining observed in NMJs, nerve terminals, or axons. Scale bar=200 μm for all images. (Šoštarić et al., 2024; Appendix II)

4.4.2. BoNT-A enzymatic activity in central second-order synapses

Previously, prepared and cut spinal cords from the level of L3-L5 were subjected to free-floating immunohistochemistry to determine cleaved SNAP25 as a marker of BoNT-A enzymatic activity in spinal synapses. Cryoprotected spinal cords were washed three times for 5 minutes with PBS and then incubated for 1 hour with 150 µl of hydrogen peroxide (H_2O_2) in each well to block the endogenous peroxidase activity. Next, the wells were thoroughly washed with PBST and then blocked for nonspecific signals with 10% NGS in PBST for another hour. After the blocking incubation, spinal cords were incubated overnight at room temperature with the primary antibody recognizing the BoNT-A-cleaved SNAP-25 fragment (SNAP-25197; National Institute for Biological Standards and Control, Potters Bar, UK) at a ratio of 1:8000. The following day, samples were washed again three times with PBST and then incubated for 1 hour with HRP-polyconjugated (polyHRP) goat anti-rabbit secondary antibody (Tyramide SuperBoost Kit B40923/Invitrogen), washed, and subjected to a short 10-12 minute incubation with tyramide Atto-488 HRP substrate prepared as described previously (265). Subsequently, slices were washed again, transferred to glass slides, and coverslipped with a mounting agent. The images were captured using a fluorescent microscope (Olympus BX-51) at 4x and 40x magnification and processed using CellSens Dimension visualization and quantification software (Olympus, Tokyo, Japan). Microphotographs from L4 coronal sections were selected for the quantification of clSNAP25 signal (average pixel-thresholded area, the average of 6 non-overlapping visual fields from 4 spinal slices of each animal), as previously described (13), (Šoštarić et al., 2022; Appendix I, Šoštarić et al., 2024; Appendix II).

4.4.3. Localization of BoNT-A- cleaved SNAP-25 in relation to other synaptic and neuronal markers

Spinal cord slices were prepared as previously described for free-floating immunohistochemistry (13). The protocol for the visualization of cleaved SNAP-25 was performed as previously described. However, for colocalization purposes, on the second day of the free-floating technique, after incubation with the first secondary antibody, samples were washed and then blocked again for 1 hour with 10% NGS, followed by overnight incubation with different primary antibodies (see Table 4). The following day, slices were washed and incubated for 2 hours with Alexa 555 secondary antibody (see Table 4), diluted in 1% NGS and PBS with 0.25% Triton X-100 (PBST). Subsequently, the samples were washed and coverslipped on glass as previously described. The microphotographs of colocalization of the spinal ventral horn level were captured using a confocal Olympus FV3000 microscope and a 60× oil immersion objective (UplanSApo, NA1.35, Olympus, Tokyo, Japan) using FV10-ASW software with a 5X scan zoom at a resolution of 1024×1024 pixels. Colocalization of MAP-2 was performed with a Leica SP5 confocal microscope equipped with a 40× HCX PL APO NA 1.4 oil immersion objective. All images were processed using Fiji software without altering the intensity of the signals, as explained previously. The representative images shown in the figures were adjusted for brightness and contrast in Adobe Photoshop (Adobe Systems, San Jose, CA, USA).

Table 4. The list of primary and secondary antibodies *used in the immunofluorescent colocalization stainings, with dilutions and incubation conditions, adapted from Šoštarić et al., 2024; Appendix II.*

Primary antibody	dilution	incubation temperature and period	catalog no/company	host species
anti-ChAT monoclonal	1:2500	4 °C overnight	AMAB91130/Atlas Antibodies	mouse
anti-SV2C[a] clone 4C8.1 monoclonal	1:1000	4 °C overnight	MABN367/Milipore	mouse
anti-K_v2.1.[b] monoclonal	1:1000	4 °C overnight	ab192761/Abcam	mouse
anti-Synaptophysin monoclonal	1:1000	4 °C overnight	S5678/Sigma Aldrich	mouse
anti-Vglut1[c] polyclonal	1:5000	4 °C overnight	135304/Synaptic Systems	guinea pig
Anti- MAP-2[d]	1:1000	4 °C overnight		mouse
secondary antibody				
anti-rabbit polyHRP[e]	undiluted	room temperature, 1 h	B40923/Invitrogen (from Tyramide SuperBoost Kit)	goat
anti-mouse IgG Fab2 Alexa Fluor 555	1:400-1:500	room temperature, 2 h	4490S/CellSignaling Technology	goat
anti-guinea pig IgG H&L Alexa Fluor 555	1:400	room temperature, 2 h	ab150186 /abcam	goat
anti-rabbit IgG Fab2 Alexa Fluor 555	1:400	room temperature, 2 h	4413S/CellSignaling Technology	goat

[a]synaptic vesicle protein 2 C, [b] potassium voltage channel K_v2.1., [c] vesicular glutamate transporter 1, [d] microtubule-associated protein 2, [f]horseradish peroxidase-polyconjugated

4.5.   Statistical analysis

The data were presented as mean ± SEM or individual values with the median. Repeated measurements were analyzed by repeated measurements two-way analysis of variance (RM two way ANOVA), followed by Bonferroni's post hoc test ($P < 0.05$ considered significant) for between-group comparisons. In case of missing values linear mixed effects models was applied instead of RM two-way ANOVA. The non-normal distribution of clSNAP25 immunoreactivity was analyzed by non-parametric ANOVA (Kruskal-Wallis) and Dunn's post hoc test (median ± range with $P < 0.05$ considered significant), while single measurements of gastrocnemius and soleus muscle weight were analyzed by one-way ANOVA followed by Bonferroni's multiple comparison test. Electromyography values, non-repeated CMAP measurements after TeNT injections, were evaluated using a two-tailed Student's t-test or by one-way ANOVA with $P < 0.05$ considered statistically significant.

The determination of the number of animals per treatment group was performed according to *a priori* power analysis conducted with G*power software version 3.1 (University of Düsseldorf, Germany) based on an estimated effect size ($F = 0.4$), α error probability = 0.05, power ($1-\beta$) = 0.9, and statistical test: ANOVA: repeated measures, within-between interaction (Šoštarić et al., 2022; Appendix I) (266). Additionally, we extended the group size from 6 to 8 to account for possible attrition of animals during the experiment.

5. RESULTS

5.1. Intramuscular BoNT-A induces fast onset, dose-independent early antispastic action, which is peripherally mediated

Experimental hypertonia was induced in rats by TeNT injection (1.5 ng) into the gastrocnemius muscle. This resulted in reversable local spastic paralysis peaking at day 3 post TeNT injections, and gradually started recovering from day 14, with complete recovery observed by day 28. Spastic paralysis and muscle rigidity in the lower limb, induced by TeNT injection, were evident through limb spasms and reduced joint mobility, exhibited as increased force required for passive ankle dorsiflexion (Figure 13 B) and reduced locomotor score observed with Basso Beattie Bresnahan (BBB) scale (Figure 13 A). BoNT-A i.m. injections (1, 2 and 5 U/kg) at day 7 post-TeNT reversed signs of hypertonia in rats, across all doses, restoring ankle flexibility and locomotor function, assessed by BBB scale (Šoštarić et al., 2022; Appendix I). The muscle weakening was visible already at day 1 post BoNT-A application which led to noticeable impairment in toe spreading reflex function (Figure 13 C). This impairment began to recover in a dose-dependent manner by day 49 post BoNT-A application (Figure 13 C), (Šoštarić et al., 2022; Appendix I).
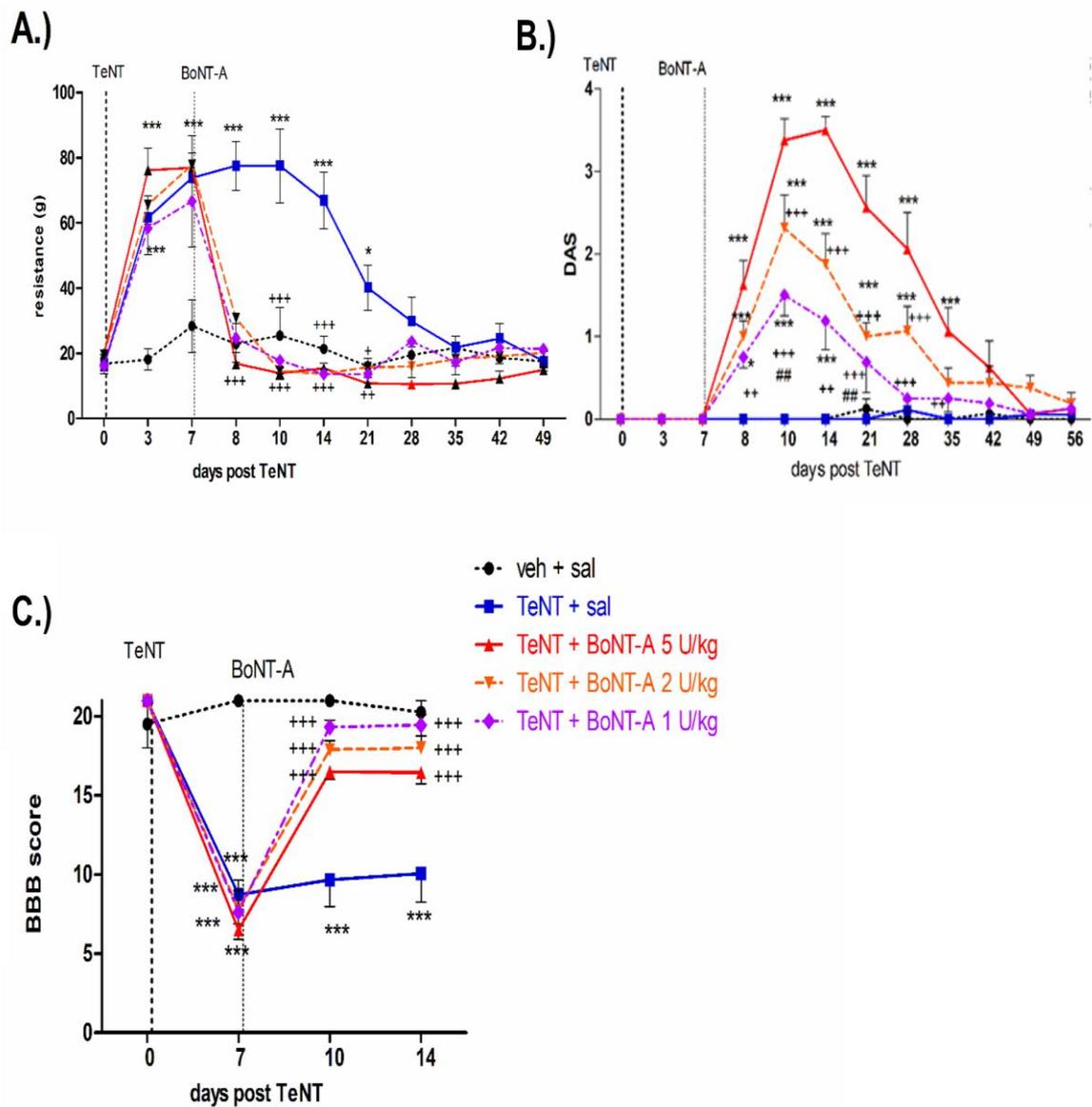
Figure 13. Early effects of different doses of intramuscular BoNT-A on TeNT-induced hypertonia and hind-paw flaccid paralysis. *The effect of different doses (1, 2 and 5 U/kg) of BoNT-A injected into gastrocnemius muscle (i.m.) on TeNT-evoked spasticity evaluated by Basso Beattie Bresnahan (BBB) scale (A.) and dorsiflexion resistance (C.), and the effect on impairment of toe-spreading reflex (B.) assessed by digit abduction score (DAS). Veh, vehicle; sal, saline i.m. treatment; DAS, digit abduction score; Horizontal bars indicate the time points of TeNT and BoNT-A i.m. application. N = 8 to 9 animals/group; mean ± SEM, * and ***: p < 0.05 and < 0.001 vs. veh + sal, +, ++ and +++: p < 0.05, < 0.01 and < 0.001 vs. TeNT + sal (two-way RM ANOVA, followed by Bonferroni's post hoc test; p < 0.05 considered significant) (Šoštarić et al., 2022; Appendix I).*

5.2. The late BoNT-A antispastic action is dose- and central trans-synaptic transport-dependent.

Animals that recovered from spastic paralysis and muscle weakness were re-injected with TeNT on day 49 post-BoNT-A injection (day 56 post first TeNT injection). This resulted in reappearance of local spasticity by day 3 post-TeNT. The antispastic effect of BoNT-A persisted over 2 months, successfully opposing high resistance during dorsiflexion test and reducing locomotor deficits noted by BBB scale, in a dose-dependent manner, with the two higher doses (5 and 2 U/kg) completely opposing the TeNT-evoked spasm and exerting a better preventive effect on locomotor deficit compared to 1 U/kg dose (Figure 14, Šoštarić et al., 2022; Appendix I).
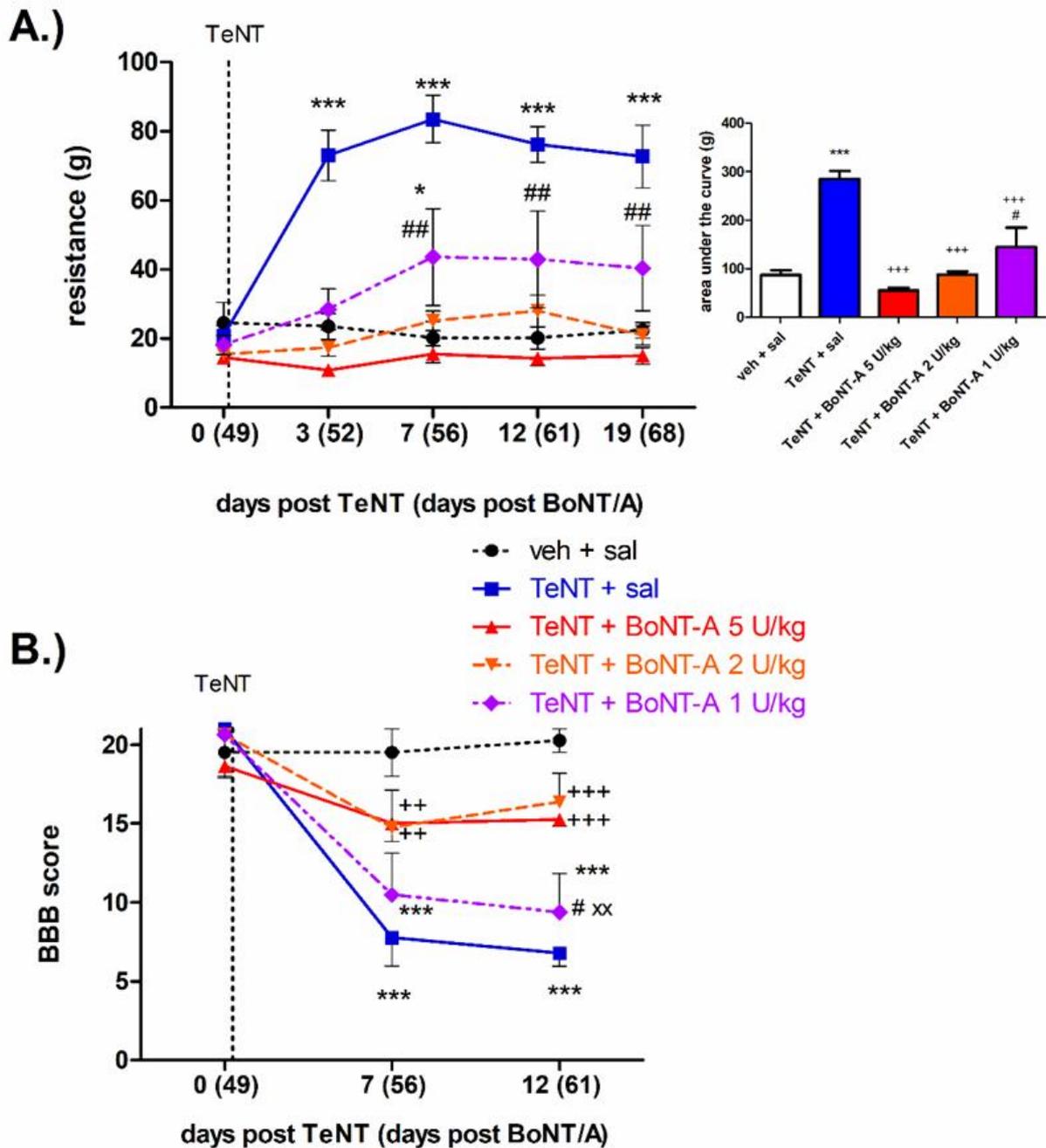
Figure 14. Late dose-dependent antispastic effects of BoNT-A on re-evoked TeNT spasticity. *On day 49 post BoNT-A administration, rats received a reinjection of TeNT into the right gastrocnemius muscle, resulting in the development of local spasticity. Assessment of motor function using the BBB score (A) and dorsiflexion resistance test (B). Veh, vehicle; sal, saline; BBB- Basso Beattie Bresnahan. Horizontal bars indicate the time points of repeated TeNT treatment. N = 8 to 9 animals/group; mean ± SEM, * and ***: p < 0.05 and < 0.001 vs. veh + sal, +, ++ and +++: p < 0.05, < 0.01 and < 0.001 vs. TeNT + sal, # and ##: p < 0.05*

and < 0.01 vs. TeNT + 5 U/kg BoNT-A; XX: p < 0.01 vs. TeNT + 2 U/kg BoNT-A (two-way RM ANOVA, followed by Bonferroni's post hoc test; p < 0.05 considered significant) (Šoštarić et al., 2022; Appendix I)

In order to assess if BoNT-A antispastic effects are centrally mediated, in a separate experiment, i.m. BoNT-A (5 U/kg) was injected into gastrocnemius muscle. Then, 24 hours post i.m. BoNT-A, we employed i.t. BoNT-A neutralising antitoxin to prevent the toxin's central transcytosis to spinal synapses. On day 50 post BoNT-A, we injected animals with TeNT (1.5 ng) in the same gastrocnemius muscle to induce local spasticity and challenge antispastic BoNT-A activity. As shown previously (Figure 14) i.m. BoNT-A (5 U/kg) decreased resistance during ankle-dorsiflexion and reduced locomotor deficits assessed by BBB locomotor scale (Figure 15). The BoNT-A antispastic effect was partially reduced by i.t. applied antitoxin, evident as increased muscle resistance and greater motor impairment assessed by BBB scale (Figure 15), (Šoštarić et al., 2022; Appendix I). This suggest that the late antispastic action of BoNT-A is centrally mediated and dependent on central transcytosis.
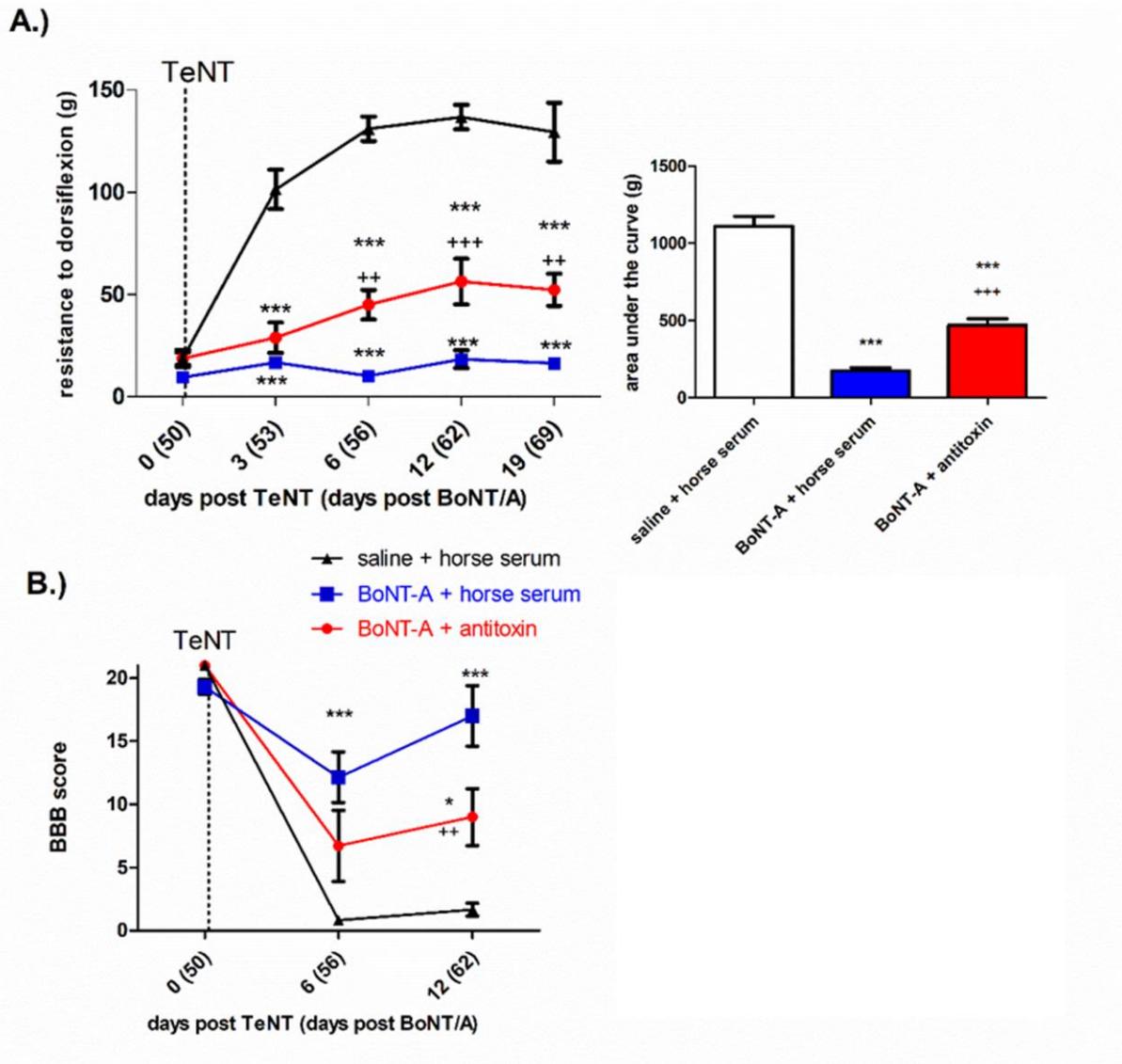
Figure 15. Long-term antispastic activity of BoNT-A on experimental hypertonia is dependent on transsynaptic central action. *The antispastic activity was evaluated after i.m. BoNT-A (5 U/kg) and re-injection with TeNT (1.5 ng) on day 49 and assessed by resistance to dorsiflexion test (A.) and motor locomotion assessed by BBB scores (B.). Sal, saline i.m. treatment. BBB, Basso Beattie Bresnahan. N = 6 to 7 animals/group; mean ± SEM, *, ** and ***: p < 0.05, < 0.01 and < 0.001 vs. sal + horse serum, ++ and +++: p < 0.01 and < 0.001 vs. BoNT-A + horse serum (two-way RM ANOVA, followed by Bonferroni's post hoc test; p < 0.05 considered significant). (Šoštarić et al., 2022; Appendix I)*

5.3. Centrally transported BoNT-A targets premotor inputs participating in normal locomotion

We explored BoNT-A effects on normal muscle tone and motor function by employing bilateral i.n. BoNT-A injection (2 U/kg) into the sciatic nerves. We assessed the possibility that BoNT-A effects are centrally mediated, by challenging its action in combination with intrathecally injected BoNT-A neutralizing antitoxin, which prevents the toxin transcytosis (10,13), (Šoštarić et al., 2024; Appendix II). The i.n. BoNT-A induced mild impairment of toe-spreading reflex (DAS=1) that quickly recovered by day 21 (Figure 16; Šoštarić et al., 2024; Appendix II).

The i.n. BoNT-A altered the appearance of hind paws during sitting, and disrupted their normal gait. This was particularly evident during walking on a slope, where animals exhibited heel-supported gait, and the inability to lift the heel from the ground during terminal stance (Figure 16). Impaired appearance of the paws together with disrupted gait resulted in reduced combined gait ability score. Prevented BoNT-A spinal transcytosis by i.t. lumbar injection of BoNT-A neutralizing antitoxin resulted with accelerated recovery of motor function and milder gait impairment (Figure 16) (Šoštarić et al., 2024; Appendix II).
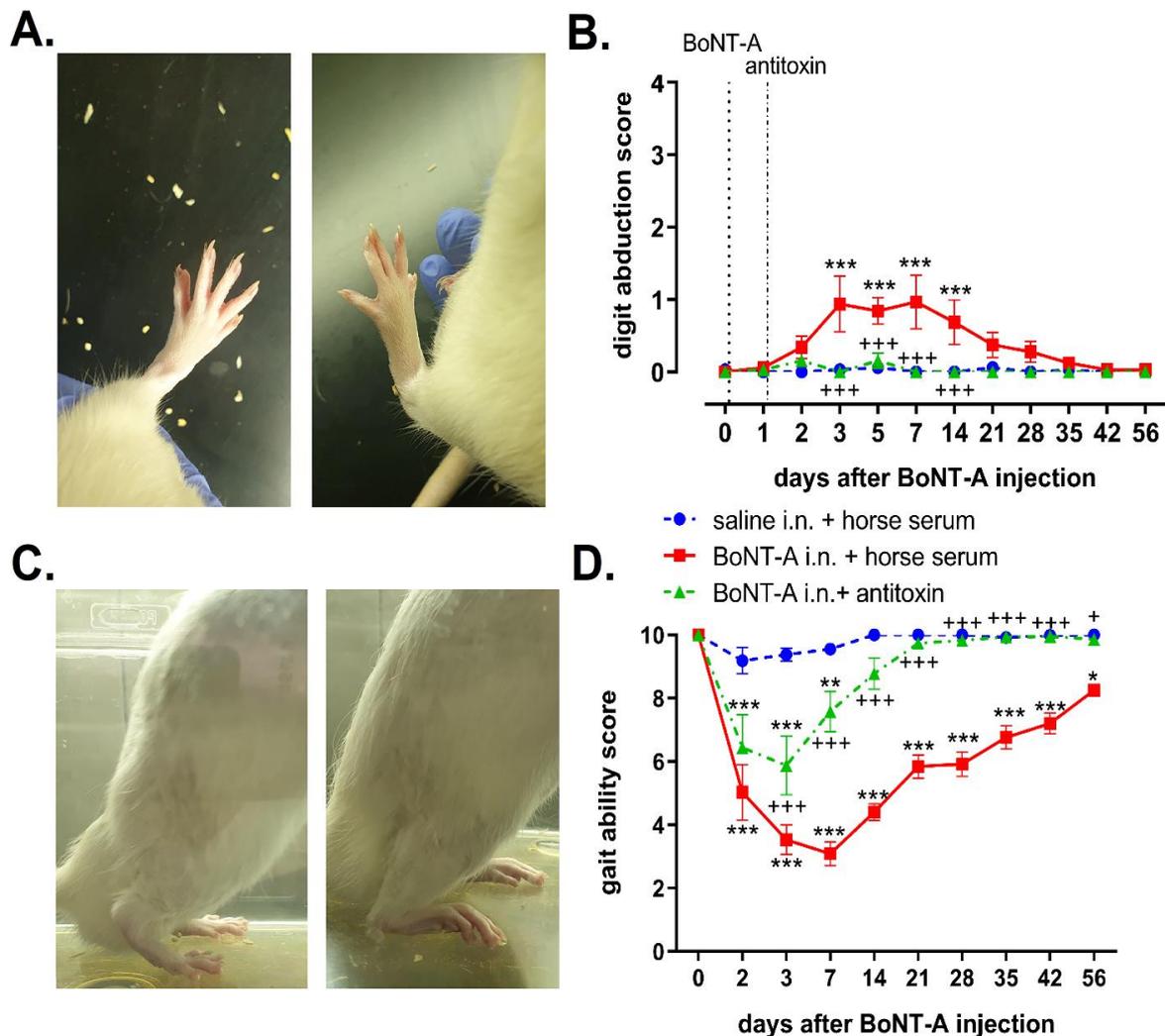
Figure 16. Intrasciatic BoNT-A induces lower leg muscle weakness dependently on its central trans-synaptic action. *The combined effect of bilateral intraneural BoNT-A (2 U per sciatic nerve) with BoNT-A-neutralizing antitoxin (5 iu, intrathecally) was evaluated by the toe spreading reflex (measured by digit abduction score) (A. and B.) and gait ability (C. and D.). Hind paw appearance in BoNT-A-treated rats revealed an inability to abduct all toes (A.) and an arch-like appearance of the hind paw (C.) with heel-supported weight bearing during bipedal stance (left vs right: saline + horse serum vs BoNT-A + horse serum). Horizontal lines in graphs (B.) indicate the time points of application of BoNT-A and BoNT-A neutralizing antitoxin. N = 8 animals/ group; mean ± SEM, *,**,*** - P < 0.05, 0.01, 0.001 vs saline + horse serum; +, ++, +++ - P < 0.05, 0.01, 0.001 vs BoNT-A + horse serum (two way RM ANOVA followed by Bonferroni's post hoc). (Šoštarić et al., 2024; Appendix II)*

Fine motor coordination and balance was evaluated by rotarod test and beam walking after i.n. BoNT-A injections. Animals were pre trained to walk swiftly on a beam walk, without stumblingor falling, and to maintain balance walking on a rotating rod for a maximal trial duration time. Animals treated with i.n. BoNT-A exhibited impaired coordination and doubled the time needed for crossing the beamwalk, which peaked at days 3-7, and then gradually recovered. Following prevention of spinal transcytosis of BoNT-A with specific antitoxin, i.n. treated animals developed milder locomotor impairment that quickly started to recover after day 3rd (Figure displayed in Šoštarić et al., 2024; Appendix II).

The i.n. BoNT-A induced a notable impairment in the animal's ability to maintain balance on the rotarod, which was indicated by reduced latency to fall, with peak toxin activity between 7-14 day that then started to gradually recover, but never fully by day 56 (Figure displayed in Šoštarić et al., 2024; Appendix II).

Effect of i.n. BoNT-A was examined during swimming performance, a high-output motor task, that requires activation of cholinergic C-boutons synapses (267,268). The i.n. BoNT-A affected swimming velocity, reducing its mean and maximal values, that recovered by day 36 post treatment (Figure 17). However, spinal intrathecal injection of BoNT-A neutralizing antitoxin (5 i.u.) prevented the reduction induced by BoNT-A, indicating possible BoNT-A cholinergic alteration on motoneuron firing rates (Figure 17; Šoštarić et al., 2024; Appendix II).
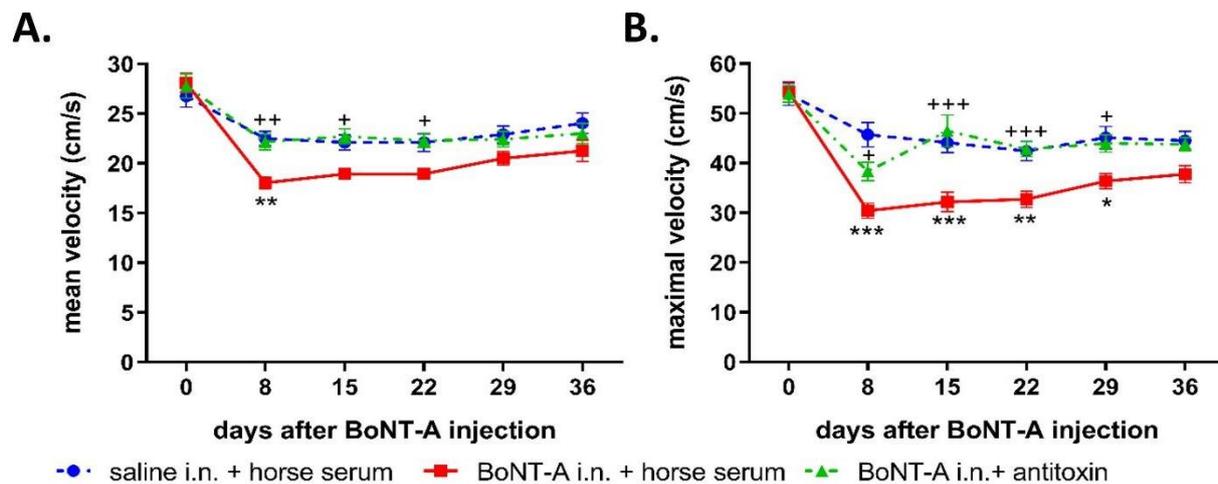
Figure 17. Impairment of swimming velocity by i.n. BoNT-A involves trans-synaptic action of the toxin. *The graphs show the effect of bilateral intrasciatic BoNT-A (2 U injected intra-nerve, i.n.) in combination with intrathecal (i.t.) horse serum or BoNT-A-neutralising antitoxin (administered 24 h post BoNT-A) on mean (A) and maximum (B) swimming velocities, N = 8 animals/ group; mean ± SEM, *,**,*** - P < 0.05, 0.01, 0.001 vs saline + horse serum; +, ++, +++ - P < 0.05, 0.01, 0.001 vs BoNT-A + horse serum (two way RM ANOVA followed by Bonferroni's post hoc).*

5.4.   Central effects of BoNT-A are not accompanied by modulation of monosynaptic reflex

Following the recovery of significant motor functions approximately two months post BoNT-A injection, we investigated the persistence of its antispastic effects by inducing TeNT-evoked disinhibition of motoneuronal inhibitory control. The BBB locomotor scale, utilized for assessing locomotor recovery in various spinal cord injuries, was employed to evaluate limb functionality during locomotion on a flat surface (261). From day 3 post-TeNT, control animals exhibited pronounced spastic paralysis in the injected right hindlimb, characterized by rigid leg extension and an inability to fully flex the joint. This locomotor impairment was evident as sweeping of the affected hind limb against the table surface without weight support or plantar stepping, resulting in a markedly reduced BBB score. The i.n. administration of BoNT-A reduced dorsiflexion resistance from days 3-15 and partially mitigated locomotor impairment on day 15 post-TeNT, demonstrating improved use of the plantar hind paw surface and higher

weight-bearing scores on the BBB scale (Figure displayed in Šoštarić et al., 2024; Appendix II). However, the beneficial effects of BoNT-A were prevented in rats treated with intrathecal antitoxin, as evidenced by high passive resistance during dorsiflexion testing (Figure displayed in Šoštarić et al., 2024; Appendix II) and impaired locomotor scores similar to those of saline-treated animals (Figure displayed in Šoštarić et al., 2024; Appendix II).

Furthermore, we employed EMG to investigate potential BoNT-A effects on monosynaptic H-reflex excitability after TeNT evoked spasticity. In order to measuree the H-reflex transmitted by central synapse between Ia afferents and motoneurons, we electrically stimulated the sciatic nerve by subcutaneous electrodes with increasing voltages. Intramuscular TeNT caused a significant increase in H_{max} amplitude, peaking on day 8 post-injection. Interestingly, the H-reflex excitability recovered faster than leg spasm intensity or locomotor deficits by day 15 post-TeNT, suggesting that sustainement of muscle spasms is not influenced by overactivity of the monosynaptic reflex. M-wave and H-reflex maximal amplitude was reduced by i.n. BoNT-A, prior and on day 8 following TeNT injection. However, when the H- reflex amplitude was adjusted for both M amplitude (their ratio and muscle weight, no notable distinction was found between the control group and the effect of BoNT-A on the excitability of the monosynaptic reflex. This suggests that the reduction of CMAP and H reflex in BoNT-A-treated animals is mediated by atrophic muscle size reduction.
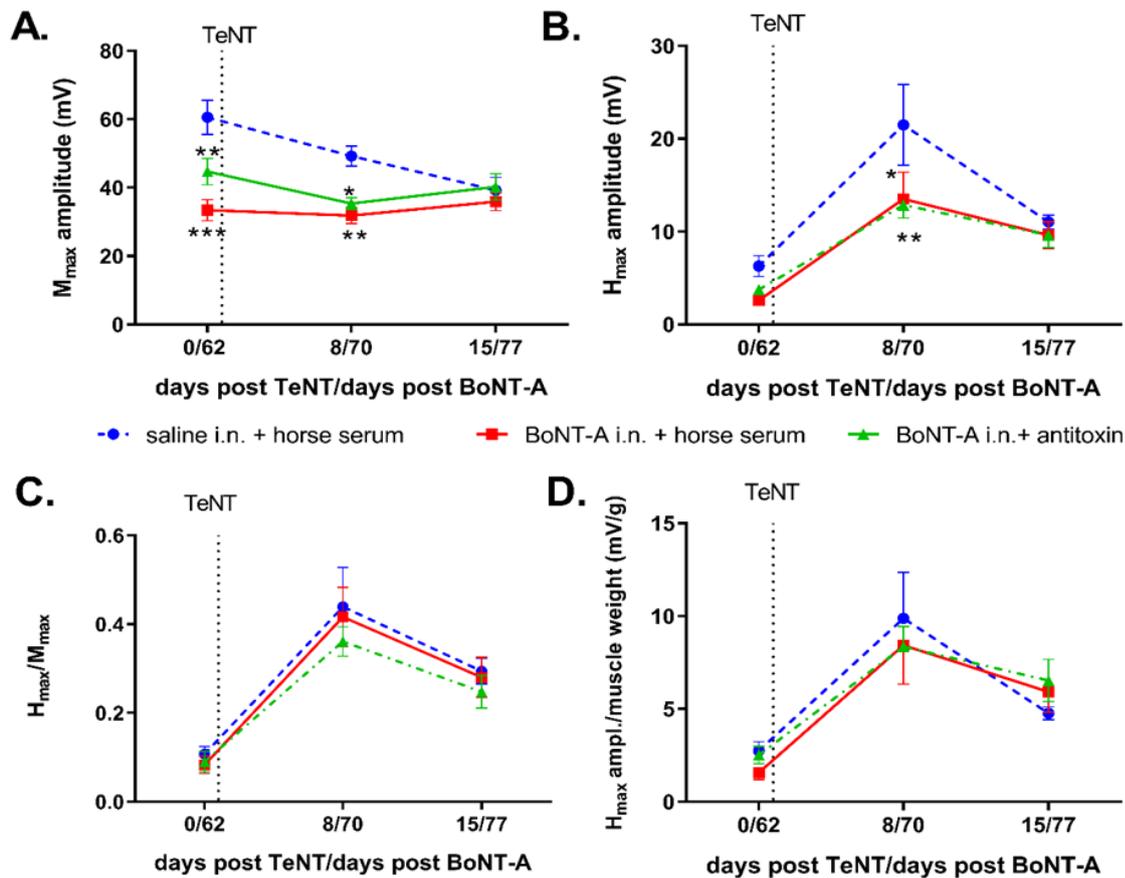
Figure 18. The lack of BoNT-A action on the monosynaptic H reflex excitability. *BoNT-A injected into the sciatic nerve (2 U per nerve) along with intrathecal BoNT-A-neutralizing antitoxin (5 i.u.) did not affect monosynaptic reflex excitability at the Ia central afferent synapse. Electromyographic measurements of compound action muscle potential (CMAP) were measured before TeNT i.m. injection (on day 60) and after TeNT evoked muscle spasm. Peak-to-peak maximal M-wave (M_{max}) and Hoffman or H-reflex (H_{max}) amplitudes, are shown on graphs (A.) and (B.), respectively, while graphs (C.) and (D.) represent H reflex to M wave relative ratio, and also H-reflex ratio to individual muscle weight.. Horizontal lines in graphs denote TeNT treatment timepoint. N = 8 animals/group; mean ± SEM, *,** - P< 0.05, 0.01 vs saline + horse serum (two-way RM ANOVA followed by Bonferroni's post hoc).*

5.5. Centrally transported BoNT-A targets defined post-synaptic neuronal synapses

According to long term synaptic silencing of peripheral nerve terminals, we examined ventral horn of the spinal cord for the presence of BoNT-A-cleaved SNAP-25 enzymatic product. After i.m. BoNT-A injections (1, 2 and 5 U/kg), its enzymatic activity persisted more than 2 months in spinal synapses. Comparable to the dose-dependent presence of cleaved SNAP-25 in muscles, a similar dose-dependent abundance was observed upon evaluation of BoNT-A enzymatic activity in the ipsilateral and contralateral sides of the ventral horn (Figure displayed in Šoštarić et al., 2022; Appendix I).

At the end of a separate experiment, on day 78 following i.n. BoNT-A (2 U/kg), we examined the central sites for immunoreactivity of cleaved SNAP-25. Product of BoNT-A enzymatic activity was notably evident following i.n. BoNT-A injections, observed in the ventral horn of the spinal cord (Figure displayed in Šoštarić et al., 2024; Appendix II). However, treatment with intrathecal (i.t.) antitoxin substantially decreased the presence of clSNAP25 in the ventral horn (Figure displayed in Šoštarić et al., 2024; Appendix II), indicative of retroaxonal transport and central transcytosis of the toxin. The presence of cleaved SNAP-25 near ventral horn motoneurons did not co-occur with microtubule-associated protein 2 (MAP-2) immunoreactivity, indicating the lack of toxin's enzymatic effect in the somatodendritic compartment primarily associated with motoneurons.

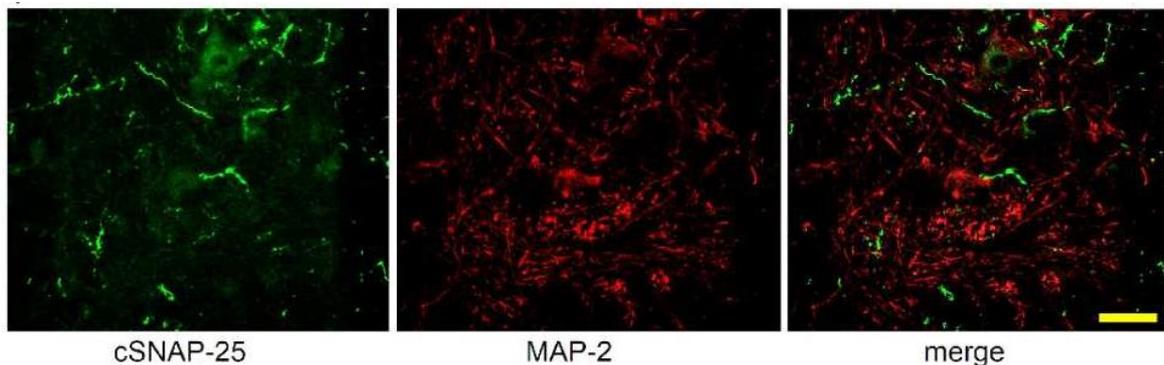cSNAP-25   MAP-2   merge

Figure 19. The BoNT-A enzymatic activity in ventral horn cleaved SNAP25 in spinal synapses does not colocalize with the motoneuronal somatodendritic compartment immunoreactive for microtubule-associated protein 2 (MAP-2). *The confocal microscope image was obtained from animals injected with 5 U/kg BoNT-A (scale bar = 50 μm). (Šoštarić et al., 2022; Appendix I)*

In accordance with absence of BoNT-A effect on monosynaptic H reflex during EMG measurements, we noted the absence of colocalization between BoNT-A-cleaved SNAP-25 and the VGlut1 isoform of the glutamate transporter (Figure 20), indicating a lack of direct toxin impact on the central afferent terminal of different muscular afferents that express this transporter isoform (type Ia and II primary afferents innnervating the muscle spindle and Ib afferents that innervate the Golgi tendon organ) which are responsible for the muscular proprioception and reflex regulation of stretch and tension.

cSNAP-25   VGlut1   merge
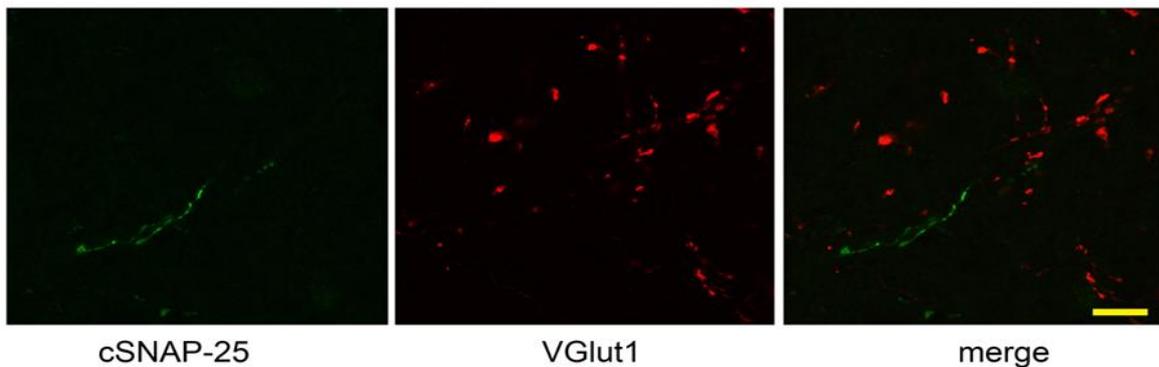
Figure 20. Centrally transported BoNT-A does not affect central afferent terminals of VGlut-1 expressing muscular sensory afferents in ventral horn. *In the L4 ventral horn of animals treated with i.n. BoNT-A, the BoNT-A-cleaved SNAP-25 does not exhibit colocalization with vesicular glutamate transporter 1 (VGlut1), the isoform of the transporter found in muscle spindle and Golgi tendon organ primary afferents. The confocal microscope image depicts a single optical slice (0.42 μm thickness) from a confocal z-stack, chosen as representative from a minimum of three different animals (scale bar = 20 μm). (Šoštarić et al., 2024; Appendix II)*

We conducted additional analysis to examine the co-localization of active BoNT-A enzymatic activity with other synaptic markers. We observed that BoNT-A-cleaved SNAP-25 was partially present in ChAT-expressing neurons, indicating a relationship with Kv2.1 immunoreactivity at C-boutons (refer to Figure 21A, Figure 21B). However, the majority of terminals containing cleaved SNAP-25 co-localized with SV2C (BoNT-A protein ectoacceptor with highest affinity) and synaptophysin (marker of synaptic vesicular release sites), suggesting susceptibility to BoNT-A across various nerve terminals, including both cholinergic and non-cholinergic types (figure 21 ; Šoštarić et al., 2024; Appendix II).
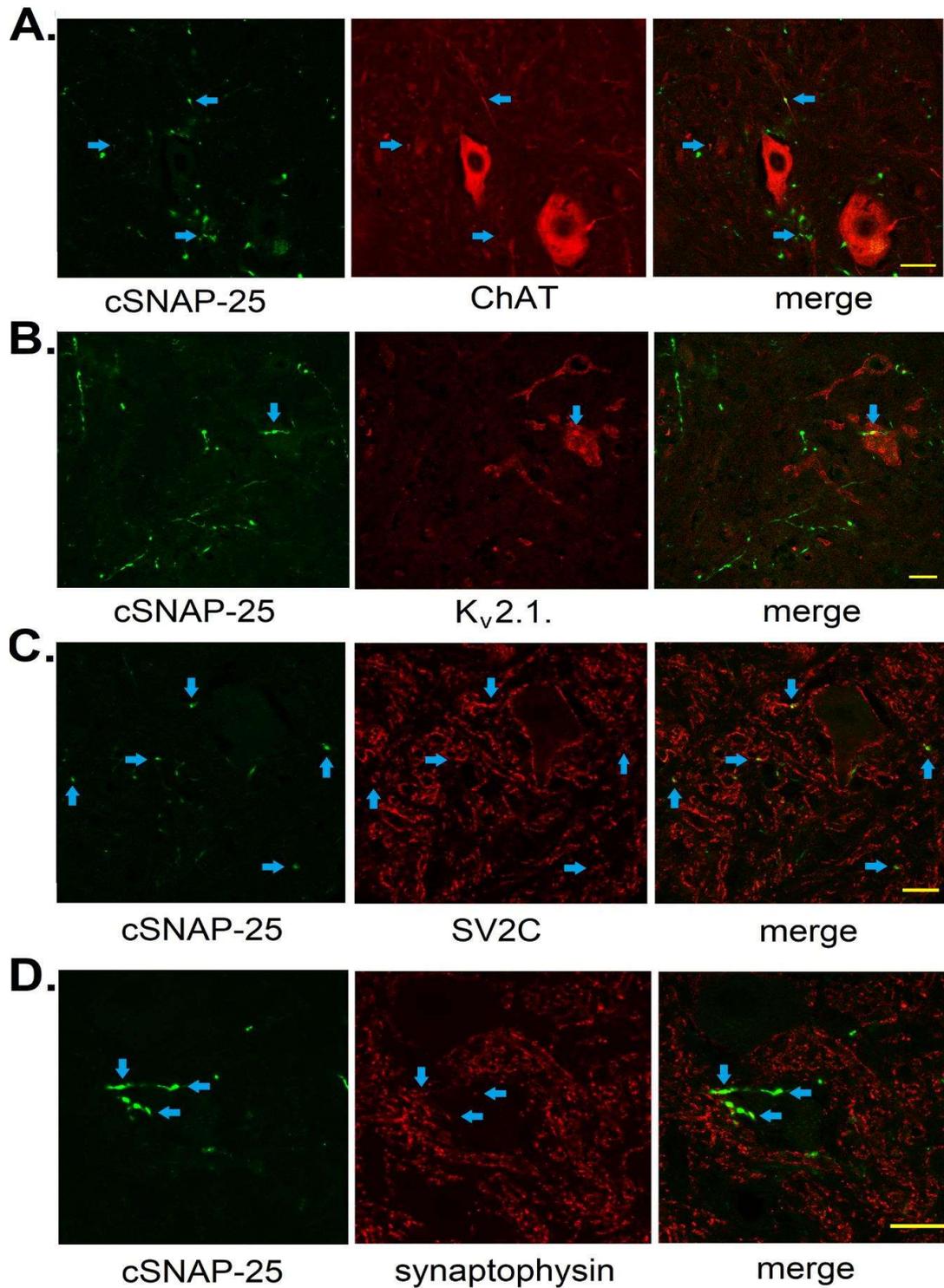
Figure 21. Colocalization of central neuronal markers and BoNT-A enzymatic activity.
Lumbar part of ventral horn (level of L4) was stained for cleaved SNAP25 immunoreactivity after i.n. injections of BoNT-A (2 U/kg) along with A.) choline acetyltransferase (ChAT) and B.) potassium voltage-gated channel Kv2.1, both indicative of cholinergic C-boutons and their associated postsynaptic channels. Additionally, colocalization of cSNAP-25 was assessed with C.) high-affinity BoNT-A binding acceptor synaptic vesicle protein 2C (SV2C) and D.) the

general synaptic marker synaptophysin. Confocal microscope images depicted a single optical slice (0.42 μm thickness), representative of at least three different animals injected with i.n. BoNT-A + horse serum (blue arrows indicate overlap of the immunoreactivities suggestive of colocalization spots on merge images, and on separate images, scale bars = 20 μm). (Šoštarić et al., 2024; Appendix II)

5.6. Characterization of muscular effects of BoNT-A

5.6.1. Intramuscularly and intrasciatically-injected BoNT-A induces lasting muscular enzymatic activity and slowly-recovering atrophy

Injections of BoNT-A into the gastrocnemius lead to visible muscle atrophy, characterised by thinning of the hindlimb's muscles and reduced muscle mass. To evaluate muscle atrophy over the course of the experiment, non-invasive measurements of hind-leg diameter was carried out using a digital caliper, and measuring muscle weights at the end of experiment. Different doses of i.m. BoNT-A (5, 2 and 1 U/kg) caused similar reduction in a cross-section area, persistent during the experiment (Figure 22 A). In next two separate experiments, we examined if central mechanisms are involved in BoNT-A action on muscle atrophy by employing i.t. BoNT-A neutralizing antitoxin to block the BoNT-A transcytosis. I.m. BoNT-A (5 U/kg) caused reduction in hind-limb diameter and estimated cross-sectional area due to muscle atrophy. However, i.t. antitoxin treatment did not significantly influence indicators of muscle atrophy, suggesting lack of functional central action on persistent muscle atrophy. We further assessed i.n. BoNT-A (2 U/kg) effects on muscle atrophy, and observed a significant reduction of measured mid-calf cross section area of BoNT-A treated hindlimbs (Figure 22). This was concomitant with reduction of final muscle weight (Figure 22). Antitoxin-treated animals seemingly showed a slightly wider estimated cross section area, however, the effect was not significant (Figure 22).
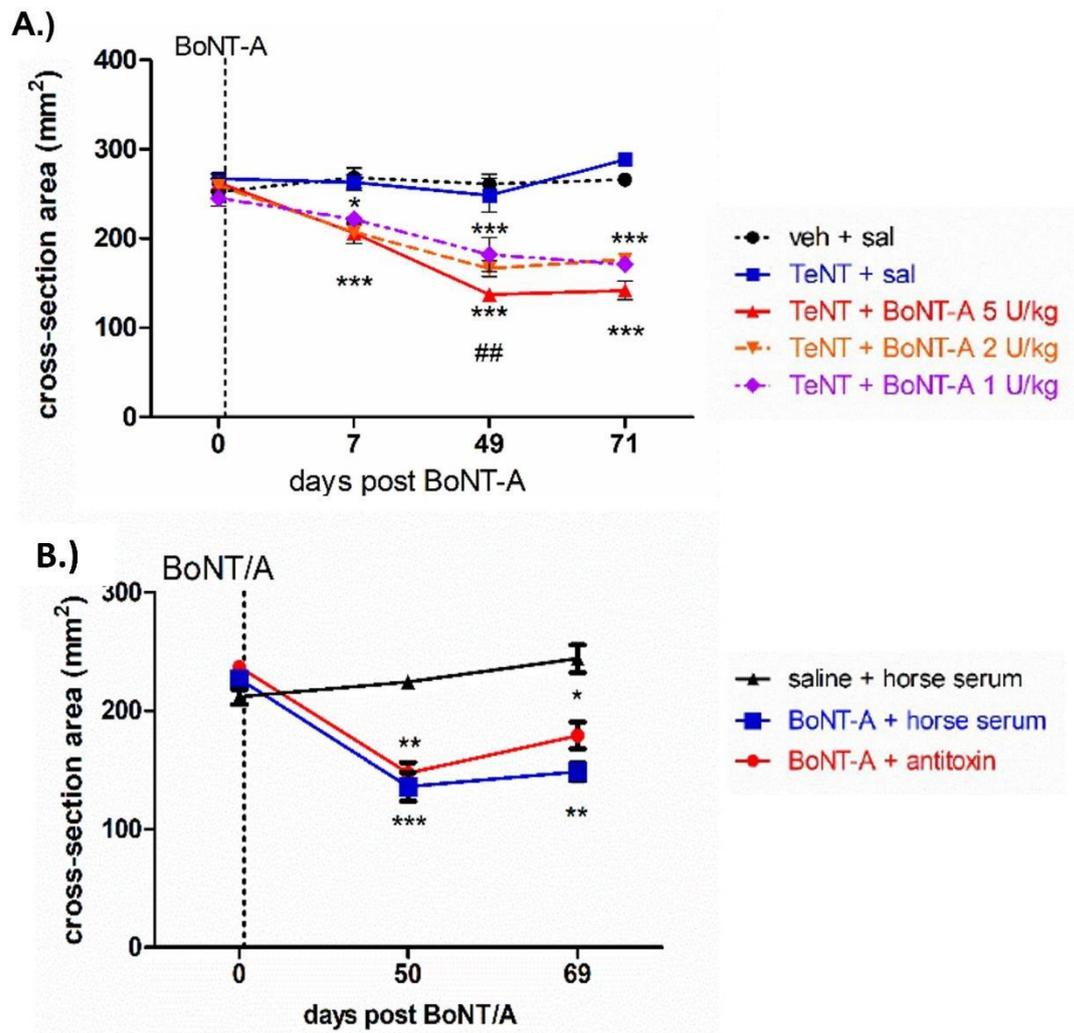
Figure 22. BoNT-A induces non-recovering lower leg calf muscle atrophy independent of its central action. *All doses of BoNT-A (1,2, and 5 U/Kg) treatment caused non-recovering muscle atrophy of lower leg estimated cross-sectional area (A.) (Šoštarić et al., 2022; Appendix I). However, atrophic loss of the lower leg is not mediated by central action of i.m. BoNT-A (5 U/kg) (B) (Šoštarić et al., 2022; Appendix I). Horizontal lines are makrs of BoNT-A treatment days. Sal, saline i.m. treatment. N = 6 to 7 animals/group; mean ± SEM, *, ** and ***: p < 0.05, < 0.01 and < 0.001 vs.sal + horse serum, ++ and +++: p <0.01 and <0.001 vs. BoNT-A + horse serum (two-way RM ANOVA, followed by Bonferroni's post hoc test; p < 0.05 considered significant). (Šoštarić et al., 2022; Appendix I)*

Morever, the gastrocnemius muscle weight did not show a significant difference compared to the i.n. BoNT-A treatment, indicating that muscle weight is not influenced by toxin's central transcytosis (Figure 23). However, soleus muscle weight was not changed when compared among the different experimental treatments (Figure 23). Additionally, alterations in muscle size did not accompany overall changes in body mass, thus ruling out the possibility of a systemic effect following i.n. BoNT-A.
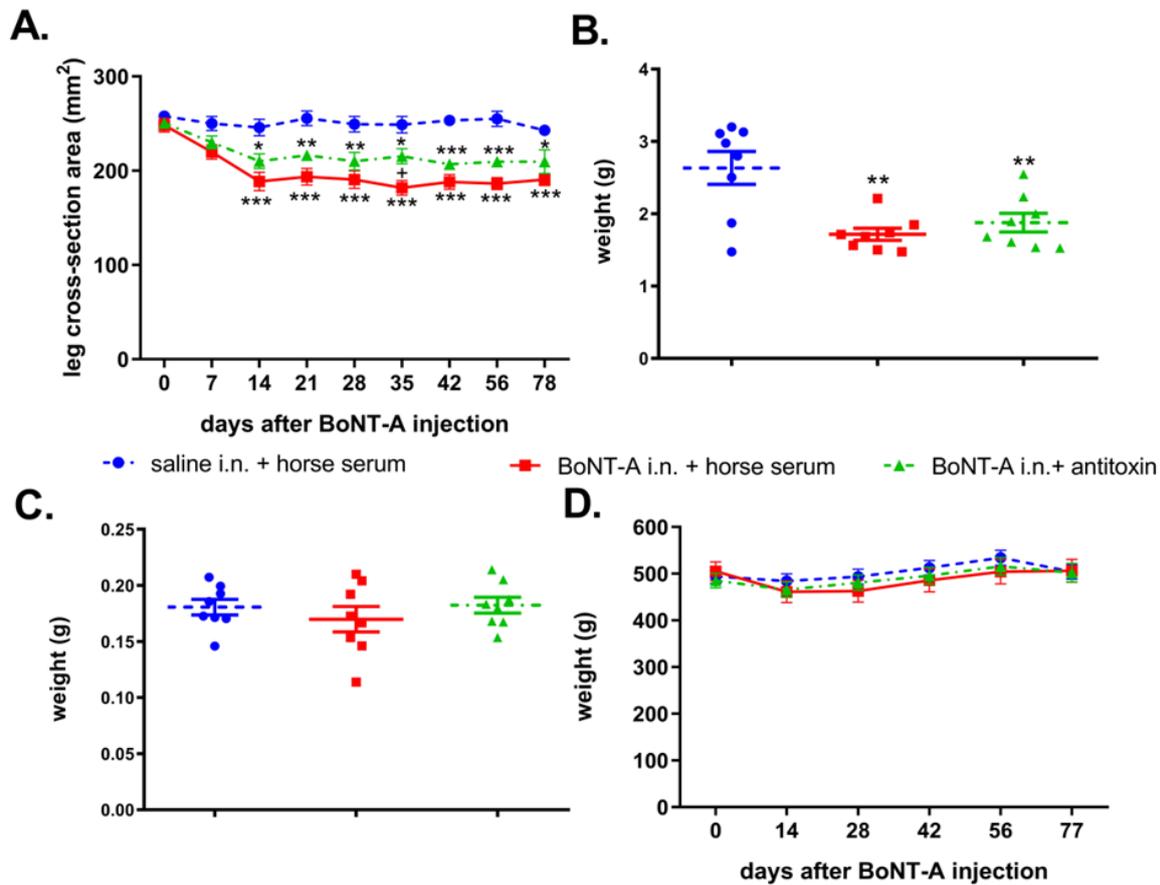
Figure 23. Intrasciatic BoNT-A leads to persistent non-recovering atrophy in the lower leg calf muscles. *The graphs above indicate lower leg cross section area A) and muscle weights of gastrocnemius B) and soleus C), 78 days post BoNT-A i.n. injections (2 U), and subsequent i.t. antitoxin injection (5 i.u.), to prevent BoNT-A central transcytosis. As depicted in graph D), total weight of the animals did not differ significantly throughout the experiment. N = 8 animals/ group; mean ± SEM, *,**,*** - P < 0.05, 0.01, 0.001 vs saline + horse serum (two-way RM ANOVA followed by Bonferroni's post hoc). (Šoštarić et al., 2024; Appendix II)*

To assess the possible presence of BoNT-A enzymatic activity 2 months post single BoNT-A treatment, we examined immunoreactivity of cleaved SNAP-25 in gastrocnemius muscle of injected hindlimbs. Following intramuscular injections of different doses of BoNT-A (5, 2, and 1 U/kg), enzymatic activity persisted in the neuromuscular junctions (NMJs) up to day 71 post-injection across all administered doses (Figure 24 A). Cleaved SNAP-25 was notably present in both NMJs and axons following all three doses, with a slightly lower score observed in muscles treated with 1 U/kg, as evaluated by a semi-quantitative method (264) (Šoštarić et al., 2022; Appendix I).

Furthermore, the presence of cl-SNAP-25 was examined in peripheral nerve terminals 78 days after BoNT-A injection into the sciatic nerve. Immunodetection revealed abundant presence of cl-SNAP25 in neuromuscular junctions, axons, and nerve terminals in BoNT-A treated animals. Notably, the substantial presence of BoNT-A enzymatic activity in peripheral nerve terminals remained unaffected by antitoxin treatment (Figure 24) (Šoštarić et al., 2024; Appendix II).
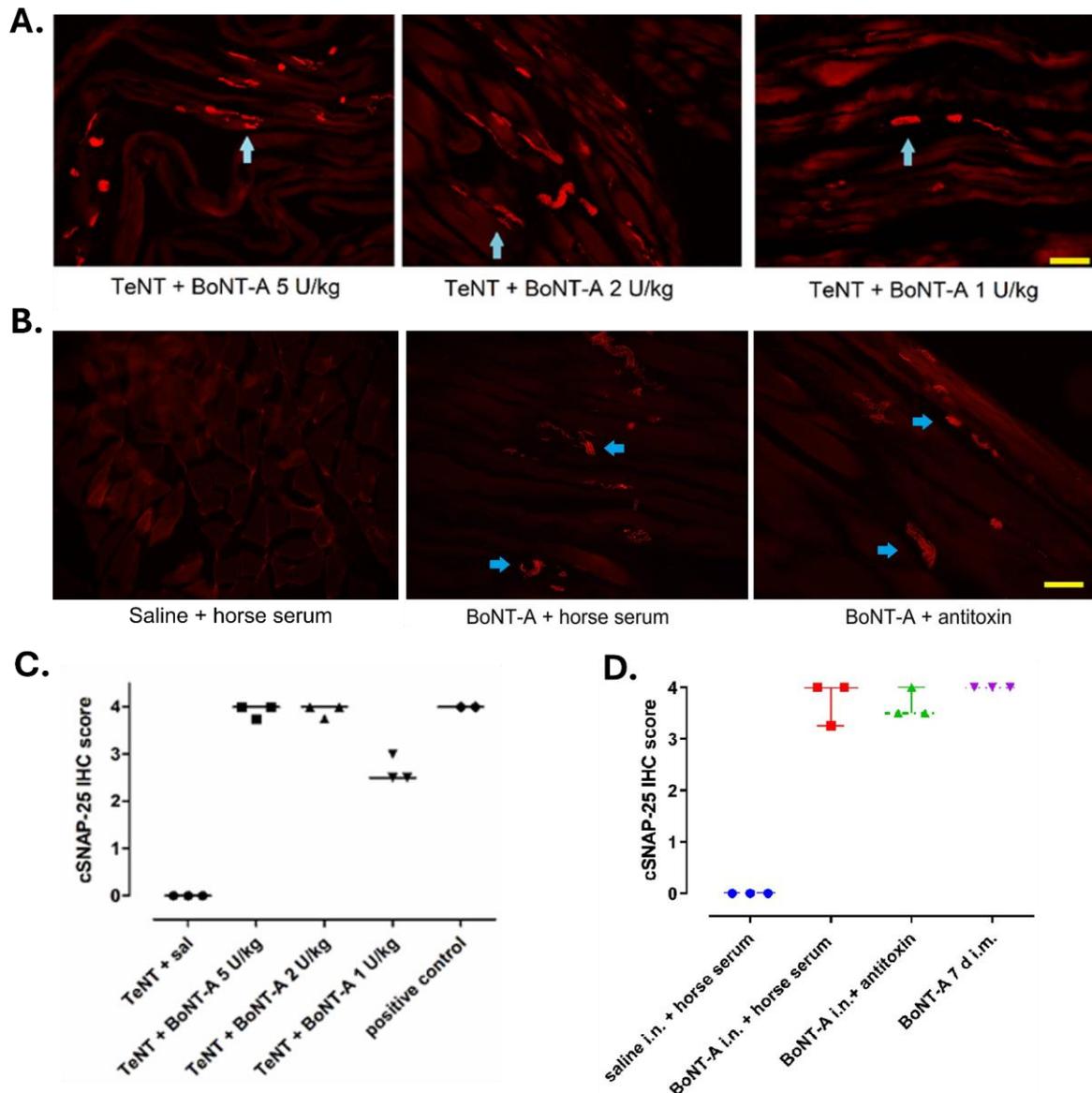
Figure 24. The peripheral muscular enzymatic activity of BoNT-A following its injections in hind leg muscle or sciatic nerve. *Presence of cleaved SNAP-25 (cSNAP-25) was assessed in muscles on day 71 post BoNT-A (5,2, and 1 U/kg) injections into gastrocnemius muscle. In (A), red immunoreactivity indicates the presence of neuromuscular junctions and nerve terminals positive for cl-SNAP-25 (cyan arrow; scale bar = 100 μm). The scoring method C), adapted from Périer et al., reveals a significant abundance of cleaved SNAP-25 in muscles, 2 months post treatment with BoNT-A (N = 3 animals per group, with 4 visual fields per animal from distinct sections), as well as in 2 positive controls (muscles treated with 5 U/kg BoNT-A 7 days before perfusion), (264) (Šoštarić et al., 2022; Appendix I). Images B.) and graph D.) represent peripheral enzymatic activity of axonally transported BoNT-A. After intraneural (i.n.)*

injection of BoNT-A at a dosage of 2 U/kg into the sciatic nerve, central trans-synaptic traffic was subsequently blocked using intrathecal (i.t.) administration of BoNT-A antitoxin. The presence of immunoreactivity for cleaved SNAP-25 was examined on day 78 post BoNT-A injection, with abundant immunoreactivity appearance of neuromuscular junctions and axons in the gastrocnemius muscle B.) (scale bar=200 µm). In panel D.), individual animal score values are represented by data points, with the horizontal bar indicating the median (N = 3 animals/group). (Šoštarić et al., 2024; Appendix II).

5.6.2. The role of BoNT-A entrance and peripheral action at neuromuscular junction

In a separate experiment we assessed the role of BoNT-A peripheral action on NMJ by employing latrotoxin i.m. injection (4 µg), before and post BoNT-A (5 U/kg) i.m. injection. The effects of α-latrotoxin are marked by rapid neuromuscular deterioration triggered by calcium influx, subsequently followed by swift axonal regeneration and restoration of motor function (254), consequently, serving as an effective model for investigating the action and entry of BoNT-A on peripheral motor terminals.

Destruction and fast regeneration of peripheral motor terminals by α-latrotoxin accelerated the recovery of motor function, both visible on digit abduction score analysis and as a performance during gait ability. I.m. BoNT-A injections induced substantial impairment of toe-spreading reflex (DAS=2) that recovered slowly by day 43 (Figure 25 A, unpublished data). Neuromuscular destruction following latrotoxin injection one day prior BoNT-A (group Latrotoxin + BoNT-A) induced slightly higher impairment of toe-spreading reflex that reached its peak at day 3 post BoNT-A and recovered by day 21. The latrotoxin treated animals 3 days post BoNT-A (BoNT-A + latrotoxin) exhibited greatly reduced ability to spread their toes, yet intoxicated neuromuscular junctions quickly recovered, with almost normal toe reflex occurring at day 15 (Figure 25, unpublished data), suggesting a slightly quicker recovery than the Latrotoxin + BoNT-A group.

Intramuscular injections of BoNT-A led to diminished functional use of hindlimbs and notable alterations in the stance of injected hind paw, that displayed an arched appearance of the foot soles and toes, similar as portrayed in figure 16. This characteristic indicative of weakened paw plantar flexors, with other gait ability parameters ended in reduced gait ability score, with substantially longer recovery compared to DAS score (incomplete at day 71 vs almost complete

by day 43) (Figure 25, unpublished data). Similarly to DAS score, the latrotoxin treated animals exhibited shorter recovery of the gait ability score compared to BoNT-A + horse serum group, with somewhat faster recovery in the BoNT-A + latrotoxin vs Latrotoxin + BoNT-A group, which was also evident as differences in area under the curve (AUC) during recovery period between days 3-71 post BoNT), (Figure 25, unpublished data).
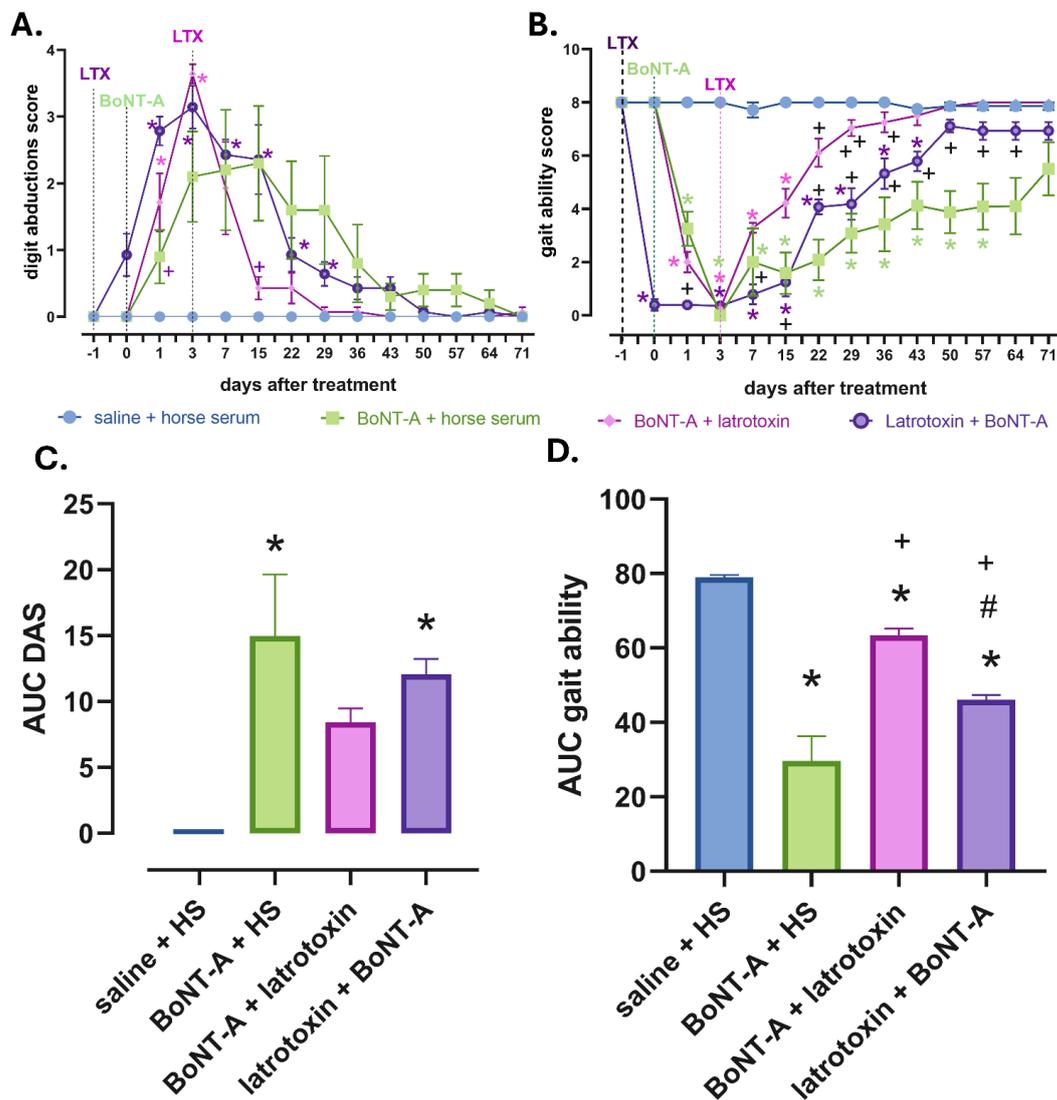
Figure 25: The recovery of BoNT-A-evoked local muscle weakness and impaired motor function depends on toxin entry and established action at the neuromuscular junction. *The time course of the effects of intramuscular (i.m.) BoNT-A (5 U/kg) in combination with destruction and fast regeneration of peripheral motor terminals by i.m. injections of α-latrotoxin (4 µg, administered either before or after BoNT-A) on digit abduction score (DAS) (A) and gait ability (B), as well as their AUC values calculated for the recovery period (days 3-71) (C and D). Horizontal lines in graphs (A and B) indicate the time points of latrotoxin*

Automated gait lab analysis was employed to assess static and dynamic parameters of motor function following intramuscular (i.m.) BoNT-A application following latrotoxin-induced neuromuscular destruction. Animals were pre-trained to walk freely on the LED-lighted, transparent plexiglass walkway and return to the home cage. Rodents' normal gait is characterized by a symmetrical pattern, balanced with an equal amount of time spent on their left and right limbs (269). While control animals exhibited consistent velocity and normal gait characteristics, all BoNT-A treated animals showed a significant decline in speed on day 15, gradually recovering after day 22. Both latrotoxin-treated groups showed variably decreased speed throughout the experiment (Figure 26). We further investigated static and dynamic parameters specifically related to balance and gait pattern, such as the length of the hindlimb, swing time, and base of support, which can be affected by both muscular weakness and spinal motor activity. The length of the right hindlimb print, a parameter describing the length of the right hindlimb paw that leans against the surface during stride, was increased in BoNT-A animals, peaking between day 3-15, followed by a gradual decline after day 22. The elongation of the hind paw print was consequent to the weakness of the injected plantar flexors (gastrocnemius) and heel weight bearing (see the gait ability analysis). Latrotoxin + BoNT-A animals showed a milder peak in longer paw length between day 8-15, which recovered by day 43. BoNT-A + latrotoxin animals had increased length on day 8 and quickly recovered by day 22, remaining consistent throughout the experiment (Figure 26). Similarly, the swing time of the right hindlimb (the time during which the animal does not put the paw on the soil) was increased for both BoNT-A and latrotoxin treatment groups (Figure 26), contributing to slow and unbalanced motion. This was also evidenced by another static parameter, hindlimb base of support (BoS), which describes the distance between two hindlimb paws. BoNT-A treated rats exhibited a decreasing BoS of hindlimbs, which did not recover during the experiment. BoNT-A + latrotoxin animals peaked in decline between day 8-15 and then gradually recovered by day 29. Latrotoxin injected one day prior to BoNT-A caused a sudden decrease in BoS, probably induced by its prominent muscular weakness. This weakness exhibited a sudden improvement on day 3 but subsequently declined again between days 3 and 8, with the base of support remaining consistently decreased throughout the experiment in these animals (Figure 26).
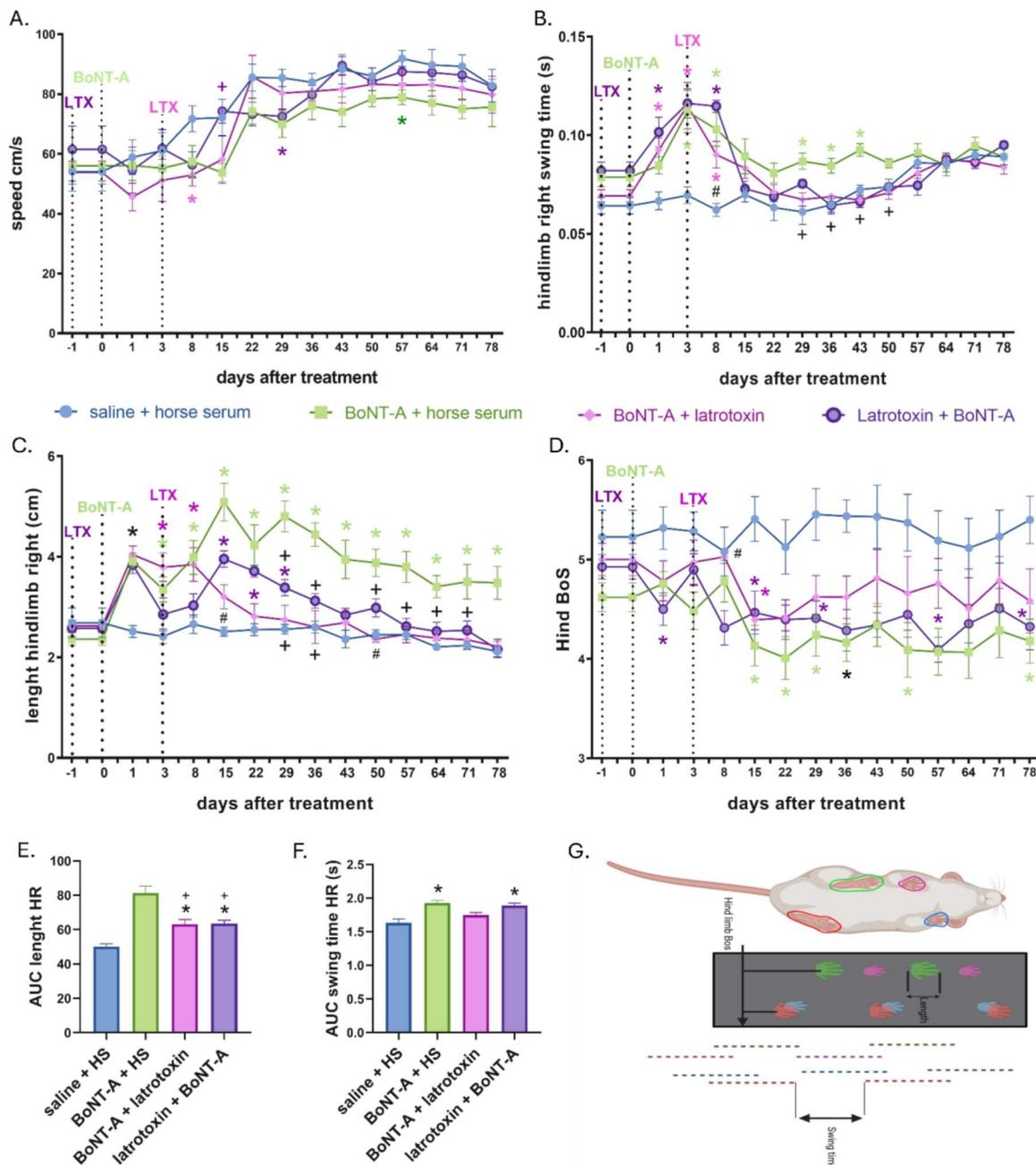
Figure 26. Effects of BoNT-A and latrotoxin on the impairment and recovery of static and dynamic gait parameters. *The effect of i.m. BoNT-A 5 U/kg in combination with i.m. latrotoxin (pre- or post treatment) on gait speed (panel A), static (panels C and D), and dynamic (panel B) gait parameters. The intensity of recovery of motor functions and muscle paralysis was quantified by length of paw prints (elongated by heel weight bearing) (panel C and E) and swing time (panel B and F). Image (panel G) represents a schematic interpretation of parameters assessed by the Gait Lab catwalk analysis software in graphs. Horizontal lines in graphs (panels A, B, C, and D) indicate the time points of latrotoxin and BoNT-A treatments.*

Furthermore, we investigated the long-term antispastic effects following intramuscular injections of BoNT-A (5 U/kg). On day 80 post i.m. BoNT-A, TeNT was injected in the same gastrocnemius muscle to induce local muscle spasm of the hindlimb. BoNT-A effect on spasm and locomotor deficits after TeNT injection were evaluated by previously explained test (dorsiflexion resistance test and BBB score) (Figure 27, unpublished data). Beneficial antispastic effects of i.m. BoNT-A persisted up until day 109 post i.m. injection, evident as reduced dorsiflexion resistance or less impaired locomotor function scored by BBB scale (Figure 27). The beneficial effects of BoNT-A on TeNT-evoked muscle spasm assessed by dorsiflexion was reduced by the latrotoxin treatments. However, the influence of latrotoxin-evoked destruction of NMJs on BBB locomotor scale indicating the beneficial functional effects of BoNT-A depended whether the latrotoxin blocked BoNT-A entrance via NMJs (latrotoxin + BoNT-A), or whether latrotoxin destroyed the BoNT-A-poisoned NMJs (BoNT-A + latrotoxin). The beneficial action of BoNT-A on the locomotor BBB scale was unaltered by latrotoxin pretreatment, while it was deficient in rats treated with latrotoxin on day 3 post BoNT-A, exhibited as high scores in dorsiflexion test (Figure 27) and impaired locomotor scores (Figure 27) resembling those observed in control-treated animals. These results suggest important functional role of peripheral motor terminals in long lasting antispastic activity of BoNT-A, however, the locomotor function amelioration can ensue if BoNT-A is allowed to enter the nerve through the remaining or recovering muscle terminals.
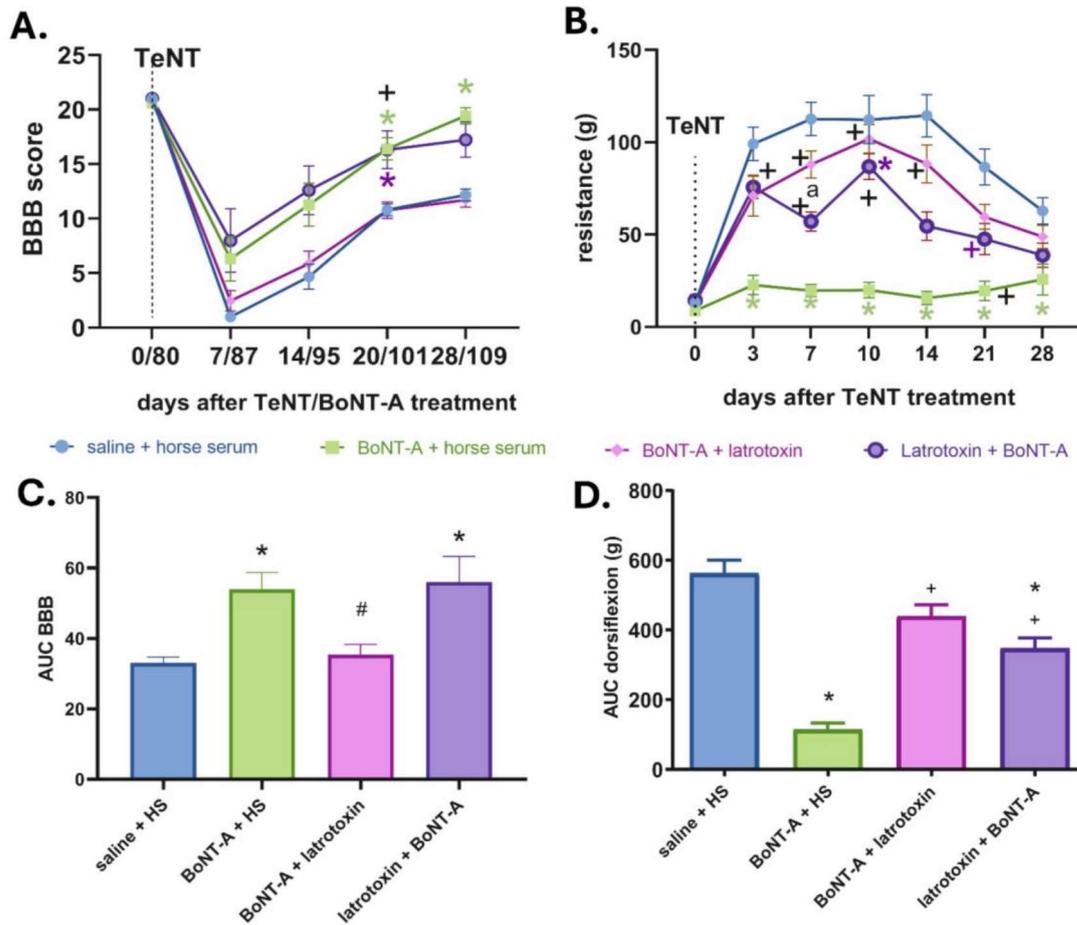
Figure 27. Peripheral effects of BoNT-A on muscle spasm and locomotor deficit. *These graphs demonstrate the enduring antispastic activity of intramuscular BoNT-A (5 U/kg) and underscore the significant contribution of the neuromuscular junction to the persistence of BoNT-A antispastic effects. Elevated dorsiflexion resistance, depicted as the ratio of resistance to muscle weight due to muscle atrophy (B and D), and the recovery of motor performance evaluated through BBB scores (A and C), are observed in latrotoxin-treated animals following TeNT-induced spasticity. Horizontal lines indicate days of TeNT treatment. Mean ± SEM, N=6-8/group. *- P < 0.05, vs. saline + horse serum; +, P < 0.05, vs. BoNT-A + horse serum, a, P < 0.05 vs. latrotoxin + BoNT-A; # P < 0.05, vs. latrotoxin + BoNT-A (two-way RM ANOVA or one-way ANOVA followed by Tukey's post hoc analysis), (Unpublished data).*

Further we assessed peripheral action of BoNT-A and its role on reduction in muscle mass after i.m. injections of BoNT-A (5 U/kg) and pre or post administrated latrotoxin. Soleus and gastrocnemius muscles exhibited significantly reduced total muscle weight after i.m. BoNT-A injections, while tibialis anterior muscle, showed mild reduction in mass. Latrotoxin treatments

showed less reduced total muscle weight, suggesting that recovery of muscle atrophy after BoNT-A treatment is at least partially dependent on peripheral motor terminals and sustained peripheral synaptic activity (Figure 28, unpublished data).
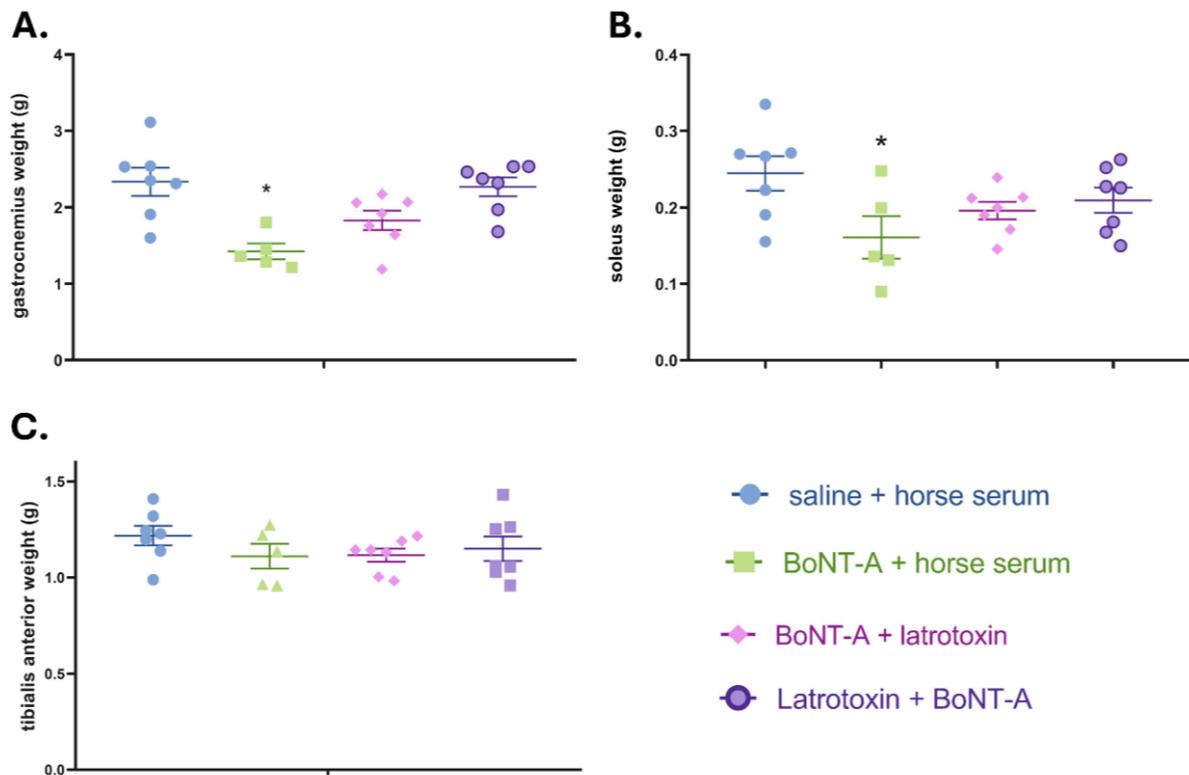
Figure 28. Peripheral motor terminals are involved in a recovery of BoNT-A induced muscle atrophy. *I.m. BoNT-A (5 U/kg) induced significant loss in muscle weight of gastrocnemius A.) and soleus muscle B.), but not the uninjected tibialis anterior C.) (Unpublished data). Latrotoxin treated animals (1 day prior BoNT-A and 3 days post BoNT-A) both showed less reduction and greater recovery of muscle weight in all three dissected muscles, thus suggesting an important role of neuromuscular junctions in mediating BoNT-A induced muscle atrophy. Mean ± SEM, N=6-8/group. *- P < 0.05, vs saline + horse serum (one way ANOVA analysis), (Unpublished data).*

Furthermore, we assessed the presence of cleaved SNAP-25, 109 days after administering BoNT-A (5 U/kg) into the rat gastrocnemius. To challenge the entry of BoNT-A, we pre-damaged NMJs in the gastrocnemius muscle by injecting latrotoxin one day before BoNT-A administration. Subsequently, in separate animals, latrotoxin was injected on day 3 after BoNT-A treatment to examine the toxin's effects on peripheral terminals. In the gastrocnemius muscles

of animals treated with BoNT-A (5 U/kg), we observed abundant cleavage of SNAP-25 in the ventral horn of the spinal cord (Figure 29). However, pre-damage of NMJs induced by latrotoxin injection in the gastrocnemius muscle reduced the amount of SNAP-25 cleavage in spinal synapses (Figure 29). A similar, less profound effect was observed in post BoNT-A-induced intoxication of muscles with latrotoxin, resulting in apparent (non-significant) reduction of SNAP-25 cleavage (Figure 29), suggesting that an existing nerve terminal in the periphery is important for the axonal transport of BoNT-A.
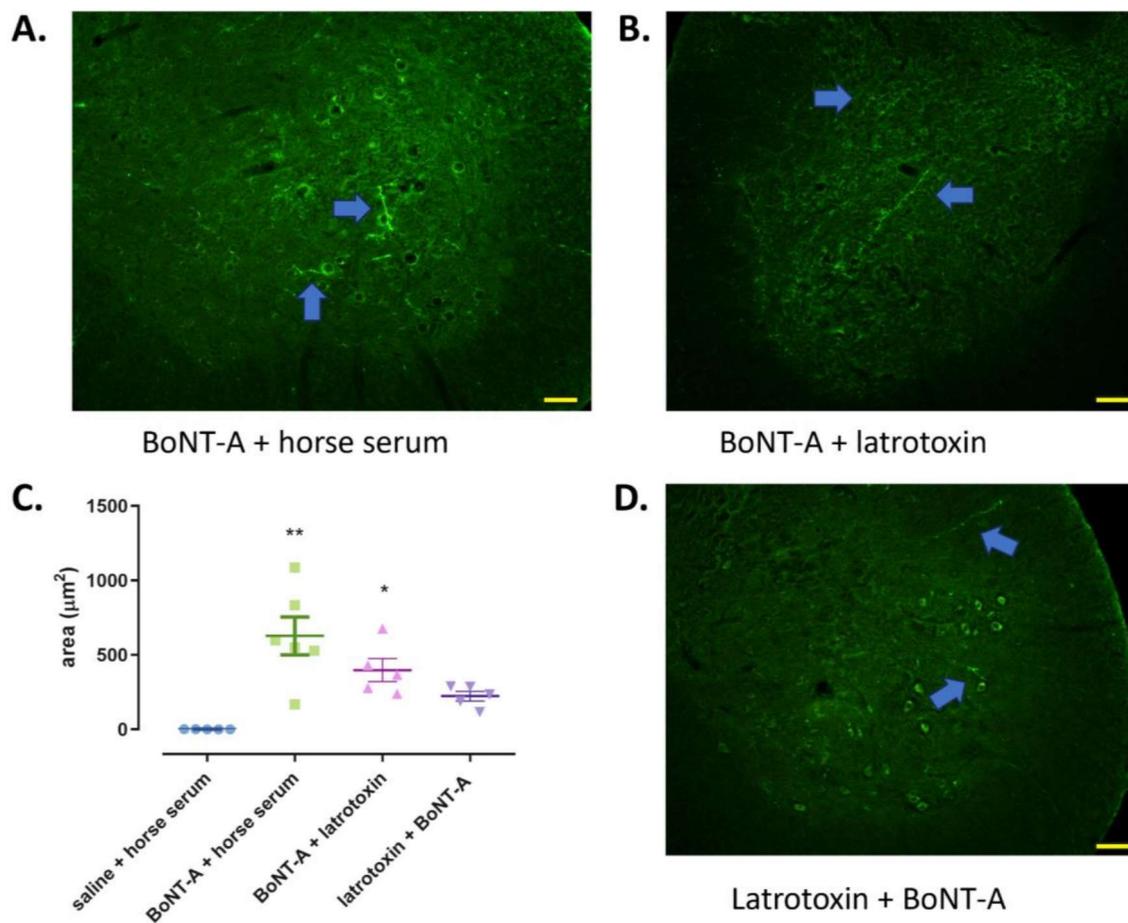
Figure 29. The effects of latrotoxin pre- or post-treatment on the occurrence of BoNT-A enzymatic product in the spinal cord following 109 days, post BoNT-A i.m. treatments. *BoNT-A (5 U/kg) and latrotoxin (4 µg, 1 day before or 3 days post BoNT-A) were injected in the gastrocnemius muscle and the presence of BoNT-A cleaved SNAP-25 was examined in ventral horn of spinal cord (L3-L5) on day 109 post BoNT-A, as depicted on images A), B) and D). The quantification of cleaved SNAP-25 in the ventral horn of the spinal cord involved summing the pixel intensity-thresholded area across six distinct visual fields as showed in graph C). These fields, each measuring 0.14 mm^2, were evenly distributed with three fields assessed*

per side (left and right). An average of four slices per animal were analyzed for this purpose. The study encompassed five animals per group, and statistical analysis was conducted using Kruskal-Wallis followed by Dunn's post hoc test (*,**- P < 0.05, 0.01 vs. saline i.m. + horse serum; median ± range), (Unpublished data).

5.7. Characterization of intramuscular and central effects of BoNT-B and TeNT

5.7.1. Characterization of antibody to cleaved VAMP-2 in muscle and cell culture of central neurons

To assess antibody specificity in detecting cleavage by TeNT and other clostridial neurotoxins targeting vesicle-associated membrane protein (VAMP), cerebellar granule neurons were intoxicated for 12 hours, and their protease activity was monitored using Western blotting (Figure 30). TeNT proteolytic activity was typically monitored using a VAMP-2 specific commercial antibody, which exhibits a decreasing signal upon cleavage, as demonstrated with increasing TeNT concentrations (0.5-50 pM) (Figure 30). Moreover, a bright signal at lowest TeNT concentration (0.05 pM) suggests insufficient sensitivity to observe reduction of VAMP-2 signal. However, when stained with Ab-VAMP77, a clear bend is observed at lower, less detectable toxin concentrations, indicating that Ab-VAMP77 is more sensitive in detecting TeNT-mediated VAMP-2 proteolysis (Fabris et al., 2022, Appendix III).
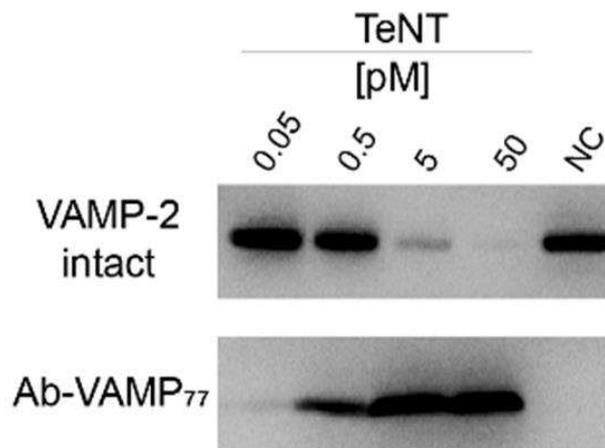
Figure 30. The Ab-VAMP77 exhibits a high level of efficacy in detecting cleaved VAMP-2 within neuronal cultures. *A Western blot comparison illustrates the heightened sensitivity of Ab-VAMP77 relative to a conventional antibody when exposed to low concentrations of TeNT (0.05 and 0.5 pM). NC - neurons not treated, acting as a negative control (Fabris et al., 2022; Appendix III).*

5.7.2. Cranially-injected TeNT (and BoNT-B) induces muscular paralysis of facial muscles dependent on VAMP-1

Injecting TeNT locally into the mouse whisker pad mimics human botulism toxin effects, as well as the cephalic tetanus-evoked flaccid paralysis, providing a model for studying its pathophysiology. This approach allows for real-time monitoring of neuromuscular activity through vibrissae movement analysis and electromyography. While naïve mice freely move their vibrissae, unilaterally treated mice with TeNT injection in WP, progressively lose vibrissae movement capability, displaying ipsilateral flaccid paralysis starting as early as 1 day post TeNT and persisting for several days.

However, on the other hand contralateral vibrissae show delayed spastic paralysis, fully visible on day 5 post TeNT (Fabris et al., 2023; Appendix IV). Characterisation of paralysis type was assessed by CMAP electromyographic analysis. When facial nerve stimulation exhibited normal CMAP values in contralateral WP, ipsilateral side of injected WP exhibit reduced CMAP values at all time points. This sudden reduction in NMJs on ipsilateral side characteristic feature of flaccid paralysis induced by botulinum neurotoxins. Interestingly, comparison with BoNT/B-induced paralysis revealed similar effects (Fabris et al., 2023; Appendix IV). These results suggest that TeNT-induced paralysis is reversible within days and remains localized to injected muscles.

To provide further evidence of VAMP cleavage and TeNT induced flaccid paralysis, separate experiment was conducted in rats. Rats are carrying a point mutation at cleavage site of VAMP-1, making it resistant to TeNT proteolysis. Vibrissae movements were examined and monitored from proximal and distal positions with respect to caudal part of the body, in both naïve (control) and injected WP of treated rats. However, no visible alterations in both treatments and injected and uninjected WPs was observed (Figure 31), until day 3 and full paralysis developed at day 5 (Fabris et al., 2023; Appendix IV). To determine is developed paralysis of WP, flaccid or spastic, facial nerve of both, ipsilateral and contralateral side was stimulated by electrodes and CMAP was measured for analysis. Normal neuromuscular transmission was noticed in both sides of WP, with unaltered CMAP values at day 7, at the time of fully developed spastic paralysis (Figure 31). Muscle of WP underwent immunohistochemical detection of possible cleavage of VAMP in the nerve terminals. However, there was no detectable signal of cleaved VAMP in injected WP of the rat (Fabris et al., 2023; Appendix IV). Taken together, these results are suggesting that TeNT can cleave VAMP-1 in the cytosol of peripheral nerve terminal of

injected muscles, thus causing a reversible flaccid paralysis similar to the one caused by botulinum toxin (in susceptible species like humans and mice), which may explain the seemingly paradoxical occurrence of flaccid paralysis in cephalic tetanus (Fabris et al., 2023; Appendix IV).
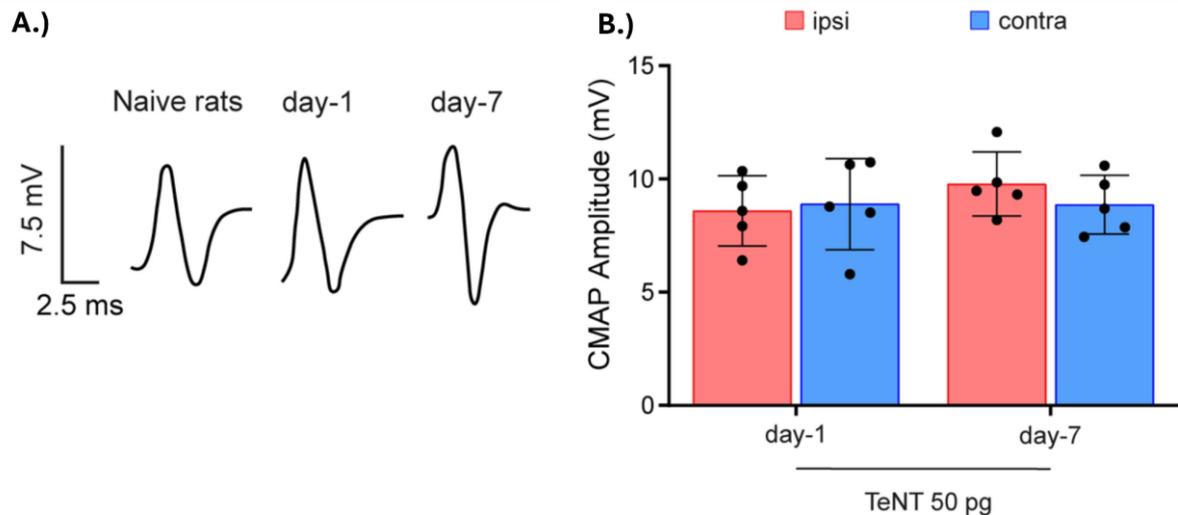
Figure 31. Rat's VAMP-1 at peripheral motor terminals insensitive to TeNT cleavage and its subsequent peripheral neuroparalysis. *Representative CMAP recordings post-TeNT injection in the WP A) and their quantification B) suggesting a lack of peripheral neuroparalytis due do single point mutation. Data are presented as means ± SD, 1 black circle=1 animal; (Fabris et al., 2023; Appendix IV).*

6. DISCUSSION

In the present PhD thesis we characterized the central effects of BoNT-A in the motor nervous system, having in mind the peculiarities of its clinical action. By characterising the duration of the toxin's antispastic activity in relation to its central actions, we attempted to clarify the clinical observations that beneficial actions may exceed the intensity and duration of peripheral paralysis (Šoštarić et al., 2022; Appendix I). In addition, for the first time we examined if the central premotor inputs targeted by BoNT-A are involved in normal locomotor performance, which might explain the normalisation of hyperactive muscles and poor motor control in BoNT-A-treated dystonic patients (Šoštarić et al., 2024; Appendix II). In addition, we characterized the effects of TeNT on the neuromuscular transmission and peripheral VAMP cleavage in rats and compared it to the known effects in mice, to explain the seemingly paradoxical flaccid neuroparalysis in highly severe form of tetanus poisoning called the cephalic tetanus.

6.1. The duration of beneficial effects of BoNT-A is determined by the dose and is dependent on central toxin action

In the initial set of preclinical experiments made in rats, we found that the dose employed in the spastic muscle determines the duration of beneficial BoNT-A effects, but not their initial intensity. In addition, we found that the toxin's central actions contribute to the long duration of the toxin's antispastic actions (Šoštarić et al., 2022 Appendix I).

The discovery by A. Burgen and his colleagues in 1949 (36), linking the paralytic effect of botulinum toxin to the prevention of acetylcholine release from peripheral motor terminals, proposed the neuromuscular junctions as the primary site of toxin activity and, upon the inclusion of BoNT-A into clinical use, also as the primary site for therapeutic efficacy for the toxin. In clinical practice, local delivery of this neurotoxin has proven successful in reducing muscle hyperactivity in conditions like spasticity and dystonia, while also providing long-lasting pain relief. Injection of low dose BoNT-A into smaller human muscles induces muscle relaxation that persists for several months (270). Despite the ongoing presence of the neurotoxin and the need to reinject the patients as the beneficial effects wane, intoxication of peripheral nerve endings with BoNT-A is completely reversible and does not induce terminal degeneration (161). The reversible muscle-weakening effect of BoNT-A, coupled with the preservation of neuromuscular junctions, has made it a widely popular therapeutic "denervation" agent. However, there are quite a few inconsistencies with beneficial effect of the toxin that can not

be explained solely by its "denervating" action on the peripheral nerve terminals. Physicians reported dissociation of the neuroparalytic weakness of the muscle and clinical benefit, which sometimes outlasts the paralytic effect of the injected muscle, or, oppositely, patients demanding sooner re-treatment due to experiencing lower duration of BoNT-A beneficial effect, despite evident muscle flaccidity (7,9,200,188). Furthermore, BoNT-A antispastic effect is mostly correlated with its muscle weakening action. However, BoNT-A decreases not only the severity but also the frequency of muscular spasms, as shown in patients with blepharospasm and torticollis (90,197,199,271); thus, indicating a possible additional effect of the toxin. In line with the lasting belief that peripheral neuroparalysis is the sole mechanism of BoNT-A action, preclinical studies of BoNT-A effect on muscle with increased muscle tone have been scarce (196). Furthermore, experimental models characterized by muscle hypertonia have its limitations such as irreversible damage at the level of cortex or spinal cord and a more generalized presentation in wider body regions, thus possibly not allowing the investigation of BoNT-A actions in individual muscles. To avoid these limitations, Matak used single low dose-TeNT (1.5 ng) injection into the gastrocnemius muscle of the rat to induce transient focal spasticity (lasting approx 2-3 weeks), thus mimicking disbalance between excitatory and inhibitory input on spinal motor pools present in spasticity and hyperkinetic movement disorders (13). Presently, we employed the transient nature of TeNT-evoked spasticity to examine the effect of single dose BoNT-A at different time points: during the early prominent neuroparalytic phase of BoNT-A action (first 2 weeks), as well as at a later phase when its neuroparalytic effects largely recover (after day 49), (Šoštarić et al., 2022; Appendix II).

We evaluated the progression of spasticity subsequent to first TeNT injection, as well as the subsequent treatment with BoNT-A injection into spastic muscles, using various established behavioral motor tests designed for locomotor evaluation in rodents. Dose response of antispastic effect was evaluated by employing a range of doses (1-5 U/kg) in rats which also correspond to low-moderate doses commonly employed in clinical practice (corresponding to 70–350 U in an average 70 kg human). TeNT injection into the muscle induced slow onset increase in muscle tone (evident as increased passive resistance to dorsiflexion, as well as compromised locomotion assessed by BBB scale) first visible after 2-3 days, peaking at day 7; and recovering by day 21 post TeNT.

In the early period following BoNT-A injection into the spastic gastrocnemius muscle, (injected 7 days post TeNT), we observed rapid and complete reversal of TeNT-induced hindlimb

spasticity and locomotor impairments (Figure 13). Additionally, an early onset of flaccid paralysis was indicated by the impaired toe-abduction reflex starting one day after BoNT-A treatment (Figure 13). Thus, seemingly, this rapid onset of BoNT-A antispastic activity, observed in clinical setting, is characterized by its initial neuromuscular paralytic effect, which is not necessarily associated with higher BoNT-A doses (6,272). In contrast, the toe spreading reflex impairment (evident as elevated DAS score), varied depending on the dosage, affecting both peak intensity and duration (Figure 13). Considering that the fascial boundaries between muscles as potential barriers appear to be penetrable to the toxin (273), allowing nearby muscles to potentially be affected, it is essential to recognize that DAS impairment reflects the diffusion of BoNT-A into adjacent muscles involved in toe abduction, rather than solely its localized action within the injected gastrocnemius (256,264). The doses employed (1-5 U/kg) in this experiment likely caused significant to almost complete synaptic silencing of neuromuscular junctions in the injected muscle in a brief period following BoNT-A treatment (217,274). This could explain the absence of dose-dependent variation in the antispastic action of BoNT-A during the early period following intramuscular treatment. However, it may account for the observation of more prevalent local side-effects in patients evoked by diffusion into unwanted muscles, when treated with higher toxin doses.

Previous research indicates that the function of the neuromuscular junction, as characterized by CMAP values, shows a recovery of approximately 35% within one month and 86% within 84 days when a similar intramuscular dose is employed (274). By comparing the recovery of CMAP following BoNT-A application as an indicator of muscle function recovery, it can be inferred that animals treated with the doses administered (1-5 U/kg) are likely to recover within 1-2 months. In accordance, the arch-like appearance of the paralyzed hind paw or weight-bearing using the heel during stance was restored in all BoNT-A-treated animals. However, the reduction in lower leg muscle size remained consistent across all doses, with no notable improvement observed throughout the experiment.

To explore the lasting effects of BoNT-A at the later time point when the recovery was considerable, we induced muscle hypertonia once again with a second tetanus toxin injection on day 49 after the initial BoNT-A treatment. Higher doses (5 and 2 U/kg) maintained their antispastic effect by completely normalising the TeNT-evoked muscle spasm, proving to be beneficial for over two months. However, the lowest dose (1 U/kg) lost efficacy against the tetanus toxin-induced locomotor deficit and showed less effectiveness in reducing muscle tone.

These results are in line with clinical observations reporting longer treatment duration with higher doses. In a comparative study on cervical dystonia, the highest dose group (1000 U) demonstrated the longest duration of effect after 8 weeks compared to lower dose groups (250 and 500 U (275). Later study in patients with spastic hemiparesis and upper limb spasticity after stroke, also supported the theory of dose dependent duration of BoNT-A treatment, respectively (276). Different conversion ratios of abobotulinumtoxinA vs onabotulinumtoxinA also exhibited different efficacy at 12 weeks post-treatment, in line with higher amount of toxin protease delivered after abobotulinumtoxinA treatment (277). Careful consideration of doses and potential adverse effects is crucial before using higher toxin doses in patients. When referring to late beneficial effects of BoNT-A we are referring to the effects that persist beyond the period of prominent local muscle weakness associated with peripheral neuroparalysis. During this phase, patients may continue to experience a lack of pain or discomfort, and may also see a reduction in spastic co-contractures. Occasionally, beneficial effects can emerge even with the use of very small doses of BoNT-A, to the extent that muscle weakness may not be visibly apparent, yet the positive effects are still exerted (201).

Furthermore, clinical observations have identified a distinct time gap in the antispastic action of BoNT-A, characterized by either a prolonged or shortened interval between BoNT-A injection and observable clinical improvement, thereby suggesting two distinct phases of clinical response. The delayed clinical response is difficult to explain solely by only peripheral blockage of neuroexocytosis. In some cases of torticollis, clinical improvement was present after 6 weeks post BoNT-A treatment (193). In spastic paralysis, abnormal muscle synergies and/or cocontraction may be a major factor limiting active movements. Clinical benefit, that is, a wider range of movement at the ankle joint in spastic patients, is present 1 month after BoNT-A injection into the soleus muscle, in spite of little peripheral blockade (201).

Following the observation that higher toxin dose correlates with prolonged antispastic action, we explored the possibility of its action at central synapses contributing to this sustained efficacy. In line with the results of our previous studies (10,13) this led us to investigate whether BoNT-A antispastic effects could be attributed to its activity at central second-order synapses targeted by the toxin's trans-synaptic traffic. To examine this, in a separate experiment we administered BoNT-A i.m. into the right gastrocnemius, followed by intrathecal injection of BoNT-A neutralizing antitoxin one day later to inhibit its central transcytosis. This experimental setup allowed the toxin to exert its activity on peripheral motor terminals in the

injected muscle while preventing its axonal transport and transsynaptic activity in spinal motor circuits. After animals recovered from peripheral muscle weakness, local muscle spasm was induced by small doses of TeNT on day 50 post BoNT-A in the same gastrocnemius muscle (Šoštarić et al., 2022; Appendix I). We found that the antitoxin partially counteracts the beneficial BoNT-A effects on the muscular spasm, as well as the locomotor deficits assessed by the BBB score. To clarify the interpretation of the antitoxin experiment results, it is important to note that animals receiving i.m. BoNT-A (with i.t. horse serum as a control), experienced unopposed BoNT-A activity in both peripheral muscular and central spinal sites. However, animals treated with BoNT-A + i.t. antitoxin should have experienced unopposed peripheral toxin effects, while central effects should depend on the transcytosis being prevented by the neutralizing antitoxin. Given the short half-life of synaptic proteins such as SNAP-25 (278), the persistent presence of actively cleaving BoNT-A, even two months post-application in peripheral muscles, underscores the enduring enzymatic potency of BoNT-A. In the ventral spinal cord, the cleaved SNAP-25 suggests a continuous central presence of active BoNT-A protease. Notably, the quantity of cleaved SNAP-25 in the central nervous system correlates with the administered dose of BoNT-A suggesting that the maintained antispastic efficacy of the higher doses (2 and 5 U/kg) is associated with the higher amount of centrally active protease. This phenomenon of delayed role of central antispastic action can be theoretically attributed to the gradual reduction in active BoNT-A protease at pivotal synaptic sites in both peripheral and central regions over time, with higher doses preserving their antispastic efficacy for an extended duration period (Šoštarić et al., 2022; Appendix I).

6.2. Centrally transported BoNT-A affects premotor inputs participating in normal locomotion

In the aforementioned study (Šoštarić et al., 2022; Appendix I) we found that the antispastic effects of intramuscularly applied BoNT-A are at least partially contributed by the toxin's central actions at the spinal cord level, mediated by its trans-synaptic traffic into premotor synapses that regulate pathological motoneuronal excitability. This possibility is in line with previous studies from our laboratory, wherein enzymatic BoNT-A actions were found to be present at the level of cholinergic synapses surrounding the motor neurons (10,83), possibly indicating the BoNT-A action at C-boutons derived from V0C excitatory propriospinal cholinergic interneurons. This type of synapse is known to reduce the afterhyperpolarization (AHP) phase of motor neuron activation and, thus, upregulate the motoneuronal activity. In

normal mice, only certain types of locomotor behavior requiring high intensity task such as swimming are mediated by this type of neurons (279,267), while the role of these synapses in modulating the hyperreflexia and pathologically elevated muscle tone has not been examined. However, this type of synapse is dispensable for most other lower intensity motor tasks, and, in addition, TeNT-evoked disinhibition may target different inhibitory spinal circuits.

Thus, we examined the effect of trans-synaptic BoNT-A on the swimming performance vs other types of normal locomotion performance. The findings that BoNT-A actions in dystonia that restore the normal locomotor function requiring a defined task e.g. writing or playing a musical instrument in occupational dystonia (99), indicate the possibility that its beneficial actions on muscle hyperactivity may address locomotor circuits regulating the task-directed complex voluntary movement. To maximise the chance of detecting the effects of BoNT-A on normal motor function and locomotor circuits, we investigated its impact on tasks requiring the activation of different muscle groups in both hind limbs. BoNT-A was therefore bilaterally injected into the sciatic nerve at the mid-thigh level to affect all motor units of the lower leg and foot. We then assessed the toxin's effect on fine motor coordination and balance in tasks involving simultaneous use of different muscle groups. We observed a significant reduction in motor performance in these tasks following BoNT-A administration, with faster recovery observed in the beam walk test compared to the rotarod test. When comparing the outcomes of bilateral and unilateral BoNT-A intrasciatic injections characterized before (13), previously it was observed that unilateral injection resulted in non-significant decline in beam walk performance, possibly attributable to compensation by the untreated contralateral limb during the specified motor tasks. Furthermore, rodents are more capable of compensating unilateral motor deficit when performing different motor test (259). Additionally, we monitored the development of classic signs of local muscle weakness. Animals exhibited a mild deficit in toe abduction reflex, which quickly recovered 14 days post BoNT-A treatment (Figure 16). Furthermore, an arch-like appearance of the paw during sitting or walking and inability to lift the heel during terminal stance by reliance on interdigital paw pads and toes only during slope walking, indicated long-term weakness of the plantar flexors (257,258).

These motor deficits took longer to recover compared to the toe abduction reflex, with recovery time-course similar to the rotarod test. As previously discussed, not all the beneficial effects of BoNT-A can be solely attributed to its peripheral action on extrafusal muscle fibers responsible for muscle contraction force, and/or intrafusal fibers containing muscle spindles. The muscle

spindles are delicate structures sensitive to muscle stretch and are innervated by gamma motoneurons and Ia primary afferents. While some effects of BoNT-A can be explained by its action on both extra- and intrafusal fibers, recent clinical observations and research suggest the involvement of additional action sites reached via retrograde transport and central transcytosis (10,13,84).

Clinical benefits are evident in observations of spastic and dystonic patients, while basic research sheds light on BoNT-A transport and the presence of its enzymatic products in central synapses. However, studies providing functional evidence of BoNT-A effects on motor synapses, correlated with findings of central BoNT-A cleavage, are limited (13), (Šoštarić et al., 2022; Appendix I). Similarly as before, in order to evaluate the contribution of the BoNT-A effect on central synapses we administered i.t. BoNT-A neutralizing antitoxin into cauda equina. As it would be expected if BoNT-A affected the cholinergic C-bouton premotor inputs (V0$_C$ interneurons), we observed the transient reduction of swimming performance that is dependent on the central trans-synaptic toxin action (Figure 17). However, other examined motor tasks involving coordinated skilled locomotion (not mediated by C-boutons) were also affected by the central toxin action, including the transient hind-paw weakness affecting the DAS and gait ability (Figures 16). These findings suggest that centrally transported and transcytosed BoNT-A may affect different types of premotor inputs that participate in different motor tasks. Moreover, in the same animals we investigated whether the central activity of i.n. BoNT-A on motor circuits could also exhibit the late antispastic effect. We re-injected the animals with TeNT (1.5 ng) on day 62 post BoNT-A to evaluate the i.n. BoNT-A antispastic effects. We noted that BoNT-A continued to alleviate the calf spasm induced by TeNT between days 65 and 77, even though all peripheral motor indicators had largely or fully recovered by day 56 (see Figure in Šoštarić et al., 2024; Appendix II). Thus, it may be posited that central premotor inputs involved in both regular locomotion and involuntary muscle spasms may be important targets of BoNT-A clinical action, resulting, in turn, in normalisation of motor performance. We further addressed these possibilities by characterizing the synaptic sites targeted by BoNT-A (see section 5.5.).

6.3.   Relieving effect of BoNT-A on TeNT-induced spasticity is not associated with its action on monosynaptic H reflex and Ia primary afferents

Following the evaluation of locomotor recovery, we further investigated whether BoNT-A might influence the central modulation of exaggerated monosynaptic stretch reflex, a characteristic feature observed in spasticity (280,281). Variations in the amplitude of the H-reflex following a conditioning stimulus are frequently employed to clinically assess either post-synaptic phenomena or adjustments in the degree of presynaptic inhibition affecting Ia afferent terminals (282).

For this purpose, we employed repeated H-reflex electromyographic measurement in animals that completely recovered their locomotor performance at day 62 post i.n. BoNT-A (before TeNT i.m.), but also after induction of TeNT-evoked unilateral spasm as a model of neuromuscular spasticity of central origin, which, conveniently, also exaggerates the H-reflex (283,253). As previously mentioned, despite the substantial or complete recovery of all peripheral motor parameters by day 56, BoNT-A demonstrated sustained efficacy in reducing TeNT-evoked muscle spasm from days 65 to 77. This persistent effect was once again attributed to BoNT-A central trans-synaptic action (see Figure 18). In contrast to that, the impact of BoNT-A on monosynaptic reflex excitability, as assessed by the H_{max}/M_{max} ratio, was not significant, both before and after TeNT-induced spasticity (refer to Figure 18). This observation is suggestive of the lack of direct BoNT-A effect on the synaptic strength between the Ia afferents and motoneurons, which also aligns with the absence of central cleaved SNAP-25 colocalization with large synaptic terminals positive for VGlut1, a marker of Ia terminals (Figure 20). In addition, since the elevation of H/M ratio evoked by TeNT was not altered by BoNT-A, irregardless of the antitoxin treatment, it can be posited that axo-axonal inhibitory synaptic contacts that influence the pathological elevation of monosynaptic reflex are not influenced by either peripheral intramuscular or central action of BoNT-A. This finding is consistent with previous clinical studies that have reported no significant effect of BoNT-A on the H/M ratio. Priori et al. (188) did a study on 12 patients with idiopathic segmental forearm dystonia, and when H and M were analyzed independently showed lower values, there was no change in H/M ratio. Furthermore, Mondugno et al. (284) did a study on 10 patients with essential hand tremor, and H and M waves were decreased, however the H/M ratio was not decreased. Girlanda et al. (285) performed a study on 20 patients with upper limb post stroke spasticity and showed similar results for H and M wave when measured for individual values,

but when combined for H/M wave ratio, it again showed no difference. However, recent results obtained in patients with poststroke spasticity (286), observed decrease in H/M ratio after BoNT-A injection in contrast to pretreatment values.

Regarding the possible role of BoNT-A targeting the intrafusal fibers and normal initiation of stretch reflex, it is important to note that H-reflex induction by peripheral nerve electrical stimulation circumvents the typical stretch reflex initiation at muscle spindles, thus, our findings and mentioned clinical reports did not assess potential direct or indirect actions of BoNT-A at peripheral intrafusal terminals. Nevertheless, the firm evidence for the role of BoNT-A's trans-synaptic traffic from present study demonstrates that BoNT-A beneficial antispastic action cannot be assigned entirely to its peripheral intramuscular (extrafusal or intrafusal) effects. Moreover, beneficial effects on dystonic or hyperkinetic conditions in the areas innervated by facial nerve (that does not possess muscle spindles) also suggest that intrafusal BoNT-A effects are not indispensable for exertion of its clinical benefit (10,287).

6.4. Neuromuscular junction as entry point of the toxin and its role in long-term action of BoNT-A

Following the aforementioned studies, which demonstrated that BoNT-A central activity contributes, at least in part, to its effects on normal muscle tone and its beneficial antispastic effects, we also aimed to evaluate the role of BoNT-A peripheral action and its entry at the level of the neuromuscular junction (NMJ). These studies indicated that: a) BoNT-A effects can be fully or partially circumvented by prevention of its trans-synaptic traffic, and b) that the BoNT-A injected directly into the sciatic nerve may exhibit full antispastic efficacy even with little neuroparalytic effect. Thus, as a possibility, it remained to be examined if central antispastic action of BoNT-A is sufficient for the exertion of late antispastic effect of BoNT-A, or the peripheral effect on NMJs (persisting in the muscle as evidenced by cleaved SNAP-25 in muscle) remains as a necessary contributing factor despite locomotor recovery.

In this study, to modulate and counteract the BoNT-A entry and action at the NMJs, we utilized α-latrotoxin, a potent neurotoxin derived from the black widow spider *Lactrodectus s.p.*, known for its affinity for vertebrate presynaptic membranes. Latrotoxin functions as a presynaptic pore-forming toxin, interacting with specific receptors on neuronal cell surfaces. This interaction triggers the immediate release of neurotransmitters through two main mechanisms: i) direct stimulation of exocytosis, or ii) formation of tetrameric pores in the membrane that

conduct calcium ions (288–291). After this immediate period, the influx of calcium into latrotoxin-poisoned free nerve terminals (devoid of myelin sheath) induce their transient degeneration up to the level of myelinated sheath formed by Schwann cells, effectively destroying the motor axon terminals and associated synapses. When injected in the muscle, latrotoxin cause peripheral flaccid neuroparalysis similar to BoNT-A. However, unlike BoNT-A that causes only silencing of nerve terminal, latrotoxin-evoked neuroparalysis is characterised by reversible degeneration of motor axon terminals which causes complete disappearance of NMJ. In spite of this, functional recovery of latrotoxin poisoned NMJ is much faster than with BoNT-A, terminating in functional reinnervation within a few days post injection (292,293). Moreover, the latrotoxin treatment can speed up the process of recovery of BoNT-A-mediated paralysis (254).

Herein, in one group of animals we injected latrotoxin one day prior to BoNT-A i.m. treatment in order to cause peripheral nerve degradation and evaluate the role of BoNT-A entrance at the peripheral NMJs. In the second group, we evaluated the contribution of established BoNT-A action at the NMJs, by administering the latrotoxin at a time-point when BoNT-A peripheral neuroparalytic effects at the NMJ are fully established (and any BoNT-A in the NMJ would be destroyed and its effect reverted).

To evaluate if latrotoxin would reverse the long-lasting peripheral and central effects of BoNT-A we injected latrotoxin in gastrocnemius muscle, 3 days post BoNT-A treatment. As expected, fast regeneration of destroyed NMJs by latrotoxin greatly accelerated motor function recovery, visible in various tests for local muscle weakness: DAS and gait ability (Figure 25, unpublished data). Interestingly, neuromuscular recoveries followed a slightly different time course dependently on the time point of latrotoxin injection: seemingly, destroying the NMJS after BoNT-A action was fully established resulted in quicker neuroparalytic recovery, while injecting the latrotoxin to prevent the BoNT-A entrance resulted in slower, somewhat intermediate pace of recovery (more similar to BoNT-A alone). The reasons for this are not entirely clear, however, we made preliminary stainings of muscle where it is visible that not all NMJs are destroyed by the latrotoxin. So, the BoNT-A may either enter through the remaining NMJs or myelin-free nerve terminals, or follow a slightly different nerve entry route (possibly via myelinated nerve endings as we demonstrated after toxin intrasciatic injection below the epineurium). A quicker recovery after latrotoxin injection on day 3 post BoNT-A may also signify that majority of BoNT-A remains at the NMJ, but also possibly serving as a reservoir

for additional trafficking to CNS even after day 3 (as it seems that central cleaved SNAP-25 is lower in BoNT-A + latrotoxin-treated animals compared to only BoNT-treated animals). Either way, these results demonstrate that BoNT-A must work both in the NMJs and CNS to fully exert its antispastic potential, and confirms the NMJs as the main entrance route after the intramuscular BoNT-A injection. However, robust efficacy of i.n. injections and the fact that some of the locomotor effects of BoNT-A are preserved despite the preceeding destruction of NMJs, suggests that other routes of BoNT-A delivery (possibly via Ranvier nodes of myelinated fibers) may also be important for further consideration. Evidence for exploiting the "nerve block" techniques for BoNT-A administration in movement disorders are pending.

Furthermore, similar to previous results i.m. BoNT-A resulted in reduced functional use of the hindlimbs and significant changes in the posture of the injected hind paw, characterized by an arched appearance of the foot soles and toes, which resulted in decreased gait ability score (Figure 26, unpublished results). Here latrotoxin injected animals pre BoNT-A injection, showed reduced gait score which similar to DAS score, caused synergized appearance of muscle weakness. Aside from muscle weakness, synergized action of slowly recovering latrotoxin injected NMJs and starting BoNT-A paralysis was visible during catwalk assessment, as sudden decrease in hindlimb base of support (Figure 26, unpublished results).

However animals injected with latrotoxin 3 days post BoNT-A showed faster recovery of local muscle weakness (both DAS and gait ability) already on day 7 post BoNT-A, in contrast to solely BoNT-A injections (Figure 26, unpublished data). Accelerated recovery of BoNT-A intoxicated NMJs after latrotoxin injection was evident also during catwalk assessment (Figure 26, unpublished data). This is in line with previous research by Duregotti et al., that also observed faster recovery of BoNT-A intoxicated nerve terminals after latrotoxin treatment (254).

When assessed for BoNT-A antispastic activity, we employed TeNT on day 80 post BoNT-A in the same gastrocnemius muscle. Beneficial BoNT-A antispastic effect remained until day 109 post i.m. injections, demonstrated as a decrease in dorsiflexion resistance and improved locomotor function evident on BBB scale (Figure 27, unpublished data). Nevertheless the beneficial antispastic effect of BoNT-A was deficient in rats treated with latrotoxin, evident in dorsiflexion and BBB test, suggesting the important functional and entry role of the peripheral motor terminals in a long lasting antispastic BoNT-A activity. However, latrotoxin injected animals previous to BoNT-A treatment, showed greater antispastic capacity than animals with

latrotoxin injected post BoNT-A treatment as evident during locomotion assessment by BBB scale (Figure 27 C). Additionally, cleavage of SNAP-25 was detected in the ventral horn of the spinal cord 109 days after BoNT-A injection, providing further evidence of BoNT-A functional impact and its presence in the central nervous system (Figure 29, unpublished data). Similarly, abundant cleavage of SNAP25 was observed in the BoNT-A + latrotoxin treatment group, with a lesser amount of cleavage present in the latrotoxin + BoNT-A treatment group.

One could hypothesize that animals with latrotoxin intoxicated NMJs prior to BoNT-A injection exhibited a sustained antispastic BoNT-A effect, when compared to BoNT-A+latrotoxin treatment (Figure 27 C). This could be attributed to BoNT-A intoxication of peripheral terminals following their recovery from latrotoxin. Moreover, due to "waiting out" that happened on the periphery, smaller amounts of BoNT-A entered the non-recycling endocytic vesicles for axonal transport (71), evident as lower presence of cSNAP-25 in spinal cord (Figure 29). In contrast to the animals, where the BoNT-A was injected first thus intoxicating the peripheral nerve terminals, and entering the axonal transport pathway resulting in higher accumulation in CNS (visible also by cleavage of SNAP25 in spinal cord on figure 29; unpublished data). However, due to intoxication with latrotoxin 3 days post BoNT-A, peripheral nerve terminals were destroyed and thus "freed" from BoNT-A intoxication, showing much faster regeneration and functional reassembling. Despite the higher presence of SNAP25 cleavage in the central nervous system, BoNT-A+latrotoxin lacked antispastic effect as observed from motor test. Based on these results it is evident that functional state of NMJ holds great importance for the BoNT-A entry in nerve terminal and its subsequent endocytic facilitation in vesicles undergoing axonal transport to CNS. However, as evident here, BoNT-A antispastic activity, it's not solely dependent on toxin's central action. This highlights the intricate interplay between peripheral and central mechanisms in mediating the beneficial effects of BoNT-A.

6.5.   Characterization of BoNT-A-targeted spinal premotor circuits

To delve deeper into the potential sites of action for BoNT-A on central synapses, we conducted colocalization studies of cleaved SNAP-25 alongside additional neuronal markers. We demonstrated functional assessment of long lasting BoNT-A effect on normal muscle tone and spastic muscles, followed by ongoing cleavage of SNAP-25 present in spinal synapses more than 2 months post single BoNT-A peripheral injection, but also in peripheral motor terminals.

To explore whether BoNT-A translocates from the somatodendritic compartment of motoneurons to the presynaptic axonal compartment of second-order neurons during axonal transport to spinal cord motoneurons, we conducted MAP-2 immunostaining in the ventral horn and colocalized it with BoNT-A cleaved SNAP-25. However, no colocalization of MAP-2 and SNAP-25 was observed in motoneurons following BoNT-A treatment in muscle spasticity induced by TeNT (Šoštarić et al., 2022; Appendix I).

However, previously it was that BoNT-A enzymatically does target with higher degree of selectivity large synaptic terminals containing choline-acetyltransferase (ChAT) and vesicular acetylcholine transporter (VAMP) (10,83,294). This hints at a potential trans-synaptic effect on C-boutons, which synapse with motoneuronal cell bodies and receive premotor input from $V0_C$ interneurons, crucial for activities like swimming (267). Our findings indicate that BoNT-A can indeed impair swimming velocity, with a portion of cleaved SNAP-25-containing terminals expressing ChAT (Figure 21, Šoštarić et al., 2024; Appendix II) or associating with Kv2.1-expressing postsynaptic sites typically linked to C-boutons (Figure 21, Šoštarić et al., 2024; Appendix II). However, the presence of cleaved SNAP-25 in a significantly greater number of terminals expressing SV2C and synaptophysin (Figure 21, Šoštarić et al., 2024; Appendix II) implies the transcytosis of the toxin to other central synapses beyond the cholinergic ones. Furthermore, these synapses should also possess the main protein acceptor for BoNT-A (295). The actions of BoNT-A within various premotor neurons also correspond with its effects on other examined motor functions besides swimming. According to Konsolaki research group (268), the performance of mice on the rotarod is not impaired when cholinergic C boutons are genetically removed. This findings suggest that BoNT-A impaired rotarod performance observed in this thesis (figure displayed in Šoštarić et al., 2022; Appendix I, Šoštarić et al., 2024; Appendix II) must affect some other types of spinal synapses or combination of spinal and peripheral synapses. To support its involvement in other central excitatory synapses, BoNT-A exhibits a preference for inhibiting the release of glutamate over GABA in isolated hippocampal synaptosomes (246). In addition to neurotransmitter release, BoNT-A might also modify other SNAP-25-mediated functions at synaptic and extrasynaptic sites, such as Ca^{2+} dynamics regulated by SNAP-25 interactions with synaptotagmin, presynaptic voltage-gated Ca^{2+} channels, and G proteins (296), as well as the translocation of membrane proteins and channels (297). These multifaceted actions likely result in a net reduction in premotor neuronal network activity. Such effects are expected to contribute to the beneficial restoration of muscle control in disinhibited motor circuits seen in movement disorders or spasticity (298–300).

6.6. Peripheral vs central action of BoNT-A beneficial effects in dystonia and spasticity

When seeking to understand the mechanism underlying the beneficial effects of BoNT-A on spastic muscles, it is commonly believed that its primary action occurs at the established site of peripheral muscle cholinergic terminals, a postulate set long ago (180–301). This has resulted in each observed effect of botulinum toxin being attributed to its action on peripheral motor endings. Moreover, other potential levels of action for BoNTs, such as the motor components of the central nervous system, were either not seriously considered or disregarded as insignificant and unnecessary, sometimes referring as only result of peripheral action causing "sensory trick" (184).

The initial theory proposing that the beneficial antispastic effect of BoNT-A originates solely from its action on extrafusal muscle fibers has been challenged by additional effects on intrafusal muscle fibers, as evidenced in both patient studies (188) and basic research (185,302). However, clinical observations suggest that the duration of neuromuscular paralysis may not always correlate with the treatment duration, and patients benefiting from doses producing little or no muscle-weakening effects suggest a role beyond simple neuromuscular paralysis (7,8,195). Moreover, evidence showed that BoNT-A undergoes axonal retrograde transportation similar to the one of TeNT (81,82,243,245,55).

Furthermore, (10) showed BoNT-A cleavage of SNAP-25 two synapses away from the injection site, suggesting that BoNT-A undergoes central transcytosis by which it manages to retain its enzymatic activity. However in their work, (294) disagree with the BoNT-A mechanism of central transcytosis, and action on further synapses suggesting that BoNT-A exert its beneficial effect at the presynaptic level of motoneuron and recurrent inhibition by Renshaw cells. However, there are questions regarding whether the presence of BoNT-A enzymatic degradation products in the ventral horns of the spinal cord is adequate to achieve the beneficial effect of BoNT-A in both dystonic and spastic patients.

In this PhD thesis we confirmed the axonal transport of enzymatically active BoNT-A to ventral horn spinal cord, and found that central effects are at least partly responsible for beneficial antispastic effect of BoNT-A (see Table 5 and Figure 32). Moreover, we evidenced that BoNT-A input on premotor central synapses affect high-intensity motor task as swimming, characterized also by central cleavage of SNAP25 colocalized on cholinergic ChaT and Kv 2.1. expressing neurons suggesting that part of toxins central activity is associated with C-boutons.

Moreover, in ventral horn, MAP-2 immunostaining of the somatodendritic compartment which is dominantly belonging to the motoneurons did not colocalize with BoNT-A cleaved SNAP25, in line with the evidence that BoNT-A holotoxin physically leaves the motor neurons and enters the presynaptic axonal compartment of the second-order neurons. Additionally, in our model of TeNT induced spasticity it was found that BoNT-A antispastic effects are not mediated via monosynaptic H reflex excitability, supported by lack of colocalization on VGlut1 terminals in spinal synapses. However, muscle atrophy associated with BoNT-A treatment, was demonstrated by present research as dominantly associated with peripheral aspects of the BoNT-A action.
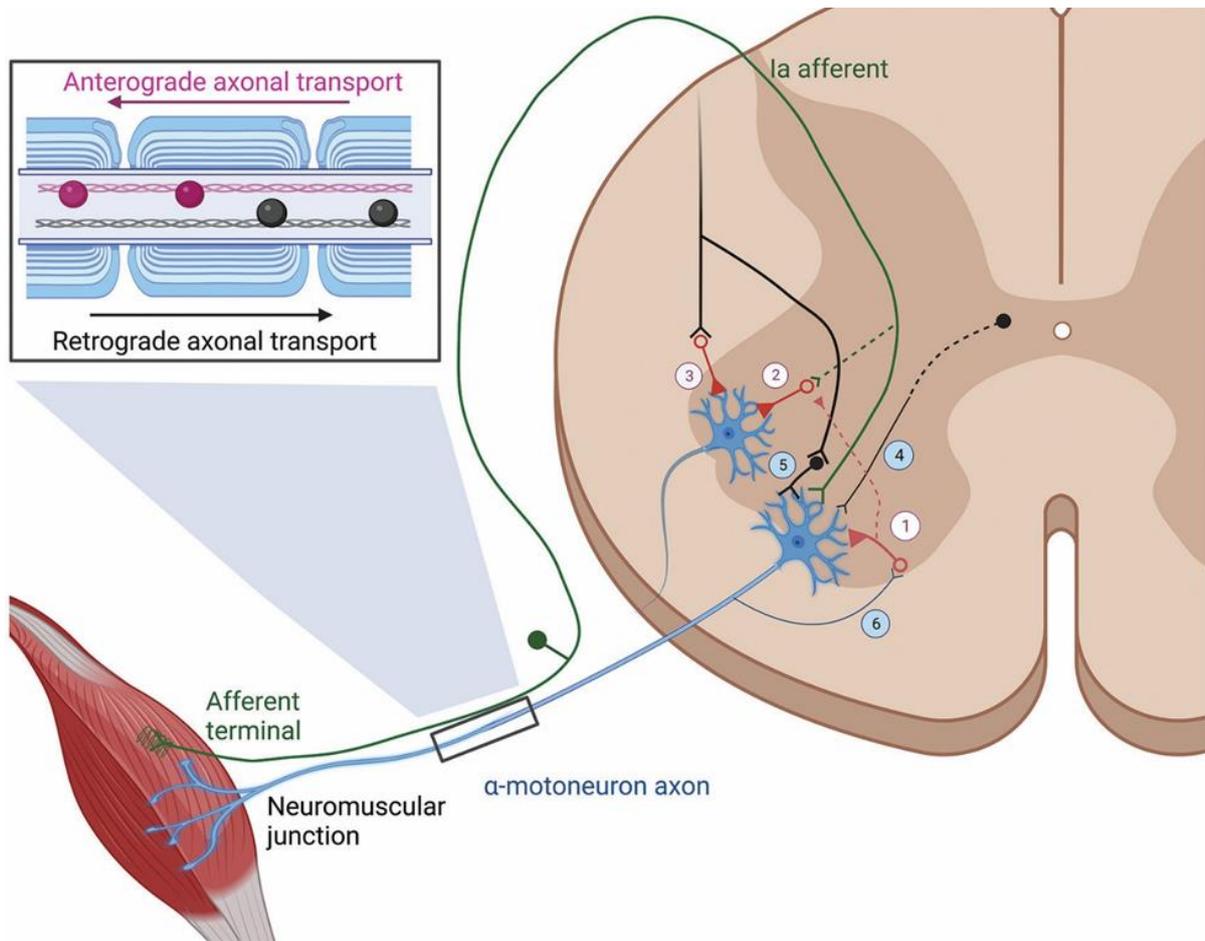
Figure 32. Schematic representation of potential actions of TeNT and BoNT-A within the spinal cord ventral horn. *TeNT, following axonal transport and transcytosis, obstructs inhibitory transmission by Renshaw cells (1), Ia inhibitory interneurons (2), and other types of inhibitory interneurons (3). Conversely, BoNT-A, administered peripherally via the sciatic nerve, undergoes anterograde axonal transport to muscles, where it silences presynaptic neuromuscular terminals. Simultaneously, retrograde axonal transport carries BoNT-A to the central nervous system, where transcytosed BoNT-A might impede excitatory transmission at C-boutons formed by V0c cholinergic interneurons (4) and other types of excitatory neurons (5). This aligns with BoNT-A's preference for targeting excitatory transmission. Additionally, potential central actions of BoNT-A at motoneuron recurrent axonal collaterals (6) synapsing with Renshaw cells may occur without transcytosis (Šoštarić et al., 2024; Appendix II).*

Table 5. Summary of peripheral vs. central effects of BoNT-A from experiments in this PhD dissertation

Dose response of BoNT-A peripheral vs central effects (see Figure 7. for schematic timeline of experiment)				
Evaluation of early antispastic effects of BoNT-A		Evaluation of late antispastic effects of BoNT-A		What does it do?
1.Treatment	Method od application	2.Treatment	Method of application	Induces muscular spasm to test the early and lasting antispastic BoNT-A effects
TeNT (day 0)	i.m (1.5 ng) gastrocnemius	TeNT (day 49)	i.m. (1.5 ng) gastrocnemius	
BoNT-A (day 7)	i.m. gastrocnemius (1, 2 and 5 U/kg)			
Motor tests	Early antispastic effect	Late antispastic effect		What have we got?
Dorsiflexion resistance BBB score DAS Caliper measurements of the injected lower leg	All doses of BoNT-A elicited similar antispastic effect	Only the higher doses (2 and 5 U/kg) showed efficient antispastic effects preventing the muscle spasm and locomotor deficits		Dose-dependent antispastic effects become more prominent in later phases, when peripheral action of BoNT-A diminishes, and central action takes lead in antispastic activity
Immunohistochemical findings: Injected gastrocnemius muscle Spinal cord (L3-L5)				What have we got?
Presence of cleaved SNAP25 activity in NMJs and axons.	Presence of cleaved SNAP25 activity in spinal synapses. MAP-2 colocalization showed no clSNAP25 in somatodendritic compartment.			Central activity of BoNT-A in a model of TeNT evoked spasticity, it is followed by ongoing presence of its enzymatic activity in both, injected muscles and spinal cord.
Peripheral vs central BoNT-A effects on motor control (see Figure 9. for schematic timeline of experiment) (P.S. see Figure 8. for timeline of BoNT-A effect after i.m. application)				
Evaluation of BoNT-A effects on normal motor processing		Peripheral vs central evaluation of late antispastic BoNT-A		What does it do?
1.Treatment	Method of application	2.Treatment	Method of application	

BoNT-A (day 0)	bilateral injections in sciatic nerve (2 U/kg)	TeNT (day 62)	i.m. (1.5 ng) gastrocnemius	Administration of TeNT in later phase induced local muscle spasm. Purpose is to test long lasting central vs peripheral BoNT-A activity, after recovery of peripheral BoNT-A effects.
Neutralizing BoNT-A antitoxin (day 1)	i.t. injection in lumbar part of cauda equina			I.t. antitoxin prevents BoNT-A transcytosis and subsequent centrally mediated effects on motor performance
Motor tests	Effects on normal muscle	Late antispastic effects		What have we got?
DAS Rotaroda Beamwalk Gait ability Swimming Dorsiflexion resistance BBB score Caliper measurements of the injected lower leg EMG[h]	The intraneural injection in *n.ischiadius* of BoNT-A, leads to long-lasting effects on normal muscle tone.	I.n. transcytosed BoNT-A decreased local spasticity induced by TeNT. In animals injected with i.t. antitoxin, BoNT-A transcytosis was prevented, which resulted in stronger TeNT evoked spasticity. The antispastic effect of BoNT-A in later stages after i.n. administration, did not change H reflex during EMG measurements.		I.n. BoNT-A effects are guided by its central trans-synaptic action on input from premotor central synapses, particularly evident during both, high-intensity and skilled locomotor tasks. The long-lasting antispastic activity of i.n. injected BoNT-A on muscle spasticity induced by TeNT, is not mediated by its action on monosynaptic H reflex excitability.
Immunohistochemical findings: Injected gastrocnemius muscle Spinal cord (L3-L5)				What have we got?
Present cleaved SNAP25 in NMJs and axons in gastrocnemius muscle, 2	Present cleaved SNAP25 in spinal premotor synapses, 2 months after i.n. sciatic BoNT-A injections, which			BoNT-A exerts its effect on motor control at the level

months after i.n. sciatic BoNT-A injections, suggesting of ongoing BoNT-A activity.	colocalized with cholinergic, but also non-cholinergic markers in higher correlation.	of secondary spinal cord synapses affecting different types of spinal premotor terminals, including both, cholinergic and non-cholinergic types.

Role of NMJs in a long -term action of BoNT-A (see Figure 10. for schematic timeline of experiment)				
Evaluation of BoNT-A entry via NMJs		Evaluation of late antispastic BoNT-A effect after peripheral NMJs destruction		What does it do?
1.Treatment	Method of application	2.Treatment	Method of application	After recovery of peripheral BoNT-A effects (and recovery of latrotoxin destruction of NMJs), TeNT was administered in later phase to induce local muscle spasm. Purpose was to test long lasting central vs peripheral BoNT-A activity,
BoNT-A (day 0)	i.m. injection in gastrocnemius muscle (5 U/kg)	TeNT (day 80)	i.m. (1.5 ng) gastrocnemius	
Latrotoxin (20-24 h prior BoNT-A, or 3 days after BoNT-A)	i.m. injection in gastrocnemius muscle (4 µg)			Latrotoxin caused short-term degeneration of NMJs, to test the role of BoNT-A muscular effects and entrance at NMJs
Motor tests and muscle atrophy assessment	BoNT-A effects on non-spastic muscles in early stages after latrotoxin degeneration of NMJs	Late antispastic effects of BoNT-A in late stages after latrotoxin degeneration of NMJs		What have we got?

DAS Catwalk Gait ability Dorsiflexion resistance BBB score Muscle weight of lower leg muscles (gastrocnemius, soleus and tibialis anterior)	Latrotoxin-induced accelerated regeneration and functional restauration of BoNT-A intoxicated lower leg NMJs, visible during functional motor assessment. Presence of high peak muscle weakness in early stage of BoNT-A treatment	BoNT-A did not show beneficial antispastic activity against TeNT-induced spasticity during functional motor assessment in later stages.	The antispastic effect of intramuscularly injected BoNT-A in the gastrocnemius muscles is not exclusively reliant on the toxin's central action on premotor spinal terminals.
Immunohistochemical findings: Spinal cord (L3-L5)			What have we got?
		clSNAP25 was present in spinal synapses, 109 days after BoNT-A injection in gastrocnemius muscle. Present clSNAP25 was also evident in animals injected with both, BoNT-A and latrotoxin, but with a lesser overall antispastic effect, as stated previously.	Functional neuromuscular junction enables BoNT-A entry into cytosol of nerve terminal and facilitates endocytic internalisation into non recycling vesicles, which undergo axonal transport, and thus is crucial for exertion of BoNT-A central effects.

TeNT, tetanus toxin; BoNT-A, botulinum toxin type A; BBB score, Basso–Beattie–Bresnahan locomotor rating sore; DAS, digit abduction score; NMJ, neuromuscular junction; L3-L5, level 3 to level 5 of lumbar part of spinal cord; cleaved SNAP25; cleaved synaptosomal-associated protein of 25 kDa; MAP-2, Microtubule-associated protein 2

6.7. Comparison of two clostridial neurotoxins: TeNT peripheral activity mimics the BoNT-A flaccid paralysis

A rare form of tetanus, cephalic tetanus is characterised by botulism like cranial nerve palsy which sometimes goes unnoticed for days, thus complicating the diagnosis of tetanus and prolonging the very much needed pharmacological therapy. Cephalic tetanus is followed by poor prognosis due to peculiar start of disease and rapid development of cardiorespiratory deficits, which mechanism of pathophysiology still remains unresolved. Previously, it was believed that the metalloproteolytic activity of TeNT primarily targeted the central VAMP for cleavage, resulting in the paralysis of inhibitory interneurons and leading to spastic paralysis. However, our study reveals that TeNT promptly cleaves VAMP subsequent to its endocytic internalization into the cytosol of the peripheral motor terminal. This cleavage occurs at VAMP located on the presynaptic membrane of the peripheral terminal, leading to the manifestation of flaccid paralysis in muscles, similar to symptoms observed in botulism.

Here we used a rodent model of cephalic tetanus based on local injections of TeNT into the whiskerpad (WP), a muscle group responsible for movement of whiskers in animals. Whisker pads sensorymotor inervation is from the facial nerve and their activity its easy to follow with live imaging and electromyographic measurements of compound muscle action potential (CMAP) (303,304). Animals treated with TeNT in the early period post TeNT injections, lost their ability to move whiskers, which after 1 day progressed to fully paralyzed appearance and persisted for 3-5 days. CMAP amplitude clarified the type of paralysis, showing TeNT provoked reduction of maximal CMAP amplitude (which is indicative of flaccid paralysis). Obtained results suggested that TeNT action on the peripheral motor terminals is very similar to the one caused by BoNT-A, characterised by synaptic silencing at the level of NMJs, but without degeneration of motor terminals, and followed by rapid reversibility (31,–306). However, in a few hours, the canonical spastic paralysis of head muscles was observed in contralateral WP muscles. This interplay of different types of paralysis is resemebeling of cephalic tetanus symptoms in human patients (307). Furthermore, flaccid paralysis caused by tetanus intoxication of peripheral NMJs was additionally evidenced by immunohistochemical stainings of TeNT injected WP and control. This was possible due to development of antibody which specifically recognize the TeNT cleaved VAMP (Fabris et al., 2022; Appendix III). Clear stainings of cleaved VAMP in TeNT injected WP evidenced that observed flaccid paralysis is caused by TeNT-mediated cleavage of VAMP (figure in Fabris et al., 2023; Appendix IV). Further evidence was obtained by experiments on rats. Interestingly rats are carriers of VAMP-

1 mutation at the cleavage site of TeNT This is making rats VAMP-1 resistant to TeNT metaloproteolytic activity. Rats were unilaterally injected with TeNT in the WP and paralysis development was assessed by live imaging and CMAP measurements. During the early onset after TeNT injection, no visible whisker paralysis was observed during video imaging. However the WP paralysis started to occur on day 3 and whiskers appeared fully paralysed by day 5. To distinguish between flaccid and spastic paralysis CMAP anaylsis was performed. Moreover, during imunohystochemical stainings cleavage of CMAP was not detected. Obtained results showed for the first time that TeNT can cleave VAMP at site of peripheral motor terminals, causing a reversible flaccid paralysis similar to the one caused by BoNT-A, thus reveling the molecular background for early symptoms of cephalic tetanus characterized by flaccid paralysis.

6.8. Possible clinical implications of present PhD study

Up until this point, the therapeutic efficacy of BoNT-A in dystonia and spasticity has primarily been associated with localized muscular neuroparalysis and consequent muscular weakness (308). Nonetheless, recent insights have shed light on potential clinical implications and the utilization of BoNT-A in the treatment of patients. In line with clinical experience, in the rat model of experimental hypertonia, we found that local muscular paralysis is the dominant factor contributing to the initial antispastic effect of i.m. BoNT-A thus explaining its early onset and intensity (Šoštarić et al., 2022; Appendix I). As the peripheral muscular effects diminish over time, the central antispastic actions become more prominent, further contributing to the overall therapeutic benefit of BoNT-A. The duration and strength of this later antispastic effect is dose dependent, with higher doses facilitating central transcytosis and subsequently amplifying the central activity of BoNT-A, thereby extending the therapeutic duration. These discoveries highlight the significance of both the peripheral dosage and the central mechanisms of the toxin in maintaining the remarkable and enduring clinical effectiveness of BoNT-A.

In the context of spastic and dystonic limb regions, conventional thinking suggests that targeting individual muscles through BoNT-A injections is the only viable approach. However, this PhD thesis reveals that injecting the toxin directly into peripheral nerves allows for the simultaneous targeting of multiple muscles at both peripheral and spinal synaptic sites crucial for neuromotor control (Šoštarić et al., 2024; Appendix II). This intraneural (i.n.) injection mode offers the advantage of avoiding complete muscle paralysis since BoNT-A does not enter via NMJs. Despite reduced peripheral paralysis, BoNT-A demonstrates sustained antispastic effects for an

extended duration following i.n. application. This finding aligns with various clinical observations indicating that the antispastic effects of BoNT-A do not necessarily correlate with significant muscle paralysis (7), (201). Hence, the i.n. delivery mode of the toxin could complement the conventional approach of muscular toxin injections in clinical practice. Moreover, employing existing nerve block techniques that spare nerve injury could provide an alternative means to target regional muscle groups innervated by common nerves or nerve branches (Šoštarić et al., 2024 Appendix II). Additionally, this approach may enhance current nerve block techniques utilizing general anesthetics or neurolytic agents for spasticity management. Notably, case studies have reported successful intra- or peri-nerve application of BoNT-A in chronic pain patients, with no apparent signs of nerve injury following i.n. injections (13,249,309,310).

Furthermore, aside from its antispastic activity and local muscle weakness, in our studies on normal muscle tone and spasticity, we found that BoNT-A affects the gait and motor function on both the peripheral and central level. This was evident from our behavioural and colocalization studies suggesting that BoNT-A activity in the spinal synapses of the ventral horn are not limited to a single-type synapse, but more likely interaction of different central circuits involved in normal locomotion and involuntary movement. It is noteworthy to consider that the action of BoNT-A extends beyond its initial perception as merely a "muscle relaxation adjuvant," as suggested by the original peripheral theory of its action. In this PhD thesis we shine light onto the effects of BoNT-A on the interplay of central motor pools in both normal locomotion and spasticity which hold possible translational implications for future clinical applications. The impact of BoNT-A on gait and motor function becomes particularly intriguing when considering its application in post-stroke patients, children with cerebral palsy, or individuals with motor disorders marked by motor neuron dysfunction and disruptions in signal transmission between motor neurons and muscles, such as seen in amyotrophic lateral sclerosis (ALS).

In our research directed at the explanation of flaccid neuroparalysis evoked by cephalic tetanus, we found that, in susceptible mouse or human synapses, the TeNT-evoked flaccid paralysis will prevail over the spastic paralysis evoked by its exclusive central action. This finding is highly relevant for explaining the paradoxical presentation of cephalic tetanus, which is a rare but very severe presentation of clinical tetanus (Fabris et al., 2023, Appendix IV). More generally, this also explains why the action of a SNARE-targeting agent such as clostridial neurotoxin at

peripheral synapses is faster, more apparent, dominant and it may mask any central effect of the toxin. This also explains why the peripheral effect of BoNT-A may mask any central effect of the toxin during early neuroparalysis, while the central toxin actions may become more apparent and important during the phase of substantial neuromuscular recovery.

7.   CONCLUSIONS

Conclusions 1 – 7. embody answers to meet both general and specific aims, forming one cohesive unit while conclusion 8. refers to the additional research resulting from the previously planned ones.

1. Central activity of BoNT-A exert its late antispastic effect in a model of TeNT evoked spasticity, followed by ongoing presence of its enzymatic activity in both injected muscles and spinal cord. In early stages, all doses (ranging from 1 to 5 U/kg) elicit similar antispastic effects, while dose-dependent antispastic effects of BoNT-A becomes more prominent in later stages post injection in gastrocnemius muscle. This is evident after repeated TeNT induced muscle spasticity, when peripheral signs of BoNT-A effects diminished, only the higher doses (2 and 5 U/kg) showed efficient antispastic effects preventing the muscle spasm and locomotor deficits.

2. The intraneural injection in *n. ischiadius* of BoNT-A leads to long-lasting effects on normal muscle tone. I.n. BoNT-A effects are guided by its central trans-synaptic action on input derived from premotor central synapes, particularly evident during both, high-intensity and skilled locomotor tasks. Long-lasting locomotor deficits were also followed by localised muscle weakness, causing significant and prolonged impairment of i.n. injected lower leg.

3. The long-lasting antispastic activity of i.n. injected BoNT-A on TeNT-induced muscle spasticity is not mediated by its action on monosynaptic H reflex excitability. This was demonstrated by EMG measurements and the absence of colocalization with the VGlut1 isoform of the glutamate transporter, which support the lack of direct toxin effect on the central afferent terminal of Ia primary afferents involved in the monosynaptic stretch reflex.

4. BoNT-A effect at the level of secondary spinal cord synapses affect different types of spinal premotor terminals, including both, cholinergic and non-cholinergic types. When BoNT-A is delivered into the sciatic nerve, it is transported axonally and cleaves SNAP-25 in both peripheral motor terminals and central premotor synapses. This cleavage occurs in neurons expressing cholinergic markers ChAT and Kv 2.1, indicating that some of the toxin's central enzymatic activity is linked to C-boutons. Additionally, in comparison to ChAT, the expression of SV2C and synaptophysin showed a higher correlation with cleaved SNAP-25, suggesting that BoNT-A affects various types of spinal neurons.

113

5. Muscle atrophy is associated with BoNT-A peripheral mechanisms of action, and it is not affected by toxin's central effects. This is evident from long lasting localised muscle weakness of lower leg muscles, after both BoNT-A i.m. injections in gastrocnemius muscle in all administered doses (1-5 U/kg) and also after BoNT-A injections in n. ischiadicus, despite the prevention of BoNT-A central action by neutralising antitoxin.

6. Antispastic activity of BoNT-A i.m. injected into gastrocnemius muscles, also depends on BoNT-A activity on NMJs, along with the toxin's central action on premotor spinal terminals. This is showed by accelerated latrotoxin induced regeneration and functional restauration of BoNT-A intoxicated lower leg NMJs. Despite the high presence of clSNAP-25 in the spinal cord, BoNT-A did not show beneficial antispastic activity against TeNT-induced spasticity.

7. Functional NMJ enables BoNT-A entry into cytosol of nerve terminal and facilitates endocytic internalisation into non recycling vesicles, which undergo axonal transport. This is showed by prevention/reduction of central clSNAP25 by the latrotoxin-induced destruction of lower leg NMJs prior to BoNT-A treatment in gastrocnemius muscle. This resulted in high peak muscle weakness in early stage of BoNT-A treatment, synergised with latrotoxin neuroparalysis, lower presence of cleaved SNAP25 in spinal cord but also a substained antispastic activity on TeNT -evoked locomotor deficit.

8. TeNT cleaves its substrate vesicle-associated membrane protein within facial neuromuscular junctions, leading to a paralysis resembling botulism that dominates over tetanus spasticity, demonstrated by both immunohistochemistry and electrophysiology.

8. ABSTRACT

Peripheral and central effects of botulinum toxin type A in the rat motor nervous system

PETRA ŠOŠTARIĆ MUŽIĆ, 2024

Introduction: Intramuscular administration of botulinum toxin type A (BoNT-A) is used to treat hyperkinetic disorders such as dystonia and spasticity. Our research suggests that BoNT-A, in addition to its primary peripheral action, also exerts effects on the central nervous system, which could explain its prolonged effect.

Methods: Studies were conducted on Wistar Han rats and primary cultures of rat cerebellar neurons. Peripheral and central effects of BoNT-A were assessed using motor tests, electromyography, intrathecal administration of antitoxin, and latrotoxin (LTX). The protease activity of the toxin was analyzed using the Western blot method.

Results: The antispastic effect of BoNT-A was dose-dependent in the later phase, with higher doses preventing spasm and improving motor performance. Intrathecal antitoxin accelerated the recovery of muscle weakness. BoNT-A reduced muscle tone induced by tetanus toxin (TeNT) without affecting the monosynaptic reflex. Central transsynaptic activity contributed to the late antispastic effect, with the presence of BoNT-A enzymatic activity in muscles and the spinal cord. LTX accelerated the recovery of neuroparalysis and reduced the late antispastic effects of BoNT-A.

Conclusion: Peripheral and central activities of BoNT-A act synergistically, with the later central effect dependent on the reduction of intense peripheral action. This is also confirmed by the initial dominance of the flaccid neuroparalytic effect of TeNT on peripheral NMJ, in relation to the central disinhibitory effect and the occurrence of spasms in cephalic tetanus.

Keywords: Botulinum toxin, neuromuscular disorders, central motor regions, SNAP-25

9.   KRATKI SADRŽAJ NA HRVATSKOM JEZIKU

Perfierni i središnji učinci botulinum toksina tipa A u motoričkom živčanom sustavu štakora

Uvod: Intramuskularna primjena botulinum toksina tipa A (BoNT-A) koristi se za liječenje hiperkinetičkih poremećaja poput distonije i spastičnosti. Naša istraživanja upućuju da BoNT-A, osim primarnog perifernog djelovanja, ostvaruje i učinke na središnji živčani sustav, što bi moglo objasniti njegov produljeni učinak.

Metode: Istraživanja su provedena na štakorima soja Wistar Han i primarnoj kulturi neurona malog mozga štakora. Periferni i središnji učinci BoNT-A procijenjeni su motoričkim testovima, elektromiografijom, intratekalnom primjenom antitoksina i latrotoxinom (LTX). Proteazna aktivnost toksina analizirana je Western blot metodom.

Rezultati: Antispastični učinak BoNT-A pokazao se ovisan o dozi u kasnijoj fazi, te su veće doze spriječile spazam i poboljšale motoričke izvedbe. Intratekalni antitoksin ubrzao je oporavak mišićne slabosti. BoNT-A je smanjio mišićni tonus induciran tetanus toksinom (TeNT), bez utjecaja na monosinaptički refleks. Središnja transsinaptička aktivnost pridonijela je kasnom antispastičkom učinku, uz prisutnost enzimske aktivnosti BoNT-A u mišićima i leđnoj moždini. LTX je ubrzao oporavak neuroparalize i smanjio kasne antispastične učinke BoNT-A.

Zaključci: Periferna i središnja aktivnost BoNT-A djeluju sinergistički, a kasniji središnji učinak ovisi o smanjenju intenzivnog perifernog djelovanja, što također potvrđuje i početna dominacija perifernog mlohavog neuroparalitičkog učinka TeNT u odnosu na središnji dezinhibicijski učinak i nastanak spazma kod cefaličkog tetanusa.

10.   REFERENCES

1. Johnson EA, Montecucco C. Botulism. Handb Clin Neurol. 2008;91:333–68.

2. Arnon S, Schechter R, Inglesby T, Henderson D, Bartlett J, Ascher M, et al. Botulinum toxin as a biological weapon: medical and public health management. JAMA. 2001;285(8):1678–84.

3. Rossetto O, Montecucco C. Tables of Toxicity of Botulinum and Tetanus Neurotoxins. Toxins. 2019;22;11(12):686.

4. Ramirez-Castaneda J, Jankovic J. Long-term efficacy and safety of botulinum toxin injections in dystonia. Toxins. 2013;4;5(2):249–66.

5. Chen S. Clinical uses of botulinum neurotoxins: Current indications, limitations and future developments. Toxins. 2012;4(10):913–39.

6. Hallett M. Explanation of timing of botulinum neurotoxin effects, onset and duration, and clinical ways of influencing them. Toxicon. 2015;1;107:64–7.

7. Hallett M. Mechanism of action of botulinum neurotoxin: Unexpected consequences. Toxicon. 2018; 1;147:73–6.

8. Mazzocchio R, Caleo M. The Family of Clostridial Neurotoxins More than at the Neuromuscular Synapse: Actions of Botulinum Neurotoxin A in the Central Nervous System. The Neuroscientist. 2015;21(1):44–61.

9. Weise D, Weise CM, Naumann M. Central effects of botulinum neurotoxin—evidence from human studies. Toxins. 2019;6;11(1):21.

10. Caleo M, Spinelli M, Colosimo F, Matak I, Rossetto O, Lackovic Z, et al. Transynaptic Action of Botulinum Neurotoxin Type A at Central Cholinergic Boutons. J Neurosci. 2018; 28;38(48):10329–37.

11. Matak I, Lacković Z. Botulinum toxin A, brain and pain. Prog Neurobiol. 2014; 1;119–120:39–59.

12. Ramachandran R, Yaksh TL. Therapeutic use of botulinum toxin in migraine: mechanisms of action. Br J Pharmacol. 2014;171(18):4177–92.

13. Matak I. Evidence for central antispastic effect of botulinum toxin type A. Br J Pharmacol. 2020;1;177(1):65–76.

14. Popoff MR, Bouvet P. Clostridial toxins. Future Microbiol. 2009;4(8):1021–64.

15. Dover N, Barash JR, Arnon SS. Novel Clostridium botulinum toxin gene arrangement with subtype A5 and partial subtype B3 botulinum neurotoxin genes. J Clin Microbiol. 2009; 47(7):2349–50.

16. Kalb SR, Santana WI, Geren IN, Garcia-Rodriguez C, Lou J, Smith TJ, et al. Extraction and inhibition of enzymatic activity of botulinum neurotoxins /B1, /B2, /B3, /B4, and /B5 by a panel of monoclonal anti-BoNT/B antibodies. BMC Biochem. 2011; 15;12:58.

17. Smith TJ, Hill KK, Raphael BH. Historical and current perspectives on Clostridium botulinum diversity. Res Microbiol. 2015;166(4):290–302.

18. Dong M, Stenmark P. The Structure and Classification of Botulinum Toxins. Handb Exp Pharmacol. 2021;263:11–33.

19. Franciosa G, Ferreira JL, Hatheway CL. Detection of type A, B, and E botulism neurotoxin genes in Clostridium botulinum and other Clostridium species by PCR: evidence of unexpressed type B toxin genes in type A toxigenic organisms. J Clin Microbiol. 1994;32(8):1911–7.

20. Winslow CEA, Broadhurst J, Buchanan RE, Krumwiede C, Rogers LA, Smith GH. The Families and Genera of the Bacteria. J Bacteriol. 1917;2(5):505–66.

21. Jabbari B. The History of Botulinum Neurotoxins: From 1820 to 2020. In: Jabbari B, editor. Botulinum Toxin Treatment in Surgery, Dentistry, and Veterinary Medicine. Cham: Springer International Publishing; 2020; p. 1–13.

22. Anniballi F, Auricchio B, Fiore A, Lonati D, Locatelli CA, Lista F, et al. Botulism in Italy, 1986 to 2015. Euro Surveill.2017; 15;22(24):30550.

23. Kerner JAC. Neue Beobachtungen über die in Würtemberg so häusig vorfallenden tödtlichen Vergiftungen durch den Genuss geräucherter Würste. Osiander. 1820; 156 p.

24. Erbguth FJ. From poison to remedy: The chequered history of botulinum toxin. J Neural Transm. 2008;115(4):559–65.

25. Tatu L, Feugeas JP. Botulinum Toxin in WW2 German and Allied Armies: Failures and Myths of Weaponization. Eur Neurol. 2021; 20;84(1):53–60.

26. Chertow DS, Tan ET, Maslanka SE, Schulte J, Bresnitz EA, Weisman RS, et al. Botulism in 4 adults following cosmetic injections with an unlicensed, highly concentrated botulinum preparation. JAMA. 2006; 22;296(20):2476–9.

27. Crowner BE, Brunstrom JE, Racette BA. Iatrogenic botulism due to therapeutic botulinum toxin a injection in a pediatric patient. Clin Neuropharmacol. 2007;30(5):310–3.

28. Anniballi F. Lessons from a recent multicountry iatrogenic botulism outbreak. Euro surveill. 2023; 28(23):2300280

29. Antonucci L, Locci C, Schettini L, Clemente MG, Antonucci R. Infant botulism: an underestimated threat. Infect Dis Lond Engl. 2021; 24;12(2):81.

30. Rao AK, Sobel J, Chatham-Stephens K, Luquez C. Clinical Guidelines for Diagnosis and Treatment of Botulism, 2021. MMWR Recomm Rep. 2021; 7;70(2):1–30.

31. Rossetto O, Pirazzini M, Montecucco C. Botulinum neurotoxins: Genetic, structural and mechanistic insights. Nat Rev Microbiol. 2014;12(8):535–49.

32. Farrar JJ. Neurological aspects of tropical disease: Tetanus. J Neurol Neurosurg Psychiatry 2000; 1;69:292–301.

33. Miller SW. Adverse Medication Events: Tetanus Toxoid Reaction: Too Much of a Good Thing. J Pharm Pract. 1997; 1;10(6):365–6.

34. Finkelstein P, Teisch L, Allen CJ, Ruiz G. Tetanus: A potential public health threat in times of disaster. In: Prehospital and Disaster Medicine. Cambridge University Press; 2017; 32(3):339–42.

35. Thwaites CL, Beeching NJ, Newton CR. Maternal and neonatal tetanus. Lancet. 2015;24;385(9965):362-70.

36. Burgen ASV, Dickens F, Zatman LJ. The action of botulinum toxin on the neuro-muscular junction. J Physiol. 1949;109(1–2):10–24.

37. Drachman DB. Atrophy of skeletal muscle in chick embryos treated with botulinum toxin. Science. 1964; 14;145(3633):719–21.

38. Scott AB. Botulinum toxin injection into extraocular muscles as an alternative to strabismus surgery. Ophthalmology. 1980 ;87(10):1044–9.

39. Jankovic J. Botulinum toxin: State of the art. Mov Disord. 2017; 1;32(8):1131–8.

40. Truong DD, Stenner A, Reichel G. Current clinical applications of botulinum toxin. Curr Pharm Des. 2009;15(31):3671–80.

41. Botox - referral | European Medicines Agency [Internet]. [cited 2024 Apr 11]. Available from: https://www.ema.europa.eu/en/medicines/human/referrals/botox

42. R FDA, 2013. US FOOD and Drug Information: Information for Healthcare Professionals: OnabotulinumtoxinA (Marketed as Botox/Botox Cosmetic), AbobotulinumtoxinA (Marketed as Dysport) and RimabotulinumtoxinB (Marketed as Myobloc), https://www.fda.gov/drugs/postmarket-drug-safety-information-patients-and-providers/onabotulinumtoxina-marketed-botoxbotox-cosmetic-abobotulinumtoxina-marketed-dysport-and

43. Hadley HS, Wheeler JL, Petersen SW. Effects of intra-articular botulinum toxin type A (Botox®) in dogs with chronic osteoarthritis: A pilot study. Vet Comp Orthop Traumatol. 2010;23(4):254–8.

44. Heikkilä HM, Hielm-Björkman AK, Morelius M, Larsen S, Honkavaara J, Innes JF, et al. Intra-articular botulinum toxin A for the treatment of osteoarthritic joint pain in dogs: A randomized, double-blinded, placebo-controlled clinical trial. Vet J. 2014; 200(1):162–9.

45. Vilhegas S, Cassu RN, Barbero RC, Crociolli GC, Rocha TLA, Gomes DR. Botulinum toxin type A as an adjunct in postoperative pain management in dogs undergoing radical mastectomy. Vet Rec. 2015;177(15):391.

46. Grobman ME, Schachtel J, Prakash Gyawali C, Lever TE, Reinero CR. Videofluoroscopic swallow study features of lower esophageal sphincter achalasia-like syndrome in dogs. JVIM. 2019;33(5), 1954–1963.

47. Lew S, Majewski M, Radziszewski P, Kuleta Z. Therapeutic efficacy of botulinum toxin in the treatment of urinary incontinence in female dogs. Acta Vet Hung. 2010; 11;58(2):157–65.

48. Mostachio GQ, Apparício M, Motheo TF, Alves AE, Vicente WRR. Intra-prostatic injection of botulinum toxin type A in treatment of dogs with spontaneous benign prostatic hyperplasia. Anim Reprod Sci. 2012 ;133(3–4):224–8.

49. Wijnberg ID, Schrama SEA, Elgersma AE, Maree JTM, de Cocq PD, Back W. Quantification of surface EMG signals to monitor the effect of a Botox treatment in six healthy ponies and two horses with stringhalt: Preliminary study. Equine Vet J. 2009; 41(3):313–8.

50. Tighe AP, Schiavo G. Botulinum neurotoxins: mechanism of action. Toxicon. 2013; 1;67:87–93.

51. Joensuu M, Syed P, Saber SH, Lanoue V, Wallis TP, Rae J, et al. Presynaptic targeting of botulinum neurotoxin type A requires a tripartite PSG-Syt1-SV2 plasma membrane nanocluster for synaptic vesicle entry. EMBO J. 2023; 3;42(13):e112095.

52. Dong M, Yeh F, Tepp WH, Dean C, Johnson EA, Janz R, et al. SV2 is the protein receptor for botulinum neurotoxin A. Science. 2006;312(5773):592–6.

53. Yao G, Zhang S, Mahrhold S, Lam KH, Stern D, Bagramyan K, et al. N-linked glycosylation of SV2 is required for binding and uptake of botulinum neurotoxin A. Nat Struct Mol Biol. 2016 ;23(7):656–62.

54. Montecucco C, Zanotti G. Botulinum neurotoxin A1 likes it double sweet. Nat Struct Mol Biol. 2016; 6;23(7):619–21.

55. Harper CB, Martin S, Nguyen TH, Daniels SJ, Lavidis NA, Popoff MR, et al. Dynamin inhibition blocks botulinum neurotoxin type A endocytosis in neurons and delays botulism. J Biol Chem. 2011; 14;286(41):35966–76.

56. Fischer A, Montal M. Single molecule detection of intermediates during botulinum neurotoxin translocation across membranes. Proc Natl Acad Sci U S A. 2007 19;104(25):10447–52.

57. Blasi J, Chapman ER, Link E, Binz T, Yamasaki S, Camilli PD, et al. Botulinum neurotoxin A selectively cleaves the synaptic protein SNAP-25. Nature. 1993;365(6442):160–3.

58. Pirazzini M, Montecucco C, Rossetto O. Toxicology and pharmacology of botulinum and tetanus neurotoxins: an update. Arch Toxicol. 2022 ;96(6):1521–39.

59. Pantano S, Montecucco C. The blockade of the neurotransmitter release apparatus by botulinum neurotoxins. CMLS. 2014 ;71(5):793–811.

60. Shoemaker CB, Oyler GA. Persistence of Botulinum neurotoxin inactivation of nerve function. Curr Top Microbiol Immunol. 2013;364:179–96.

61. Whitemarsh RCM, Tepp WH, Johnson EA, Pellett S. Persistence of botulinum neurotoxin a subtypes 1-5 in primary rat spinal cord cells. PloS One. 2014;9(2):e90252.

62. Naumann M, Dressler D, Hallett M, Jankovic J, Schiavo G, Segal KR, et al. Evidence-based review and assessment of botulinum neurotoxin for the treatment of secretory disorders. Toxicon. 2013; 1;67:141–52.

63. Wang J, Gossing M, Fang P, Zimmermann J, Li X, von Mollard GF, et al. Epsin N-terminal homology domains bind on opposite sides of two SNAREs. Proc Natl Acad Sci U S A. 2011; 26;108(30):12277–82.

64. Šoštarić P, Članjak - Kudra E, Matak I, Smajlović A. 2022. Botulinum toxin: From the natural cause of botulism to an emerging therapeutic in veterinary medicine. Veterinaria, 71(2), 153-17.

65. Brüggemann H, Brzuszkiewicz E, Chapeton-Montes D, Plourde L, Speck D, Popoff MR. Genomics of Clostridium tetani. Res Microbiol. 2015 ;166(4):326–31.

66. Schiavo G, Papini E, Genna G, Montecucco C. An intact interchain disulfide bond is required for the neurotoxicity of tetanus toxin. Infect Immun. 1990 ;58(12):4136–41.

67. Surana S, Tosolini AP, Meyer IFG, Fellows AD, Novoselov SS, Schiavo G. The travel diaries of tetanus and botulinum neurotoxins. Toxicon. 2018; 1;147:58–67.

68. Garcia-Rodriguez C, Levy R, Arndt JW, Forsyth CM, Razai A, Lou J, et al. Molecular evolution of antibody cross-reactivity for two subtypes of type A botulinum neurotoxin. Nat Biotechnol. 2007 ;25(1):107–16.

69. Garcia-Rodriguez C, Yan S, Geren IN, Knopp KA, Dong J, Sun Z, et al. A Four-Monoclonal Antibody Combination Potently Neutralizes Multiple Botulinum Neurotoxin Serotypes C and D. Toxins. 2021; 10;13(9):641.

70. Dong M, Masuyer G, Stenmark P. Botulinum and Tetanus Neurotoxins. Annu Rev Biochem. 2019; 20;88:811–37.

71. Harper CB, Papadopulos A, Martin S, Matthews DR, Morgan GP, Nguyen TH, et al. Botulinum neurotoxin type-A enters a non-recycling pool of synaptic vesicles. Sci Rep. 2016; 25;6:19654.

72. Colasante C, Rossetto O, Morbiato L, Pirazzini M, Molgó J, Montecucco C. Botulinum neurotoxin type A is internalized and translocated from small synaptic vesicles at the neuromuscular junction. Mol Neurobiol. 2013;48(1):120–7.

73. Deinhardt K, Salinas S, Verastegui C, Watson R, Worth D, Hanrahan S, et al. Rab5 and Rab7 control endocytic sorting along the axonal retrograde transport pathway. Neuron. 2006;19;52(2):293–305.

74. Bercsenyi K, Schmieg N, Bryson JB, Wallace M, Caccin P, Golding M, et al. Tetanus toxin entry. Nidogens are therapeutic targets for the prevention of tetanus. Science. 2014; 28;346(6213):1118–23.

75. Debaisieux S, Encheva V, Chakravarty P, Snijders AP, Schiavo G. Analysis of Signaling Endosome Composition and Dynamics Using SILAC in Embryonic Stem Cell-Derived Neurons. Mol Cell Proteomics. 2016; 15(2):542–57.

76. Gibbs KL, Kalmar B, Sleigh JN, Greensmith L, Schiavo G.In vivo imaging of axonal transport in murine motor and sensory neurons. J Neurosci Methods. 2016;15;257:26-33.

77. Sleigh JN, Rossor AM, Fellows AD, Tosolini AP, Schiavo G. Axonal transport and neurological disease. Nat Rev Neurol. 2019 ;15(12):691–703.

78. Sleigh JN, Tosolini AP, Schiavo G. In Vivo Imaging of Anterograde and Retrograde Axonal Transport in Rodent Peripheral Nerves. Methods Mol Biol. 2020; 2143:271–92.

79. Antonucci F, Rossi C, Gianfranceschi L, Rossetto O, Caleo M. Long-distance retrograde effects of botulinum neurotoxin A. J Neurosci. 2008 2;28(14):3689–96.

80. Caleo M, Schiavo G. Central effects of tetanus and botulinum neurotoxins. Toxicon. 2009;54(5):593–9.

81. Matak I, Bach-Rojecky L, Filipović B, Lacković Z. Behavioral and immunohistochemical evidence for central antinociceptive activity of botulinum toxin A. Neuroscience. 2011; 186:201–7.

82. Restani L, Novelli E, Bottari D, Leone P, Barone I, Galli-Resta L, et al. Botulinum Neurotoxin A Impairs Neurotransmission Following Retrograde Transynaptic Transport. Traffic. 2012;13(8):1083–9.

83. Matak I, Riederer P, Lacković Z. Botulinum toxin's axonal transport from periphery to the spinal cord. Neurochem Int. 2012 ;61(2):236–9.

84. Restani L, Antonucci F, Gianfranceschi L, Rossi C, Rossetto O, Caleo M. Evidence for anterograde transport and transcytosis of botulinum neurotoxin A (BoNT/A). J Neurosci. 2011; 2;31(44):15650–9.

85. Jahn R, Scheller RH. SNAREs--engines for membrane fusion. Nat Rev Mol Cell Biol. 2006 ;7(9):631–43.

86. Brooks VB, Curtis DR, Eccles JC. The action of tetanus toxin on the inhibition of motoneurones. J Physiol. 1957 11;135(3):655–72.

87. Stoeckel K, Schwab M, Thoenen H. Role of gangliosides in the uptake and retrograde axonal transport of cholera and tetanus toxin as compared to nerve growth factor and wheat germ agglutinin. Brain Res. 1977 26;132(2):273–85.

88. Hassel B. Tetanus: pathophysiology, treatment, and the possibility of using botulinum toxin against tetanus-induced rigidity and spasms. Toxins. 2013; 8;5(1):73–83.

89. Pirazzini M, Grinzato A, Corti D, Barbieri S, Leka O, Vallese F, et al. Exceptionally potent human monoclonal antibodies are effective for prophylaxis and treatment of tetanus in mice. J Clin Invest. 2021; 15;131(22):e151676.

90. Jankovic J, Orman J. Botulinum A toxin for cranial-cervical dystonia: a double-blind, placebo-controlled study. Neurology. 1987;37(4):616–23.

91. Taylor AE, Lang AE, Saint-Cyr JA, Riley DE, Ranawaya R. Cognitive processes in idiopathic dystonia treated with high-dose anticholinergic therapy: implications for treatment strategies. Clin Neuropharmacol. 1991 ;14(1):62–77.

92. Tsui JK, Eisen A, Stoessl AJ, Calne S, Calne DB. Double-blind study of botulinum toxin in spasmodic torticollis. Lancet.1986; 2;2(8501):245–7.

93. Albanese A, Sorbo FD, Comella C, Jinnah HA, Mink JW, Post B, et al. Dystonia rating scales: critique and recommendations. Mov Disord. 2013;15;28(7):874–83.

94. Jinnah HA, Delong MR, Hallett M. The dystonias: past, present, and future. Mov Disord. 2013; 15;28(7):849–50.

95. Jankovic J, Brin MF. Therapeutic uses of botulinum toxin. N Engl J Med. 1991;25;324(17):1186–94.

96. Giladi N, Meer J, Kidan C, Greenberg E, Gross B, Honigman S. Interventional neurology: botulinum toxin as a potent symptomatic treatment in neurology. Isr J Med Sci. 1994 ;30(11):816–9.

97. Rothwell JC, Obeso JA, Day BL, Marsden CD. Pathophysiology of dystonias. Adv Neurol. 1983;39:851–63.

98. Berardelli A, Rothwell JC, Day BL, Marsden CD. Pathophysiology of blepharospasm and oromandibular dystonia. Brain J Neurol. 1985 ;108 (Pt 3):593–608.

99. Berardelli A, Rothwell JC, Hallett M, Thompson PD, Manfredi M, Marsden CD. The pathophysiology of primary dystonia. Brain J Neurol. 1998 ;121 (Pt 7):1195–212.

100. Sohn YH, Hallett M. Motor evoked potentials. Phys Med Rehabil Clin N Am. 2004 ;15(1):117–31,

101. Hallett M. Neurophysiology of dystonia: The role of inhibition. Neurobiol Dis. 2011;42(2):177–84.

102. Quartarone A, Hallett M. Emerging concepts in the physiological basis of dystonia. Mov Disord. 2013; 15;28(7):958–67.

103. Balint B, Mencacci NE, Valente EM, Pisani A, Rothwell J, Jankovic J, et al. Dystonia. Nat Rev Dis Primer. 2018 20;4(1):25.

104. Termsarasab P, Thammongkolchai T, Frucht SJ. Medical treatment of dystonia. J Clin Mov Disord. 2016;3:19.

105. Jankovic J. Medical treatment of dystonia. Mov Disord. 2013; 15;28(7):1001–12.

106. Ranoux D, Gury C, Fondarai J, Mas JL, Zuber M. Respective potencies of Botox and Dysport: a double blind, randomised, crossover study in cervical dystonia. J Neurol Neurosurg Psychiatry. 2002 ;72(4):459–62.

107. Jochim A, Meindl T, Mantel T, Zwirner S, Zech M, Castrop F, et al. Treatment of cervical dystonia with abo- and onabotulinumtoxinA: long-term safety and efficacy in daily clinical practice. J Neurol. 2019 ;266(8):1879–86.

108. Brin MF, Comella CL, Jankovic J, Lai F, Naumann M, CD-017 BoNTA Study Group. Long-term treatment with botulinum toxin type A in cervical dystonia has low immunogenicity by mouse protection assay. Mov Disord Off J Mov Disord Soc. 2008; 30;23(10):1353–60.

109. Gill HS, Kraft SP. Long-term efficacy of botulinum a toxin for blepharospasm and hemifacial spasm. Can J Neurol Sci. 2010 ;37(5):631–6.

110. Camargo CHF, Teive HAG, Becker N, Munhoz RP, Werneck LC. Botulinum toxin type A and cervical dystonia: a seven-year follow-up. Arq Neuropsiquiatr. 2011 ;69(5):745–50.

111. Ramirez-Castaneda J, Jankovic J. Long-term efficacy, safety, and side effect profile of botulinum toxin in dystonia: a 20-year follow-up. Toxicon. 2014 ;90:344–8.

112. Bentivoglio AR, Di Stasio E, Mulas D, Cerbarano ML, Ialongo T, Laurienzo A, et al. Long-Term Abobotulinumtoxin A Treatment of Cervical Dystonia. Neurotox Res. 2017 ;32(2):291–300.

113. Colosimo C, Bhidayasiri R, Fheodoroff K, Bhatia K, Chung TM, Landreau T, et al. Management of Spastic Paresis and Cervical Dystonia: Access to Therapeutic Innovations Through an International Program of Practical Courses. Clin Ther. 2019; 41(11):2321-2330.e4.

114. Mejia NI, Vuong KD, Jankovic J. Long-term botulinum toxin efficacy, safety, and immunogenicity. Mov Disord. 2005;20(5):592–7.

115. Papapetropoulos S, Singer C. Eating dysfunction associated with oromandibular dystonia: clinical characteristics and treatment considerations. Head Face Med. 2006; 7;2:47.

116. Fabbri M, Leodori G, Fernandes RM, Bhidayasiri R, Marti MJ, Colosimo C, et al. Neutralizing Antibody and Botulinum Toxin Therapy: A Systematic Review and Meta-analysis. Neurotox Res. 2016 ;29(1):105–17.

117. Mittal SO, Lenka A, Jankovic J. Botulinum toxin for the treatment of tremor. Parkinsonism Relat Disord. 2019 ;63:31–41.

118. Mittal SO, Machado D, Richardson D, Dubey D, Jabbari B. Botulinum Toxin in Parkinson Disease Tremor: A Randomized, Double-Blind, Placebo-Controlled Study With a Customized Injection Approach. Mayo Clin Proc. 2017 ;92(9):1359–67.

119. Mittal SO, Machado D, Richardson D, Dubey D, Jabbari B. Botulinum Toxin in Restless Legs Syndrome-A Randomized Double-Blind Placebo-Controlled Crossover Study. Toxins. 2018; 29;10(10):401.

120. Charles JA. Roadblock to the only FDA-approved treatment for chronic migraine. Headache. 2014 ;54(1):169–70.

121. Novak CB, Katz J. Neuropathic pain in patients with upper-extremity nerve injury. Physiother Can. 2010;62(3):190–201.

122. Camargo CHF, Cattai L, Teive HAG. Pain Relief in Cervical Dystonia with Botulinum Toxin Treatment. Toxins. 2015 23;7(6):2321–35.

123. Park J, Chung ME. Botulinum Toxin for Central Neuropathic Pain. Toxins. 2018;1;10(6):224.

124. Relja M, Miletić V. When movement disorders hurt: Addressing pain in hyperkinetic disorders. Parkinsonism Relat Disord. 2017 ;44:110–3.

125. Sheean G. The pathophysiology of spasticity. Eur J Neurol. 2002;9;1:3–9;53-61.

126. Kheder A, Nair KPS. Spasticity: Pathophysiology, evaluation and management. Pract Neurol. 2012 ;12(5):289–98.

127. Dressler D, Bhidayasiri R, Bohlega S, Chahidi A, Chung TM, Ebke M, et al. Botulinum toxin therapy for treatment of spasticity in multiple sclerosis: review and recommendations of the IAB-Interdisciplinary Working Group for Movement Disorders task force. J Neurol. 2017 ;264(1):112–20.

128. Patejdl R, Zettl UK. Spasticity in multiple sclerosis: Contribution of inflammation, autoimmune mediated neuronal damage and therapeutic interventions. Autoimmun Rev. 2017;16(9):925–36.

129. Pundik S, McCabe J, Skelly M, Tatsuoka C, Daly JJ. Association of spasticity and motor dysfunction in chronic stroke. Ann Phys Rehabil Med. 2019; 1;62(6):397–402.

130. Maynard FM, Karunas RS, Waring WP. Epidemiology of spasticity following traumatic spinal cord injury. Arch Phys Med Rehabil. 1990 ;71(8):566–9.

131. Watkins CL, Leathley MJ, Gregson JM, Moore AP, Smith TL, Sharma AK. Prevalence of spasticity post stroke. Clin Rehabil. 2002;16(5):515–22.

132. Dressler D, Tacik P, Adib Saberi F. Botulinum toxin therapy of cervical dystonia: duration of therapeutic effects. J Neural Transm. 2015 ;122(2):297–300.

133. Moeini-Naghani I, Hashemi-Zonouz T, Jabbari B. Botulinum Toxin Treatment of Spasticity in Adults and Children. Semin Neurol. 2016 ;36(1):64–72.

134. Simpson DM, Hallett M, Ashman EJ, Comella CL, Green MW, Gronseth GS, et al. Practice guideline update summary: Botulinum neurotoxin for the treatment of blepharospasm, cervical dystonia, adult spasticity, and headache: Report of the Guideline Development Subcommittee of the American Academy of Neurology. Neurology. 2016; 10;86(19):1818–26.

135. Bensmail D, Hanschmann A, Wissel J. Satisfaction with botulinum toxin treatment in post-stroke spasticity: results from two cross-sectional surveys (patients and physicians). J Med Econ. 2014; 1;17(9):618–25.

136. Andringa A, van de Port I, van Wegen E, Ket J, Meskers C, Kwakkel G. Effectiveness of Botulinum Toxin Treatment for Upper Limb Spasticity Poststroke Over Different ICF Domains: A Systematic Review and Meta-Analysis. Arch Phys Med Rehabil. 2019 1;100(9):1703–25.

137. Wissel J, Ward AB, Erztgaard P, Bensmail D, Hecht MJ, Lejeune TM, et al. European consensus table on the use of botulinum toxin type A in adult spasticity. J Rehabil Med. 2009 ;41(1):13–25.

138. Santamato A, Micello MF, Ranieri M, Valeno G, Albano A, Baricich A, et al. Employment of higher doses of botulinum toxin type A to reduce spasticity after stroke. J Neurol Sci. 2015; 15;350(1–2):1–6.

139. Baricich A, Picelli A, Santamato A, Carda S, de Sire A, Smania N, et al. Safety Profile of High-Dose Botulinum Toxin Type A in Post-Stroke Spasticity Treatment. Clin Drug Investig. 2018; 1;38(11):991–1000.

140. Gracies JM, Lugassy M, Weisz DJ, Vecchio M, Flanagan S, Simpson DM. Botulinum toxin dilution and endplate targeting in spasticity: a double-blind controlled study. Arch Phys Med Rehabil. 2009 ;90(1):9-16.e2.

141. Schnitzler A, Roche N, Denormandie P, Lautridou C, Parratte B, Genet F. Manual needle placement: accuracy of botulinum toxin A injections. Muscle Nerve. 2012;46(4):531–4.

142. Picelli A, Lobba D, Midiri A, Prandi P, Melotti C, Baldessarelli S, et al. Botulinum toxin injection into the forearm muscles for wrist and fingers spastic overactivity in adults with chronic stroke: a randomized controlled trial comparing three injection techniques. Clin Rehabil. 2014 ;28(3):232–42.

143. Ploumis A, Varvarousis D, Konitsiotis S, Beris A. Effectiveness of botulinum toxin injection with and without needle electromyographic guidance for the treatment of spasticity in hemiplegic patients: a randomized controlled trial. Disabil Rehabil. 2014;36(4):313–8.

144. Hesse S, Mach H, Fröhlich S, Behrend S, Werner C, Melzer I. An early botulinum toxin A treatment in subacute stroke patients may prevent a disabling finger flexor stiffness six months later: a randomized controlled trial. Clin Rehabil. 2012 ;26(3):237–45.

145. Fietzek UM, Kossmehl P, Schelosky L, Ebersbach G, Wissel J. Early botulinum toxin treatment for spastic pes equinovarus--a randomized double-blind placebo-controlled study. Eur J Neurol. 2014 ;21(8):1089–95.

146. Lagalla G, Danni M, Reiter F, Ceravolo MG, Provinciali L. Post-stroke spasticity management with repeated botulinum toxin injections in the upper limb. Am J Phys Med Rehabil. 2000;79(4):377–84; 391–4.

147. Gordon MF, Brashear A, Elovic E, Kassicieh D, Marciniak C, Liu J, et al. Repeated dosing of botulinum toxin type A for upper limb spasticity following stroke. Neurology. 2004; 23;63(10):1971–3.

148. Elovic EP, Brashear A, Kaelin D, Liu J, Millis SR, Barron R, et al. Repeated treatments with botulinum toxin type a produce sustained decreases in the limitations associated with focal upper-limb poststroke spasticity for caregivers and patients. Arch Phys Med Rehabil. 2008;89(5):799–806.

149. Santamato A, Panza F, Intiso D, Baricich A, Picelli A, Smania N, et al. Long-term safety of repeated high doses of incobotulinumtoxinA injections for the treatment of upper and lower limb spasticity after stroke. J Neurol Sci. 2017; 15;378:182–6.

150. Siparsky PN, Kirkendall DT, Garrett WE. Muscle changes in aging: understanding sarcopenia. Sports Health. 2014 ;6(1):36–40.

151. Agyei JO, Smolar DE, Hartke J, Fanous AA, Gibbons KJ. Cervical Kyphotic Deformity Worsening After Extensor Cervical Muscle Paralysis from Botulinum Toxin Injection. World Neurosurg. 2019 ;125:409–13.

152. Baizabal-Carvallo JF, Jankovic J, Pappert E. Flu-like symptoms following botulinum toxin therapy. Toxicon. 2011;58(1):1–7.

153. Baizabal-Carvallo JF, Jankovic J, Feld J. Flu-like symptoms and associated immunological response following therapy with botulinum toxins. Neurotox Res. 2013 ;24(2):298–306.

154. Dressler D, Bigalke H. Immunological aspects of botulinum toxin therapy. Expert Rev Neurother. 2017 ;17(5):487–94.

155. Oshima M, Deitiker P, Jankovic J, Aoki KR, Atassi MZ. Submolecular recognition of the C-terminal domain of the heavy chain of botulinum neurotoxin type A by T cells from toxin-treated cervical dystonia patients. Immunobiology. 2016 ;221(4):568–76.

156. Sethi KD, Rodriguez R, Olayinka B.Satisfaction with botulinum toxin treatment:a cross-sectional survey of patients with cervical dystonia. J Med Econ. 2012;15(3):419-23.

157. Kaňovský P, Rosales R. Debunking the pathophysiological puzzle of dystonia--with special reference to botulinum toxin therapy. Parkinsonism Relat Disord 2011; 7-1;11-14

158. Foran PG, Mohammed N, Lisk GO, Nagwaney S, Lawrence GW, Johnson E, et al. Evaluation of the therapeutic usefulness of botulinum neurotoxin B, C1, E, and F compared with the long lasting type A: Basis for distinct durations of inhibition of exocytosis in central neurons. J Biol Chem. 2003;278(2):1363–71.

159. Meunier F, Lisk G, Sesardic D, Dolly J. Dynamics of motor nerve terminal remodeling unveiled using SNARE-cleaving botulinum toxins: the extent and duration are dictated by the sites of SNAP-25 truncation. Mol Cell Neurosci. 2003; 1;22(4):454–66.

160. Montecucco C, Molgó J. Botulinal neurotoxins: revival of an old killer. Curr Opin Pharmacol. 2005 ;5(3):274–9.

161. de Paiva A, Meunier FA, Molgó J, Aoki KR, Dolly JO. Functional repair of motor endplates after botulinum neurotoxin type A poisoning: biphasic switch of synaptic activity between nerve sprouts and their parent terminals. Proc Natl Acad Sci U S A. 1999 16;96(6):3200–5.

162. Keller JE, Cai F, Neale EA. Uptake of botulinum neurotoxin into cultured neurons. Biochemistry. 2004; 20;43(2):526–32.

163. Chen R, Karp BI, Goldstein SR, Bara-Jimenez W, Yaseen Z, Hallett M. Effect of muscle activity immediately after botulinum toxin injection for writer's cramp. Mov Disord. 1999; 1;14(2):307–12.

164. Fortuna R, Vaz MA, Youssef AR, Longino D, Herzog W. Changes in contractile properties of muscles receiving repeat injections of botulinum toxin (Botox). J Biomech. 2011; 4;44(1):39–44.

165. Inagi K, Connor NP, Schultz E, Ford CN, Cook CH, Heisey DM. Muscle fiber-type changes induced by botulinum toxin injection in the rat larynx. Otolaryngol Head Neck Surg. 1999;120(6):876–83.

166. Dodd SL, Selsby J, Payne A, Judge A, Dott C. Botulinum neurotoxin type A causes shifts in myosin heavy chain composition in muscle. Toxicon. 2005;46(2):196–203.

167. Clowry GJ, Walker L, Davies P. The effects of botulinum neurotoxin A induced muscle paresis during a critical period upon muscle and spinal cord development in the rat. Exp Neurol. 2006 ;202(2):456–69.

168. Hufschmidt A, Mauritz KH. Chronic transformation of muscle in spasticity: a peripheral contribution to increased tone. J Neurol Neurosurg Psychiatry. 1985 ;48(7):676–85.

169. Gracies JM. Pathophysiology of spastic paresis. II: Emergence of muscle overactivity. Muscle Nerve. 2005 ;31(5):552–71.

170. Shaari CM, Sanders I. Quantifying how location and dose of botulinum toxin injections affect muscle paralysis. Muscle Nerve. 1993 ;16(9):964–9.

171. Cavarsan CF, Gorassini MA, Quinlan KA. Animal models of developmental motor disorders: parallels to human motor dysfunction in cerebral palsy. J Neurophysiol. 2019 1;122(3):1238–53.

172. Gibson CL, Arnott GA, Clowry GJ. Plasticity in the rat spinal cord seen in response to lesions to the motor cortex during development but not to lesions in maturity. Exp Neurol. 2000 ;166(2):422–34.

173. Andreani JCM, Guma C. New animal model to mimic spastic cerebral palsy: the brain-damaged pig preparation. Neuromodulation. 2008 ;11(3):196–201.

174. Stigger F, do Nascimento PS, Dutra MF, Couto GK, Ilha J, Achaval M, et al. Treadmill training induces plasticity in spinal motoneurons and sciatic nerve after sensorimotor restriction during early postnatal period: new insights into the clinical approach for children with cerebral palsy. Int J Dev Neurosci. 2011 ;29(8):833–8.

175. Stigger F, Felizzola AL de S, Kronbauer GA, Couto GK, Achaval M, Marcuzzo S. Effects of fetal exposure to lipopolysaccharide, perinatal anoxia and sensorimotor restriction on motor skills and musculoskeletal tissue: implications for an animal model of cerebral palsy. Exp Neurol. 2011;228(2):183–91.

176. Brandenburg JE, Gransee HM, Fogarty MJ, Sieck GC. Differences in lumbar motor neuron pruning in an animal model of early onset spasticity. J Neurophysiol. 2018 1;120(2):601–9.

177. Wilson BK, Hess EJ. Animal models for dystonia. Mov Disord. 2013; 15;28(7):982–9.

178. Kita M, Goodkin DE. Drugs used to treat spasticity. Drugs. 2000 ;59(3):487–95.

179. Hassel B. Tetanus: pathophysiology, treatment, and the possibility of using botulinum toxin against tetanus-induced rigidity and spasms. Toxins. 2013 8;5(1):73–83.

180. Drachman DB. Botulinum toxin as a tool for research on the nervous system. In: Simpson LL, editor. Neuropoisons. Boston (MA): Springer; 1971. p. 479-92.

181. Johnson EA. Clostridial toxins as therapeutic agents: benefits of nature's most toxic proteins.: Benefits of Nature's Most Toxic Proteins. Annu Rev Microbiol. 1999; 53, 551–575.

182. Scott AB. Botulinum toxin injection of eye muscles to correct strabismus. Trans Am Ophthalmol Soc. 1981;79:734–70.

183. Scott AB, Magoon EH, McNeer KW, Stager DR. Botulinum treatment of strabismus in children. Trans Am Ophthalmol Soc. 1989;87:174–80;

184. Giladi N. The mechanism of action of Botulinum toxin type A in focal dystonia is most probably through its dual effect on efferent (motor) and afferent pathways at the injected site. Vol. 152, Journal of Neurological Sciences. 1997; 25;152(2):132–5.

185. Filippi GM, Errico P, Santarelli R, Bagolini B, Manni E. Botulinum A toxin effects on rat jaw muscle spindles. Acta Otolaryngol. 1993 ;113(3):400–4.

186. Rosales RL, Arimura K, Takenaga S, Osame M. Extrafusal and intrafusal muscle effects in experimental botulinum toxin-A injection. Muscle Nerve. 1996 ;19(4):488–96.

187. Nakashima K, Rothwell JC, Day BL, Thompson PD, Shannon K, Marsden CD. Reciprocal inhibition between forearm muscles in patients with writer's cramp and other occupational cramps, symptomatic hemidystonia and hemiparesis due to stroke. Brain J Neurol. 1989 ;112 (Pt 3):681–97.

188. Priori A, Berardelli A, Mercuri B, Manfredi M, Neurologiche S, La R, et al. Changes in reciprocal inhibition between forearm muscles. Brain. 1995;118:801–7.

189. Gracies JM. Physiological effects of botulinum toxin in spasticity. Mov Disord. 2004;19 -8;120–128.

190. Pestronk A, Drachman DB, Griffin JW. Effect of botulinum toxin on trophic regulation of acetylcholine receptors. Nature. 1976; 23;264(5588):787–9.

191. Simpson LI. The binary toxin produced by Clostridium botulinum enters cells by receptor-mediated endocytosis to exert its pharmacologic effects. J Pharmacol Exp Ther. 1989;251(3):1223–8.

192. Hamjian JA, Walker FO. Serial neurophysiological studies of intramuscular botulinum-A toxin in humans. Muscle Nerve. 1994;17(12):1385–92.

193. Greene P, Kang U, Fahn S, Brin M, Moskowitz C, Flaster E. Double-blind, placebo-controlled trial of botulinum toxin injections for the treatment of spasmodic torticollis. Neurology. 1990; 40(8):1213–8.

194. Davis D, Jabbari B. Significant improvement of stiff-person syndrome after paraspinal injection of botulinum toxin A. Mov Disord. 1993;8(3):371–3.

195. Nix WA, Butler IJ, Roontga S, Gutmann L, Hopf HC. Persistent unilateral tibialis anterior muscle hypertrophy with complex repetitive discharges and myalgia: report of two unique cases and response to botulinum toxin. Neurology. 1992;42(3 Pt 1):602–6.

196. Cosgrove AP, Corry IS, Graham HK. Botulinum toxin in the management of the lower limb in cerebral palsy. Dev Med Child Neurol. 1994 ;36(5):386–96.

197. Brin MF, Fahn S, Moskowitz C, Friedman A, Shale HM, Greene PE, et al. Localized injections of botulinum toxin for the treatment of focal dystonia and hemifacial spasm. Mov Disord.1987;2(4):237–54.

198. Tolosa E, Martí MJ, Kulisevsky J. Botulinum toxin injection therapy for hemifacial spasm. Adv Neurol. 1988;49:479–91.

199. Denislic M, Pirtosek Z, Vodusek DB, Zidar J, Meh D. Botulinum toxin in the treatment of neurological disorders. Ann N Y Acad Sci. 1994;710:76–87.

200. Hardie RJ. Botulinum toxin in muscle spasticity. J Neurol Neurosurg Psychiatry. 2000;68(6):689–90.

201. Mazzocchio R, Spidalieri R, Dominici F, Popa T, Hallett M, Rossi A. Putative central effects of botulinum toxin, possibly mediated by changes in Renshaw cell activity, following intramuscular injection in humans. Mov Disord. 2007;22(Suppl 16)

202. Gracies JM. Pathophysiology of impairment in patients with spasticity and use of stretch as a treatment of spastic hypertonia. Phys Med Rehabil Clin N Am. 2001;12(4):747–68.

203. Miscio G, Del Conte C, Pianca D, Colombo R, Panizza M, Schieppati M, et al. Botulinum toxin in post-stroke patients: stiffness modifications and clinical implications. J Neurol. 2004 ;251(2):189–96.

204. Elston JS. Long-term results of treatment of idiopathic blepharospasm with botulinum toxin injections. Br J Ophthalmol. 1987 ;71(9):664–8.

205. Elston JS. The management of blepharospasm and hemifacial spasm. J Neurol. 1992;239(1):5–8.

206. Jankovic J. Botulinum toxin in the treatment of dystonic tics. Mov Disord. 1994;9(3):347–9.

207. Shulman LM, Singer C, Weiner WJ. Improvement of both tardive dystonia and akathisia after botulinum toxin injection. Neurology. 1996 ;46(3):844–5.

208. Naumann M, Reiners K. Long-latency reflexes of hand muscles in idiopathic focal dystonia and their modification by botulinum toxin. Brain J Neurol. 1997 ;120 (Pt 3):409–16.

209. Kanovský P, Streitová H, Dufek J, Znojil V, Daniel P, Rektor I. Change in lateralization of the P22/N30 cortical component of median nerve somatosensory evoked potentials in patients with cervical dystonia after successful treatment with botulinum toxin A. Mov Disord. 1998 ;13(1):108–17.

210. Park ES, Park CI, Kim DY, Kim YR. The effect of spasticity on cortical somatosensory-evoked potentials: changes of cortical somatosensory-evoked potentials after botulinum toxin type A injection. Arch Phys Med Rehabil. 2002;83(11):1592–6.

211. Frascarelli F, Di Rosa G, Bisozzi E, Castelli E, Santilli V. Neurophysiological changes induced by the botulinum toxin type A injection in children with cerebral palsy. Eur J Paediatr Neurol. 2011;15(1):59–64.

212. Byrnes ML, Thickbroom GW, Wilson SA, Sacco P, Shipman JM, Stell R, et al. The corticomotor representation of upper limb muscles in writer's cramp and changes following botulinum toxin injection. Brain J Neurol. 1998 ;121 (Pt 5):977–88.

213. Thickbroom GW, Byrnes ML, Stell R, Mastaglia FL. Reversible reorganisation of the motor cortical representation of the hand in cervical dystonia. Mov Disord. 2003;18(4):395–402.

214. Byrnes ML, Mastaglia FL, Walters SE, Archer SAR, Thickbroom GW.Primary writing tremor:motor cortex reorganisation and disinhibition. J Clin Neurosci.2005;12(1):102–4.

215. Gilio F, Currà A, Lorenzano C, Modugno N, Manfredi M, Berardelli A. Effects of botulinum toxin type A on intracortical inhibition in patients with dystonia. Ann Neurol. 2000 ;48(1):20–6.

216. Ridding MC, Sheean G, Rothwell JC, Inzelberg R, Kujirai T. Changes in the balance between motor cortical excitation and inhibition in focal, task specific dystonia. J Neurol Neurosurg Psychiatry. 1995;59(5):493–8.

217. Ceballos-Baumann AO, Sheean G, Passingham RE, Marsden CD, Brooks DJ. Botulinum toxin does not reverse the cortical dysfunction associated with writer's cramp. A PET study. Brain J Neurol. 1997 ;120 (Pt 4):571–82.

218. Senkárová Z, Hlustík P, Otruba P, Herzig R, Kanovský P. Modulation of cortical activity in patients suffering from upper arm spasticity following stroke and treated with botulinum toxin A: an fMRI study. J Neuroimaging. 2010 ;20(1):9–15.

219. Nevrlý M, Hluštík P, Hok P, Otruba P, Tüdös Z, Kaňovský P. Changes in sensorimotor network activation after botulinum toxin type A injections in patients with cervical dystonia: a functional MRI study. Exp Brain Res. 2018;236(10):2627–37.

220. Chang CL, Weber DJ, Munin MC. Changes in Cerebellar Activation After Onabotulinumtoxin A Injections for Spasticity After Chronic Stroke: A Pilot Functional Magnetic Resonance Imaging Study. Arch Phys Med Rehabil. 2015 ;96(11):2007–16.

221. Hok P, Hvizdošová L, Otruba P, Kaiserová M, Trnečková M, Tüdös Z, et al. Botulinum toxin injection changes resting state cerebellar connectivity in cervical dystonia. Sci Rep. 2021 15;11(1):8322.

222. Hok P, Veverka T, Hluštík P, Nevrlý M, Kaňovský P. The Central Effects of Botulinum Toxin in Dystonia and Spasticity. Toxins. 2021; 17;13(2):155.

223. Kojovic M, Caronni A, Bologna M, Rothwell JC, Bhatia KP, Edwards MJ. Botulinum toxin injections reduce associative plasticity in patients with primary dystonia. Mov Disord. 2011 ;26(7):1282–9.

224. Redman TA, Gibson N, Finn JC, Bremner AP, Valentine J, Thickbroom GW. Upper limb corticomotor projections and physiological changes that occur with botulinum toxin-A therapy in children with hemiplegic cerebral palsy. Eur J Neurol. 2008 ;15(8):787–91.

225. Koizumi H, Goto S, Okita S, Morigaki R, Akaike N, Torii Y, et al. Spinal central effects of peripherally applied botulinum neurotoxin A in comparison between its subtypes A1 and A2. Front Neurol. 2014;5:1–9.

226. Rosales L, Giribaldi F, Manich M, et al. Botulinum neurotoxins A and E undergo retrograde axonal transport in primary motor neurons. PLoS Patho. 2012; 31;8(12).

227. Rosales RL, Arimura K, Takenaga S, Osame M. Extrafusal and intrafusal muscle effects in experimental botulinum toxin-A injection. Muscle Nerve. 1996;19(4):488–96.

228. Sanna PP, Celio MR, Bloom FE, Rende M. Presumptive Renshaw cells contain decreased calbindin during recovery from sciatic nerve lesions. Proc Natl Acad Sci U S A. 1993;1;90(7):3048–52.

229. Gonzalez-Forero D, Pastor AM, Geiman EJ, Benítez-Temiño B, Alvarez FJ. Regulation of gephyrin cluster size and inhibitory synaptic currents on Renshaw cells by motor axon excitatory inputs. J Neurosci. 2005;12;25(2):417–29.

230. Hagenah R, Benecke R, Wiegand H. Effects of type A botulinum toxin on the cholinergic transmission at spinal Renshaw cells and on the inhibitory action at Ia inhibitory interneurones. Naunyn Schmiedebergs Arch Pharmacol. 1977 ;299(3):267–72.

231. Wiegand H, Wellhöner HH. The action of botulinum A neurotoxin on the inhibition by antidromic stimulation of the lumbar monosynaptic reflex. Naunyn Schmiedebergs Arch Pharmacol. 1977; 298(3):235–8.

232. Pinter MJ, Vanden Noven S, Muccio D, Wallace N. Axotomy-like changes in cat motoneuron electrical properties elicited by botulinum toxin depend on the complete elimination of neuromuscular transmission. J Neurosci.1991;11(3):657–66.

233. Watson WE. The response of rat hypoglossal neurones to injection of botulinum toxin into the tongue. J Physiol. 1969; 202(2):101

234.Jung HH, Lauterburg T, Burgunder JM. Expression of neurotransmitter genes in rat spinal motoneurons after chemodenervation with botulinum toxin. Neuroscience. 1997 78(2):469–79.

235. Moreno-López B, De la Cruz RR, Pastor AM, Delgado-García JM. Effects of botulinum neurotoxin type A on abducens motoneurons in the cat: alterations of the discharge pattern. Neuroscience. 1994;78;81(2):437–55.

236. Moreno-López B, Pastor AM, de la Cruz RR, Delgado-García JM. Dose-dependent, central effects of botulinum neurotoxin type A: a pilot study in the alert behaving cat. Neurology. 1997;48(2):456–64.

237. Pastor AM, Moreno-López B, De La Cruz RR, Delgado-García JM. Effects of botulinum neurotoxin type A on abducens motoneurons in the cat: ultrastructural and synaptic alterations. Neuroscience. 1997;81(2):457–78.

238. Marchand-Pauvert V, Aymard C, Giboin LS, Dominici F, Rossi A, Mazzocchio R. Beyond muscular effects: depression of spinal recurrent inhibition after botulinum neurotoxin A. J Physiol. 2013;591:1017–29.

239. Aymard C, Giboin LS, Lackmy-Vallée A, Marchand-Pauvert V. Spinal plasticity in stroke patients after botulinum neurotoxin A injection in ankle plantar flexors. Physiol Rep. 2013;1(6):e00173.

240. Habermann E. 125I-labeled neurotoxin from Clostridium botulinum A: preparation, binding to synaptosomes and ascent to the spinal cord. Naunyn Schmiedebergs Arch Pharmacol. 1974;281(1):47–56.

241. Wiegand H, Erdmann G, Wellhöner HH. 125I-labelled botulinum A neurotoxin: pharmacokinetics in cats after intramuscular injection. Naunyn Schmiedebergs Arch Pharmacol. 1976;292(2):161–5.

242. Schmieg N, Menendez G, Schiavo G, Terenzio M. Signalling endosomes in axonal transport:travel updates on the molecular highway. Semin Cell Dev Biol.2014;27:32–43.

243. Harper CB, Papadopulos A, Martin S, Matthews DR, Morgan GP, Nguyen TH, et al. Botulinum neurotoxin type-A enters a non-recycling pool of synaptic vesicles. Sci Rep. 2016; 25;6:19654.

244. Rind HB, Butowt R, Bartheld CS von. Synaptic Targeting of Retrogradely Transported Trophic Factors in Motoneurons: Comparison of Glial Cell Line-Derived Neurotrophic Factor, Brain-Derived Neurotrophic Factor, and Cardiotrophin-1 with Tetanus Toxin. J Neurosci. 2005;1;25(3):539.

245. Restani L, Giribaldi F, Manich M, Bercsenyi K, Menendez G, Rossetto O, et al. Botulinum neurotoxins A and E undergo retrograde axonal transport in primary motor neurons. PLoS Pathog. 2012 ;8(12):e1003087.

246. Verderio C, Grumelli C, Raiteri L, Coco S, Paluzzi S, Caccin P, et al.Traffic of botulinum toxins A and E in excitatory and inhibitory neurons.Traffic.2007;8(2):142–53.

247. Bomba-Warczak E, Vevea JD, Brittain JM, Figueroa-Bernier A, Tepp WH, Johnson EA, et al. Interneuronal Transfer and Distal Action of Tetanus Toxin and Botulinum Neurotoxins A and D in Central Neurons. Cell Rep. 2016 16;16(7):1974–87.

248. Marinelli S, Vacca V, Ricordy R, Uggenti C, Tata A, Luvisetto S, et al. The analgesic effect on neuropathic pain of retrogradely transported botulinum neurotoxin A involves Schwann cells and astrocytes. PloS One 2012; 7(10).

249. Bach-Rojecky L, Lacković Z. Central origin of the antinociceptive action of botulinum toxin type A. Pharmacol Biochem Behav. 2009;94(2):234–8.

250. Bach-Rojecky L, Salković-Petrisić M, Lacković Z. Botulinum toxin type A reduces pain supersensitivity in experimental diabetic neuropathy: bilateral effect after unilateral injection. Eur J Pharmacol. 2010; 10;633(1–3):10–4.

251. Filipović B, Matak I, Bach-Rojecky L, Lacković Z. Central action of peripherally applied botulinum toxin type a on pain and dural protein extravasation in rat model of trigeminal neuropathy. PLoS ONE. 2012;7(1):1–8.

252. Percie du Sert N, Hurst V, Ahluwalia A, Alam S, Avey MT, Baker M, et al. The ARRIVE guidelines 2.0: Updated guidelines for reporting animal research. Br J Pharmacol. 2020;177(16):3617–24.

253. Matthews CC, Fishman PS, Wittenberg GF. Tetanus toxin reduces local and descending regulation of the H-reflex. Muscle Nerve. 2014;49(4):495–501.

254. Duregotti E, Zanetti G, Scorzeto M, Megighian A, Montecucco C, Pirazzini M, et al. Snake and spider toxins induce a rapid recovery of function of botulinum neurotoxin paralysed neuromuscular junction. Toxins. 2015; 8;7(12):5322–36.

255. Tehran DA, Pirazzini M. Preparation of Cerebellum Granule Neurons from Mouse or Rat Pups and Evaluation of Clostridial Neurotoxin Activity and Their Inhibitors by Western Blot and Immunohistochemistry. Bio-Protoc. 2018; 5;8(13):e2918.

256. Broide R, Rubino J, GS Nicholson, Ardila M, Brown M, Aoki K, et al. The rat Digit Abduction Score (DAS) assay: a physiological model for assessing botulinum neurotoxin-induced skeletal muscle paralysis. Toxicon. 2013 1;71:18–24.

257. Brent MB, Lodberg A, Thomsen JS, Brüel A. Rodent model of disuse-induced bone loss by hind limb injection with botulinum toxin A. MethodsX. 2020; 3;7:101079 1;7.

258. Warner SE, Sanford DA, Becker BA, Bain SD, Srinivasan S, Gross TS. Botox induced muscle paralysis rapidly degrades bone. Bone. 2006 ;38(2):257–64.

259. Carter RJ, Morton J, Dunnett SB. Motor coordination and balance in rodents. Curr Protoc Neurosci. 2001; 8:8.12.

260. Ho SM, Waite PME. Effects of different anesthetics on the paired-pulse depression of the h reflex in adult rat. Exp Neurol. 2002;177(2):494–502.

261. Basso DM, Beattie MS, Bresnahan JC. A sensitive and reliable locomotor rating scale for open field testing in rats. J Neurotrauma. 1995;12(1):1–21.

262. Ekong TAN, Feavers IM, Sesardic D. Recombinant SNAP-25 is an effective substrate for Clostridium botulinum type A toxin endopeptidase activity in vitro. Microbiol Read Engl. 1997 ;143 (Pt 10):3337–47.

263. Jones RGA, Ochiai M, Liu Y, Ekong T, Sesardic D. Development of improved SNAP25 endopeptidase immuno-assays for botulinum type A and E toxins. J Immunol Methods. 2008 1;329(1–2):92–101.

264. Périer C, Martin V, Cornet S, Favre-Guilmard C, Rocher MN, Bindler J, et al. Recombinant botulinum neurotoxin serotype A1 in vivo characterization. Pharmacol Res Perspect. 2021;9(5):e00857

265. Homolak J, Babic Perhoc A, Knezovic A, Osmanovic Barilar J, Koc F, Stanton C, et al. Disbalance of the Duodenal Epithelial Cell Turnover and Apoptosis Accompanies Insensitivity of Intestinal Redox Homeostasis to Inhibition of the Brain Glucose-Dependent Insulinotropic Polypeptide Receptors in a Rat Model of Sporadic Alzheimer's Disease. Neuroendocrinology. 2022;112(8):744–62.

266. Charan J, Kantharia ND. How to calculate sample size in animal studies? J Pharmacol Pharmacother. 2013 1;4(4):303–6.

267. Zagoraiou L, Akay T, Martin JF, Brownstone RM, Jessell TM, Miles GB. A Cluster of Cholinergic Premotor Interneurons Modulates Mouse Locomotor Activity. Neuron. 2009;64(5):645–62.

268. Konsolaki E, Koropouli E, Tsape E, Pothakos K, Zagoraiou L. Genetic Inactivation of Cholinergic C Bouton Output Improves Motor Performance but not Survival in a Mouse Model of Amyotrophic Lateral Sclerosis. Neuroscience. 2020; 1;450:71–80.

269. Jacobs BY, Kloefkorn HE, Allen KD. Gait analysis methods for rodent models of osteoarthritis. Curr Pain Headache Rep. 2014 ;18(10):456.

270. Eleopra R, Tugnoli V, Rossetto O, De Grandis D, Montecucco C. Different time courses of recovery after poisoning with botulinum neurotoxin serotypes A and E in humans. Neurosci Lett. 1998; 13;256(3):135–8.

271. Martí MJ, Kulisevsky J, Tolosa E.Treatment of dystonic blepharospasm and hemifacial spasm with botulinum toxin: preliminary studies. Med Clin (Barc).1987;19;89(8):321–3.

272. Sätilä H, Kotamäki A, Koivikko M, Autti-Rämö I. Low- and high-dose botulinum toxin A treatment: a retrospective analysis. Pediatr Neurol. 2006;34(4):285–90.

273. Shaari CM, George E, Wu BL, Biller HF, Sanders I. Quantifying the spread of botulinum toxin through muscle fascia. The Laryngoscope. 1991; 101(9):960–4.

274. Cichon JV, McCaffrey TV, Litchy WJ, Knops JL. The effect of botulinum toxin type A injection on compound muscle action potential in an in vivo rat model. The Laryngoscope. 1995 ;105(2):144–8.

275. Poewe W, Deuschl G, Nebe A, Feifel E, Wissel J, Benecke R, et al. What is the optimal dose of botulinum toxin A in the treatment of cervical dystonia? Results of a double blind, placebo controlled, dose ranging study using Dysport. German Dystonia Study Group. J Neurol Neurosurg Psychiatry. 1998 ;64(1):13–7.

276. Childers MK, Brashear A, Jozefczyk P, Reding M, Alexander D, Good D, et al. Dose-dependent response to intramuscular botulinum toxin type a for upper-limb spasticity in patients after a stroke. Arch Phys Med Rehabil. 2004 ;85(7):1063–9.

277. Rystedt A, Zetterberg L, Burman J, Nyholm D, Johansson A. A Comparison of Botox 100 U/mL and Dysport 100 U/mL Using Dose Conversion Ratio 1: 3 and 1: 1.7 in the Treatment of Cervical Dystonia: A Double-Blind, Randomized, Crossover Trial. Clin Neuropharmacol. 2015;38(5):170–6.

278. Sanders JD, Yang Y, Liu Y. Differential turnover of syntaxin and SNAP-25 during synaptogenesis in cultured cerebellar granule neurons. J Neurosci Res. 1998; 15;53(6):670–6.

279. Miles GB, Hartley R, Todd AJ, Brownstone RM. Spinal cholinergic interneurons regulate the excitability of motoneurons during locomotion. Proc Natl Acad Sci U S A. 2007 13;104(7):2448–53.

280. Rosales RL, Dressler D. On muscle spindles, dystonia and botulinum toxin. Eur J Neurol. 2010 ;17; 1 :71–80.

281. Stampacchia G, Bradaschia E, Rossi B. Change of stretch reflex threshold in spasticity: effect of botulinum toxin injections. Arch Ital Biol. 2004 ;142(3):265–73.

282. Pierrot-Deseilligny E, Burke D. The circuitry of the human spinal cord: its role in motor control and movement disorders. Cambridge: Cambridge University Press; 2005

283. Megighian A, Pirazzini M, Fabris F, Rossetto O, Montecucco C. Tetanus and tetanus neurotoxin: From peripheral uptake to central nervous tissue targets. J Neurochem. 2021;158(6):1244–53.

284. Modugno N, Priori A, Berardelli A, Vacca L, Mercuri B, Manfredi M. Botulinum toxin restores presynaptic inhibition of group Ia afferents in patients with essential tremor. Muscle Nerve. 1998;21(12):1701–5.

285. Girlanda P, Quartarone A, Sinicropi S, Nicolosi C, Roberto ML, Picciolo G, et al. Botulinum toxin in upper limb spasticity: study of reciprocal inhibition between forearm muscles. Neuroreport. 1997;29;8(14):3039–44.

286. Fawzi SM, Hamdan FB, Jaafar IF, Gawwam GAASA. Botulinum neurotoxin-A in a patient with post-stroke spasticity: a neurophysiological study. Folia Neuropathol. 2023;61(4):412–8.

287. Kröger S, Watkins B. Muscle spindle function in healthy and diseased muscle. Skelet Muscle. 2021;7;11:3.

288. Chen M, Blum D, Engelhard L, Raunser S, Wagner R, Gatsogiannis C. Molecular architecture of black widow spider neurotoxins. Nat Commun. 2021;29;12(1):6956.

289. Garb JE, Hayashi CY. Molecular Evolution of α-Latrotoxin, the Exceptionally Potent Vertebrate Neurotoxin in Black Widow Spider Venom. Mol Biol Evol. 2013;30(5):999.

290. Grasso A, Alemà S, Rufini S, Senni MI. Black widow spider toxin-induced calcium fluxes and transmitter release in a neurosecretory cell line. Nature. 1980; 283(5749):774–6.

291. Rizo J. Mechanism of neurotransmitter release coming into focus. Protein Sci. 2018;27(8):1364–91.

292. Duchen LW, Gomez S, Queiroz LS. The neuromuscular junction of the mouse after black widow spider venom. J Physiol. 1981;316:279–91.

293. Rossetto O, Morbiato L, Caccin P, Rigoni M, Montecucco C. Presynaptic enzymatic neurotoxins. J Neurochem. 2006;97(6):1534–45.

294. Cai BB, Francis J, Brin MF, Broide RS. Botulinum neurotoxin type A-cleaved SNAP25 is confined to primary motor neurons and localized on the plasma membrane following intramuscular toxin injection. Neuroscience. 2017;352:155–69.

295. Mahrhold S, Rummel A, Bigalke H, Davletov B, Binz T. The synaptic vesicle protein 2C mediates the uptake of botulinum neurotoxin A into phrenic nerves. FEBS Lett. 2006;3;580(8):2011–4.

296. Pozzi D, Corradini I, Matteoli M. The Control of Neuronal Calcium Homeostasis by SNAP-25 and its Impact on Neurotransmitter Release. Neuroscience. 2019;10;420:72–8.

297. Shimizu T, Shibata M, Toriumi H, Iwashita T, Funakubo M, Sato H, et al. Reduction of TRPV1 expression in the trigeminal system by botulinum neurotoxin type-A. Neurobiol Dis. 2012;48(3):367–78.

298. Liu YB, Tewari A, Salameh J, Arystarkhova E, Hampton TG, Brashear A, et al. A dystonia-like movement disorder with brain and spinal neuronal defects is caused by mutation of the mouse laminin β1 subunit, Lamb1. eLife. 2015; 24;4:e11102.

299. Bellardita C, Caggiano V, Leiras R, Caldeira V, Fuchs A, Bouvier J, et al. Spatiotemporal correlation of spinal network dynamics underlying spasms in chronic spinalized mice. Life. 2017; 13:6:e23011

300. Pocratsky AM, Nascimento F, Özyurt MG, White IJ, Sullivan R, O'Callaghan BJ, et al. Pathophysiology of Dyt1-Tor1a dystonia in mice is mediated by spinal neural circuit dysfunction. Sci Transl Med. 2023; 3;15(694):eadg3904.

301. Johnson EA. Biomedical aspects of Botulinum Toxin. J Toxicol Toxin Rev. 1999;18(1):1–15.

302. Rosales RL, Arimura K, Takenaga S, Osame M. Extrafusal and intrafusal muscle effects in experimental botulinum toxin-A injection. Muscle Nerve. 1996;19(4):488–96.

303. Campagner D, Evans MH, Bale MR, Erskine A, Petersen RS. Prediction of primary somatosensory neuron activity during active tactile exploration. eLife. 2016; 15;5:e10696.

304. Takeuchi K, Takemura M, Shimono T, Miyakawa S. Baseline muscle tendon unit stiffness does not affect static stretching of the ankle plantar flexor muscles. J Phys Ther Sci. 2018;30(11):1377–80.

305. Pirazzini M, Rossetto O, Eleopra R, Montecucco C. Botulinum neurotoxins: Biology, pharmacology, and toxicology. Pharmacol Rev. 2017;69(2):200–35.

306. Pirazzini M, Montecucco C, Rossetto O. Toxicology and pharmacology of botulinum and tetanus neurotoxins: an update. Arch Toxicol. 2022 ;96(6):1521–39.

307. Nascimento FA, Hammoud N, Augusto FD. Teaching Video NeuroImages: Cephalic tetanus: Not every facial weakness is Bell palsy. Neurology. 2019;93(21).

308. Jankovic J. Botulinum toxin: State of the art. Mov Disord. 2017;1;32(8):1131–8.

309. Lu L, Atchabahian A, Mackinnon SE, Hunter DA. Nerve injection injury with botulinum toxin. Plast Reconstr Surg. 1998;101(7):1875–80.

310. Mercado M del PA, Olea MS, Rodrigues AT, Morales KE, Ros JJL, Altinpulluk EY, et al. Intraneural Injection of Botulinum Toxin-A in Palliative Care and Unresponsive Neuropathic Pain. Asia Pac J Pain. 2022 1–6.

11. PUBLISHED ARTICLES

Appendix I

Šoštarić P, Vukić B, Tomašić L, Matak I. **Lasting Peripheral and Central Effects of Botulinum Toxin Type A on Experimental Muscle Hypertonia in Rats.** Int J Mol Sci. 2022;23(19):11626. (Q1)

Petra Šoštarić Mužić made significant contributions to the conception and design of the work, acquisition, analysis, and interpretation of data for the work, writing, reviewing, and editing the manuscriot for publication.

Vukić Barbara- acquisition of data, review and editing of the manuscript for publication.

Tomašić Lucija- acquisition of data, review and editing of the manuscript for publication.

Matak Ivica- made significant contributions to the conception and design of the work, acquisition, analysis, and interpretation of data for the work, writing, reviewing, and editing the manuscriot for publication, writing, reviewing and editing manuscript for publication.

Web link: https://www.mdpi.com/1422-0067/23/19/11626

Article

Lasting Peripheral and Central Effects of Botulinum Toxin Type A on Experimental Muscle Hypertonia in Rats

Petra Šoštarić [1], Barbara Vukić [1], Lea Tomašić [1,2] and Ivica Matak [1,*]

1 Department of Pharmacology, University of Zagreb School of Medicine, Šalata 11, 10000 Zagreb, Croatia
2 University Psychiatric Hospital Vrapče, University of Zagreb School of Medicine, Bolnička Cesta, 10090 Zagreb, Croatia
* Correspondence: ivica.matak@mef.hr; Tel.: +38-514590198

Abstract: Recent animal experiments suggested that centrally transported botulinum toxin type A (BoNT-A) might reduce an abnormal muscle tone, though with an unknown contribution to the dominant peripheral muscular effect observed clinically. Herein, we examined if late BoNT-A antispastic actions persist due to possible central toxin actions in rats. The early effect of intramuscular (i.m.) BoNT-A (5, 2 and 1 U/kg) on a reversible tetanus toxin (TeNT)-induced calf muscle spasm was examined 7 d post-TeNT and later during recovery from flaccid paralysis (TeNT reinjected on day 49 post-BoNT-A). Lumbar intrathecal (i.t.) BoNT-A–neutralizing antiserum was used to discriminate the transcytosis-dependent central toxin action of 5 U/kg BoNT-A. BoNT-A-truncated synaptosomal-associated protein 25 immunoreactivity was examined in the muscles and spinal cord at day 71 post-BoNT-A. All doses (5, 2 and 1 U/kg) induced similar antispastic actions in the early period (days 1–14) post-BoNT-A. After repeated TeNT, only the higher two doses prevented the muscle spasm and associated locomotor deficit. Central trans-synaptic activity contributed to the late antispastic effect of 5 U/kg BoNT-A. Ongoing BoNT-A enzymatic activity was present in both injected muscle and the spinal cord. These observations suggest that the treatment duration in sustained or intermittent muscular hyperactivity might be maintained by higher doses and combined peripheral and central BoNT-A action.

Keywords: botulinum toxin type A; antispastic activity; duration of action; central effect

1. Introduction

Botulinum neurotoxin type A (BoNT-A) and other immunogenically distinct serotypes (BoNT-B–BoNT-G) are potent clostridial neurotoxins that cause botulism, a potentially fatal neuroparalytic illness characterized by the long-term synaptic silencing of peripheral muscular and autonomic nerve terminals [1,2]. Their extreme potency (estimated LD_{50} of BoNT-A is around 1 ng/kg [2,3]) due to selective nerve terminal uptake and inhibition of the neurotransmitter release machinery within the presynaptic active zones [4,5]. The BoNT-A serotype enzymatically cleaves off only a small C-terminal part (amino-acids 197–206) of synaptosomal-associated protein 25 (SNAP-25) involved in the Ca^{2+}-triggered synaptic vesicle exocytosis [5]. Used as a standardized low-dose pharmaceutical preparation, locally injected BoNT-A (A1 subtype BoNT synthesized by the *Clostridium botulinum* strain Hall) has become the first-choice treatment of several neurological disorders characterized by sustained or intermittent focal muscular hyperactivity, such as strabismus, upper limb spasticity, oromandibular and cervical dystonia, etc. [6].

Transient, reversible synaptic silencing has been the basis of BoNT-A clinical efficacy and safe use. In individual patients, the treatment duration (the time period between the toxin's application and the cessation of its beneficial actions requiring reinjection) may depend on several factors related to appropriate targeting, dosing and mechanism of the toxin action, as well as the mechanism of the underlying disease [7]. Ideally, an appropriate

mode of toxin application and dosage should produce sufficiently lasting beneficial actions with minimal local or systemic adverse effects [8]. In the muscles targeted for cosmetic or neurological use, the primary toxin action involves an initial prominent blockade of motor unit activity, followed by remodeling of the neuromuscular junction and reversible recovery of the quantal acetylcholine (ACh) release at the original muscular endplate zone [9]. Careful muscle targeting with appropriate techniques (e.g., muscle identification by electrophysiology and ultrasound and endplate targeting by appropriate toxin dilution and volumes) provides optimal and reliable clinical effects emphasizing the importance of peripheral muscular action [10,11]. However, the toxin treatment may exert a variable extent and duration of antispastic or anti-dystonic action in comparison to separately assessed local neuromuscular paralytic actions. Several clinical reports suggest that the toxin's beneficial actions may surpass the duration of the peripheral muscle weakness. On the other hand, patients may experience an unsatisfactory therapeutic duration and require sooner reinjections, even if local muscular action is still present [12–14]. Clinical evidence suggests that BoNT-A modifies muscle spindle activation and the consequent proprioceptive afferent input associated with the exaggerated stretch reflex, either directly by the blockage of encapsulated intrafusal terminals or indirectly due to extrafusal muscle relaxation [15,16]. Additional, nonlocal actions have also been hypothesized based on reported BoNT-A neurophysiological effects on distant muscles located far from treated NMJ or the muscle spindle zone. A reduction of spinal recurrent inhibition and the reciprocal facilitation in noninjected muscles of the same limb [17–19] and F-wave alterations in hand muscles after cervical muscle treatment [20,21] indicated that BoNT-A may induce distant effect on motor pools, innervating different, noninjected muscles.

Possible direct central effect of the toxin on the neuromotor control has been supported by animal studies. After high-dose BoNT-A injected into ocular or hind limb muscles, a reduced firing activity accompanied by structural alterations of synaptic contacts suggested the toxin's action on the presynaptic input that controls the motoneuron activity [22–24]. The occurrence of BoNT-A-truncated SNAP-25 fragments in central motor and sensory nuclei supports direct central enzymatic actions after toxin axonal transport from the injected peripheral site [25–29]. Moreover, peripherally injected BoNT-A induces proteolytic SNAP-25 cleavage in cholinergic terminals presynaptic to motoneurons [28] and reduced the tetanus neurotoxin (TeNT)-evoked local muscular spasm dependently on transcytosis [30]. However, in the later study [30], central antispastic effects were evident when the toxin was injected into the sciatic nerve, and the translation of this finding to clinically employed intramuscular injections, with strong muscular paralysis possibly masking the central toxin effect, is unclear. Herein, we examined the possibility that the central antispastic action might be influencing the duration of the BoNT-A beneficial antispastic effect once the local muscular toxin action starts to fade. Thus, in rats with a tetanus toxin (TeNT)-evoked transient local muscular spasm, we investigated the toxin's antispastic activity during the later time period when flaccid paralysis recovered and, further on, the possible involvement of the central action of BoNT-A in the late beneficial antispastic effect.

2. Results

2.1. Early Effects of BoNT-A on Spastic Paralysis Are Concomitant with Local Muscular Neuroparalytic Effect

Rats developed spastic paralysis starting at 3 days post-TeNT i.m. injection, which peaked at 7 d post-toxin treatment and subsequently started to wear off after day 14 and fully recovered by day 28. The spastic paralysis and lower limb plantar flexor muscle rigidity was evident as a spasm of the injected limb, resulting in limb extension or a reduced range of motion of the tibiotarsal joint. This was evident as the elevated force required for passive ankle dorsiflexion (Figure 1A) and reduced Basso Beattie Bresnahan (BBB) locomotor rating score (Figure 1B). BoNT-A i.m. injections at day 7 post-TeNT fully restored the elevated resistance to passive ankle dorsiflexion already within 1 day after BoNT-A injection, with the effects of different doses of BoNT-A being similar throughout

the duration period of TeNT-evoked spastic hypertonia. In addition, all BoNT-A doses similarly restored the locomotor deficit assessed by the BBB scale.
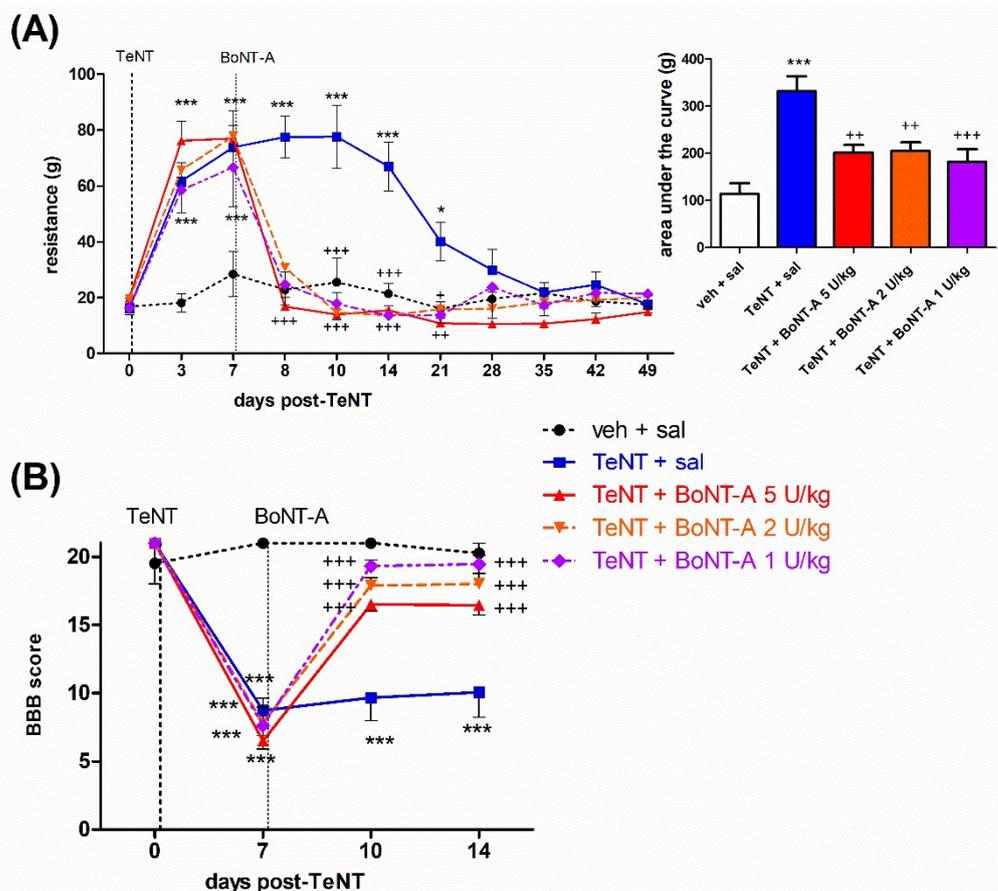

Figure 1. The fast-onset antispastic effect of botulinum toxin type A (BoNT-A) on tetanus toxin (TeNT)-evoked hind limb rigidity and locomotor deficit in rats. The BoNT-A (1–5 U/kg) intramuscular (i.m.) injection into gastrocnemius reduces the preestablished TeNT (1.5 ng, i.m.)-evoked resistance to ankle dorsiflexion (reaching a 90° tibiotarsal angle) (**A**), and the locomotor deficit assessed by the Basso Beattie Bresnahan (BBB) scale (**B**). Veh, vehicle; sal, saline i.m. treatment. Horizontal bars indicate the time points of TeNT and BoNT-A i.m. application. N = 8 to 9 animals/group; mean ± SEM, * and ***: $p < 0.05$ and < 0.001 vs. veh + sal, +, ++ and +++: $p < 0.05$, < 0.01 and < 0.001 vs. TeNT + sal (two-way RM ANOVA, followed by Bonferroni's post hoc test; $p < 0.05$ considered significant).

The muscle-weakening effect of BoNT-A resulting in impaired toe spreading reflex function was quantified, as an increase in the digit abduction score (DAS) was evident already 1 day post-BoNT-A application and started to recover dose-dependently by day 49 post-BoNT-A application. Compared to 5 U/kg, lower BoNT-A doses (2 and 1 U/kg) induced a less intensive and shorter-lasting toe spreading reflex impairment (Figure 2A). In addition to an impaired toe spreading reflex, during the plantar ground placement, we observed the arch-like appearance of the foot and heel weight bearing during the stance in all BoNT-A-treated animals (not shown). The mentioned hind paw appearance change was fully (2 and 1 U/kg) or partially (5 U/kg) recovered by day 49 post-BoNT-A. Weight bearing with plantar surface during initial contact and mid stance recovered by day 49 in all animals, while normal propulsion by using toes and interdigital plantar pads during a terminal stance was only partially recovered in 5 U/kg-treated animals, suggesting some residual local muscular toxin effect from the use of plantar flexion muscles. The atrophic loss of the hind-limb muscle volume was evident as a reduction of the lower leg width at the mid-calf point. Different BoNT-A doses evoked a similar reduction in the lower

leg cross-sectional area, which did not show signs of recovery throughout the experiment duration (Figure 2B).
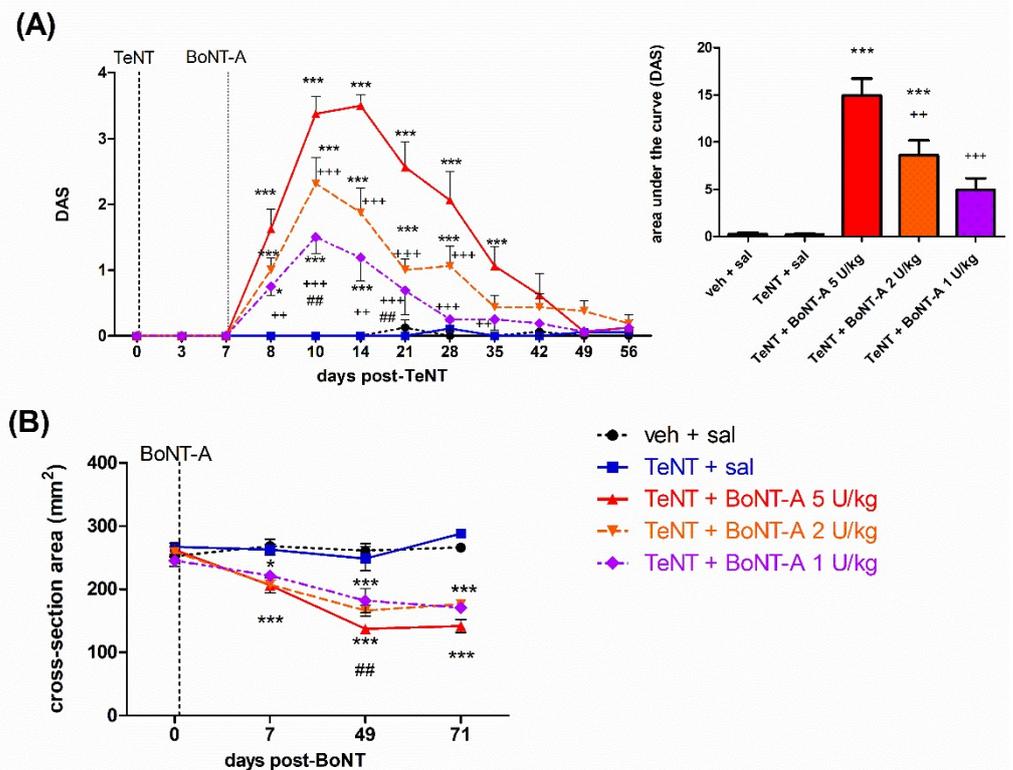

Figure 2. Intramuscular BoNT-A induces reversible impairment of local hind-limb muscle function and non-recovering atrophy in rats. The BoNT-A (1–5 U/kg) intramuscular (i.m.) injections into gastrocnemius induces dose-dependent lasting toe spreading reflex inhibition (**A**), assessed by the digit abduction score (DAS), and atrophic reduction of the lower leg muscles (**B**), represented as the estimated cross-section area of the lower leg at the middle calf muscle level (calculated as the area of ellipse defined by dorsoventral and mediolateral leg diameters). Veh, vehicle; sal, saline i.m. treatment. Horizontal bars indicate the time points of TeNT and BoNT-A i.m. application. N = 8 to 9 animals/group; mean $\pm$ SEM, * and ***: $p < 0.05$ and < 0.001 vs. veh + sal, ++ and +++: $p < 0.01$ and < 0.001 vs. TeNT + sal; ##: $p < 0.01$ vs. TeNT + BoNT-A 1 U/kg (two-way RM ANOVA, followed by Bonferroni's post hoc test; $p < 0.05$ considered significant).

2.2. Late Effects of BoNT-A on Spastic Paralysis Are Dose-Dependent and Augmented by Central Toxin Action

The animals that previously recovered from signs of spastic and flaccid paralysis were reinjected with TeNT on day 49 post-BoNT-A intramuscular injection (day 56 post-first TeNT) and redeveloped the focal spasm starting from day 3 after TeNT injection. The antispastic activity of BoNT-A persisted for more than 2 months in a dose-dependent manner. While the antispastic activity of the 5 and 2 U/kg doses reversed the dorsiflexion resistance to the level of the saline-treated vehicle and normalized the locomotor deficit assessed by the BBB scale, the effect of 1 U/kg was significantly lower (Figure 3A), and no significant locomotor improvement was observed (Figure 3B).
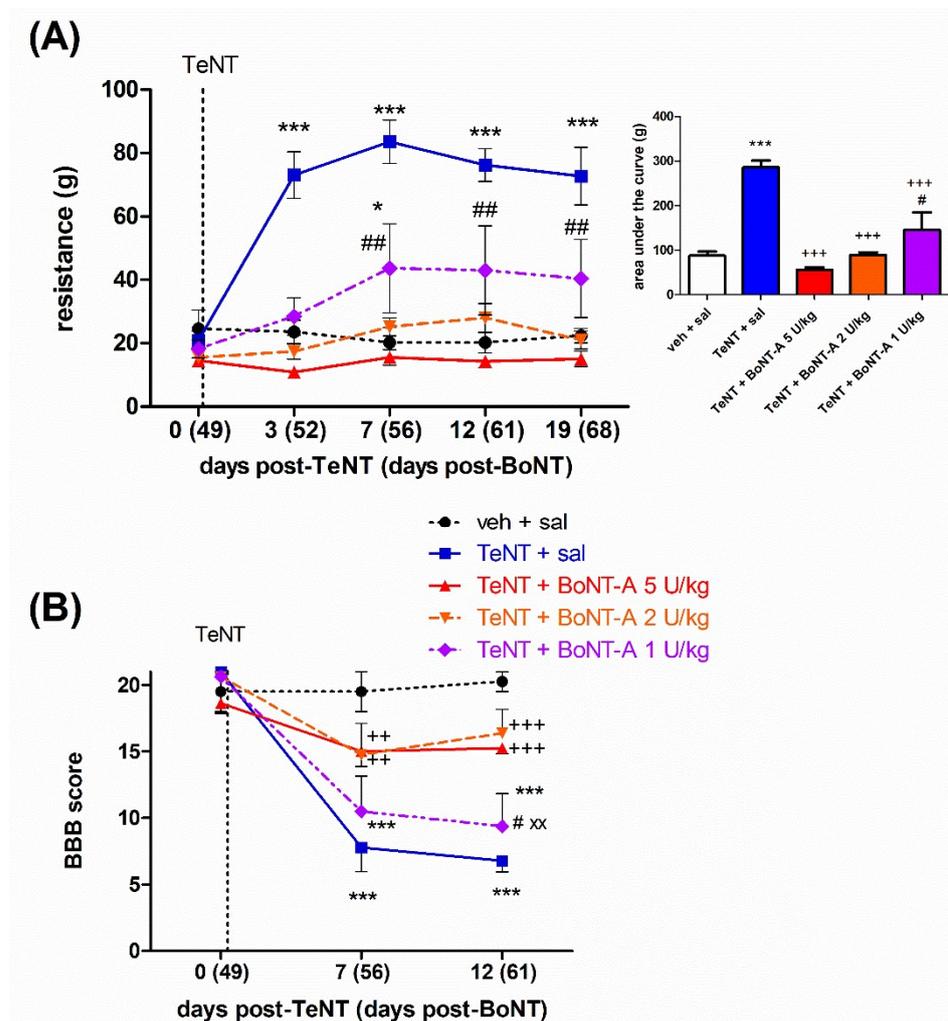
Figure 3. The late dose-dependent BoNT-A antispastic effect persists two months post-i.m. treatment. The effect of BoNT-A (1–5 U/kg) intramuscular (i.m.) injection into the gastrocnemius on a TeNT (1.5 ng, i.m.)-evoked local muscle spasm reinduced 49 days post-BoNT-A was assessed by measuring the resistance to passive ankle dorsiflexion reaching a 90° tibiotarsal angle (**A**) and the locomotor deficit assessed by BBB scale (**B**). Veh, vehicle; sal, saline i.m. treatment. Horizontal bars indicate the time point of TeNT i.m. application. N = 8 to 9 animals/group; mean ± SEM, * and ***: $p < 0.05$ and < 0.001 vs. veh + sal; ++ and +++: $p < 0.01$ and < 0.001 vs. TeNT + sal; # and ##: $p < 0.05$ and < 0.01 vs. TeNT + 5 U/kg BoNT-A; XX: $p < 0.01$ vs. TeNT + 2 U/kg BoNT-A (two-way RM ANOVA, followed by Bonferroni's post hoc test; $p < 0.05$ considered significant).

In a separate experiment, we assessed the possibility that the late BoNT-A antispastic action is centrally mediated by examining its effect in combination with intrathecally injected BoNT-A-neutralizing antitoxin, which prevents the toxin transcytosis [28,30]. The antispastic action of 5 U/kg BoNT-A on both the dorsiflexion resistance (Figure 4A), as well as the locomotor performance (Figure 4B), was partially reduced by the antitoxin, suggesting the involvement of a central, transcytosis-dependent toxin action. The atrophic reduction of the hind-limb diameter and estimated cross-sectional area was not significantly affected by the intrathecal antitoxin treatment, suggestive of a lack of involvement of a central action of the toxin on muscle atrophy (Figure 4C).
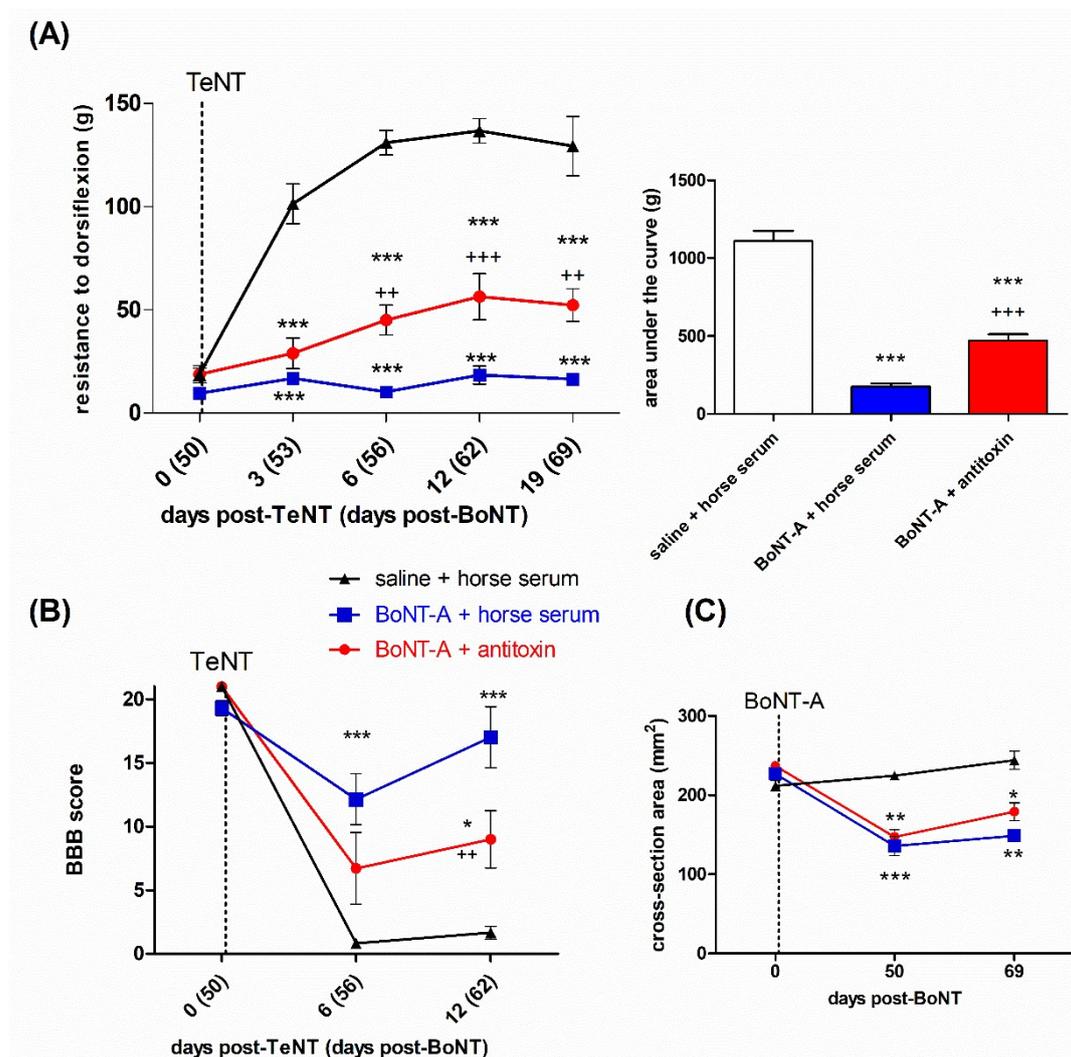
Figure 4. The late BoNT-A antispastic effect involves transcytosis-dependent central action. The rats were treated with i.m. BoNT-A (5 U/kg) and, then, after 24 h, injected i.t. into the lumbar spinal canal with the neutralizing equine antitoxin (or horse serum as the control) to prevent its central transcytosis-dependent action. Then, after a further 49 days, its effect on the TeNT (1.5 ng, i.m.)-evoked local muscle spasm was assessed by measuring the resistance to ankle dorsiflexion (reaching a 90° tibiotarsal angle) (**A**) and the locomotor deficit assessed by the BBB scale (**B**). The central toxin action does not affect the atrophic loss of the lower leg estimated cross-sectional area at the widest calf point (**C**). Sal, saline i.m. treatment. Horizontal bars indicate the time points of TeNT i.m. application. N = 6 to 7 animals/group; mean ± SEM, *, ** and ***: $p < 0.05$, < 0.01 and < 0.001 vs. sal + horse serum, ++ and +++: $p < 0.01$ and < 0.001 vs. BoNT-A + horse serum (two-way RM ANOVA, followed by Bonferroni's post hoc test; $p < 0.05$ considered significant).

2.3. Lasting Effects of BoNT-A Are Accompanied by Toxin's Ongoing Enzymatic Activity in Both, Injected Muscle and Spinal Cord

After observing that the behaviorally assessed beneficial antispastic actions of BoNT-A persist for more than 2 months after a single treatment in animals, we assessed the possible persistence of BoNT-A–cleaved SNAP-25 (cSNAP-25) immunoreactivity in injected gastrocnemius muscles and the spinal cord. The enzymatic activity in NMJ persisted up to day 71 post-BoNT-A injection at all BoNT-A doses injected (Figure 5A). In line with the nonuniform distribution of NMJs in the examined muscle, the staining of cSNAP-25 was not visible in all visual fields but within the single longitudinal section of gastrocnemius, it was easy to identify elongated motor endplate zones containing cSNAP-25 immunoreactivity

at all the examined doses. A semiquantitative evaluation showed a similar occurrence of NMJs and nerve terminals in the examined visual fields that contained the staining, with a slightly lower number of stained NMJs and axons in 1 U/kg-treated muscle (Figure 5C).
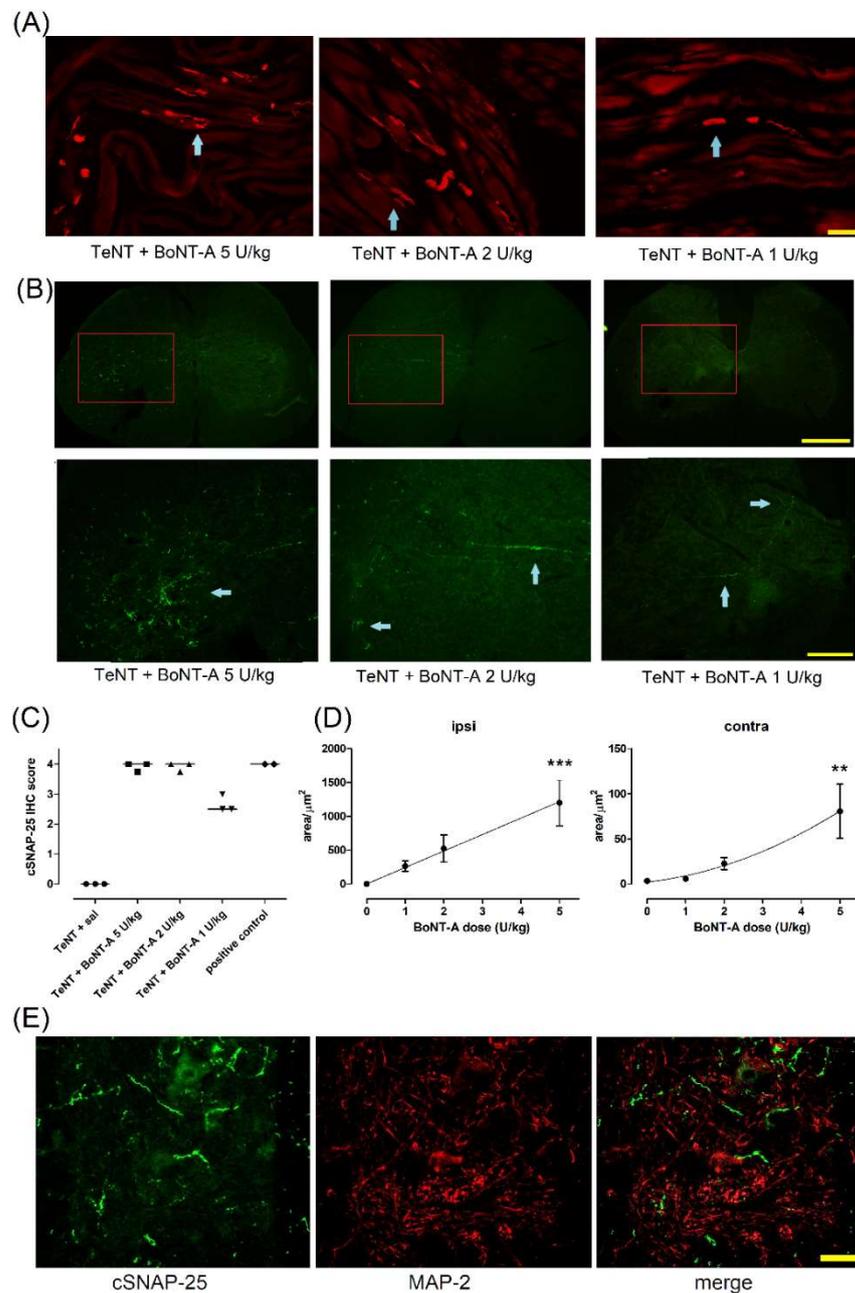

Figure 5. Enzymatic product of BoNT-A in the muscle and spinal cord persists for more than 2 months post-BoNT-A i.m. treatments. BoNT-A (1–5 U/kg) was injected into the gastrocnemius muscle, and the presence of BoNT-A-cleaved SNAP-25 (cSNAP-25) was examined in the injected muscle (**A**) and spinal cord (**B**) on day 71 post-toxin treatment. (**A**) Red immunoreactivity shows neuromuscular junctions and nerve terminals (cyan arrow; scale bar = 100 μm). (**B**) Upper and lower-panel microphotographs indicate the low (2×) and higher (5×) magnification images of the same representative L4 spinal cord sections with green immunoreactivity indicating cSNAP (arrow) (scale bars = 500 μm and 200 μm, respectively). The scoring method suggests an abundant presence of neuromuscular junctions, nerve terminals or axons immunoreactive for cleaved SNAP-25 in BoNT-A-treated muscle at more than 2 months post-BoNT-A (N = 3 animals per group, 4 visual fields per animal each taken from different section), as well as in 2 positive controls (obtained from the muscle

treated with 5 U/kg BoNT-A 7 days prior to perfusion (**C**)). Under (**C**), the data points represent individual animal score values and the horizontal bar represents median. The immunoreactive cSNAP-25 area quantity in the ipsilateral (ipsi) and contralateral (contra) ventral horn is dose-dependent (**D**). The data were obtained by analysis of the pixel intensity threshold area of cleaved SNAP-25 immunoreactivity in 3 nonoverlapping high-magnification ($20\times$) visual fields (433 μm $\times$ 323 μm = 0.14 mm^2) located in the lateral L4 ventral horn, average of 4 slices per animal (N = 5 to 6 animals per group; mean $\pm$ SEM, ** and ***: $p < 0.01$ and < 0.001 vs. BoNT-A dose = 0 from TeNT + saline animals (Kruskal–Wallis test, followed by Dunn's post hoc). In the L4 ventral horn, the cSNAP-25 does not colocalize with the somatodentritic compartment immunoreactive for microtubule-associated protein 2 (MAP-2) (**E**). The confocal microscope image was obtained from animals injected with 5 U/kg BoNT-A (scale bar = 50 μm).

In addition to long-term synaptic silencing in the periphery, the product of BoNT-A enzymatic activity was also present in the spinal cord ventral horn (Figure 5B). The area of cleaved SNAP-25 immunoreactivity in the muscle in the ipsilateral and contralateral spinal cord ventral horn was shown to be dose-dependent (Figure 5D). The cleaved SNAP-25 surrounding the ventral horn motoneurons did not colocalize with MAP-2 immunoreactivity, suggesting the lack of toxin activity in the somatodendritic compartment belonging dominantly to motoneurons (Figure 5E).

3. Discussion

To account for the BoNT-A therapeutic action in hyperactive muscle, it is widely assumed that the desirable therapeutic benefit is entirely due to the toxin's well-known long-term neuroparalytic activity at peripheral muscular cholinergic terminals as its natural, dominant target. Hence, possible actions at additional levels of the motor nervous system, including CNS, might have been supposed to be unwarranted and unnecessary. However, clinical observations suggesting that the period of neuromuscular paralysis does not necessarily coincide with the treatment duration, or that the patients may benefit from doses producing little or no muscle-weakening effect, and alterations of neurophysiological activity of noninjected muscles exceed the simple functional role of neuromuscular paralysis [12–14,31,32]. Herein, we found that the maximal beneficial actions in rat spastic muscle may persist beyond the local neuroparalytic effect with participation of the central toxin action.

A preclinical assessment of the muscle-weakening effect, i.e., toxin-mediated flaccid paralysis in the normal muscle of non-spastic animals or isolated ex vivo preparations, is considered a correlate of its antispastic action, thus, overlooking possible additional mechanisms of action relevant only for pathological muscle hyperactivity. In line with that, studies of BoNT-A action in experimental disorders of elevated muscle activity have been scarce [29,33,34]. In the present study, we employed repeated low-dose TeNT i.m. injections to induce local spastic paralysis mimicking the disinhibition of the synaptic input to motor neurons in spasticity and hyperkinetic movement disorders responsive to commonly employed antispasmodic baclofen, as well as BoNT-A [30]. Herein, we examined the long-term effects of intramuscularly injected BoNT-A by behavioral scoring methods for the evaluation of both flaccid and spastic paralysis and locomotor deficits in rodents. The chosen peripheral BoNT-A doses (1–5 U/kg) in rats corresponded to low–moderate doses commonly employed in clinical practice (corresponding to 70–350 U in an average 70 kg human).

During the early period post-BoNT-A (injected 7 d post-TeNT), we observed the fast and complete reversal of TeNT-mediated spastic paralysis and locomotor deficits evident as increased dorsiflexion resistance or an impaired BBB locomotor scale (Figure 1). The early onset of BoNT-A antispastic action cooccurred with the toxin-mediated toe spreading reflex impairment (assessed by DAS), which started within 24 h (Figure 2A). This is in line with the commonly observed fast clinical onset of BoNT-A action starting together with a neuromuscular paralytic effect [8]. In line with clinical observations that higher doses are not necessarily related to a higher therapeutic efficacy of BoNT-A [35], we found no dose-dependent differences in the early BoNT-A antispastic activity (Figure 1). The

DAS score impairment was, however, shown to be dose-dependent in terms of the peak intensity and duration (Figure 2A), keeping in mind that this impairment is indicative of BoNT-A diffusion into the noninjected nearby muscles mediating the toe abduction rather than the local action within the injected gastrocnemius [36,37]. The 1–5 U/kg doses employed here are expected to produce substantial to near-complete muscular paralysis of gastrocnemius in the immediate period post-BoNT-A [27,38], which may account for the lack of dose-dependent difference in the BoNT-A antispastic action in the early time period post i.m. treatment. The gastrocnemius CMAP recovers up to 30–35% of the original value by day 35 and up to 68% after 84 days post-i.m. 2.5 U BoNT-A [38]. This suggest that a significant recovery of muscular function (albeit slower and incomplete compared to DAS) is expected after 1 to 2 months at the doses examined here. In line with that, the arch-like appearance of the paralyzed hind paw or weight bearing by employing the heel during the stance was recovered in all BoNT-A-treated animals (not shown). In contrast to the significant functional recovery of the hind-limb appearance and use, the atrophic reduction of the lower leg muscles was similar at all doses employed here, and notable recovery was not observed throughout the experiment (Figures 2B and 4C).

To study the late effect of BoNT-A, we reinstated the muscle hypertonia by using a second TeNT injection on day 49 after the BoNT-A pretreatment. The higher two doses (5 and 2 U/kg) maintained their antispastic action, normalizing the muscle hypertonia and locomotor deficit for more than two months post-BoNT-A. On the other hand, the lowest examined 1 U/kg dose lost its ability to block the TeNT-evoked locomotor deficit assessed by the BBB and was shown to be less effective in reducing the elevated muscle tone (Figure 4A,B). Thus, our results are in line with clinical observations reporting a longer treatment duration with higher doses. A comparative study of the beneficial effects of BoNT-A (abobotulinumtoxinA) on cervical dystonia, assessed by a modified Tsui severity scale, suggested the longest duration of effect and lowest need for reinjection after 8 weeks in the highest dose-treated patient group (1000 U total dose vs. lower dose groups (250 and 500 U)) [39]. Compared to onabotulinumtoxinA, abobotulinumtoxinA administered at a higher conversion ratio (3:1) was more efficacious than the same preparation administered at a 1.7:1 ratio at 12 weeks post-treatment [40]. However, a careful balance between the doses employed, as well as other factors such as adverse local or systemic effects of a given treatment, should be taken into account before considering the use of higher toxin doses in patients.

Based on the findings that BoNT-A-mediated therapeutic benefits are not concurrent or outlast the flaccid paralysis [31,32,41], we hypothesized that a central action may contribute to the overall toxin-mediated benefit when the muscular effects start to fade. Thus, after observing that a BoNT-A-mediated antispastic effect might persist for 2 months post-BoNT-A despite the functional neuromuscular recovery, we further went on to examine the possible contribution of the central toxin action. In additional animals treated with 5 U/kg BoNT-A, we blocked the toxin's transcytosis by a BoNT-A-neutralizing antibody administered intrathecally 24 h post-BoNT-A (and not at the same time to avoid any possible interference with BoNT-A binding and entrance at the neuromuscular endplate zones) and then injected the same muscle with TeNT at day 50 post-BoNT-A to establish muscle hypertonia. Importantly, to be able to interpret the results of the antitoxin experiment, it has to be pointed out that the animals treated with i.m. BoNT-A (and i.t. horse serum as a control for i.t. equine antitoxin) exerted unopposed BoNT-A activity at both the peripheral muscular and central spinal sites, while the BoNT-A + antitoxin- treated animals should have an unopposed peripheral toxin effect and central effect, depending only on the transcytosis being prevented by the neutralizing antitoxin. We found that the antitoxin partially counteracted the beneficial effects of BoNT-A on the TeNT-evoked elevated muscle tone and locomotor deficit, which suggests a combination of peripheral and central toxin actions simultaneously contributing to the observed late antispastic activity of BoNT-A. The possibility that the direct central toxin effects contribute to the observed overall beneficial effect adds to our understanding of the mechanisms of this toxin's long-term central actions.

At the end of the behavioral assessment, we examined the persistence of the toxin's enzymatic activity in both the injected muscle and the corresponding spinal cord segment. In line with the short turnover half-time of synaptic proteins such as SNAP-25 lasting only few days, this points to the ongoing presence of SNAP-25 cleaving protease for over 2 months post-toxin i.m. injection. Thus, despite the obvious functional muscle recovery, our results are in line with the long-term muscular actions of enzymatically active BoNT-A. In the spinal cord ventral horn, central SNAP-25 cleavage indicated the continuous central presence of BoNT-A protease as well. At the dose range employed here, the quantity of cleaved SNAP-25 in the CNS was shown to be dependent on the amount of injected BoNT-A. Although all BoNT-A doses employed here produced similar antispastic actions during the early period of BoNT-A action, only the higher two doses (5 and 2 U/kg) continued to show the full antispastic effect at a later time period. Theoretically, as the level of active BoNT-A protease at the relevant synaptic sites in both the muscle and spinal cord drops with time, a higher BoNT-A dose may maintain its antispastic effect for a longer time period. In other central motor regions, its lasting action on the basal ganglia circuitry and reduction of the motor deficits in experimental parkinsonism has been demonstrated after its direct injection into the striatum [42,43], which is most likely associated with the ongoing BoNT-A enzymatic activity lasting for several months after the toxin central injection [25].

In the ventral horn, MAP-2 immunostaining of the somatodendritic compartment dominantly belonging to the motoneurons did not colocalize with BoNT-A-cleaved SNAP-25, in line with the evidence that BoNT-A holotoxin physically leaves the motor neurons and enters the presynaptic axonal compartment of the second-order neurons [28,29]. In the ventral horn and brainstem motor regions, cSNAP-25's distinctive localization within large synaptic terminals containing choline-acetyltransferase and vesicular acetylcholine transporter often in contact with motoneuronal cell bodies suggested toxin action within the cholinergic C-boutons [26,28,44], a premotor synaptic input from V0$_C$ lineage-derived excitatory interneurons that support sustained motoneuronal firing during intense motor activities (e.g., swimming) [45]. This is in line with the possibility that BoNT-A reduces the motoneuronal excitability by inhibiting the excitatory cholinergic drive onto motoneurons, which, apart from immunohistochemical evidence, has not been conclusively demonstrated yet. The involvement of additional synaptic sites expressing lower levels of cleaved SNAP-25 and/or the simultaneous synaptic blockade of other central neurotransmitters cannot be ruled out as well.

4. Materials and Methods

4.1. Animals

Male Wistar Han rats (Department of Pharmacology, University of Zagreb School of Medicine), 2.5–3 months old and weighing 350–400 g at the beginning of experiment, were used in all the experiments. The animals were kept under a 12-h light and dark cycle regime with unlimited access to the standardized diet (Mucedola Srl., Milano, Italy) and drinking water. The experiments were approved by the review boards of the University of Zagreb School of Medicine and Croatian Ministry of Agriculture (No. EP 229/2019).

4.2. Pharmacological Treatment

For intramuscular neurotoxin injections, the rats were briefly anesthetized with isoflurane (Forane, Abbot Laboratories, Abbot Park, IL, USA), 5% induction and 1–1.5% maintenance by using a gas anesthesia system for small animals (Ugo Basile, Varese, Italy). The rats were intramuscularly injected with 1.5 ng tetanus neurotoxin (TeNT, Sigma, St. Louis, MO, USA) and BoNT-A (INN: Clostridium botulinum type A neurotoxin complex, Allergan Inc., Irvine, CA, USA). Different doses of BoNT-A were employed: 1, 2 or 5 international units per kg (U/kg, each unit consisting of 48 pg of a 900-kDa toxin complex). The neurotoxins were injected into the right gastrocnemius in a total volume of 20 μL divided into the medial and lateral muscle belly (10 μL each) by employing a 50-μL Hamilton syringe as previously described [30]. To block the central BoNT-A transcytosis, animals were in-

jected with BoNT-A-neutralizing antitoxin (National Institute for Biological Standards and Control, NIBSC code 14/174, Potters Bar, UK; a kind gift from Dr. Thea Sesardic, 10 I.U. in 10-μL volume) into the intrathecal lumbar space at the level of cauda equina by employing a 0.3-mL 27 G tuberculin syringe (BD, Franklin Lakes, NJ, USA). The rats were anesthetized by intraperitoneal (i.p.) ketamine and xylazine (70 and 7 mg/kg, respectively). Then, the rat's hair covering the lumbar spine was clipped, and a small skin incision was made to visualize the midline joining area of the paraspinal muscles. Subsequently, a needle was advanced between the lumbar vertebrae into the spinal canal, which was confirmed by brief tail or hind-leg movement as the needle touched the spinal nerve roots within the cauda equina. Next, the antiserum or horse serum was injected slowly into the lumbar space and the needle carefully withdrawn after 10–15 s. The incision was joined by 1 to 2 sutures using the 5–0 surgical thread (Mersilk, Ethicon, Cincinnati, OH, USA) and disinfected by povidone-iodine (Alkaloid, Skopje, North Macedonia).

4.3. Behavioral Motor Assessment
4.3.1. Digit Abduction Score

To measure the local flaccid paralysis of the hind-limb, the reflex toe abduction was used to evaluate the digit abduction score (DAS), similar to as previously described [36]. The rats were lifted by their waist, and then, the DAS score was determined as the number of hind-paw toes that could not abduct normally after the loss of contact with the ground (0 = all fingers abduct from each other, 1 = 2 toes cannot abduct, 2 = 3 toes cannot abduct, 3 = 4 toes cannot abduct and 4 = no toe abduction).

4.3.2. Resistance to Ankle Dorsiflexion

We measured the intensity of the TeNT-evoked muscular rigidity by assessing the force needed to overcome the resistance of spastic hind-paw plantar flexors during passive ankle dorsiflexion in trained calm animals, as previously described [29]. In brief, the animals were held around the waist with the experimenter's hand gently pressing the interdigital paw pad against an elevated plastic platform mounted on a digital kitchen scale to flex the spastic joint. When the 90° tibiotarsal angle was achieved or slightly exceeded, the pressure exerted by the experimenter was slightly relieved, and the resistance in grams was noted just before the point when further pressure relief would return the tibiotarsal angle to values above 90°. The average of two values per limb was taken per each single measurement.

4.3.3. Basso Beattie Bresnahan Locomotor Scale

To assess the hind-limb usage and the range of motion of hind-limb joints during walking, we employed a modified version of the Basso Beattie Bresnahan (BBB) locomotor score [46] originally devised to assess the motor effect of experimental spinal cord injuries. The BBB scale consists of 21 defined grade points assessing the range of motion of hind-limb joints, stepping, coordination, paw position, trunk stability and tail position in their gait. Presently, the non-spastic left limb contralateral to i.m. TeNT was not included into the quantification to obtain the overall score; however, it conveniently served as a reference for normal non-spastic joint range of motion during gait. The rats were allowed to walk across a flat black table surface and freely return to their home cage with its opened top placed level with the table. The videos were taken with a web camera with an unopposed view of the spastic limb during walk across the table towards the cage. The BBB score was assessed offline by two independent observers unaware of the animal treatment, and the two scoring results were averaged as a single animal measurement.

4.3.4. Measurement of Lower Leg Muscle Atrophy

Gastrocnemius injection of BoNT-A results in notable muscle reduction and visible thinning of the lower leg. Thus, throughout the course of the experiment, we estimated the muscle atrophy by noninvasive external measurement of the hind-leg diameter by using a digital caliper. The mediolateral diameter value was noted at the widest point of the rat calf

belly with the jaws of the caliper gently touching the skin of both sides perpendicularly to the Achilles tendon while dorsoventral diameter was noted at the same level by touching the tibial bone on one side and the skin overlaying the middle of the calf on the other side. The approximate cross-sectional area of the rat lower leg was calculated by using the formula for the area of an ellipse (in mm^2) defined by the two diameters obtained (dorsoventral $\times$ mediolateral $\times$ $\pi/4$).

4.4. Time-Course of Experiments

4.4.1. Experiment No 1. The Dose-Response Assessment of Early and Late BoNT-A Antispastic Action

The animals were assigned to 5 experimental groups (N = 8/group) and treated i.m. with TeNT or the 2% BSA-containing saline vehicle. After the development of spasticity, on day 7 post-TeNT, the animals were treated with different BoNT-A doses (1, 2 and 5 U/kg) or physiological saline (control non-spastic and spastic groups). The motor behavioral effect of the toxins was assessed at different time points (pretreatment, days 3 and 7, and then after BoNT-A i.m. days 8 and 10 post-TeNT (on days 1 and 3 post-BoNT-A). From then on, the measurements were conducted once a week until day 56 post-TeNT/49 post-BoNT-A, when another 1.5 ng TeNT injection was made to reinduce the spasticity. Then, afterwards, the measurements were repeated on days 3, 7, 12 and 19 post-the second TeNT (days 52, 56, 61 and 68 post-BoNT-A)

4.4.2. Experiment No 2. Assessment of the Role of Central Action and Transcytosis in the Late BoNT-A Antispastic Activity

The rats (N = 6/group) were injected with 5 U/kg BoNT-A and then, after 24 h, with BoNT-A-neutralizing antitoxin into the lumbar intrathecal space, as described in the previous section. On day 50 post-BoNT-A, the animals were injected with TeNT into the right gastrocnemius. Then, the measurements were repeated on days 3, 7, 12 and 19 post-the second TeNT injection (days 53, 57, 62 and 69 post-BoNT-A).

4.5. Immunohistochemistry

The animals from experiment no. 1 were deeply anesthetized with ketamine-xylazine and sacrificed by transcardial perfusion with physiological saline, followed by cold 4% paraformaldehyde + phosphate-buffered saline (PBS) fixative. The gastrocnemius muscle and spinal cord were excised, post-fixed and cryoprotected overnight in 15% sucrose + fixative and, the next day, transferred to 30% sucrose in 1 $\times$ PBS. Then, after the tissue sank, it was removed from sucrose + PBS and kept in an ultra-freezer at $-80\ ^{\circ}$C. The muscles were cut in the cryostat at a 20-μm per slice thickness and immediately transferred to glass adhesion slides (Super Frost Plus Gold, Thermo Scientific, Waltham, MA, USA), while the spinal cord slices were cut at 35-μm slices and placed in free-floating wells.

The muscles were washed with PBS + 0.25% triton-X-100 (PBST), blocked in 10% NGS and incubated overnight at room temperature with nonaffinity purified rabbit polyclonal antibody to BoNT-A-cleaved SNAP-25 recognizing the SNAP-25 1–197 fragment (1:4000, National Institute for Biological Standards and Control, Potters Bar, UK), followed the next day by 1:400–500 goat anti-rabbit Alexa 555 secondary antibody (Cell Signaling, Danvers, MA, USA). Primary and secondary antibodies were diluted in 1% NGS and PBST. After that, the slides were coverslipped with antifading agent. The cleaved SNAP-25 occurrence in muscles was quantified by a previously reported semiquantitative method [37] assigning a defined score to observable neuromuscular junctions, nerve terminals and nerve profiles. Score 1 was assigned when only a few or weak NMJ staining was observed; score 2 = the moderate staining of frequent NMJs; score 3 = the strong staining of frequent NMJ and nerve terminals and score 4 = the strong staining of frequent NMJs, terminals and intramuscular nerves (no. of axons $\geq$ 10). The individual score assigned for each animal was derived from the average score of 4 visual fields, each taken from different muscle slices at 20 $\times$ 0.5 magnification. Spinal cord slices were incubated with 3% H$_2$O$_2$ for the inhibition of endogenous peroxidase and washed in PBS. Then, the slices were blocked with 10% NGS

and incubated overnight at 4 °C with mouse monoclonal antibody to somatodendritic marker microtubule-associated protein 2 (MAP-2) (Sigma Aldrich, St. Louis, MO, USA, 1:1000 dilution in 1 % NGS). The next day, the tissue was incubated with goat anti-rabbit Alexa 555 secondary antibody (Cell Signaling, Danvers, MA, USA) and washed. After that, the spinal cord sections were incubated with the antibody to BoNT-A-cleaved SNAP-25 (1:8000) overnight at room temperature. The following day, the tissue was incubated with poly-HRP-conjugated goat anti-rabbit secondary antibody and then reacted with tyramide Atto-488 HRP substrate prepared as described previously [47] diluted 1:100 in PBS with 100 mM imidazole and 0.001% H_2O_2 for 10 min. After that, the slices were washed 3 times, mounted on glass slides and coverslipped with antifading agent. Then, the images were visualized by an Olympus BX-51 fluorescent microscope and processed using Cell Sens Dimension imaging and quantification software (Olympus, Tokyo, Japan). The cSNAP-25 immunoreactivity was quantified as reported previously [30]. If brief, microphotographs taken at 40×0.5 magnification were acquired at constant exposure in the ipsilateral and contralateral ventral horns. Then, the area containing the cSNAP-25 immunoreactivity was quantified from separated green channel images by using a constant pixel threshold range (100–256 by employing cell Sens Dimension software). The value representing the ventral horn cSNAP-25 immunoreactive area was calculated as the total area from 3 nonoverlapping visual fields (3×0.14 mm^2) and the average of 4 slices per single animal. Samples with MAP-2/cSNAP-25 colocalization were visualized with a Leica SP5 Confocal microscope equipped with a $40\times$ HCX PL APO NA 1.4 oil immersion and, afterwards, processed by ImageJ without altering the intensity of the signals.

4.6. Statistical Analysis

The data were presented as mean ± SEM or individual values with the median. Repeated measurements were analyzed by two-way analysis of variance (two-way RM ANOVA), followed by Bonferroni's post hoc test for between-group comparisons. The statistical analysis of the results of the cleaved SNAP-25 immunoreactive area was not normally distributed; hence, nonparametric ANOVA and Dunn's post hoc were employed. A *p*-value lower than 0.05 was considered significant.

5. Conclusions

In rat model of local spasticity, we found that the persistence of BoNT-A effect and the relative importance of central toxin action change depending on the doses injected and the time point examined. In line with clinical experience, local muscular paralysis is the dominant factor contributing to the initial antispastic effect of i.m. BoNT-A, explaining its early onset and intensity. Later, when peripheral muscular effects start to fade, central antispastic actions become a more apparent contributor to the overall BoNT-A-mediated benefit. These results suggest the relevance of peripheral doses employed and central toxin action as additional factors contributing to extraordinarily long BoNT-A clinical action.

References

1. Dong, M.; Masuyer, G.; Stenmark, P. Botulinum and Tetanus Neurotoxins. *Annu. Rev. Biochem.* **2019**, *88*, 811–837. [CrossRef] [PubMed]
2. Rossetto, O.; Montecucco, C. Tables of Toxicity of Botulinum and Tetanus Neurotoxins. *Toxins* **2019**, *11*, 686. [CrossRef] [PubMed]
3. Arnon, S.S.; Schechter, R.; Inglesby, T.V.; Henderson, D.A.; Bartlett, J.G.; Ascher, M.S.; Eitzen, E.; Fine, A.D.; Hauer, J.; Layton, M.; et al. Botulinum Toxin as a Biological Weapon. *JAMA* **2001**, *285*, 1059. [CrossRef]
4. Schiavo, G.; Benfenati, F.; Poulain, B.; Rossetto, O.; Polverino de Laureto, P.; DasGupta, B.R.; Montecucco, C. Tetanus and Botulinum-B Neurotoxins Block Neurotransmitter Release by Proteolytic Cleavage of Synaptobrevin. *Nature* **1992**, *359*, 832–835. [CrossRef] [PubMed]
5. Blasi, J.; Chapman, E.R.; Link, E.; Binz, T.; Yamasaki, S.; De Camilli, P.; Südhof, T.C.; Niemann, H.; Jahn, R. Botulinum Neurotoxin A Selectively Cleaves the Synaptic Protein SNAP-25. *Nature* **1993**, *365*, 160–163. [CrossRef] [PubMed]
6. Jankovic, J. Botulinum Toxin: State of the Art. *Mov. Disord.* **2017**, *32*, 1131–1138. [CrossRef]
7. Ledda, C.; Artusi, C.A.; Tribolo, A.; Rinaldi, D.; Imbalzano, G.; Lopiano, L.; Zibetti, M. Time to Onset and Duration of Botulinum Toxin Efficacy in Movement Disorders. *J. Neurol.* **2022**, *269*, 3706–3712. [CrossRef] [PubMed]
8. Hallett, M. Explanation of Timing of Botulinum Neurotoxin Effects, Onset and Duration, and Clinical Ways of Influencing Them. *Toxicon* **2015**, *107*, 64–67. [CrossRef]
9. Rogozhin, A.A.; Pang, K.K.; Bukharaeva, E.; Young, C.; Slater, C.R. Recovery of Mouse Neuromuscular Junctions from Single and Repeated Injections of Botulinum Neurotoxin A. *J. Physiol.* **2008**, *586*, 3163–3182. [CrossRef] [PubMed]
10. Nijmeijer, S.W.R.; Koelman, J.H.T.M.; Standaar, T.S.M.; Postma, M.; Tijssen, M.A.J. Cervical Dystonia: Improved Treatment Response to Botulinum Toxin after Referral to a Tertiary Centre and the Use of Polymyography. *Park. Relat. Disord.* **2013**, *19*, 533–538. [CrossRef]
11. Gracies, J.-M.; Lugassy, M.; Weisz, D.J.; Vecchio, M.; Flanagan, S.; Simpson, D.M. Botulinum Toxin Dilution and Endplate Targeting in Spasticity: A Double-Blind Controlled Study. *Arch. Phys. Med. Rehabil.* **2009**, *90*, 9–16.e2. [CrossRef] [PubMed]
12. Hallett, M. Mechanism of Action of Botulinum Neurotoxin: Unexpected Consequences. *Toxicon* **2018**, *147*, 73–76. [CrossRef]
13. Mazzocchio, R.; Caleo, M. More than at the Neuromuscular Synapse: Actions of Botulinum Neurotoxin A in the Central Nervous System. *Neuroscientist* **2015**, *21*, 44–61. [CrossRef] [PubMed]
14. Weise, D.; Weise, C.M.; Naumann, M. Central Effects of Botulinum Neurotoxin-Evidence from Human Studies. *Toxins* **2019**, *11*, 21. [CrossRef]
15. Gracies, J.-M. Physiological Effects of Botulinum Toxin in Spasticity. *Mov. Disord.* **2004**, *19* (Suppl. S8), S120–S128. [CrossRef]
16. Rosales, R.L.; Dressler, D. On Muscle Spindles, Dystonia and Botulinum Toxin. *Eur. J. Neurol.* **2010**, *17* (Suppl. S1), 71–80. [CrossRef]
17. Vinti, M.; Costantino, F.; Bayle, N.; Simpson, D.M.; Weisz, D.J.; Gracies, J.-M. Spastic Cocontraction in Hemiparesis: Effects of Botulinum Toxin. *Muscle Nerve* **2012**, *46*, 917–925. [CrossRef]
18. Aymard, C.; Giboin, L.-S.; Lackmy-Vallée, A.; Marchand-Pauvert, V. Spinal Plasticity in Stroke Patients after Botulinum Neurotoxin A Injection in Ankle Plantar Flexors. *Physiol. Rep.* **2013**, *1*, e00173. [CrossRef]
19. Marchand-Pauvert, V.; Aymard, C.; Giboin, L.-S.; Dominici, F.; Rossi, A.; Mazzocchio, R. Beyond Muscular Effects: Depression of Spinal Recurrent Inhibition after Botulinum Neurotoxin A. *J. Physiol.* **2013**, *591*, 1017–1029. [CrossRef]
20. Wohlfarth, K.; Schubert, M.; Rothe, B.; Elek, J.; Dengler, R. Remote F-Wave Changes after Local Botulinum Toxin Application. *Clin. Neurophysiol.* **2001**, *112*, 636–640. [CrossRef]
21. Ishikawa, M.; Takashima, K.; Kamochi, H.; Kusaka, G.; Shinoda, S.; Watanabe, E. Treatment with Botulinum Toxin Improves the Hyperexcitability of the Facial Motoneuron in Patients with Hemifacial Spasm. *Neurol. Res.* **2010**, *32*, 656–660. [CrossRef] [PubMed]
22. Moreno-López, B.; de la Cruz, R.R.; Pastor, A.M.; Delgado-García, J.M. Effects of Botulinum Neurotoxin Type A on Abducens Motoneurons in the Cat: Alterations of the Discharge Pattern. *Neuroscience* **1997**, *81*, 437–455. [CrossRef]
23. Pastor, A.M.; Moreno-López, B.; De La Cruz, R.R.; Delgado-García, J.M. Effects of Botulinum Neurotoxin Type A on Abducens Motoneurons in the Cat: Ultrastructural and Synaptic Alterations. *Neuroscience* **1997**, *81*, 457–478. [CrossRef]
24. Gonzalez-Forero, D.; Pastor, A.M.; Geiman, E.J.; Benítez-Temiño, B.; Alvarez, F.J. Regulation of Gephyrin Cluster Size and Inhibitory Synaptic Currents on Renshaw Cells by Motor Axon Excitatory Inputs. *J. Neurosci.* **2005**, *25*, 417–429. [CrossRef] [PubMed]

25. Antonucci, F.; Rossi, C.; Gianfranceschi, L.; Rossetto, O.; Caleo, M. Long-Distance Retrograde Effects of Botulinum Neurotoxin A. *J. Neurosci.* **2008**, *28*, 3689–3696. [CrossRef]

26. Matak, I.; Riederer, P.; Lacković, Z. Botulinum Toxin's Axonal Transport from Periphery to the Spinal Cord. *Neurochem. Int.* **2012**, *61*, 236–239. [CrossRef]

27. Koizumi, H.; Goto, S.; Okita, S.; Morigaki, R.; Akaike, N.; Torii, Y.; Harakawa, T.; Ginnaga, A.; Kaji, R. Spinal Central Effects of Peripherally Applied Botulinum Neurotoxin A in Comparison between Its Subtypes A1 and A2. *Front. Neurol.* **2014**, *5*, 98. [CrossRef]

28. Caleo, M.; Spinelli, M.; Colosimo, F.; Matak, I.; Rossetto, O.; Lackovic, Z.; Restani, L. Transynaptic Action of Botulinum Neurotoxin Type a at Central Cholinergic Boutons. *J. Neurosci.* **2018**, *38*, 10329–10337. [CrossRef]

29. Marinelli, S.; Vacca, V.; Ricordy, R.; Uggenti, C.; Tata, A.M.; Luvisetto, S.; Pavone, F. The analgesic effect on neuropathic pain of retrogradely transported botulinum neurotoxin A involves Schwann cells and astrocytes. *PLoS ONE* **2012**, *7*, e47977. [CrossRef]

30. Matak, I. Evidence for Central Antispastic Effect of Botulinum Toxin Type A. *Br. J. Pharmacol.* **2020**, *177*, 65–76. [CrossRef]

31. Bjornson, K.; Hays, R.; Graubert, C.; Price, R.; Won, F.; McLaughlin, J.F.; Cohen, M. Botulinum Toxin for Spasticity in Children with Cerebral Palsy: A Comprehensive Evaluation. *Pediatrics* **2007**, *120*, 49–58. [CrossRef] [PubMed]

32. Eek, M.N.; Himmelmann, K. No Decrease in Muscle Strength after Botulinum Neurotoxin-A Injection in Children with Cerebral Palsy. *Front. Hum. Neurosci.* **2016**, *10*, 506. [CrossRef]

33. Cosgrove, A.P.; Graham, H.K. Botulinum Toxin A Prevents the Development of Contractures in the Hereditary Spastic Mouse. *Dev. Med. Child Neurol.* **1994**, *36*, 379–385. [CrossRef]

34. Wei, X.M.; Dou, Z.L.; Zhang, Y.W.; Dai, M.; Yu, F.; Wang, Q.Y.; Jiang, L. Effects of Botulinum Toxin Type A Injection for Pathological Characteristic of Calf in Rats with Spinal Cord Injure. *Zhonghua Yi Xue Za Zhi* **2017**, *97*, 1809–1814. [CrossRef] [PubMed]

35. Sätilä, H.; Kotamäki, A.; Koivikko, M.; Autti-Rämö, I. Low- and High-Dose Botulinum Toxin A Treatment: A Retrospective Analysis. *Pediatr. Neurol.* **2006**, *34*, 285–290. [CrossRef]

36. Broide, R.S.; Rubino, J.; Nicholson, G.S.; Ardila, M.C.; Brown, M.S.; Aoki, K.R.; Francis, J. The Rat Digit Abduction Score (DAS) Assay: A Physiological Model for Assessing Botulinum Neurotoxin-Induced Skeletal Muscle Paralysis. *Toxicon* **2013**, *71*, 18–24. [CrossRef] [PubMed]

37. Périer, C.; Martin, V.; Cornet, S.; Favre-Guilmard, C.; Rocher, M.; Bindler, J.; Wagner, S.; Andriambeloson, E.; Rudkin, B.B.; Marty, R.; et al. Recombinant Botulinum Neurotoxin Serotype A1 in Vivo Characterization. *Pharmacol. Res. Perspect.* **2021**, *9*, e00857. [CrossRef] [PubMed]

38. Cichon, J.V.; McCaffrey, T.V.; Litchy, W.J.; Knops, J.L. The Effect of Botulinum Toxin Type A Injection on Compound Muscle Action Potential in an in Vivo Rat Model. *Laryngoscope* **1995**, *105*, 144–148. [CrossRef]

39. Poewe, W.; Deuschl, G.; Nebe, A.; Feifel, E.; Wissel, J.; Benecke, R.; Kessler, K.R.; Ceballos-Baumann, A.O.; Ohly, A.; Oertel, W.; et al. What Is the Optimal Dose of Botulinum Toxin A in the Treatment of Cervical Dystonia? Results of a Double Blind, Placebo Controlled, Dose Ranging Study Using Dysport. German Dystonia Study Group. *J. Neurol. Neurosurg. Psychiatry* **1998**, *64*, 13–17. [CrossRef]

40. Rystedt, A.; Zetterberg, L.; Burman, J.; Nyholm, D.; Johansson, A. A Comparison of Botox 100 U/ML and Dysport 100 U/ML Using Dose Conversion Ratio 1. *Clin. Neuropharmacol.* **2015**, *38*, 170–176. [CrossRef]

41. Priori, A.; Berardelli, A.; Mercuri, B.; Manfredi, M. Physiological Effects Produced by Botulinum Toxin Treatment of Upper Limb Dystonia. Changes in Reciprocal Inhibition between Forearm Muscles. *Brain* **1995**, *118 Pt 3*, 801–807. [CrossRef] [PubMed]

42. Wree, A.; Mix, E.; Hawlitschka, A.; Antipova, V.; Witt, M.; Schmitt, O.; Benecke, R. Intrastriatal botulinum toxin abolishes pathologic rotational behaviour and induces axonal varicosities in the 6-OHDA rat model of Parkinson's disease. *Neurobiol. Dis.* **2011**, *41*, 291–298. [CrossRef] [PubMed]

43. Hawlitschka, A.; Wree, A. Experimental Intrastriatal Applications of Botulinum Neurotoxin-A: A Review. *Int. J. Mol. Sci.* **2018**, *19*, 1392. [CrossRef]

44. Cai, B.B.; Francis, J.; Brin, M.F.; Broide, R.S. Botulinum Neurotoxin Type A-Cleaved SNAP25 Is Confined to Primary Motor Neurons and Localized on the Plasma Membrane Following Intramuscular Toxin Injection. *Neuroscience* **2017**, *352*, 155–169. [CrossRef] [PubMed]

45. Zagoraiou, L.; Akay, T.; Martin, J.F.; Brownstone, R.M.; Jessell, T.M.; Miles, G.B. A Cluster of Cholinergic Premotor Interneurons Modulates Mouse Locomotor Activity. *Neuron* **2009**, *64*, 645–662. [CrossRef] [PubMed]

46. Basso, D.M.; Beattie, M.S.; Bresnahan, J.C. A Sensitive and Reliable Locomotor Rating Scale for Open Field Testing in Rats. *J. Neurotrauma* **1995**, *12*, 1–21. [CrossRef] [PubMed]

47. Homolak, J.; Babic Perhoc, A.; Knezovic, A.; Osmanovic Barilar, J.; Koc, F.; Stanton, C.; Ross, R.P.; Salkovic-Petrisic, M. Disbalance of the Duodenal Epithelial Cell Turnover and Apoptosis Accompanies Insensitivity of Intestinal Redox Homeostasis to Inhibition of the Brain Glucose-Dependent Insulinotropic Polypeptide Receptors in a Rat Model of Sporadic Alzheimer's Disease. *Neuroendocrinology* **2022**, *112*, 744–762. [CrossRef]

Appendix II

Šoštarić P, Matić M, Nemanić D, Lučev Vasić Ž, Cifrek M, Pirazzini M, Matak I. **Beyond neuromuscular activity: botulinum toxin type A exerts direct central action on spinal control of movement.** Eur J Pharmacol. 2024;962:176242. (Q1)

Petra Šoštarić Mužić made significant contributions to the conception and design of the work, acquisition, analysis, and interpretation of data for the work, writing, reviewing, and editing the manuscriot for publication.

Matić Magdalena-acquisition of data, review and editing of the manuscript for publication

Nemanić Dalia- acquisition of data, review and editing of the manuscript for publication

Lučev Vasić Željka-acquisition of data, review and editing of the manuscript for publication

Cifrek Mario- acquisition of data, review and editing of the manuscript for publication

Pirazzini Marco- acquisition of data, review and editing of the manuscript for publication

Matak Ivica- significant contributions to the conception and design of the work, acquisition, analysis, and interpretation of data for the work, writing, reviewing, and editing the manuscriot for publication.
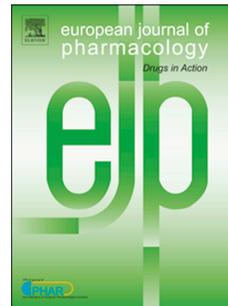
Weblink:

https://www.sciencedirect.com/science/article/abs/pii/S0014299923007562?via%3Dihub

Journal Pre-proof

Beyond neuromuscular activity: Botulinum toxin type a exerts direct central action on spinal control of movement

Petra Šoštarić, Magdalena Matić, Dalia Nemanić, Željka Lučev Vasić, Mario Cifrek, Marco Pirazzini, Ivica Matak

AUTHOR CONTRIBUTIONS

IM: Conception and design of the study; PŠ, MM, DV, ŽLV, MP, MC, IM: Acquisition and analysis of the data; PŠ, IM: Draft of the manuscript and figures; All authors revised and approved the final manuscript.

Beyond neuromuscular activity: botulinum toxin type A exerts direct central action on spinal control of movement

- Botulinum toxin A (BoNT-A) is a standard therapy for spasticity & dystonia

- It potently blocks NMJs and possibly intrafusal transmission

- Possible role of spinal premotor networks in dystonia and spasticity is so far unknown

Treatment 1. (days 0, 1)

Blocked trans-synaptic action on **premotor inputs**

BoNT-A (2 U)

antitoxin (5 iu)

BoNT-A (2 U)

Treatment 2. day 62

testing effects of BoNT-A on **local spasm**

TeNT (1.5 ng)

Combined **peripheral and spinal trans-synaptic** BoNT-A action (↓motor control, ↓spasm, SNAP-25 cleavage)

Ia afferent
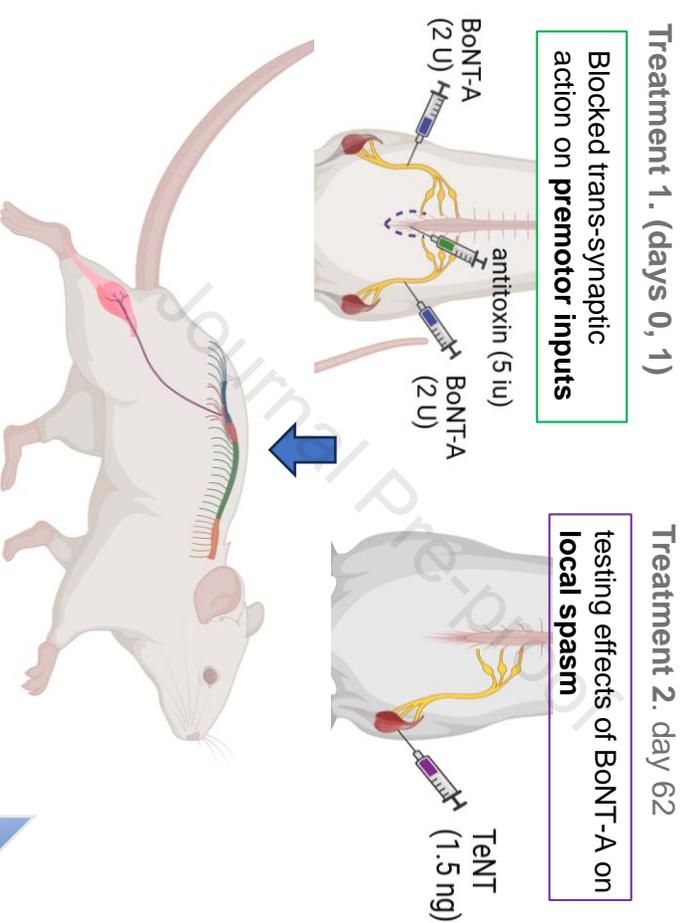
Functional motor tests

(days 0-56) motor control: balance & fatigue, swimming, local muscle weakness
(days 62-78) spasm: resistance to flexion; locomotor scale, EMG (H/M)

Beyond neuromuscular activity: botulinum toxin type A exerts direct central action on spinal control of movement

Petra Šoštarić[1]**, Magdalena Matić**[1,2]**, Dalia Nemanić**[3]**, Željka Lučev Vasić**[4]**, Mario Cifrek**[4]**, Marco Pirazzini**[5,6]**, Ivica Matak**[1]*

1 Laboratory of Molecular Neuropharmacology, Department of Pharmacology and Croatian Institute of Brain Research, University of Zagreb School of Medicine, Šalata 11, 10000 Zagreb, Croatia

2 Division of Neurobiology, Department of Neurology, Medical University of Innsbruck, Innsbruck, Austria

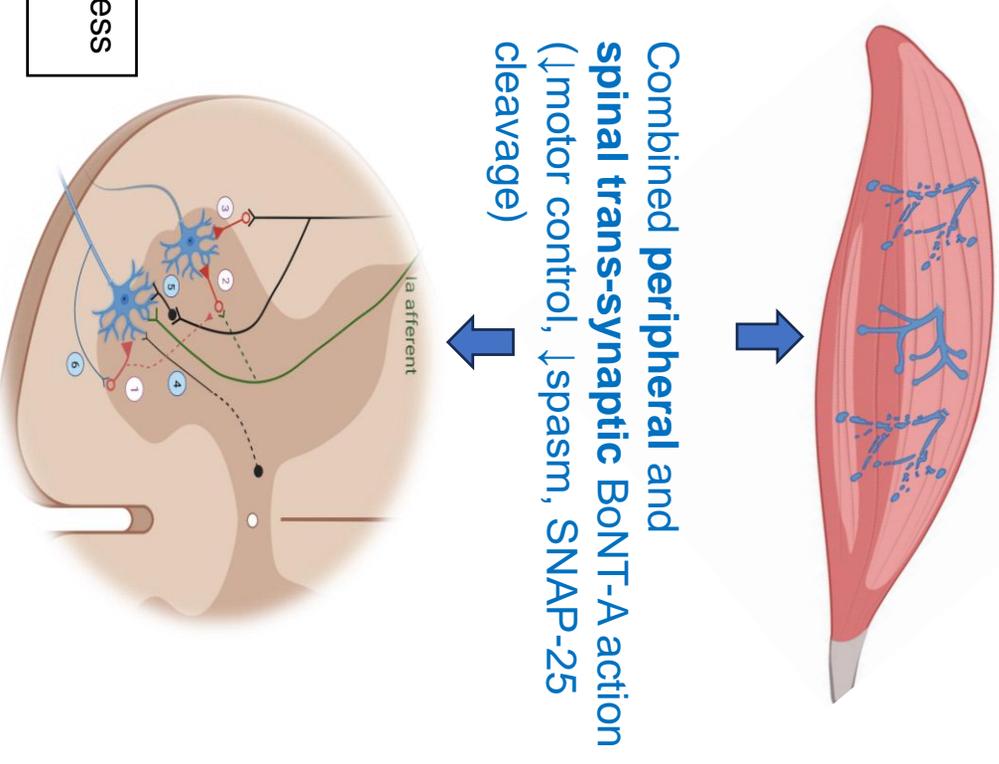3 Department of Pharmacology, Faculty of Pharmacy and Biochemistry, University of Zagreb, Domagojeva 2, 10 000 Zagreb, Croatia

4 University of Zagreb, Faculty of Electrical Engineering and Computing, Zagreb, Croatia

5 Department of Biomedical Sciences, University of Padova, via Ugo Bassi 58/B 35131, Padova, Italy

6 Interdepartmental Research Center of Myology CIR-Myo, University of Padova, Via Ugo Bassi 58/B, 35131 Padova, Italy

*Correspondence: ivica.matak@mef.hr; Tel.: 0038514590198

Type of article: Original research article

ABSTRACT

Overt muscle activity and impaired spinal locomotor control hampering coordinated movement is a hallmark of spasticity and movement disorders like dystonia. While botulinum toxin A (BoNT-A) standard therapy alleviates mentioned symptoms presumably due to its peripheral neuromuscular actions alone, the aim of present study was to examine for the first time the toxin's trans-synaptic activity within central circuits that govern the skilled movement. The rat hindlimb motor pools were targeted by BoNT-A intrasciatic bilateral injection (2 U per nerve), while its trans-synaptic action on premotor inputs was blocked by intrathecal BoNT-A-neutralising antitoxin (5 i.u.). Effects of BoNT-A on coordinated and high intensity motor tasks (rotarod, beamwalk swimming), and localised muscle weakness (digit abduction, gait ability) were followed until their substantial recovery by day 56 post BoNT-A. Later, (day 62-77) the BoNT-A effects were examined in unilateral calf muscle spasm evoked by tetanus toxin (TeNT, 1.5 ng). In comparison to peripheral effect alone, combined peripheral and central trans-synaptic BoNT-A action induced a more prominent and longer impairment of different motor tasks, as well as the localised muscle weakness. After near-complete recovery of motor functions, the BoNT-A maintained the ability to reduce the experimental calf spasm evoked by tetanus toxin (TeNT 1.5 ng, day 62) without altering the monosynaptic reflex excitability. These results indicate that, in addition to muscle terminals, BoNT-A-mediated control of hyperactive muscle activity in movement disorders and spasticity may involve the spinal premotor inputs and central circuits participating in the skilled locomotor performance.

Key words: botulinum toxin type A; motor control; axonal transport; spinal cord; trans-synaptic effect

1. Introduction

Used as a pharmaceutical-grade purified low dose preparation, botulinum neurotoxin serotype A (BoNT-A) is employed in various disorders involving motor, autonomic and sensory nerve hyperactivity (Rosseto and Montecucco, 2019; Jankovic 2017; Anandan and Jankovic 2021). It poisons the presynaptic nerve terminals for several months by first binding to

polysialoganglioside and synaptic vesicle 2 (SV2) protein, followed by endocytic entry into recycled synaptic vesicles. Upon vesicle acidification, the toxin translocates its 50 kDa neurotoxic light chain into the presynaptic cytosol, and cleaves synaptosomal-associated protein of 25 kDa (SNAP-25) (Schiavo et al., 1993; Rossetto et al., 2014) with consequent long-term blockage of the Ca^{2+}-triggered release of ACh and other neurotransmitters Gundersen 1980; Pirazzini et al., 2017). In focal dystonias and spasticity, its therapeutic benefits have been commonly attributed to local neuromuscular paralysis of injected muscles, in turn, leading to indirect central plastic changes (Rosales and Dressler, 2010). However, mounting data point to a direct central interaction with sensory and motor systems (Matak and Lacković 2014; Ramachandran and Yaksh, 2014; Ramirez-Castaneda et al., 2013; Mazzocchio and Caleo, 2015). The BoNT-A may normalise the spastic co-contraction of agonists and antagonists and recover the reciprocal inhibition in uninjected muscles, possibly by influencing the recurrent inhibition at a synapse between motoneuronal collaterals and Renshaw interneurons (Hallett 2018; Gracies 2004; Matak et al., 2016; Vinti et al., 2012; Marchand-Pauvert et al., 2013; Aymard et al., 2013; Caleo and Mazzocchio, 2018; Weise et al., 2019). Peripherally injected BoNT-A is axonally transported to spinal cord and brainstem nuclei (Antonucci et al., 2008; Matak et al., 2012; Restani et al.,2012; Koizumi et al., 2014; Caleo et al., 2018). Furthermore, its central antispastic effect has been reported in rat focal muscle hypertonia induced by tetanus toxin (TeNT) (Matak 2020; Šoštarić et al., 2022), a neurotoxin that blocks the inhibitory transmission (Brooks et al.,1957; Megighian et al., 2021). The BoNT-A central trans-synaptic traffic was found to be necessary for its antispastic effect when local muscular effects of BoNT-A are minimised or start to recover (Matak 2020; Šoštarić et al., 2022). Other motor consequences of BoNT-A trans-synaptic transport in ventral horn are, up to now, unknown. Spinal premotor inputs regulate the precise activation of different muscle groups during normal locomotion (Laliberte et al., 2019). In dystonia and spasticity, spinal locomotor circuits produce altered patterns of motor pool activation leading to sustained or intermittent muscular hyperactivity (Liu et al., 2015; Bellardita et al., 2017; Pocratsky et al., 2023). Building on our previous research that demonstrated the BoNT-A axonal transport and

transcytosis (Caleo et al., 2018; Matak 2020; Šoštarić et al., 2022), we hypothesised that spinal synapses sensitive to BoNT-A may belong to premotor inputs regulating the precise activation of different muscle groups during locomotion.

To examine this hypothesis, we studied the effect of BoNT-A in the motor system by targeting the bilateral lower leg and hind-paw motor pools in adult rats. We employed direct toxin injections into the sciatic nerves (i.n.) rather than into multiple hindlimb muscles. This enabled a slower-onset toxin effect at the NMJ due to anterograde transport resulting in milder weakness, however with ongoing muscle atrophy, and a central enzymatic action similar to the one seen after i.m. BoNT-A in previous studies (Matak 2020; Šoštarić et al., 2022). We further characterised the effect of unopposed vs opposed BoNT-A spinal trans-synaptic action on the motor performance by blocking its trans-synaptic transport with intrathecal BoNT-A-neutralising antitoxin. Then, its motor effects were regularly assessed by different behavioural tests up to 56 days after BoNT-A injection. Later, in the same animals we examined BoNT-A central action on TeNT-evoked spasm and exaggerated monosynaptic H reflex and, at the end of experiment, analysed the localization of the toxin enzymatic activity in relation to synaptic markers and known toxin acceptors.

2. Material and methods

2.1. Animals

Adult male Wistar Han rats (University of Zagreb School of Medicine, Croatia), 6 months old and weighing 494 ± 9 g at the beginning of the experiment, were used. Three rats per home cage supplied with cardboard play tunnel enrichment were kept under a 12 hour light/dark cycle and *ad libitum* access to food and water. All procedures involving animals and animal care were carried out in accordance with the European Union Directive (2010/63/EU), the ARRIVE guidelines 2.0: Updated guidelines for reporting animal research (Percie et al., 2020) and approved by the institutional review board (University of Zagreb School of Medicine) and Croatian Ministry of Agriculture ethical committees (permit no. EP 229/2019). The adult

rats of single sex (male) were chosen to achieve more uniform weight and dosing that is not affected by differences related to sexual dimorphism e.g. muscle size, total weight of rats, length of the nerves, as well as to minimise any possible systemic effect of the injected BoNT-A (lower dosage/body weight ratio).

2.2. Drugs

Following drugs were used: lyophilized BoNT-A (INN: clostridium botulinum type A neurotoxin complex, Allergan, Irvine, CA, USA) was reconstituted in physiological saline. Lyophilized polyclonal equine IgG-based BoNT-A antitoxin (NIBSC code 14/174, National Institute for Biological Standards and Control, Potters Bar, United Kingdom; a kind gift from Dr. Thea Sesardic), validated by Li et al. (2012) , was reconstituted in 0.9% sterile saline to obtain1000 international units (iu)/ml concentration (single iu can neutralise 10 000 mouse LD_{50} doses of BoNT-A), and further kept in ultrafreezer, until use. Lyophilized TeNT (Sigma Aldrich, St Louis, MO, USA, Cat. No T3194) was reconstituted in saline vehicle containing 2% bovine serum albumin (BSA) (Sigma Aldrich), kept in concentrated aliquots at −80°C, and further diluted with vehicle containing 2% BSA to the necessary volume for i.m. injections

2.3. Pharmacological treatment

Animals were assigned randomly into different experimental groups by using block randomisation. For bilateral i.n. injection of BoNT-A or saline, the rats were deeply anaesthetised with a mixture of ketamine (Ketamidor® 10%, Richter Pharma AG, Wels, Austria; 70 mg/kg i.p.) and xylazine (Xylased® Bio, Bioveta, Ivanovice na Hané, Czech Republic; 7 mg/kg i.p.). The fur of the rat thigh was clipped and disinfected with 70% ethanol, and then a lateral skin incision (1.5 cm) at mid-femoral level was made. The sciatic nerve was exposed by blunt dissection through the thigh muscles and exposed with curved forceps. The BoNT-A injection into the nerve trunk was performed with a 0-10 µl Hamilton syringe needle (Cat. No. #701, Hamilton, Bonadouz, Switzerland) as previously described (Bach-Rojecky and Lacković 2009). The nerve was left in place for three minutes following the treatment and

retracted to its natural position by leg extension, followed by skin suturing. Then, the operation and injection procedure were repeated on the contralateral limb (fig 1).

The next day (24 h post BoNT-A), animals were injected i.t. into the spinal canal at level of cauda equina with equine serum containing 5 iu of BoNT-A-neutralizing equine antitoxin (National Institute for Biological Standards and Control, NIBSC code 14/174, Potters Bar, United Kingdom,) or horse serum administered as a control treatment for equine serum (Gibco, ThermoFisher Scientific, Waltham, MA, USA). Prior to i.t. treatment, both neutralising antiserum solution and control horse serum (5 µl each per animal) were diluted with equal amount of saline to obtain the total volume of 10 µl per animal. The i.t. administration was performed under isoflurane anaesthesia (5% induction, 2 % maintenance) by 28G x ½" tip of 0.5 ml tuberculin syringe inserted between the lumbar vertebrae (L4-L6) into vertebral canal at the level of cauda equina, as previously described (Matak 2020; Šoštarić et al., 2022). Brief, sudden movement of hind limb or tail was monitored as a confirmation of successful targeting of lumbar spinal canal.

Tetanus toxin (TeNT; Sigma Aldrich, Cat. No T3194) diluted in saline vehicle containing 2% BSA was administered on day 62 after BoNT-A into the calf to induce local hindlimb spasticity. The rats were i.m. injected under anaesthesia with 10 µL of neurotoxin divided into 2 injection sites (5 µL each site) i.m. into the lateral and medial belly of the right gastrocnemius by employing 10 µL Hamilton syringe. The 1.5 ng TeNT dose was chosen based on previously used non-systemic doses (Matak 2020; Šoštarić et al., Matthews et al.,2014).

Figure 1.

2.4. Behavioural motor tests

Experimenters were blinded to the animal treatment during performance of i.n. and i.t. treatments and measurements. All motor tests were conducted during the day at similar time periods (from 9 a.m. to 2 p.m.).

2.4.1. Narrow beam walking

Rats were trained to cross an elevated rectangular horizontal beam (2.5 cm ✕ 2.5 cm ✕ 100 cm) connecting a rectangular platform (10 cm ✕ 10 cm) exposed to lamp light on one side and an enclosed "safe" dark platform (25 cm × 25 cm × 25 cm, 10 cm × 10 cm entrance) on the other side, as previously described (Šoštarić et al., 2022; Carter et al.,2001). The latency was defined as the transit time between the markings placed at 10 cm from both ends of the beam (80 cm total distance), with the average calculated from two successful trials per single measurement (Matak 2020). Animals were pre-trained daily during the week preceding the BoNT-A i.n. treatment to cross the bar swiftly without stumbling, stopping or falling.

2.4.2. Rotarod test

The animals were placed on a rotarod device rotating at constant rate (13 r.p.m.). The time that the animal spent on the rotating bar (8-cm diameter) before falling was then measured, with the maximal trial duration set to 180 s. Animals were pre trained to easily maintain the balance for 3 minutes before the toxin treatment. The latency value was calculated based on two trials per a single measurement session, with at least 20 min resting period between the trials.

2.4.3. Swimming performance

Individual rats were placed inside the circular swimming pool filled with water (180 cm diameter, water depth 30 cm, temperature 24 ˚C), and observed with a wide-angle video camera (Basler AG, Basler, Ahrensburg, Germany) mounted above. The swimming mean and maximal velocity during a time period of 120 s per trial were assessed by video analysis software (Noldus Ethovision XT ver. 11.5; Noldus, Wageningen, Netherlands) monitoring the animal's body centre position every 0.133 s (7.5 Hz). To exclude the low values when animals did not swim (e.g. during passive floating), or erroneously high values, only the velocities between 10 to 100 cm/s were considered. The parameters were calculated based on two trials per measurement session with at least 30 min resting period between the trials. The animals

exhibit an innate ability to swim and did not require pre-training prior to the baseline measurement.

2.4.4. Digit abduction score (DAS)

To assess the toe-spreading reflex impairment, animals were gently grasped around the waist and lifted, and the toe spreading was quantified with scores based on toe abduction defined as 0 = separation of all toes; 1 = separation of four toes; 2 = separation of three toes; 3 = separation of two toes; and 4 = no toe separation (Broide et al., 2013). The DAS value was based on the average score of both hind-limbs and by the two independent observers unaware of the animal treatment.

2.4.5. Gait ability test

The appearance of rat hind paws and leg use during gait and climbing, indicative of lower leg muscle weakness, was assessed by the gait ability score as previously explained in details (Brent et al., 2020; Warner et al., 2006). The total score ranging from 0-10 was based on the sum of scores from five different parameters: 1) hindlimb abduction during suspension by the animal's tail; the hind paw appearance that evaluated the weight bearing by interdigital paw pad and toes (normal) vs the use of heel (abnormal) during 2) sitting on the ground; 3) bipedal stance while leaning against the cage side, 4) while walking on a slope, 5) gripping with toes and propulsion by both toes and interdigital paw pad during climbing on the inclined mesh floor. Each set of observations was scored with scale of individual parameter ranging from disabled (0) to normal (2) (e.g. markedly arch-like appearance of the hind-paw in contact with the ground scored as 0; intermediate foot sole arching with partially curled toes scored 1, no arching and normal foot appearance with toe extension and interdigital paw pad in contact with the ground scored as 2). The gait ability value from single measurement was based on the average score of both hind-limbs and by the two independent observers unaware of the animal treatment.

2.4.6. Resistance to passive ankle flexion

Digital zeroed kitchen scale with a plastic platform attached on its surface (dimensions in cm: 1.5 × 4 × 4) was used for assessing the passive ankle flexion resistance. Animals were lifted by the examiner's hand and the ankle joint was flexed by pressing the hind paw interdigital pad area against the platform. The dorsiflexion of TeNT-treated spastic hind-limb was performed until > 90° tibiotarsal angle was reached, after which the pressure was slightly relieved until the tibiotarsal angle returned to 90°. At that point the resistance value in grams (g) was noted and the average of two measurements per session was calculated (Matak 2020; Šoštarić et al., 2022).

2.4.7. Basso Beattie Bresnahan locomotor scale

The appearance of TeNT-treated hind limb and its use during gait was examined by employing the Basso Beattie Bresnahan (BBB) locomotor rating scale. The BBB score range (0-21) consists of a combination of defined elements describing the hind limb joint movement, paw placement, weight support, forelimb-hindlimb coordination, paw position during locomotion, toe clearance during limb advancement, tail position, and trunk stability during gait (Basso et al., 1995). The rats were video-recorded while walking across a table to return to their home cage opened in level with the table surface, as previously described (Šoštarić et al., 2022). Two observers unaware of the animal treatment assessed the BBB score from coded video footage, and the mean of their independent scoring counted as a single measurement. Only the right hind limb injected with TeNT was used to assign the score, while contralateral non-spastic limb served as a reference for normal range of motion of joints.

2.4.8. Measurement of lower leg muscle atrophy

Changes of the lower leg width were used to assess the muscle atrophy throughout the experiment. The approximate cross section area of the lower leg was modelled as ellipse defined by the mediolateral (ML) and dorsoventral (DV) calf diameter at its widest mid-belly part (DV × ML × π/4) measured by calliper (Šoštarić et al., 2022). The values representing single animal measurements were calculated as average value obtained from both legs. The calf diameters were measured prior to the treatment and at different experimental points after

i.n. BoNT-A. At the end of the experiment, the gastrocnemius and soleus muscles from saline and fixative-perfused animals were dissected and their weights measured on a laboratory scale. The cross section area and weight values were based on the average score of both hind-limbs.

2.5. Electromyography (EMG)

The CMAP (M-wave) and monosynaptic reflex (Hoffmann's reflex or H-reflex) were recorded from right gastrocnemius muscle on day 62 after BoNT-A treatment (prior to TeNT treatment) and on days 8 and 15 after TeNT. The EMG measurements were performed under general anaesthesia with ketamine/xylazine (70/7 mg/kg i.p.). Rats were placed in a prone position inside a narrow wooden box slightly elevated from the ground (5 cm) with tail and hind limbs protruding out. The stimulating 29 G stainless steel needle electrodes (Cat. #. MLA1203, AD Instruments, Oxford, UK) were inserted s.c. over the sciatic notch and mid-thigh femur. The recording needle electrode was inserted perpendicularly into the lateral gastrocnemius head belly to the depth that just penetrated the skin and entered the muscle. The reference electrode was inserted s.c. over the lateral malleolus, and the ground electrode was placed subcutaneously into the thoracolumbar back. Both stimulation and recording electrodes were connected to the two-channel extracellular amplifier (EXT-02B, NPI electronic GmbH, Germany) via two headstages. The recording of muscle potentials was performed in differential mode. Analog signals obtained from the amplifier were digitised via data acquisition unit (Micro1401-4, CED, UK) and then fed to a PC for both online visualisation and offline analysis using Spike2 software version 10 (CED, Cambridge, UK). The PC-controlled transistor–transistor logic signal pulses fed via the same acquisition unit switched one of the amplifier channels from recording to stimulation mode, and activated the stimulus isolator (ISO 01 D, NPI electronic, GmbH, Germany) to generate the 200 μs rectangular voltage pulses that were, in turn, redirected via amplifier and headstage to the stimulating electrodes. From the stimulated sciatic nerve trunk, orthodromic and antidromic depolarization waves travelling via myelinated fibres generated a short latency CMAP or M wave, and a delayed Hoffmann's or

H-reflex muscle activation evoked by monosynaptic activation of motoneurons by electrically stimulated Ia afferents. The maximal peak-to-peak amplitudes of M wave and H-reflex in mV (M_{max} and H_{max}) were measured by stimulation with increasing voltages. The H-reflex was confirmed by eliciting the rate-dependent depression by repeated pulse train (10 x, 4 Hz, delivered at voltage that elicits H_{max}). Mean H_{max} and M_{max} were determined based on 3 independent waveforms generated with at least 5 s delay between the pulses (Matthews et al.,2014; Ho and Waite, 2002).

2.6. Immunohistochemistry

At the end of the experiment, animals were deeply anaesthetised with ketamine/xylazine and killed by transcardial perfusion with physiological saline (400-500 ml), followed by 250 ml 4% paraformaldehyde fixative. Left and right gastrocnemius, soleus and spinal cord were excised. All tissues were post-fixed and cryoprotected overnight in 15 % sucrose with fixative, and the next day transferred to 30 % sucrose in 1 x phosphate buffered saline (PBS). After the tissue sank it was further stored at -80 ºC. Spinal cords were cut in cryostat at 35 µm thick slices and transferred to free floating wells for immunohistochemistry, while muscles were cut at 20 µm slice thickness and immediately transferred to glass adhesion slides (Super Frost Plus Gold, Thermo Scientific, Waltham, USA), kept at -20 ºC. Spinal cord slices were washed with PBS and incubated with 3 % H_2O_2 for inhibition of endogenous peroxidase. Then the slices were washed again, followed by blocking with 10 % normal goat serum (NGS), and incubated overnight at room temperature with non-affinity purified rabbit polyclonal antibody recognizing the BoNT-A-cleaved SNAP-25 fragment (SNAP-25$_{197}$; 1:8000, National Institute for Biological Standards and Control, Potters Bar, UK) validated in previous studies (Ekong et al., 1997; Jones et al., 2008). Next day the tissue was incubated with HRP-polyconjugated (polyHRP) goat anti rabbit secondary antibody (Tyramide SuperBoost Kit B40923/Invitrogen), and then with tyramide Atto-488 HRP substrate prepared as described previously (Homolak et al., 2022), for 10 minutes. After that, the slices were washed, mounted on glass slides and coverslipped with anti-fading agent. For colocalization

analyses the slices were incubated overnight with different primary antibodies (Table1.). After overnight incubation, the slices were washed and then incubated for 2 hours with Alexa 555 secondary antibody (Table1.) diluted in 1% NGS and PBS with 0.25% triton X-100 (PBST), and later mounted on glass as previously stated. The fluorescent microphotographs were taken at constant exposure time at 40x magnification by employing Olympus BX-51 microscope coupled to DP-70 digital camera, and CellSens Dimension visualisation and quantification software (Olympus, Tokyo, Japan). The unprocessed green channel images were converted to grayscale, and the ventral horn cSNAP-25 immunoreactivity was quantified as an average pixel-thresholded area (pixel intensity 100-256) in 6 non-overlapping visual fields per each L4 coronal section (6 x 0.14 mm^2 total analysed area per slice). This was performed in 4 randomly chosen L4 coronal spinal cord slices per each animal as previously described (Matak 2020). The confocal imaging of stained spinal cord slices at level of ventral horn to evaluate colocalization was done with Olympus FV3000 microscope and a 60× oil-immersion objective (UplanSApo, NA1.35, Olympus, Tokyo, Japan) using FV10-ASW software with 5 X scan zoom at a resolution of 1024×1024 pixels. Signal bleed-through was minimised by adjusting the excitation line of laser, power intensity, and emission range chosen independently for each fluorophore and different samples. The Fiji software was used for raw picture processing without altering the intensity of the signal. The representative images shown in figures were processed for brightness and contrast in Adobe Photoshop (Adobe Systems, San Jose, CA, USA). Muscle slices on glass were washed by PBST and blocked in 10% NGS. Incubation with anti BoNT-A-cleaved SNAP-25 (1:4000, diluted in 1% NGS and PBST) was carried out overnight at room temperature, followed next day by 1:400-500 goat anti-rabbit Alexa 555 secondary antibody (Cell Signalling, Danvers, USA), and coverslipped with anti-fading agent. Semi-quantification of the cleaved SNAP-25 was performed as previously described (Šoštarić et al., 2022; Perier et al., 2021). Briefly, in muscle slices from each animal, 4 visual fields from 4 different slices were chosen and scored (0-4) based on presence and abundance of clSNAP-25 in NMJs, nerve terminals and axons (Supplementary file S1).

Table 1. The list of primary and secondary antibodies used in the immunofluorescent colocalization stainings, with dilutions and incubation conditions.

Primary antibody	dilution	incubation temperature and period	catalog no/company	host species
anti-ChAT monoclonal	1:2500	4 °C overnight	AMAB91130/Atlas Antibodies	mouse
anti-SV2C [a] clone 4C8.1 monoclonal	1:1000	4 °C overnight	MABN367/Milipore	mouse
anti-K$_v$2.1.[b] monoclonal	1:1000	4 °C overnight	ab192761/Abcam	mouse
anti-Synaptophysin monoclonal	1:1000	4 °C overnight	S5678/Sigma Aldrich	mouse
anti-Vglut1[c] polyclonal	1:5000	4 °C overnight	135304/Synaptic Systems	guinea pig
secondary antibody				
anti-rabbit polyHRP[d]	undiluted	room temperature, 1 h	B40923/Invitrogen (from Tyramide SuperBoost Kit)	goat
anti-mouse IgG Fab2 Alexa Fluor 555	1:400-1:500	room temperature, 2 h	4490S/CellSignaling Technology	goat
anti-guinea pig IgG H&L Alexa Fluor 555	1:400	room temperature, 2 h	ab150186 /abcam	goat

anti-rabbit IgG Fab2 Alexa Fluor 555	1:400	room temperature, 2 h	4413S/CellSignaling Technology	goat

[a]synaptic vesicle protein 2 C, [b] potassium voltage channel $K_v2.1.$, [c] vesicular glutamate transporter 1, [d]horseradish peroxidase-polyconjugated

2.7. Statistical analysis

Results are presented as mean ± SEM and analysed by two-way ANOVA for repeated measurements, followed by Bonferroni's multiple post hoc test ($P<0.05$ considered significant) for between-group comparisons. The non-parametric ANOVA (Kruskal Vallis) and Dunn's post hoc were employed for statistical analysis of non-normally distributed Csnap-25 immunoreactive area (median ± range with $P<0.05$ considered significant). Single measurement of gastrocnemius and soleus muscle weight was analysed by one-way ANOVA followed by Bonferroni's multiple comparison test.

The number of animals per treatment group determination was performed according to *a priori* power analysis performed with G*power software version 3.1. (University of Düsseldorf, Germany) based on estimated effect size F=0.4, α error probability = 0.05, power (1-β) = 0.9, statistical test: ANOVA: repeated measures, within-between interaction (Šoštarić et al., 2022; Charan and Kantharia, 2013). In addition, we extended the group size from 6 to 8 to account for possible attrition of animals during the experiment.

3. Results

Presently, to assess the BoNT-A actions on central locomotor circuits, we characterised its trans-synaptic effect on normal motor performance involving coordinated use of hind limbs. An optimised method to study its central effects includes BoNT-A injection into the peripheral sciatic nerve trunk that, in contrast to i.m. injection, avoids the masking of the central toxin action (Matak 2020). The participation of central toxin effect through its action on second order central synapses was assessed by combining the BoNT-A treatment with

subsequent intrathecal lumbar injection of equine BoNT-A-neutralising antitoxin to prevent the central transcytosis, as previously reported (Matak 2020).

3.1. Lasting impairment of motor coordination and performance is mediated by transcytosis-dependent central action of BoNT-A

Firstly, we examined the effect of BoNT-A on fine motor coordination and balance by employing beam walking and rotarod tests. Prior to BoNT-A i.n. injection, the animals were pre-trained to traverse swiftly across the narrow beam and maintain balance on the rotating rod during the maximal trial duration. The animals injected i.n. with saline and i.t. with horse serum did not show signs of motor impairment after surgeries, suggesting the lack of effect due to control treatments and i.n. or i.t. injection procedures itself. Animals treated with i.n. BoNT-A (+ horse serum i.t.) approximately doubled the transit time across the narrow beam at day 3 after the toxin injection. The performance started to recover gradually after day 7, and returned to normal pretreatment values by day 28-35 (figure 2A). The BoNT-A also induced a prominent impairment of the animals' ability to maintain the balance on the rotarod (reduced latency to fall) which peaked between day 7-14 and thereafter started to recover gradually, yet never fully by day 56 (figure 2B). Prevention of spinal toxin transcytosis by intrathecal lumbar injection of BoNT-A-neutralizing antitoxin prevented the motor deficits evoked by i.n. BoNT-A in both of these motor performance tests. Animals injected with i.n. BoNT-A in combination with the i.t. antitoxin exhibited a very mild deficit in the rotarod performance by day 3, which subsequently recovered, and did not display any apparent deficit in the beam transit time at any experimental time point (figure 2).

To account for the possible effect of the BoNT-A on motor activity involving intense motoneuronal activation, we examined its effect on swimming performance. Swimming as a high-output motor task, is dependent on cholinergic modulation mediated by C-boutons, synapses responsible for alterations in motoneuron firing rate (Zagoraiou et al., 2009; Konsolaki et al., 2020). We found that i.n. BoNT-A significantly reduces mean (figure 2C) and maximal swimming velocities (figure 2D), which recovered by day 36 post toxin treatment.

Again, the toxin-mediated swimming velocity reduction was fully prevented by the i.t. antitoxin (figure 2C, figure 2D).

Figure 2.

In addition to motor performance tests, we examined the hind paw appearance suggestive of localised muscle weakness during reflex toe spread and gait. The rats showed mild impairment of the toe-spreading reflex (DAS ≈ 1) that quickly recovered by day 21 (figure 3A). The BoNT-A i.n. treatment reduced the functional use of hindlimbs and markedly changed the appearance of hind paws during stance. The hind paws exhibited arch-like appearance of foot soles and toes, and the heel-supported weight bearing, indicative of the weakness of paw plantar flexors (figure 3B) Moreover, the animals were unable to perform a normal foot propulsion during terminal stance by using interdigital paw pads and toes. This resulted in reduced combined gait ability score (sum of scores from five different parameters ranging from 0-10) used to evaluate voluntary motor function. The antitoxin-treated animals also exhibited a reduced gait ability following i.n. BoNT-A, however, with milder impairment and accelerated recovery of motor function (figure 3B).

Figure 3.

3.2. The BoNT-A induces muscle atrophy independent of its central action

We further assessed the i.n. BoNT-A effect on measurable signs of muscular atrophy by monitoring the calf diameter throughout the experiment and by measuring muscle weights at the end of experiment. We observed a significant reduction of the estimated mid-calf cross-section area of BoNT-A-treated hind limbs (figure 4A), as well as the final gastrocnemius muscle weight (figure 4B). Seemingly, the BoNT-A + antitoxin - treated animals showed slightly lower reduction of estimated cross section area (figure 4A), however, the reduction of the gastrocnemius muscle weight by i.n. BoNT-A was not dependent on the toxin central transcytosis (figure 4B). In contrast to gastrocnemius, there was no observable difference of the soleus muscle weight between the experimental groups (figure 4C). Changes in muscle

size were not accompanied by significant changes in animal body weight throughout the experiment, eliminating possible systemic effect of i.n. BoNT-A (figure 4D).

Figure 4.

3.3. Axonally transported and transcytosed BoNT-A reduces local spastic paralysis without altering the exaggerated monosynaptic H-reflex

After the recovery of major motor functions roughly two months after BoNT-A injection, we examined the persistence of its antispastic action by using TeNT-evoked disinhibition of motoneuronal inhibitory control. The BBB locomotor scale, which is used to evaluate locomotor recovery after different spinal cord injuries, was used to assess the functional use of limbs during locomotion on a flat surface. Animals' locomotion and lower limb movement was monitored and evaluated with scores (with 21 rating highest and validating normal locomotion, to 0 rating the lowest and describing no observable movement of the limb) (Basso et al., 1995). Starting from day 3 after TeNT, control animals treated with saline developed a prominent spastic paralysis of the injected right hindlimb, manifested as the leg rigid extension and inability to fully flex the joint. The locomotor impairment, evident as sweeping of affected hind limb against the table surface without weight support or plantar stepping during locomotion, resulted in markedly reduced BBB score. The i.n. BoNT-A reduced the dorsiflexion resistance from days 3-15 (figure 5C) and partly counteracted the locomotor impairment on day 15 post TeNT, showing improved use of plantar hind paw surface and weight bearing scoring higher on the BBB scale (figure 5A, figure 5D) The beneficial BoNT-A action was prevented in the i.t. antitoxin-treated rats, evident as high passive resistance during dorsiflexion test (figure 5C) and impaired locomotor score similar to saline-treated animals (figure 5B and figure 5D).

Figure 5.

In addition to behavioural assessment, we employed EMG to examine possible BoNT-A effects on monosynaptic H reflex transmitted by central synapse between Ia afferents and

motoneurons, evoked by subcutaneous electrical stimulation over the sciatic nerve. As previously shown (Matthews et al., 2014), the i.m. TeNT induced a large increase of H_{max} amplitude peaking on day 8 post injection in all experimental groups. Interestingly, the H-reflex excitability started to recover faster than the leg spasm intensity or locomotor deficit by day 15 post TeNT, suggesting that the sustenance of TeNT-evoked muscle spasm (figure 5) is not associated with persistence of overactive monosynaptic reflex. We found that i.n. BoNT-A reduced the maximal amplitude of M-wave and H-reflex prior to, and on day 8 post TeNT with no apparent difference with the antitoxin treatment (figure 6A, figure 6B). However, when the H-reflex amplitude was corrected for the size of M_{max} and the muscle weight, the effect of the BoNT-A was not significantly different compared to controls (figure 6C, figure 6D), indicating the lack of BoNT-A effects on monosynaptic reflex excitability. In accordance, we observed lack of colocalization of BoNT-A-cleaved SNAP-25 with VGlut1 isoform of the glutamate transporter figure 6E), suggesting the lack of direct toxin effect on the central afferent terminal of Ia primary afferents involved in the monosynaptic stretch reflex.

Figure 6.

3.4. The i.n. BoNT-A cleaves SNAP-25 in peripheral motor terminals and central second order synapses

At the end of the experiment (day 78) we examined the sites of BoNT-A enzymatic action by immunodetection of its enzymatic products in the periphery and CNS. In the gastrocnemius muscles of animals treated with BoNT-A we found cleaved SNAP-25 in neuromuscular junctions, nerve terminals and axons. Their relative abundance was not affected by the antitoxin treatment (figure 7A, figure 7C). On the other hand, the amount of cSNAP-25 in the ventral horn was reduced by the i.t. antitoxin (figure 7B, figure 7D), indicating central toxin transcytosis.

Figure 7.

In addition to VGlut1, we analysed the colocalization of the toxin enzymatic activity in relation to other synaptic markers and known toxin acceptors. We found that a portion of BoNT-A-cleaved SNAP-25 was present in ChAT-expressing neurons and contacted the $K_v2.1.$ immunoreactivity, suggesting that at least the fraction of toxin's central effect is associated with the C-boutons (figure 8A, figure 8B). In contrast to partial colocalization with ChAT, the majority of cleaved-SNAP-25-containing terminals colocalized with the BoNT-A nerve terminal protein acceptor SV2C and synaptic marker synaptophysin (figure 8C, figure 8D). Apparently, both SV2C and synaptophysin were present in higher number of cSNAP-25-immunopositive terminals in comparison to the ChAT and $K_v2.1.$, suggesting that different types of nerve terminals, including both cholinergic and non-cholinergic, are susceptible to BoNT-A enzymatic activity following its axonal transport and transcytosis.

Figure 8.

4. Discussion

Intramuscular BoNT-A is a standard treatment for different movement disorders characterised by sustained or intermittent muscle hyperactivity. The currently dominant opinion is that BoNT-A actions in hyperkinetic/hypertonic muscle result from direct toxin's action on extrafusal plus either direct or indirect modulation of intrafusal muscle terminals, followed by indirect plastic changes in the CNS (Rosales and Dressler, 2010; Hallet 2018). In the rat motor system, as previously mentioned, we found that the toxin transcytosis at spinal cord level participates in the lasting reduction of TeNT-evoked local spasm (Matak 2020; Šoštarić et al., 2022). Though its peripheral action is well described at the level of extrafusal neuromuscular junction, a general picture of all the possible sites of BoNT-A actions at multiple levels of motor processing is still lacking. In addition, it remains so far unknown if the central toxin action affects different spinal synapses as vital elements of circuits involved in normal locomotion.

To address this later question, we studied the behavioural actions of BoNT-A on motor tasks involving multiple muscle groups on both hindlimbs. The BoNT-A was injected bilaterally

into the sciatic nerve trunk at mid-thigh level to affect all the motor units of the lower leg and foot (indirectly innervated by sciatic nerve via common peroneal and tibial nerve) by anterograde and retrograde axonal transport (Antonucci et al., 2008; Restani et al., 2011). We then examined the effect of BoNT-A on fine motor coordination and balance in skilled motor performance tasks involving simultaneous bilateral use of multiple muscle groups with quick alternations of contractions of flexors and extensors. The BoNT-A bilateral injection into the sciatic nerves markedly reduced the motor performance in both tasks (figure 2A, figure 2B), with faster recovery of the beam walk performance by day 28 in comparison to rotarod performance incomplete recovery (examined up to day 56). In contrast to bilateral i.n. BoNT-A, unilateral i.n. BoNT-A induces only mild impairment in the beamwalk performance, and no observable impairment in the rotarod latency (Matak 2020), suggesting the compensation of motor deficits by the untreated contralateral limb in mentioned motor tasks. In addition to neuromuscular coordination we monitored the development of classical signs of local muscle weakness by assessing the reflex digit abduction and paw appearance during gait. The animals developed very mild toe-spreading reflex deficit (DAS ≈ 1 out of maximal 4 normally observed for the same toxin dose injected i.m.) that quickly recovered within 14 days after BoNT-A treatment (figure 3A). Other signs of muscle weakness such as the arched position of hind paws during motor activities like sitting, bipedal stance or climbing measured by combined „gait ability" score (Brent et al., 2020; Warner et al., 2006) suggested lasting weakness of plantar flexors that support the body weight and mediate the limb propulsion during the terminal stance (figure 3B). Mentioned impairment took longer to recover compared to DAS with recovery time-course comparable to rotarod.

We assessed the role of central transcytosis-dependent toxin activity by employing the BoNT-A-specific antitoxin injection into the spinal canal at the level of cauda equina 24 h after i.n. toxin injection. In all the aforementioned motor tests or functional outcomes, the BoNT-A-evoked motor deficits were either prevented or reduced in intensity and duration in rats injected with i.t. antitoxin (figure 2, figure 3). This suggests that BoNT-A trans-synaptic

activity in second order spinal synapses, in concert with peripheral toxin action, affects motor performance in different tests and contributes to local muscle weakness. Consistent with the dual site of toxin action, we found that cSNAP-25 occurred both peripherally and centrally, with only the central enzymatic activity being dependent on the toxin transcytosis (figure 7). On the other hand, calf muscle weight and CMAP reduction occurred at similar intensity in all toxin-treated animals, suggesting a peripheral toxin action as the main driver of muscle atrophy and residual effect on NMJ transmission (figure 4B, figure 6A). In contrast to gastrocnemius, the dominantly slow-twitch fibre soleus muscle did not show atrophy, indicating possible faster recovery of this type of muscle (figure 4C).

After assessment of locomotor recovery, in the same animals we additionally examined if BoNT-A may induce central modulation of exaggerated monosynaptic stretch reflex that is clinically observed in spasticity (Rosales and Dressler, 2010; Stampacchia et al., 2004), with TeNT-evoked unilateral spasm used as a convenient model of neuromuscular spasticity of central origin (Megighian et al., 2021). We observed that BoNT-A retained the ability to reduce the TeNT-evoked calf spasm on days 65-77 despite all peripheral motor parameters being substantially or completely recovered by day 56. This effect was, again, found to be dependent on BoNT-A central trans-synaptic effect (figure 5). In contrast to BoNT-A-mediated reduction of spasm and locomotor deficit, the effect of BoNT-A on the monosynaptic reflex excitability (assessed by H_{max} / M_{max} ratio) was not significant, both prior to and after TeNT-evoked spasticity (figure 6C) and in line with a lack of cleaved SNAP-25 colocalization with large synaptic terminals positive for VGlut1, the marker of Ia terminals (Rotterman et al., 2014) (figure 6E). This suggests lack of BoNT-A central activity on the synaptic strength between Ia central afferent terminals and motoneurons, in line with previous clinical studies reporting the lack of BoNT-A on the H/M ratio (Priori et al., 1995; Modugno et al., 1998; Phadke et al., 2013; Manca et al., 2010). However, H-reflex induction by peripheral nerve electrical stimulation bypasses the normal stretch reflex initiation at muscle spindles, thus, not assessing possible BoNT-A direct or indirect actions at peripheral intrafusal terminals. Nevertheless, our findings

show that normalisation of experimental spasm involves central trans-synaptic action of the toxin, thus, indicating a more complex mechanism of BoNT-A action other than stretch reflex direct modulation.

To further address the possible sites of BoNT-A action in the CNS we performed colocalization of cleaved SNAP-25 with additional neuronal markers. It was observed that BoNT-A may enzymatically cleave the SNAP-25 in ChAT- and VAChT-expressing cholinergic terminals (Matak et al., 2012; Caleo et al., 2018; Cai et al., 2017), with comparably higher selectivity for cholinergic synapses compared to other types (Caleo et al., 2018), suggesting its possible trans-synaptic effect on C-boutons synapsing with motoneuronal cell bodies. This premotor input derived from $V0_C$ interneurons supports the motoneuronal firing in demanding motor tasks such as swimming (Zagoraiou et al., 2009). In accordance, we found that BoNT-A impairs the swimming velocity (Figure 3), and that a fraction of cSNAP-25-containing terminals expressed ChAT or contacted the $K_v2.1$-expressing postsynaptic sites typically associated with C-boutons (figure 8A, figure 8B). Yet, the occurrence of cSNAP-25 in comparably more numerous SV2C- and synaptophysin-expressing terminals (figure 8C, figure 8D) suggests toxin transcytosis to additional non-cholinergic central synapses that possess the main protein acceptor for BoNT-A (Verderio et al., 2007) and the synaptic neurotransmitter release machinery (Figure 9). The BoNT-A action within different premotor neurons is also in line with behavioural effect on other examined motor functions besides swimming. Interestingly, genetic ablation of cholinergic C boutons does not affect the rotarod performance in mice (Konsolaki et al., 2020), suggesting that BoNT-A action in C-boutons cannot explain the reduction of rotarod performance observed here. In support of its action in other central excitatory synapses, BoNT-A preferentially inhibits the release of glutamate in comparison to GABA in isolated hippocampal synaptosomes (Mahrhold et al., 2006). Apart from neurotransmitter release, BoNT-A may alter other SNAP-25-mediated functions in synaptic and extrasynaptic sites, e.g. Ca^{2+} dynamics mediated by SNAP-25 interactions with synaptotagmin, presynaptic voltage-gated Ca^{2+} channels and G proteins (Pozzi et al., 2019) ,

as well as the translocation of membrane proteins and channels (Shimizu et al., 2012). These complex actions might be associated with net balance in favour of reduction of premotor neuronal network activity. These effects are likely to contribute to desirable restoration of muscle control in disinhibited motor circuits in movement disorders or spasticity (Liu et al., 2015; Bellardita et al., 2017; Pocratsky et al., 2023).

Figure 9.

Some of the cleaved SNAP-25 may be present in recurrent axonal collaterals due to BoNT-A axonal transport without trans-synaptic transport, since the toxin would not necessarily need to exit and re-enter the motoneuron from extracellular fluid (and be neutralized by antitoxin). Our experiments do not exclude this option, however, given the specific role of recurrent collaterals only partially contributing to activation of Renshaw cells in recurrent and reciprocal inhibition, the central BoNT/A behavioral actions on many locomotor functions and TeNT-evoked spasm (evoked by TeNT affecting different types of inhibitory interneurons along Renshaw cells), preventable by antitoxin, likely cannot be explained exclusively by such action.

In spastic or dystonic limb/regions, targeting different muscles is assumed to be the only feasible mode of BoNT-A injection. Herein we show that toxin injection into the peripheral nerve enables simultaneous targeting of different muscles at peripheral and spinal synaptic sites relevant for their neuromotor control. The characterization of antero-retrograde effects of the toxin substantiates that the effect is similar to i.m. injection, with the advantage that the i.n. injection mode avoids the initial full paralysis due to BoNT-A entry at the NMJ. Nonetheless, it attenuates muscle hyperactivity for a long time. This better approximates the clinical observations that BoNT-A-mediated benefit is not necessarily accompanied by prominent muscle paralysis (Hallet 2018). The i.n. mode of toxin delivery might complement the muscular toxin injections employed clinically. Toxin application by existing nerve block techniques that avoid the nerve injury (Jeng and Rosenblatt , 2011) might provide an alternative way to target regional muscle groups innervated by the common nerve/nerve branches. In addition, it may

complement already existing nerve block techniques with general anaesthetics or neurolytic agents aimed at spasticity management (Picelli et al., 2023). Interestingly, case studies reported successful BoNT-A intra- or peri-nerve application in chronic pain patients (Ryu et al., 2019; Mercado et al., 2023). The studies showed no apparent signs of nerve injury occurring after BoNT-A i.n. injections (Matak 2020; Bach-Rojecky and Lacković, 2009; Mercado et al., 2023; Lu et al., 1998).

In comparison to human subjects, it is important to note that a limiting factor in this study is that the research was exclusively conducted on male rats to achieve more uniform weight and dosing. In addition, the crude measurements of muscle weight and cross-section area as a measure of atrophy performed here cannot distinguish, specifically, the possibility that the restoration of muscle mass, normal movement and force may be attributed to hypertrophy in some fibers, while others may not exhibit similar improvements.

5. Conclusion

Up to now, BoNT-A local muscular neuroparalytic effects have been regarded as its only physiological correlate of therapeutically desirable effect in spasticity and movement disorders [26]. Present study shows that its actions affect the gait and motor functions on both peripheral and central level. Further, our behavioural and colocalization studies suggest that BoNT-A activity in the ventral horn does not necessarily restrict to a single-type synapse, but rather to interplay between different central circuits involved in normal locomotion and involuntary hyperactive movement.

role in study design; collection, analysis and interpretation of data, writing and decision to submit the article.

AUTHOR CONTRIBUTIONS

IM: Conception and design of the study; PŠ, MM, DV, ŽLV, MP, MC, IM: Acquisition and analysis of the data; PŠ, IM: Draft of the manuscript and figures; All authors revised and approved the final manuscript.

ADDITIONAL INFORMATION

Conflict of interests: The authors declare no conflict of interests.

REFERENCES

Anandan C, Jankovic J. Botulinum toxin in movement disorders: An update. Toxins. 2021;13:42. doi: 10.3390/toxins13010042.

Antonucci F, Rossi C, Gianfranceschi L, Rossetto O, Caleo M. Long-distance retrograde effects of botulinum neurotoxin A. J Neurosci. 2008; 28: 3689–96. doi: 10.1523/JNEUROSCI.0375-08.2008

Aymard C, Giboin LS, Lackmy-Vallée A, Marchand-Pauvert V. Spinal plasticity in stroke patients after botulinum neurotoxin A injection in ankle plantar flexors. Physiol Rep. 2013; 1:e00173. doi: 10.1002/phy2.173.

Bach-Rojecky L, Lacković Z. Central origin of the antinociceptive action of botulinum toxin type A. Pharmacol Biochem Behav. 2009; 94:234–8. doi:10.1016/j.pbb.2009.08.012.

Basso DM, Beattie MS, Bresnahan JC. A sensitive and reliable locomotor rating scale for open field testing in rats. J Neurotrauma. 1995; 12:1–21. doi:10.1089/neu.1995.12.1.

Bellardita C, Caggiano V, Leiras R, Caldeira V, Fuchs A, Bouvier J, Löw P, Kiehn O. Spatiotemporal correlation of spinal network dynamics underlying spasms in chronic spinalized mice. Elife. 2017;6:e23011. doi: 10.7554/eLife.23011.

Brent MB, Lodberg A, Thomsen JS, Brüel A. Rodent model of disuse-induced bone loss by hind limb injection with botulinum toxin A. MethodsX. 2020; 7:101079. doi: 10.1016/j.mex.2020.101079.

Broide R, Rubino J, GS Nicholson, Ardila M, Brown M, Aoki K, et al. The rat Digit Abduction Score (DAS) assay: a physiological model for assessing botulinum

neurotoxin-induced skeletal muscle paralysis. Toxicon. 2013; 71:18–24. doi: 10.1016/j.toxicon.2013.05.004.

Brooks VB, Curtis DR, Eccles JC. The action of tetanus toxin on the inhibition of motoneurones. J Physiol. 1957; 135:655–72. doi: 10.1113/jphysiol.1957.sp005737.

Cai BB, Francis J, Brin MF, Broide RS. Botulinum neurotoxin type A-cleaved SNAP25 is confined to primary motor neurons and localized on the plasma membrane following intramuscular toxin injection. Neuroscience. 2017; 352:155–69. doi: 10.1016/j.neuroscience.2017.03.049.

Caleo M, Mazzocchio R. Direct Central Nervous System Effects of Botulinum Neurotoxin. From Dressler D; Altenmüller E, Krauss Joachim K. (2018). Treatment of Dystonia. Publisher: Cambridge University Press, pp. 111–114. doi:10.1017/9781316459324.025

Caleo M, Spinelli M, Colosimo F, Matak I, Rossetto O, Lackovic Z, et al. Transynaptic action of botulinum neurotoxin type A at central cholinergic boutons. J Neurosci. 2018; 38:10329–37. doi: 10.1523/JNEUROSCI.0294-18.2018.

Carter RJ, Morton J, Dunnett SB. Motor coordination and balance in rodents. Curr Protoc Neurosci. 2001;Chapter 8. doi: 10.1002/0471142301.ns0812s15. doi: 10.1002/0471142301.ns0812s15.

Charan J, Kantharia ND. How to calculate sample size in animal studies? J Pharmacol Pharmacother. 2013; 4:303–6. doi: 10.4103/0976-500X.119726.

Ekong TAN, Feavers IM, Sesardic D. Recombinant SNAP-25 is an effective substrate for Clostridium botulinum type A toxin endopeptidase activity in vitro. Microbiol. 1997; 143:3337–47. doi: 10.1006/exnr.2002.8013.

Gracies JM. Physiological effects of botulinum toxin in spasticity. Mov Disord. 2004;19 Suppl 8:120-128. doi: 10.1002/mds.20065.

Gundersen CB. The effects of botulinum toxin on the synthesis, storage and release of acetylcholine. Prog Neurobiol. 1980; 14 (2-3):99-119. doi:10.1016/0301-0082(80)90019-2.

Hallett M. Mechanism of action of botulinum neurotoxin: Unexpected consequences. Toxicon. 2018;147:73–6. doi: 10.1016/j.toxicon.2017.08.011.

Ho SM, Waite PM. Effects of different anesthetics on the paired-pulse depression of the H reflex in adult rat. Exp Neurol. 2002; 177:494–502.

Homolak J, Babic Perhoc A, Knezovic A, Osmanovic Barilar J, Koc F, Stanton C, et al. Disbalance of the duodenal epithelial cell turnover and apoptosis accompanies insensitivity of intestinal redox homeostasis to inhibition of the brain glucose-dependent insulinotropic polypeptide receptors in a rat model of sporadic Alzheimer's disease. Neuroendocrinology. 2022; 112:744–62. doi: 10.1159/000519988.

Jankovic J. Botulinum toxin: State of the art. Mov Disord. 2017;32:1131–8. doi: 10.1002/mds.27072.

Jeng CL, Rosenblatt MA. Considerations When performing ultrasound-guided supraclavicular perineural catheter placement. J Ultrasound Med. 2011; 30:423–423. doi: 10.7863/jum.2011.30.3.423.

Jones RGA, Ochiai M, Liu Y, Ekong T, Sesardic D. Development of improved SNAP25 endopeptidase immuno-assays for botulinum type A and E toxins. J Immunol Methods. 2008; 329:92–101. doi: 10.1016/j.jim.2007.09.014.

Koizumi H, Goto S, Okita S, Morigaki R, Akaike N, Torii Y, et al. Spinal central effects of peripherally applied botulinum neurotoxin A in comparison between its subtypes A1 and A2. Front Neurol. 2014; 5:1–9. doi: 10.3389/fneur.2014.00098.

Konsolaki E, Koropouli E, Tsape E, Pothakos K, Zagoraiou L. Genetic inactivation of cholinergic C bouton output improves motor performance but not survival in a mouse

model of amyotrophic lateral sclerosis. Neuroscience. 2020 ; 450:71–80. doi: 10.1016/j.neuroscience.2020.07.047.

Laliberte AM, Goltash S, Lalonde NR, Bui TV. Propriospinal Neurons: Essential Elements of Locomotor Control in the Intact and Possibly the Injured Spinal Cord. Front Cell Neurosci. 2019 Nov 12;13:512. doi: 10.3389/fncel.2019.00512.

Li D, Mattoo P, Keller JE. New equine antitoxins to botulinum neurotoxins serotypes A and B. Biologicals. 2012; 40:240–6. doi: 10.1016/j.biologicals.2012.03.004.

Liu YB, Tewari A, Salameh J, Arystarkhova E, Hampton TG, Brashear A, Ozelius LJ, Khodakhah K, Sweadner KJ. A dystonia-like movement disorder with brain and spinal neuronal defects is caused by mutation of the mouse laminin β1 subunit, Lamb1. Elife. 2015 Dec 24;4:e11102.

Lu L, Atchabahian A, Mackinnon SE, Hunter DA. Nerve injection injury with botulinum toxin. Plast Reconstr Surg. 1998; 101:1875–80. doi:10.1097/00006534-199806000-00015.

Mahrhold S, Rummel A, Bigalke H, Davletov B, Binz T. The synaptic vesicle protein 2C mediates the uptake of botulinum neurotoxin A into phrenic nerves. FEBS Lett. 2006; 580:2011–4. doi: 10.1016/j.febslet.2006.02.074.

Manca M, Merlo A, Ferraresi G, Cavazza S, Marchi P. Botulinum toxin type A versus phenol. A clinical and neurophysiological study in the treatment of ankle clonus. Eur J Phys Rehabil Med. 2010; 46:11–8. PMID: 20332721

Marchand-Pauvert V, Aymard C, Giboin LS, Dominici F, Rossi A, Mazzocchio R. Beyond muscular effects: depression of spinal recurrent inhibition after botulinum neurotoxin A. J Physiol. 2013; 591:1017–29. doi: 10.1113/jphysiol.2012.239178.

Matak I, Lacković Z, Relja M. Botulinum toxin type A in motor nervous system: unexplained observations and new challenges. J Neural Transm (Vienna). 2016;123:1415-21, doi: 10.1007/s00702-016-1611-9.

Matak I, Lacković Z. Botulinum toxin A, brain and pain. Prog Neurobiol. 2014 Aug-Sep;119-120:39-59. doi: 10.1016/j.pneurobio.2014.06.001. PMID: 24915026.

Matak I, Riederer P, Lacković Z. Botulinum toxin's axonal transport from periphery to the spinal cord. Neurochem Int. 2012; 61:236–9. doi: 10.1016/j.neuint.2012.05.001

Matak I. Evidence for central antispastic effect of botulinum toxin type A. Br J Pharmacol. 2020; 177:65–76. doi: 10.1111/bph.14846.

Matthews CC, Fishman PS, Wittenberg GF, Matthews CC. Tetanus toxin reduces local and descending regulation of the H-reflex. Muscle Nerve. 2014; 49:495–501. doi: 10.1002/mus.23938.

Mazzocchio R, Caleo M. More than at the neuromuscular synapse: actions of botulinum neurotoxin A in the central nervous system. Neuroscientist. 2015 Feb;21(1):44-61. doi: 10.1177/1073858414524633. PMID: 24576870.

Megighian A, Pirazzini M, Fabris F, Rossetto O, Montecucco C. Tetanus and tetanus neurotoxin: From peripheral uptake to central nervous tissue targets. J Neurochem. 2021; 158:1244–53. doi: 10.1111/jnc.15330.

Mercado M del PA, Olea MS, Rodrigues AT, Morales KE, Ros JJL, Altinpulluk EY, et al. Intraneural injection of botulinum toxin-A in palliative care and unresponsive neuropathic pain. Asia Pac J Pain. 2023. In press:1–6. doi: 10.29760/APJP.202302/PP.0001

Modugno N, Priori A, Berardelli A, Vacca L, Mercuri B, Manfredi M. Botulinum toxin restores presynaptic inhibition of group Ia afferents in patients with essential tremor. Muscle Nerve. 1998; 21:1701–5. doi: 10.1093/brain/118.3.801.

Percie du Sert N, Hurst V, Ahluwalia A, Alam S, Avey MT, Baker M, et al. The ARRIVE guidelines 2.0: Updated guidelines for reporting animal research. PLoS Biol. 2020;18:e3000410. doi: 10.1371/journal.pbio.3000410.

Périer C, Martin V, Cornet S, Favre-Guilmard C, Rocher MN, Bindler J, et al. Recombinant botulinum neurotoxin serotype A1 in vivo characterization. Pharmacol Res Perspect. 2021; 9:e00857. doi: 10.1002/prp2.857.

Phadke CP, On AY, Kirazli Y, Ismail F, Boulias C. Intrafusal effects of botulinum toxin injections for spasticity: revisiting a previous paper. Neurosci Lett. 2013; 541:20–3. doi: 10.1016/j.neulet.2013.02.025.

Picelli A, Di Censo R, Zadra A, Faccioli S, Smania N, Filippetti M. Management of spastic equinovarus foot in children with cerebral palsy: An evaluation of anatomical landmarks for selective nerve blocks of the tibial nerve motor branches. J Rehabil Med. 2023; 55:jrm00370. doi: 10.2340/jrm.v55.4538.

Pirazzini M, Rossetto O, Eleopra R, Montecucco C. Botulinum neurotoxins: Biology, pharmacology, and toxicology. Pharmacol Rev. 2017; 69:200–35. doi:10.1124/pr.116.012658

Pocratsky AM, Nascimento F, Özyurt MG, White IJ, Sullivan R, O'Callaghan BJ, Smith CC, Surana S, Beato M, Brownstone RM. Pathophysiology of Dyt1-Tor1a dystonia in mice is mediated by spinal neural circuit dysfunction. Sci Transl Med. 2023; 15(694):eadg3904. doi: 10.1126/scitranslmed.adg3904.

Pozzi D, Corradini I, Matteoli M. The control of neuronal calcium homeostasis by SNAP-25 and its impact on neurotransmitter release. Neuroscience. 2019; 420:72–8. doi: 10.1016/j.neuroscience.2018.11.009.

Priori A, Berardelli A, Mercuri B, Manfredi M, Neurologiche S, La R, et al. Physiological effects produced by botulinum toxin treatment of upper limb dystonia. Changes in reciprocal inhibition between forearm muscles. Brain. 1995; 118:801–7. doi: 10.1093/brain/118.3.801.

Ramachandran R, Yaksh TL. Therapeutic use of botulinum toxin in migraine: mechanisms of action. Br J Pharmacol. 2014 Sep;171(18):4177-92. doi: 10.1111/bph.12763. PMID: 24819339; PMCID: PMC4241086.

Ramirez-Castaneda J, Jankovic J, Comella C, Dashtipour K, Fernandez HH, Mari Z. Diffusion, spread, and migration of botulinum toxin. Mov Disord. 2013 Nov;28(13):1775-83. doi: 10.1002/mds.25582. Epub 2013 Jul 18. PMID: 23868503.

Restani L, Antonucci F, Gianfranceschi L, Rossi C, Rossetto O, Caleo M. Evidence for anterograde transport and transcytosis of botulinum neurotoxin A (BoNT/A). J Neurosci. 2011; 31:15650–9. doi: 10.1523/JNEUROSCI.2618-11.2011.

Restani L, Novelli E, Bottari D, Leone P, Barone I, Galli-Resta L, et al. Botulinum neurotoxin A impairs neurotransmission following retrograde transynaptic transport. Traffic. 2012; 13:1083–9. doi: 10.1111/j.1600-0854.2012.01369.x.

Rosales RL, Dressler D. On muscle spindles, dystonia and botulinum toxin. Eur J Neurol. 2010;17 Suppl 1:71-80. doi: 10.1111/j.1468-1331.2010.03056.x. PMID: 20590812.

Rossetto O, Montecucco C. Tables of toxicity of botulinum and tetanus neurotoxins. Toxins. 2019; 11:686. doi: 10.3390/toxins11120686.

Rossetto O, Pirazzini M, Montecucco C. Botulinum neurotoxins: Genetic, structural and mechanistic insights. Nat Rev Microbiol. 2014;12:535–49. doi: 10.1038/nrmicro3295.

Rotterman TM, Nardelli P, Cope TC, Alvarez FJ. Normal distribution of VGLUT1 synapses on spinal motoneuron dendrites and their reorganization after nerve injury. J Neurosci. 2014;34:3475–92. doi: 10.1523/JNEUROSCI.4768-13.2014.

Ryu JH, Shim JH, Yeom JH, Shin WJ, Cho SY, Jeon WJ. Ultrasound-guided greater occipital nerve block with botulinum toxin for patients with chronic headache in the

occipital area: a randomized controlled trial. Korean J Anesthesiol. 2019; 72:479–85. doi: 10.4097/kja.19145.

Schiavo G, Santucci A, Dasgupta BR, Mehta PP, Jontes J, Benfenati F, et al. Botulinum neurotoxins serotypes A and E cleave SNAP-25 at distinct COOH-terminal peptide bonds. FEBS Lett. 1993; 335:99–103. doi: 10.1016/0014-5793(93)80448-4.

Shimizu T, Shibata M, Toriumi H, Iwashita T, Funakubo M, Sato H, et al. Reduction of TRPV1 expression in the trigeminal system by botulinum neurotoxin type-A. Neurobiol Dis. 2012; 48:367–78. doi: 10.1016/j.nbd.2012.07.010.

Stampacchia G, Bradaschia E, Rossi B. Change of stretch reflex threshold in spasticity: effect of botulinum toxin injections. Arch Ital Biol. 2004; 142:265–73. Doi: 10.4449/aib.v142i3.375

Šoštarić P, Vukić B, Tomašić L, Matak I. Lasting peripheral and central effects of botulinum toxin type A on experimental muscle hypertonia in rats. Int J Mol Sci. 2022; 23:11626. doi: 10.3390/ijms231911626.

Verderio C, Grumelli C, Raiteri L, Coco S, Paluzzi S, Caccin P, et al. Traffic of botulinum toxins A and E in excitatory and inhibitory neurons. Traffic. 2007; 8:142-53. doi: 10.1111/j.1600-0854.2006.00520.x.

Vinti M, Costantino F, Bayle N, Simpson DM, Weisz DJ, Gracies JM. Spastic cocontraction in hemiparesis: Effects of botulinum toxin. Muscle Nerve. 2012;46:917–25. doi: 10.1002/mus.23427.

Warner SE, Sanford DA, Becker BA, Bain SD, Srinivasan S, Gross TS. Botox induced muscle paralysis rapidly degrades bone. Bone. 2006; 38:257–64. doi:10.1016/j.bone.2005.08.009.

Weise D, Weise CM, Naumann M. Central effects of botulinum neurotoxin—evidence from human studies. Toxins. 2019 Jan 1;11:21 doi: 10.3390/toxins11010021.

Zagoraiou L, Akay T, Martin JF, Brownstone RM, Jessell TM, Miles GB. A cluster of cholinergic premotor interneurons modulates mouse locomotor activity. Neuron. 2009; 64:645–62. doi: 10.1016/j.neuron.2009.10.017.

FIGURE LEGENDS

Figure 1. The time course and schematic representation of experimental treatments with bilateral intraneural (i.n.) botulinum toxin type A (BoNT-A), i.t. BoNT-A-neutralising antitoxin and unilateral i.m. tetanus toxin (TeNT), and functional behavioural motor testing in rats. The numbers above the timeline indicate experimental days following the i.n. BoNT-A treatment. H-reflex; Hoffmann's monosynaptic reflex; BBB, Basso Beattie Bresnahan locomotor scale. The figure was created with Biorender.com (*accessed on 22/09/2023*).

Figure 2. Botulinum toxin type A (BoNT-A) reduces the performance in motor coordination assays and swimming velocity dependently on its central trans-synaptic action. Spinal i.t. injection of BoNT-A-neutralizing antitoxin (5 iu) prevents the bilateral intraneural (i.n.) BoNT-A (2 U per sciatic nerve)-mediated impairment in beam walking A.) and rotarod B.) performances (evaluated by latency times) and reduces C.) mean swimming velocity and D.) maximal swimming velocity. N = 8 animals/ group; mean ± SEM, *,**,*** - $P < 0.05, 0.01, 0.001$ vs saline + horse serum; +, ++, +++ - $P < 0.05, 0.01, 0.001$ vs BoNT-A + horse serum (two-way RM ANOVA followed by Bonferoni's post hoc).

Figure 3. Intrasciatic BoNT-A induces mild temporary digit abduction inability and long-term prominent gait impairment, dependently on its central trans-synaptic action. The effect of bilateral intraneural (i.n.) BoNT-A (2 U per sciatic nerve) was assessed in combination with BoNT-A-neutralising antitoxin (5 iu, i.t.) on toe spreading reflex (assessed by digit abduction score) (A. and B.) and gait ability (C. and D.). The appearance of hind paws from BoNT-A-treated rats show the inability to abduct all toes A.) and the arch-like hind paw appearance C.) with heel-supported weight bearing during bipedal stance (left vs right: saline + horse serum vs BoNT-A + horse serum). In graph B.), horizontal lines indicate the time points of BoNT-A and antitoxin treatments. N = 8 animals/ group; mean ± SEM, *,**,*** - $P < 0.05, 0.01, 0.001$ vs saline + horse serum; +, ++, +++ - $P < 0.05, 0.01, 0.001$ vs BoNT-A + horse serum (two-way RM ANOVA followed by Bonferroni's post hoc).

Figure 4. The i.n. BoNT-A induces non-recovering lower leg calf muscle atrophy. The graphs indicate A.) estimated lower leg cross section area during the experiment, and muscle weights of B.) gastrocnemius and C.) soleus on day 78 following i.n. BoNT-A (2 U per nerve) in combination with BoNT-A-specific antitoxin (5 iu). The effects of BoNT-A were unrelated to changes in total animal weight during the experiment D.). The leg cross section area was estimated as an ellipse area defined by dorsoventral and mediolateral diameter of the calf muscle (average of both legs). N = 8 animals/ group; mean ± SEM, *,**,*** - P < 0.05, 0.01, 0.001 vs saline + horse serum; + - P < 0.05 vs BoNT-A + horse serum (two-way RM ANOVA followed by Bonferroni's post hoc).

Figure 5. Lasting central antispastic activity of axonally transported BoNT-A. The intraneural (i.n.) BoNT-A (2 U per sciatic nerve) was administered in combination with BoNT-A-neutralising antitoxin (5 iu, i.t., 24 h post BoNT-A), and the spastic paralysis was evoked by i.m. tetanus toxin (TeNT) 1.5 ng injection into right gastrocnemius) on day 62 post BoNT-A. The photographs show the normal vs spastic hind-limb appearance of BoNT-A + horse serum A.) and BoNT-A + antitoxin-treated B.) animals on day 15 post TeNT. The spastic paralysis evoked by TeNT was quantified behaviourally by C.) resistance to ankle dorsiflexion and D.) Basso Beattie Bresnahan (BBB) locomotor scale. The vertical lines indicate the timepoint of TeNT treatment. N = 8 animals/ group; mean ± SEM,*** - P < 0.0015 vs saline + horse serum; ++,+++ - P < 0.01, 0.0015 vs BoNT-A + horse serum (two-way RM ANOVA followed by Bonferroni's post hoc).

Figure 6. Lack of BoNT-A action on the monosynaptic reflex excitability at the Ia central afferent synapse. The BoNT-A was injected into the sciatic nerve (2 U per nerve) in combination with intrathecal BoNT-A-neutralizing antitoxin. Electromyographic measurement of gastrocnemius CMAP was performed prior to tetanus toxin (TeNT, 1.5 ng i.m.), and after the development of TeNT-evoked local spasm by employing increasing voltage rectangular pulses (200 μs) delivered subcutaneously into the thigh over the sciatic nerve. The graphs A.)

and B.) show the effects of neurotoxins on peak to peak maximal M-wawe (M_{max}) and Hoffman or H-reflex (H_{max}) amplitudes, while C.) and D.) show the relation of H_{max} amplitude relative to M_{max}, and in relation to gastrocnemius muscle weight of individual rats, respectively. Each compound potential measurement is average of 3 maximal peak to peak amplitudes obtained during the measurement. $N = 8$ animals/ group; mean ± SEM, *,** - $P < 0.05$, 0.01 vs saline + horse serum (two-way RM ANOVA followed by Bonferroni's post hoc). In the L4 ventral horn of animals injected with i.n. BoNT-A, the BoNT-A-cleaved SNAP-25 (cSNAP-25) does not colocalize with vesicular glutamate transporter 1 (VGlut1) – the transporter isoform present in Ia muscle spindle primary afferents E.). The confocal microscope image represents a single optical slice (0.42 µm thickness) from confocal z-stack, representative from at least 3 different animals injected with i.n. BoNT-A + horse serum (scale bar = 20 µm).
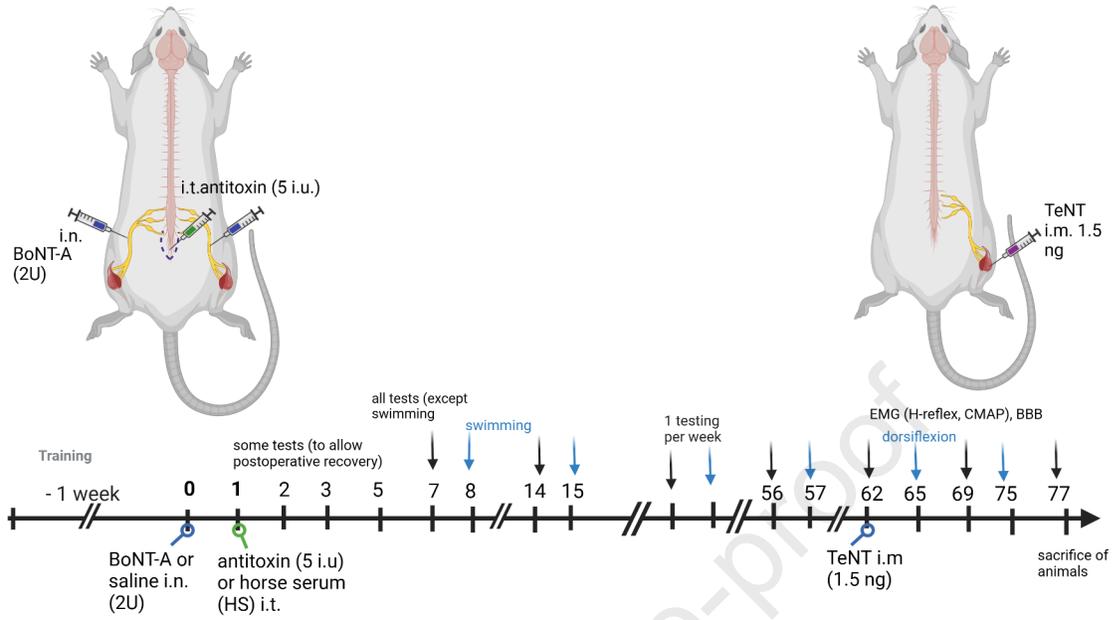
Figure 7. Peripheral and central enzymatic activity of axonally transported BoNT-A. The intraneural (i.n.) BoNT-A (2 U per sciatic nerve) was administered in combination with BoNT-A-neutralising antitoxin (5 iu, i.t., 24 h post BoNT-A), and the immunoreactivity of BoNT-A-cleaved synaptosomal associated protein 25 (cSNAP-25) was examined on day 78 post BoNT-A. Fluorescent microphotographs show A.) BoNT-A enzymatic activity in neuromuscular junctions, terminals and axons in gastrocnemius (scale bar = 200 µm) and B.) L4 spinal cord ventral horn (upper panel scale bar = 500 µm, lower panel scale bar = 200 µm). Immunohistochemical scoring of muscular toxin activity C.) suggests abundant presence of cSNAP-25 in BoNT-A i.n. treated groups and positive controls (assessed 7 days post 5 U kg^{-1} i.m. BoNT-A). Under C.), the data points represent individual animal score values and the horizontal bar represents median ($N = 3$ animals/group). The cSNAP-25 quantity in the spinal cord ventral horn D.), assessed by sum of pixel intensity-thresholded area in 6 non-overlapping visual fields (0.14 mm2, 3 visual fields per left and right side; average of 4 slices per animals, $N = 5$ animals/group; median ± range, **$P < 0.01$ vs. saline i.n. + horse serum; Kruskal–Wallis followed by Dunn's post hoc).
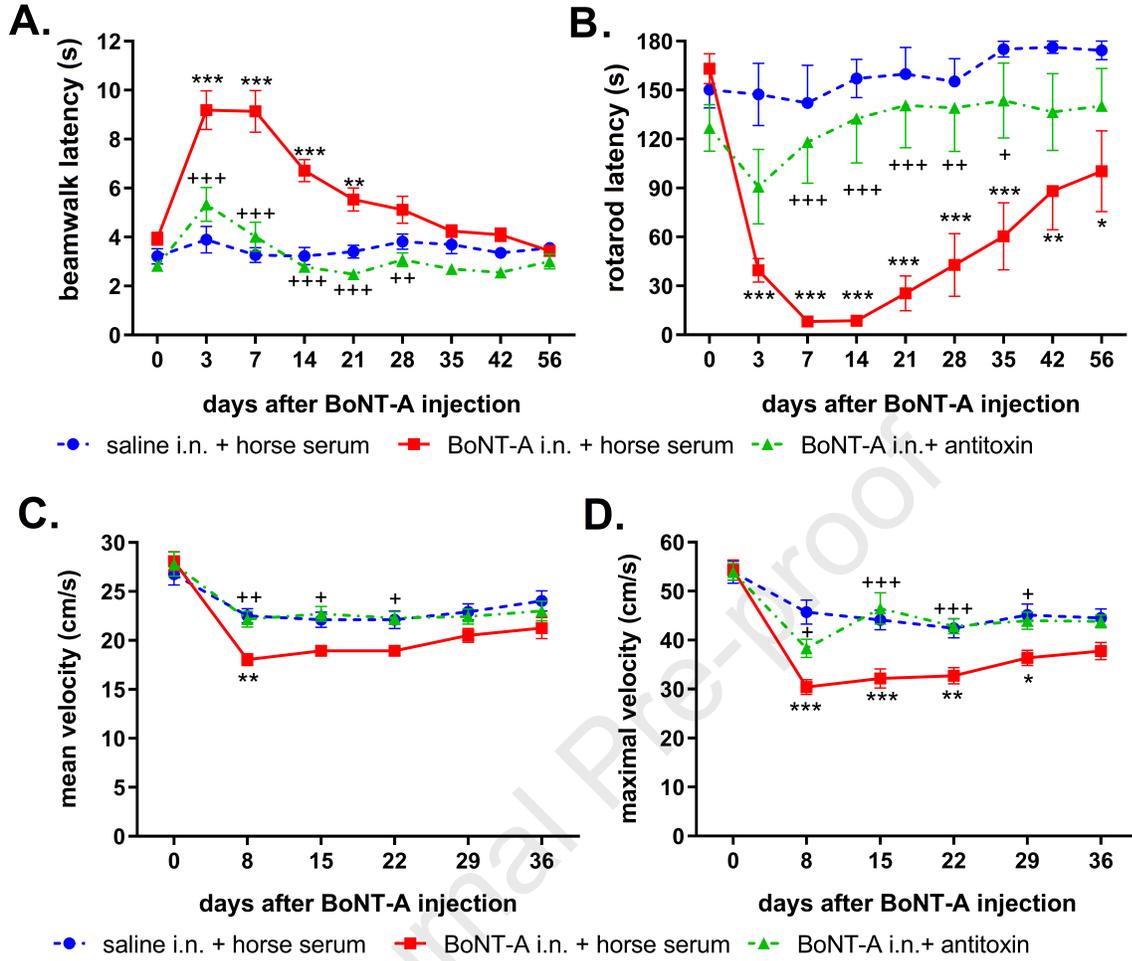
Figure 8. Localization of BoNT-A enzymatic activity in relation to different neuronal and synaptic markers. The animals were treated with i.n. BoNT-A (2 U per bilateral sciatic nerve) and the L4 ventral horn sections were co-stained with BoNT-A-cleaved SNAP-25 immunoreactivity (cSNAP-25) and A.) choline acetyltransferase (ChAT), B.), potassium voltage channel $K_v2.1.$, both markers of cholinergic C-boutons and their associated postsynaptic channels. In addition, colocalization of cSNAP-25 was performed with C.) high affinity BoNT-A binding acceptor synaptic vesicle protein 2 C (SV2C), and D.) general synaptic marker synaptophysin. The confocal microscope images represent a single optical slice (0.42 µm thickness), representative from at least 3 different animals injected with i.n. BoNT-A + horse serum (blue arrows indicate overlap of the immunoreactivities suggestive of colocalization, scale bars = 20 µm).
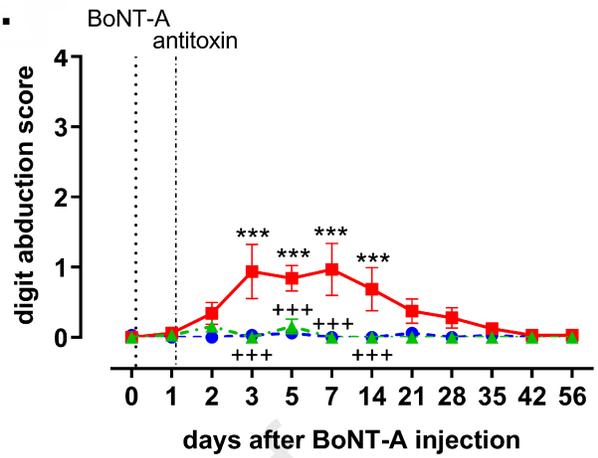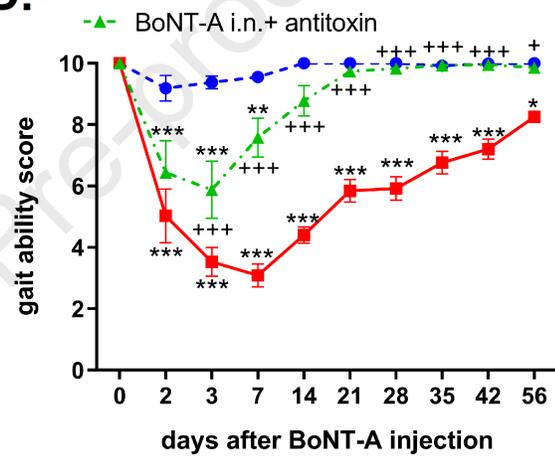
Figure 9. Schematic representation of some possible TeNT and BoNT-A actions in the spinal cord ventral horn. After its axonal transport and transcytosis, TeNT blocks inhibitory transmission by 1.) Renshaw cells, 2.) Ia inhibitory interneurons, as well as 3.) other types of inhibitory interneurons (glycinergic, GABA-ergic) not shown here for simplicity (Weise et al., 2019; Antonucci et al., 2008). When injected in sciatic nerve peripherally, BoNT-A is transported by anterograde axonal transport to muscle (where it's effect on presynaptic neuromuscular terminal of ACh exocytosis results in neuromuscular terminal silencing) and by retrograde axonal transport to central nervous system, where transcytosed BoNT-A may block the excitatory transmission by 4.) C-boutons formed by V0c cholinergic interneurons (Caleo and Mazzocchio, 2018), and 5.) other types of excitatory neurons (e.g. glutamatergic), in line with its selectivity for excitatory transmission (Restani et al., 2011). Possible BoNT-A central action at 6.) motoneuron recurrent axonal collaterals synapsing with Renshaw cells (Ramirez-Castaneda et al., 2013; Mazzocchio and Caleo, 2015) does not necessitate transcytosis. The figure was created with Biorender.com (accessed on 14/08/2023).
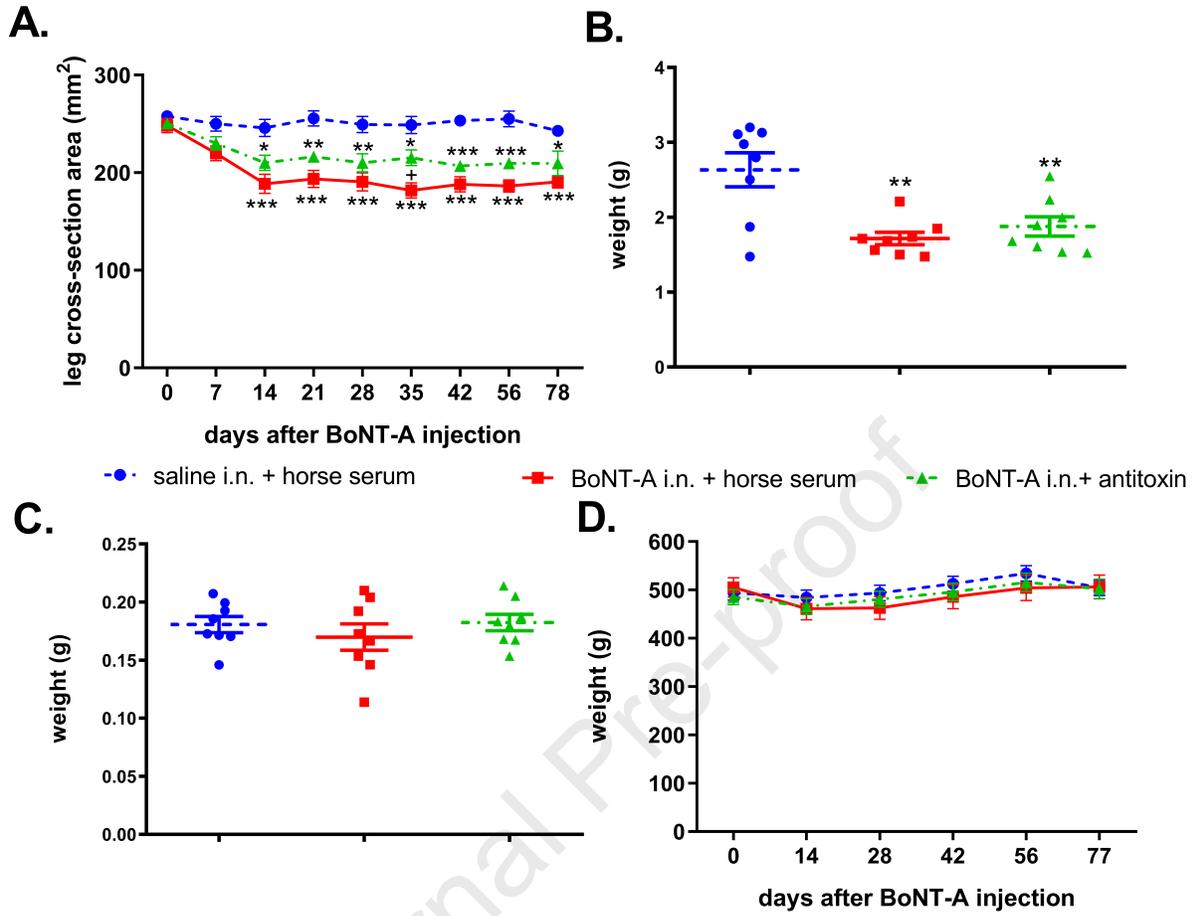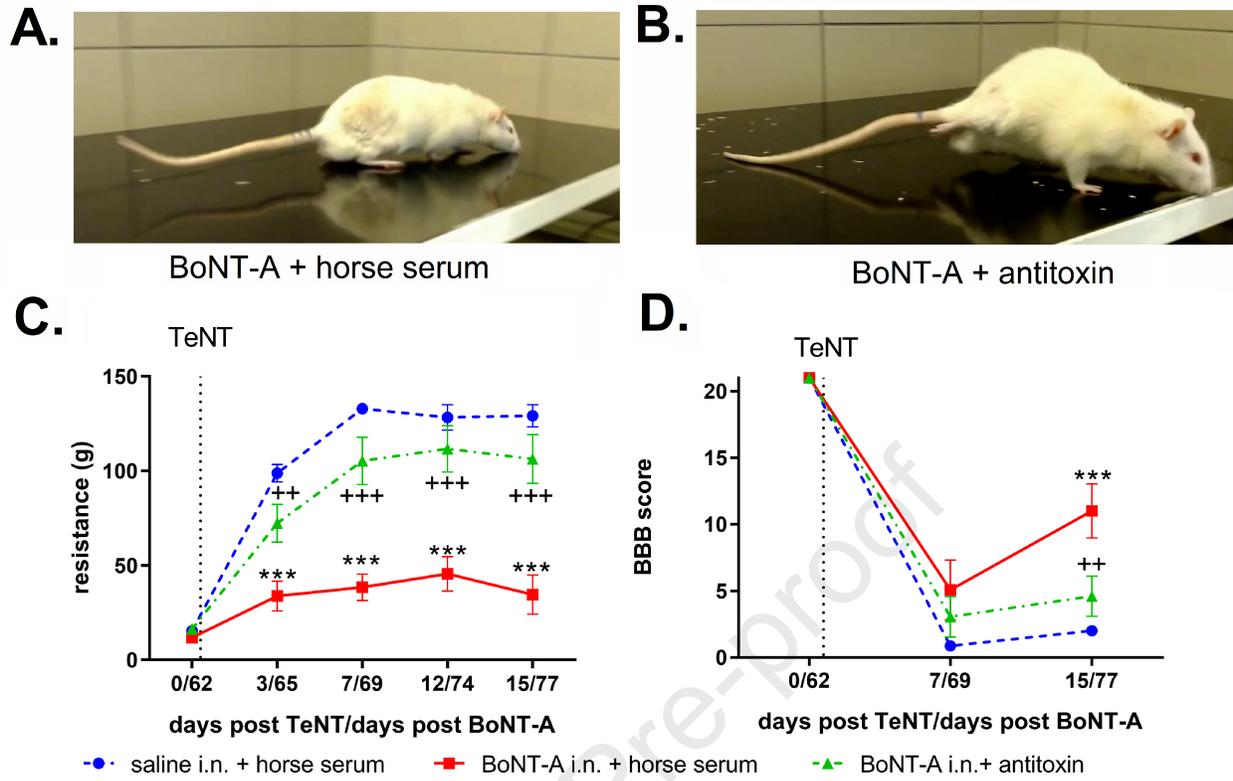
SUPPLEMENTARY FIGURE LEGEND

Supplementary figure S1. Representative images of immunohistochemical scoring system for presence of cSNAP-25 in neuromuscular junctions (NMJ) and axons, similar to Perier et al., 2021. Score 4 = the strong staining of frequent NMJs, terminals and intramuscular nerves (no. of axons ≥ 10), score 3 = the strong staining of frequent NMJ and nerve terminals; score 2 = the moderate staining of frequent NMJs; score 1 was assigned when only a few or weak NMJ staining was observed. Score 0 was given if there was no staining of NMJ, no staining of nerve terminal and no staining of axons.
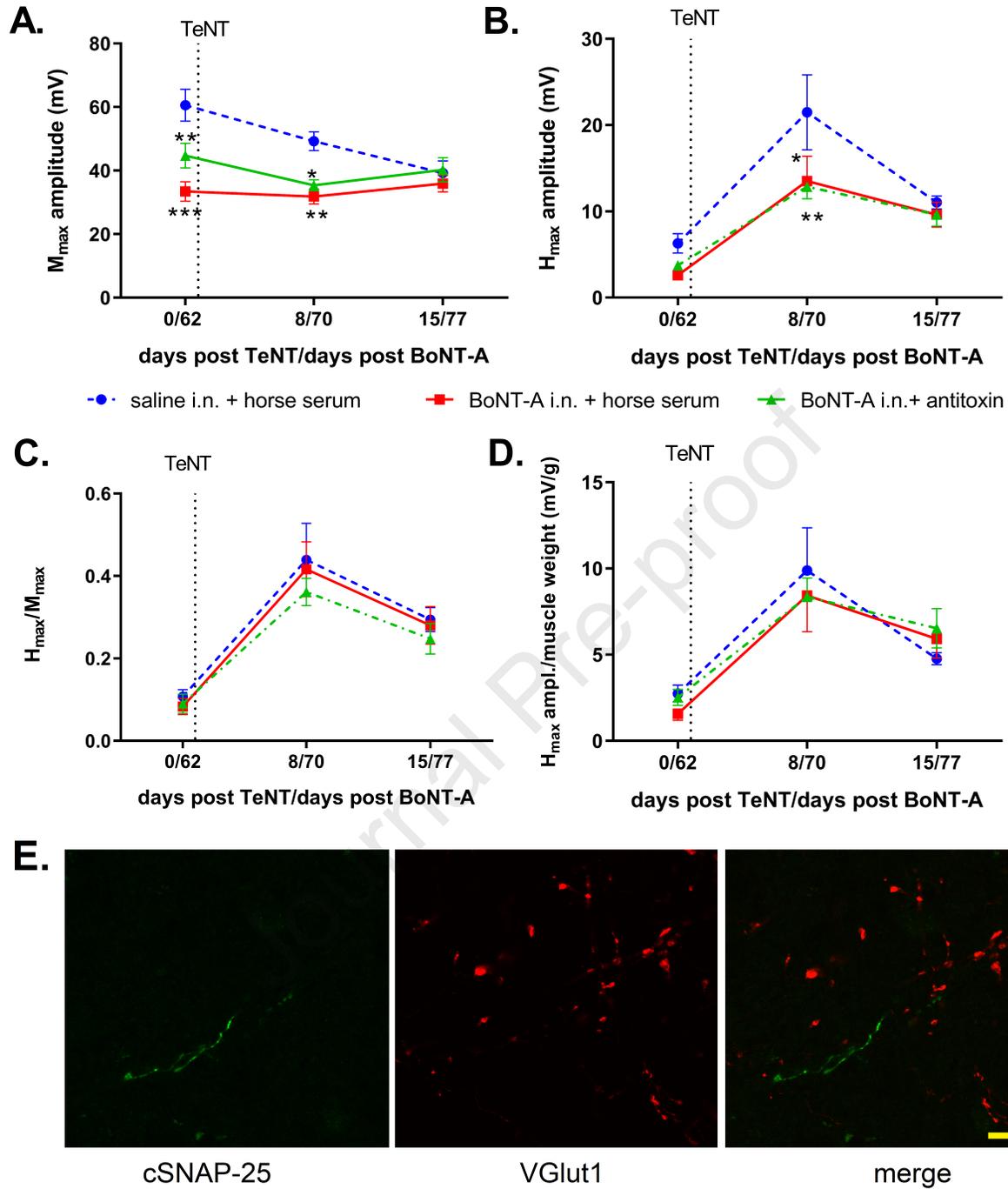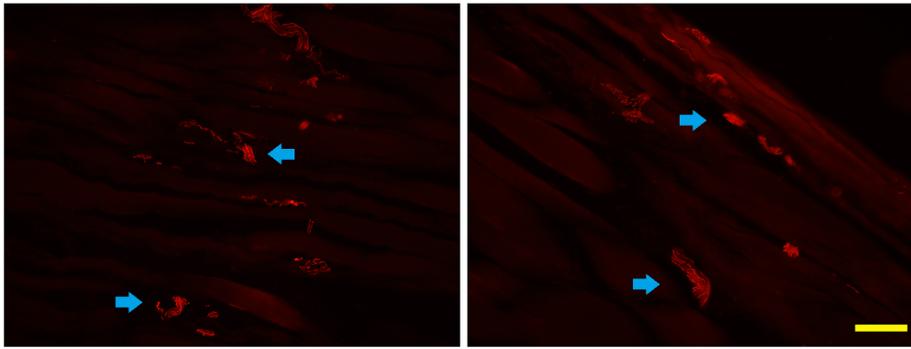
A. leg cross-section area (mm²) vs days after BoNT-A injection

B. weight (g)

Legend: saline i.n. + horse serum · BoNT-A i.n. + horse serum · BoNT-A i.n.+ antitoxin

C. weight (g)

D. weight (g) vs days after BoNT-A injection

A. BoNT-A + horse serum

B. BoNT-A + antitoxin

C.

TeNT

resistance (g)

++   +++   +++   +++
***   ***   ***   ***

0/62   3/65   7/69   12/74   15/77
days post TeNT/days post BoNT-A

D.

TeNT

BBB score

***

++

0/62   7/69   15/77
days post TeNT/days post BoNT-A

- saline i.n. + horse serum   — BoNT-A i.n. + horse serum   - BoNT-A i.n.+ antitoxin

A.

B.

saline i.n. + horse serum   ■ BoNT-A i.n. + horse serum   ▲ BoNT-A i.n.+ antitoxin

C.

D.

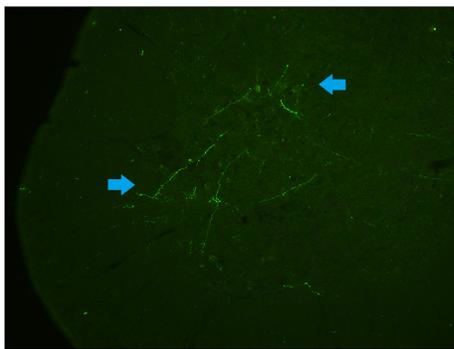**E.**

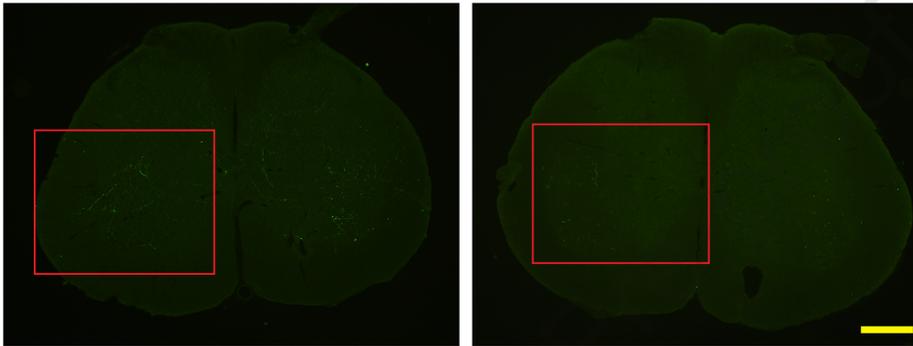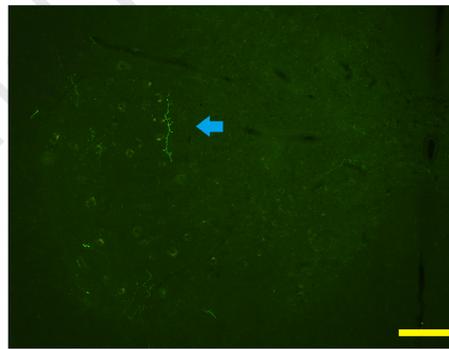cSNAP-25   VGlut1   merge

A.

BoNT-A + horse serum　　　　BoNT-A + antitoxin

B.

BoNT-A + horse serum　　　　BoNT-A + antitoxin

C.

D.

A.

cSNAP-25   ChAT   merge

B.

cSNAP-25   K$_v$2.1.   merge

C.

cSNAP-25   SV2C   merge

D.

cSNAP-25   synaptophysin   merge

Anterograde axonal transport

Retrograde axonal transport

Ia afferent

Afferent terminal

Neuromuscular junction

α-motoneuron axon
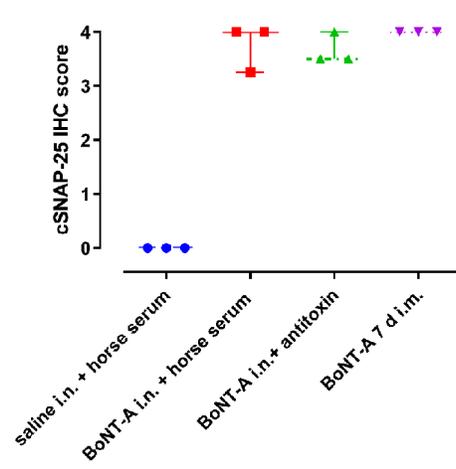
What is already known:

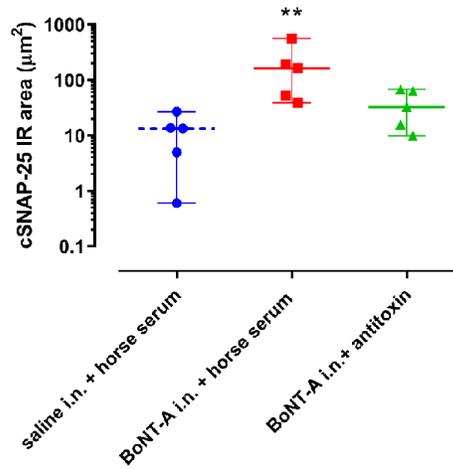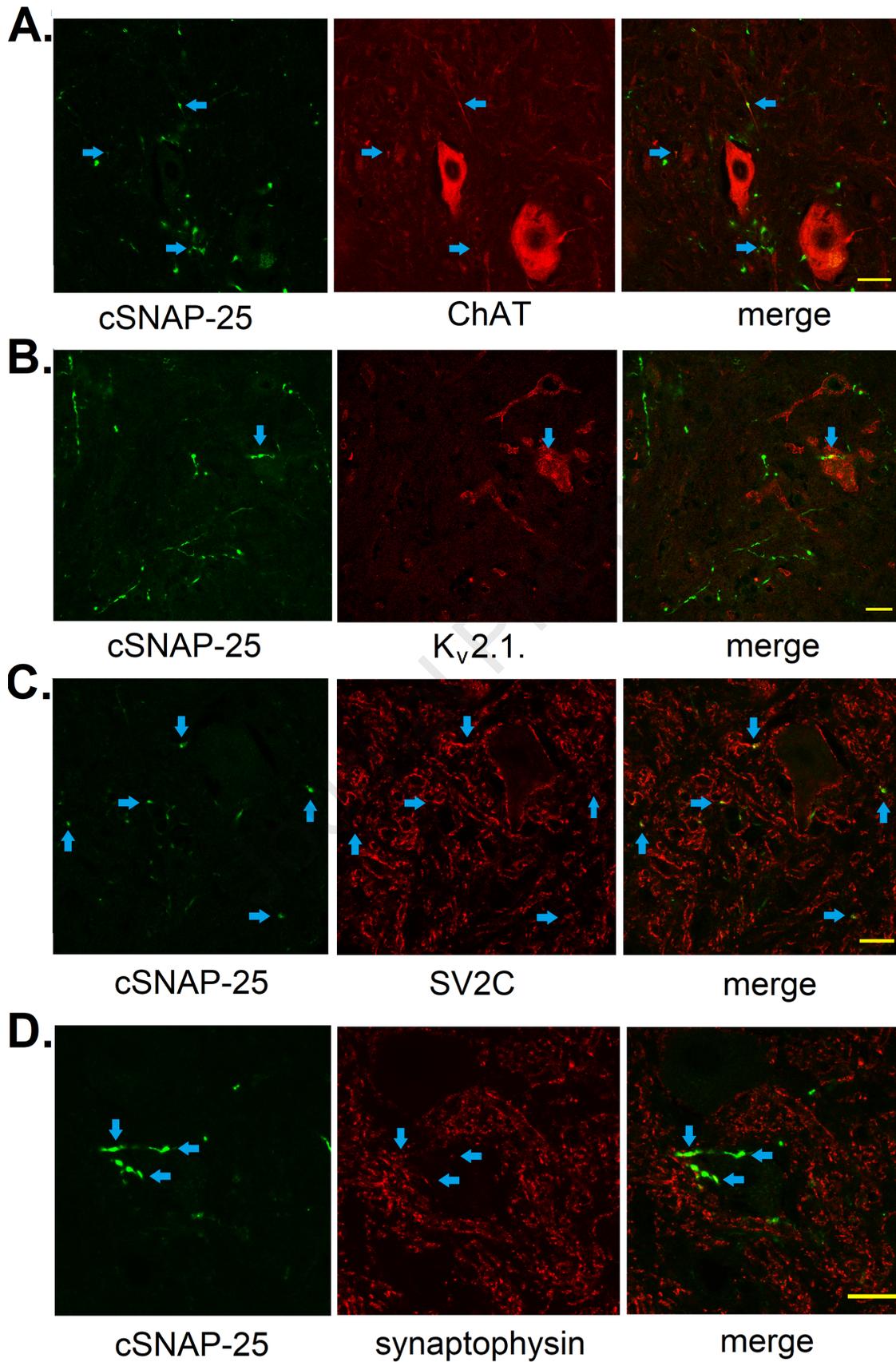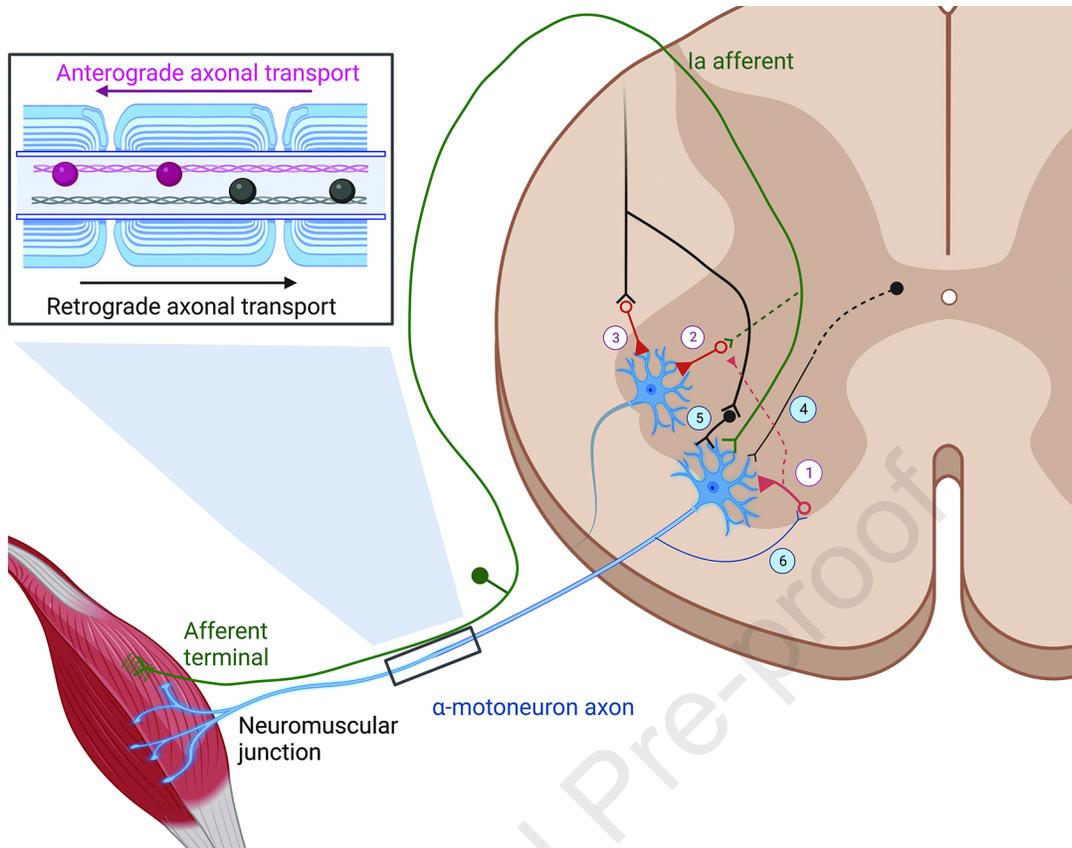-In human patients and animal models, BoNT-A may exhibit central effects in muscular hyperactivity

- the possible central BoNT-A actions on normal motor processing have not been characterized

What does this study add?

-In normal non-spastic animals, BoNT-A transported via peripheral nerve impairs spinal control of movement

-This effect is dependent on spinal transcytosis and accompanied by central enzymatic action

What is the clinical significance?

- The BoNT-A affects spinal premotor circuits participating in normal locomotion and involuntary muscle spasm

- Present study provides a novel perspective on the possible mechanisms of BoNT-A therapeutic action in movement disorders and spasticity.

Declaration of interest

The authors declare no conflict of interests.

Appendix III

Fabris F, Šoštarić P, Matak I, Binz T, Toffan A, Simonato M, Montecucco C, Pirazzini M, Rossetto O. **Detection of VAMP Proteolysis by Tetanus and Botulinum Neurotoxin Type B In Vivo with a Cleavage-Specific Antibody**. Int J Mol Sci. 2022;14;23(8):4355. (Q1)

Petra Šoštarić Mužić -acquisition, analysis, and interpretation of data for the work, writing, reviewing, and editing the manuscriot for publication.

Fabris Federico - acquisition, analysis, and interpretation of data for the work, writing, reviewing, and editing the manuscriot for publication.

Matak Ivica- acquisition, analysis, and interpretation of data for the work, writing, reviewing, and editing the manuscriot for publication.

Binz Thomas-, writing, reviewing, and editing the manuscriot for publication.

Toffan Anna- immunized the rabbit and performed the blood sampling.

Simonato Morena- reviewing and editing the manuscriot for publication.

Cesare Montecucco- contributions to the conception and design of the work, writing, reviewing, and editing the manuscriot for publication.

Pirazzini Marco- contributions to the conception and design of the work, writing, reviewing, and editing the manuscriot for publication.

Rossetto Ornella- contributions to the conception and design of the work, writing, reviewing, and editing the manuscriot for publication.

Web link: https://www.mdpi.com/1422-0067/23/8/4355

Article

Detection of VAMP Proteolysis by Tetanus and Botulinum Neurotoxin Type B In Vivo with a Cleavage-Specific Antibody

Federico Fabris [1], Petra Šoštarić [2], Ivica Matak [2], Thomas Binz [3], Anna Toffan [4], Morena Simonato [5], Cesare Montecucco [1,5], Marco Pirazzini [1,6,*] and Ornella Rossetto [1,5,6,*]

[1] Department of Biomedical Sciences, University of Padova, Via Ugo Bassi 58/B, 35131 Padova, Italy; federico.fabris.5@phd.unipd.it (F.F.); cesare.montecucco@gmail.com (C.M.)

[2] Department of Pharmacology, School of Medicine, University of Zagreb, Šalata 11, 10000 Zagreb, Croatia; petra.sostaric@mef.hr (P.Š.); ivica.matak@mef.hr (I.M.)

[3] Institute of Cellular Biochemistry, Hannover Medical School, Carl-Neuberg-Straße 1, 30625 Hannover, Germany; binz.thomas@mh-hannover.de

[4] Istituto Zooprofilattico Sperimentale delle Venezie, Viale dell'Università 10, 35020 Legnaro, Italy; atoffan@izsvenezie.it

[5] Institute of Neuroscience, Italian Research Council, University of Padova, Via Ugo Bassi 58/B, 35131 Padova, Italy; morena.simonato@cnr.it

[6] Interdepartmental Research Center of Myology CIR-Myo, University of Padova, Via Ugo Bassi 58/B, 35131 Padova, Italy

* Correspondence: marco.pirazzini@unipd.it (M.P.); ornella.rossetto@unipd.it (O.R.)

Abstract: Tetanus and Botulinum type B neurotoxins are bacterial metalloproteases that specifically cleave the vesicle-associated membrane protein VAMP at an identical peptide bond, resulting in inhibition of neuroexocytosis. The minute amounts of these neurotoxins commonly used in experimental animals are not detectable, nor is detection of their VAMP substrate sensitive enough. The immune detection of the cleaved substrate is much more sensitive, as we have previously shown for botulinum neurotoxin type A. Here, we describe the production in rabbit of a polyclonal antibody raised versus a peptide encompassing the 13 residues C-terminal with respect to the neurotoxin cleavage site. The antibody was affinity purified and found to recognize, with high specificity and selectivity, the novel N-terminus of VAMP that becomes exposed after cleavage by tetanus toxin and botulinum toxin type B. This antibody recognizes the neoepitope not only in native and denatured VAMP but also in cultured neurons and in neurons in vivo in neurotoxin-treated mice or rats, suggesting the great potential of this novel tool to elucidate tetanus and botulinum B toxin activity in vivo.

Keywords: botulinum neurotoxins; tetanus neurotoxins; vesicle-associated membrane protein VAMP; SNARE proteins; polyclonal antibodies

1. Introduction

Tetanus (TeNT) and Botulinum Neurotoxins (BoNTs) form the large family of Clostridial Neurotoxins (CNT), the deadly bacterial exotoxins made by anaerobic and sporogenic Clostridium species [1]. *C. tetani* produces one single TeNT, whereas several phylogenetically distinct clostridia, including *C. botulinum*, *butyricum*, *baratii*, and *argentinense*, produce eight different BoNT serotypes. These toxins are indicated with an alphabetical letter (BoNT/A through /G and BoNT/X) and are further subclassified as subtypes (numerals appended to the serotype) [1–3]. CNT display lethal doses in the low ng/kg range, and thus are the most poisonous substances discovered so far [4]. This potency derives from the ability of CNT to enter selectively into nerve terminals and to cleave one (or more) neuronal SNARE (Soluble NSF Attachment protein Receptors) proteins, i.e., VAMP-1/2, SNAP-25 or syntaxin-1A/1B. These three proteins form the heterotrimeric complex, known as the SNARE complex, which is responsible for synaptic vesicle fusion with the presynaptic plasma membrane

and neurotransmitter release [5,6]. SNARE cleavage by CNT prevents the formation of the complex or causes its dysfunction, thereby inhibiting neurotransmission.

BoNTs bind to and enter within both motor and autonomic peripheral cholinergic neurons, where they block the release of the neurotransmitter acetylcholine, causing the flaccid paralysis of botulism [1,7]. Accordingly, minute amounts of BoNT/A1 are used, with great success and safety, to treat neurological conditions caused by hyperactivity of nerve terminals and in aesthetic medicine [8]. Conversely, TeNT undergoes a retroaxonal transport and it is released within the spinal cord and brain stem, where it blocks neurotransmission of inhibitory interneurons causing excitatory disbalance and spastic paralysis, which is the main symptom of tetanus [9–11]. Tetanus can be prevented by a very effective vaccine [9,11], whereas no vaccine has yet been approved for BoNTs, perhaps due to the rarity of botulism and the extensive use of BoNT/A1 in human therapy [12,13].

The metalloprotease activity of CNT against SNARE proteins is sufficient to cause the cardinal symptoms of tetanus and botulism. The identification of VAMP-1/2 as the targets of TeNT and BoNT/B [14] rapidly led to the discovery of the other BoNT substrates, i.e., SNAP-25 for BoNT/A, BoNT/C, and BoNT/E [15,16], and VAMP-1/2 for BoNT/D, BoNT/F, and BoNT/G [17–19]. BoNT/C is unique as it also cleaves syntaxin-1A/1B [20], although its toxic effect is primarily due to SNAP-25 proteolysis [21].

Different experimental techniques have been developed to track SNARE cleavage as a readout to monitor CNT activity in cell and neuronal culture [22–30], in animal tissues [21,31,32], as well as for CNT detection in biological isolates [33–38]. A particularly convenient and versatile method is the use of antibodies against specific portions of VAMP, SNAP-25, or syntaxin, which can be used in cell-based assays via Western blotting [22,24,26,28,39–42], and by fluorescence microscopy [21,29,31,32,43–52].

Depending on the specific antigen used to elicit host immunization, different antibodies recognizing different portions of the SNARE proteins have been developed and detect CNT proteolytic activity very specifically. Some antibodies recognize the intact SNARE protein, and their signal decreases after cleavage [53–55]. Other antibodies recognize both the entire and the truncated form of the SNARE protein and are useful to evaluate CNT activity by Western blotting in a ratiometric manner [21,24,40,56–61]. Particularly useful are those antibodies recognizing the SNARE protein only after cleavage by a specific toxin because of the development of in vitro detection assays [62–65] and to track CNT activity in vivo, although this is thus far restricted to the BoNT/A- or BoNT/E-truncated forms of SNAP-25 [21,31,32,43–52,66–68]. These antibodies have the advantage of providing a signal that increases in parallel with the progressive CNT proteolytic activity in tissues where it is ineffective, monitoring a decreasing signal.

Here, we describe the development of a polyclonal antibody specific for segment 77-89 of mouse VAMP-2 (dubbed Ab-VAMP$_{77}$), which selectively recognizes VAMP-1/2 only after TeNT and BoNT/B cleavage that occurs at the same single site [8,14]. Notably, Ab-VAMP$_{77}$ detects the proteolytic activity of TeNT and BoNT/B, but not the one elicited by BoNT/D or BoNT/G, in neuronal cultures. More importantly, it raises a robust signal in motor axon terminals at the neuromuscular junction (NMJ) after BoNT/B injection and in the brain stem after injection of TeNT. Ab-VAMP$_{77}$ represents a novel and effective tool to visualize the proteolytic activity of these two toxins in vitro and in vivo.

2. Results and Discussion

2.1. Generation of the Polyclonal Antibody Specific for TeNT and BoNT/B Cleavage of VAMP

VAMP-1 and -2 are integral proteins with a single transmembrane domain spanning the synaptic vesicle membrane [69,70]. VAMP-1 and VAMP-2 are protein isoforms differing significantly only in the 20 N-terminal residues, and for the remaining part are highly conserved among vertebrate and invertebrate animals [71] (Supplementary Figure S1). This cytosolic portion contains the alpha-helical domain (SNARE motif) that coil-coils with two similar domains of SNAP-25 and one of syntaxin to form the SNARE complex involved in neuroexocytosis (Figure 1A) [5]. All the CNT targeting VAMP cleave single

and specific peptide bonds within the SNARE-motif (Figure 1B). TeNT and BoNT/B cleave the identical peptide bond Q78F79 in VAMP-1 and Q76F77 in VAMP-2 (with human VAMP numbering), leaving the truncated form of VAMP on the SV membrane. Notably, due to the high conservation of the two proteins, the same truncated VAMP-1 and VAMP-2 are expected to be generated in all the animal species used in the lab except for the rat and chicken VAMP-1, which are resistant to TeNT and BoNT/B cleavage [8,72] (Figure 1C).
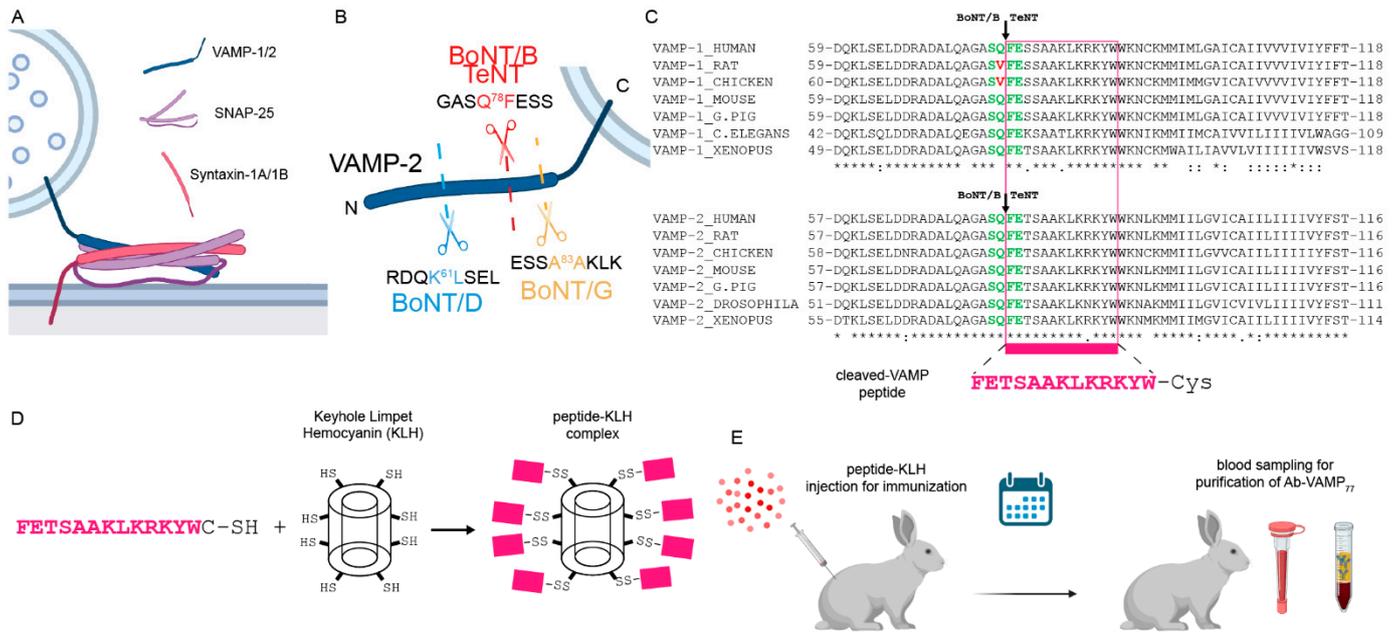

Figure 1. Generation of the Ab-VAMP₇₇ antibody. (**A**) Scheme showing the three SNARE proteins involved in neuroexocytosis that form the SNARE complex by coil-coiling their SNARE motifs, one from the vesicular VAMP-1/2 (blue), two from the membrane-anchored SNAP-25 (pink), and one from the integral membrane protein syntaxin-1A/1B (red). (**B**) Scheme showing the peptide bonds cleaved by the VAMP-specific CNT used in this study, which generate specific new N-termini to VAMP (shown is human VAMP-2). (**C**) Alignment of VAMP-1/2 showing that the FETSAAKLKRKYW peptide (pink) exposed by BoNT/B and TeNT is in all the main animal species used in research. The green residues indicate cleavage sites of TeNT and BoNT/B in VAMP-1 and VAMP-2. Red residues indicate the mutation responsible for VAMP-1 resistance to TeNT and BoNT/B in rat and chicken. (**D**) Scheme showing the generation of immunogenic carrier by chemical conjugation of the C-terminal Cysteine to the Keyhole limpet Hemocyanin. (**E**) the peptide-KLH complex was injected into a rabbit, and at the scheduled time point the blood was collected for the ensuing purification of peptide-specific IgGs.

An antibody specific to BoNT/B and TeNT cleaved VAMP, but not to the intact protein, is an invaluable tool for visualizing the action of these toxins in vivo. For this purpose, the peptide FETSAAKLKRKYW-C corresponding to the N-terminus of cleaved VAMP-2 bearing a C-terminal Cysteine was conjugated to Keyhole limpet hemocyanin, used as an immunogenic carrier (Figure 1D,E). The rabbit was immunized and, after boosting injections, scheduled blood samplings were undertaken. Sera were eventually pooled and used for affinity purification. To this end, the C-terminal Cysteine was replaced by biotin for a fast coupling to a streptavidin-agarose resin, which allowed a very fast and efficient affinity purification of the antibody (Supplementary Figure S2).

2.2. Ab-VAMP₇₇ Detects, with High Specificity, TeNT and BoNT/B Cleavage in Primary Neuronal Cultures

Neuronal cultures are widely employed to dissect the mechanism of action of CNTs. In addition, after the identification of SNARE proteins as specific targets of CNTs, TeNT

and BoNTs became major tools to study the exo–endocytosis apparatus within neurons, as well as other cell types [8,73]. Moreover, neuronal cultures are used as a screening platform to assess potential CNT inhibitors [12].

A very convenient model to assay the specificity of antibodies in detecting cleavage by TeNT and BoNT/B is Cerebellar Granule Neurons (CGNs), a primary neuronal culture that is highly susceptible to CNTs [68]. We thus intoxicated CGNs for 12 h with four CNTs targeting VAMP: TeNT, BoNT/B, BoNT/D, and BoNT/G, and monitored their protease activity via Western blotting and imaging (Figure 2A). The proteolytic activity of TeNT can be monitored with a VAMP-2 specific commercial antibody that provides a decreasing signal upon cleavage. As shown in Figure 2B, 50 pMolar TeNT causes the complete disappearance of VAMP-2, with 5 pMolar being almost equipotent. At variance, 0.5 and 0.05 pMolar TeNT do not apparently cause a decrease in the signal, indicating that these two concentrations of TeNT are not sufficient to mediate cleavage of VAMP-2. However, when the same samples were stained with Ab-VAMP$_{77}$, a clear band appeared at 0.5 pMolar and a fainter band was still visible in the 0.05 pMolar sample. This result indicates that Ab-VAMP$_{77}$, by providing a rising rather than a decreasing signal, is much more sensitive than anti-intact VAMP antibody when detecting the TeNT-mediated VAMP-2 proteolysis. The same enhanced sensitivity is also observed after VAMP-2 cleavage by BoNT/B (Figure 2B). Intact VAMP is not recognized Ab-VAMP$_{77}$, indicating its selectivity only for cleaved VAMP. This is of fundamental importance for in vivo studies.
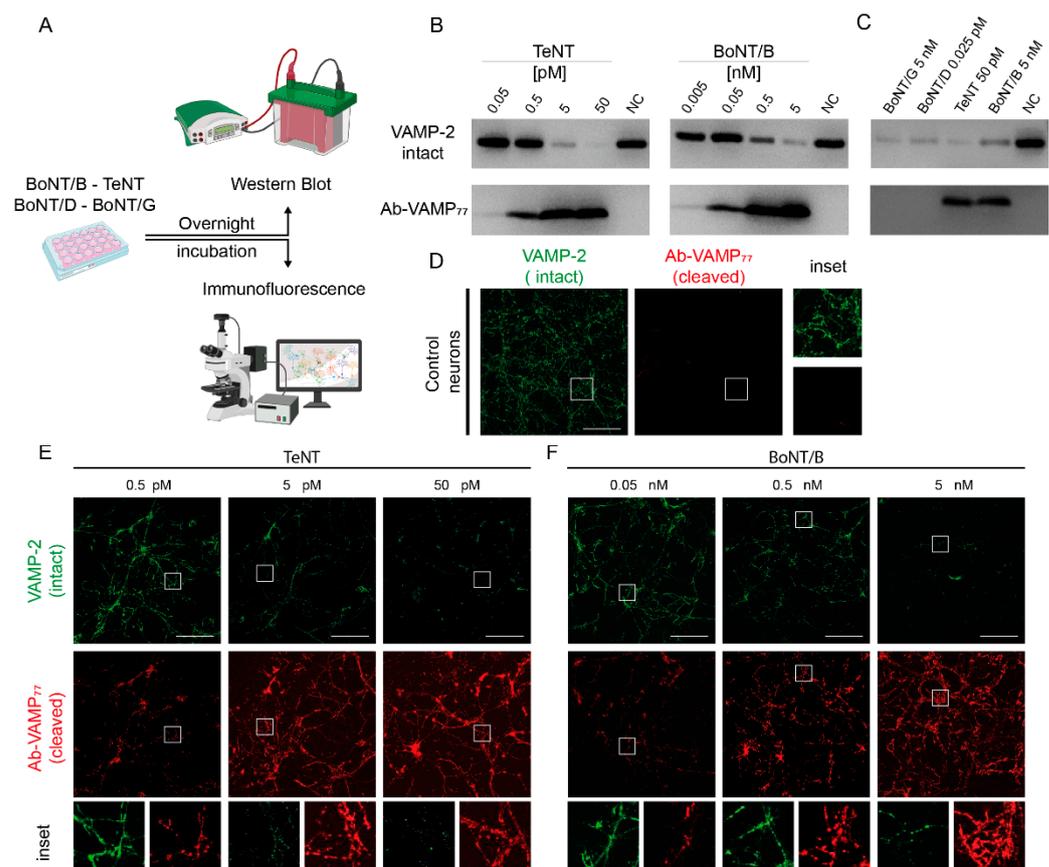
Figure 2. The Ab-VAMP$_{77}$ polyclonal antibody detects VAMP-1/2 cleavage by TeNT and BoNT/B in neuronal culture with high efficiency and toxin selectivity. (**A**) Scheme showing the experimental readout used to evaluate the specificity of Ab-VAMP$_{77}$ in rat CGNs. (**B**) Representative Western blotting showing the high sensitivity of Ab-VAMP$_{77}$ compared to a conventional antibody at low TeNT (**left**) and BoNT/B (**right**) concentrations. The NC samples are control neurons not treated with

any toxin. (**C**) Representative Western blotting showing that Ab-VAMP$_{77}$ binds only to a cleaved fragment of VAMP specifically generated by BoNT/B and TeNT, but not by BoNT/D nor BoNT/G. (**D**) Control CGNs showing the typical punctuate pattern (inset) of VAMP-2 (green) staining at presynaptic level, and no signal for Ab-VAMP$_{77}$ in the absence of TeNT or BoNT/B treatment. (**E,F**) Immunofluorescence analysis showing that at increasing concentration of TeNT (**E**) or BoNT/B (**F**) the signal of intact VAMP-2 (green) fades away, whereas the signal of Ab-VAMP$_{77}$ (red) progressively increases yet maintains the typical punctuate pattern (insets) in both cases. Scale bars in (**D**–**F**) are 100 μm.

We next tested Ab-VAMP$_{77}$ in neurons treated with BoNT/D or BoNT/G, as they generate two different cleaved-VAMP N-termini containing or not the linear epitope. In fact, BoNT/D cleaves peptide bond K61L62 in VAMP-1, K59L60 in VAMP-2 (human VAMP numbering), upstream of the TeNT-BoNT/B cleavage site and BoNT/G cleaves the A83A84 bond in VAMP-1, A81A82 in VAMP-2 (human numbering) included in the antigenic peptide (Supplementary Figure S3A). BoNT/D is very potent in CGNs and cleaved all the VAMP-2 already at fMolar concentration (Supplementary Figure S3B), while BoNT/G has an activity more similar to BoNT/B and thus required a nMolar range for complete cleavage (Supplementary Figure S3C). In both cases, Ab-VAMP$_{77}$ did not recognize the truncated VAMPs at any toxin concentration (Supplementary Figure S3B,C), including those causing complete cleavage (Figure 2C).

Comparable results were obtained when VAMP-2 cleavage was monitored by immunostaining. As shown in Figure 2D, control CGNs stained with the antibody against the whole protein displayed the typical punctuate accumulation of VAMP-2 at the level of presynaptic boutons, whilst Ab-VAMP$_{77}$ did not produce any detectable signal. When treated with increasing concentrations of TeNT and BoNT/B, the signal of intact VAMP-2 progressively faded away (Figure 2E,F), and eventually disappeared almost completely. The antibody against cleaved VAMP displayed the opposite pattern, i.e., it increased proportionally to the concentration of TeNT and BoNT/B. As shown in the insets, the signal remained almost exclusively confined at the level of the puncta, coherently with previous observations reporting that after SNARE cleavage by CNT, synaptic vesicles accumulate at the presynaptic level [22,74,75]. Notably, when the signal given by Ab-VAMP$_{77}$ was merged with the signal of the residual intact VAMP, the two signals displayed clearly segregated staining (Supplementary Figure S4). This is consistent with the fact that the two antibodies spot distinct and mutually exclusive populations of VAMP-2 corresponding to the intact and the cleaved one. Again, in spite of a complete cleavage of VAMP-2, Ab-VAMP$_{77}$ was unable to detect VAMP cleavage products after BoNT/D and BoNT/G treatment (Supplementary Figure S3D,E).

Altogether, these results indicate that Ab-VAMP$_{77}$ can detect the cleavage of VAMP by TeNT and BoNT/B with high specificity and selectivity, which are maintained both when VAMP is denatured as well as when the epitope is fixed and in native conformation, consistent with the fact that the antibody was raised with a linear peptide and that the epitope is sequential rather than conformational. Ab-VAMP$_{77}$ does not bind intact VAMP. At variance, Gray et al. developed a monoclonal antibody using the same FETSAAKLKRKYW peptide that recognizes TeNT-BoNT/B-cleaved VAMP, but also the intact protein [64]. At the same time, our finding is in agreement with the results obtained by von Berg et al., who developed a monoclonal antibody against a similar, yet shorter, peptide (FETSAAKL) that recognized specifically the cleaved, but not the intact form of VAMP [35]. It is tempting to suggest that our immunization protocol has favored an immune response specific to the very N-terminus of the peptide, raising antibodies that, similarly to that of von Berg et al., are specific to the TeNT-BoNT/B newly generated epitope in VAMP. At variance, Gray et al. might have selected a monoclonal antibody recognizing another part of the peptide, which remains exposed for binding both in intact and TeNT-BoNT/B-cleaved VAMP. Concurrently with this possibility, the Gray et al. antibody fails to detect VAMP after BoNT/G cleavage [64].

2.3. The Antibody against Cleaved VAMP Specifically Detects the Activity of BoNT/B at the Neuromuscular Junction

We next tested whether Ab-VAMP$_{77}$ can detect BoNT/B activity in vivo within motor axon terminals at the NMJ. For this purpose, we injected a sub-lethal amount of BoNT/B (or saline as a control) between the ears of mice to provide a local intoxication of the Levator Auris Longus (LAL) muscles. LAL muscles originate from the cranial midline and extend toward the external ears, and consist of a few layers of myofibers making them very convenient for NMJ imaging [76–78]. After 48 h from the injection, we collected the two LAL and stained one muscle with an antibody recognizing the intact form of VAMP-1, i.e., the major VAMP form expressed at the adult NMJ [55], and the other one with Ab-VAMP$_{77}$ (Figure 3A). Both samples were also stained with an antibody against the vesicular Acetylcholine Transporter (v-AchT), used as a marker of synaptic vesicles. As expected, LAL muscles injected with saline displayed clear presynaptic staining for intact VAMP-1 that colocalized with v-AchT, but no signal for cleaved-VAMP, indicating that Ab-VAMP$_{77}$ does not bind intact VAMP-1 in vivo (Figure 3B). Conversely, the LAL muscles injected with BoNT/B displayed very bright and robust staining only with the antibody against cleaved-VAMP and only at the presynaptic level where it completely colocalized with v-AchT (Figure 3C), consistent with the fact that the antibody recognized an epitope associated with the synaptic vesicles. In keeping with the results on cultured CGNs, Ab-VAMP$_{77}$ failed to recognize VAMP proteolysis operated by both BoNT/D (Figure 3D) and BoNT/G (Figure 3E). Importantly, it also failed to detect BoNT/B activity when injected in rats that, like chickens, express a VAMP-1 resistant to BoNT/B owing to a point mutation at the toxin cleavage site [72] (Supplementary Figure S5). This control experiment, based on a natural knock-in, further proves the high selectivity of Ab-VAMP$_{77}$ for BoNT/B proteolytic activity in vivo, which is also maintained when the epitope is in its native conformation.
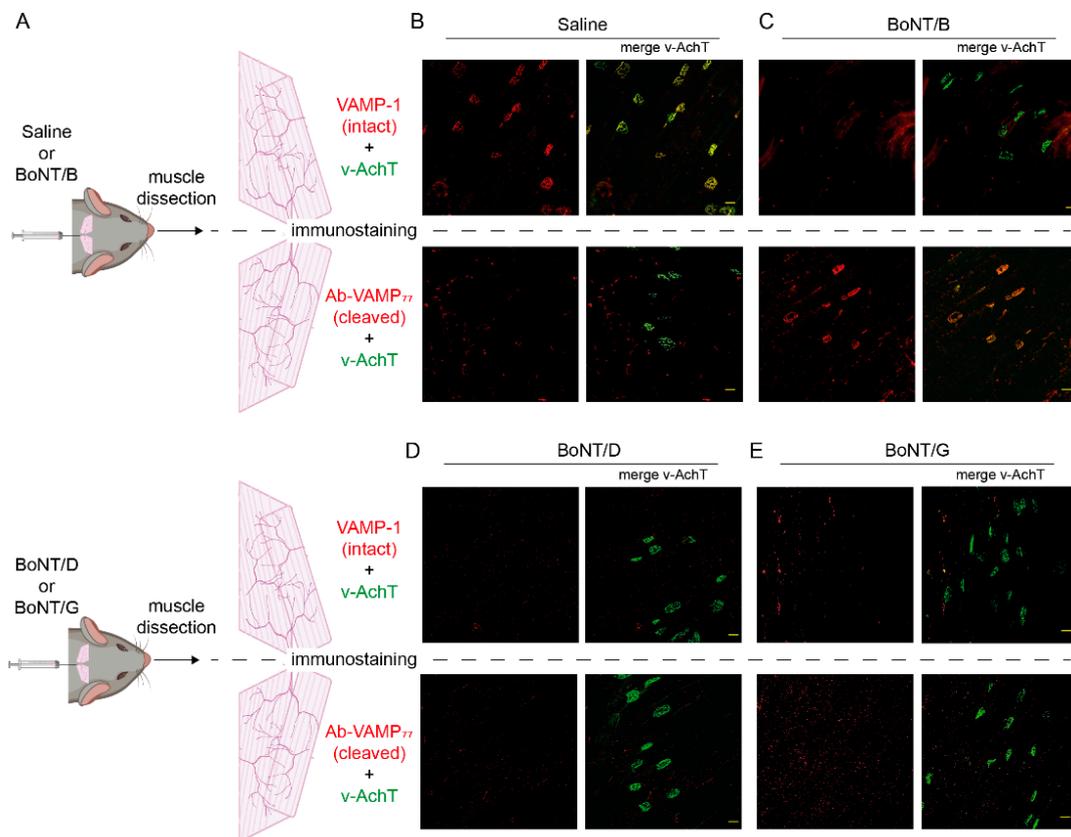

Figure 3. The Ab-VAMP$_{77}$ polyclonal antibody detects VAMP cleavage by BoNT/B at the neuromuscular junction. (**A**) Scheme showing the staining of the two LAL muscles collected after injection of either saline

or BoNT/B (top panel) or of either BoNT/D or BoNT/G (bottom panel) and the following immunostaining of one LAL with an antibody against intact VAMP-1 (top panels) or with the Ab-VAMP$_{77}$ antibody (bottom panels). In both cases, the muscles were also stained for the vesicular protein marker v-AchT. (**B**–**E**) Representative images of whole-mount LAL muscles injected with either saline (**B**) or BoNT/B (**C**) or BoNT/D (**D**) or BoNT/G (**E**) stained for intact VAMP-1 (red in top panels) or cleaved VAMP (red in bottom panels). The right panels of each condition show the merge with v-AchT (green). Scale bar = 25 μm.

2.4. The Antibody against Cleaved-VAMP Specifically Detects the Activity of TeNT in the Central Nervous System

The strategy to exploit the protease activity as an amplifying factor to track down the tissue distribution of CNT has been instrumental in showing that BoNT/A action also acts in the CNS [79–81]. Notably, an antibody recognizing the BoNT/A-cleaved SNAP-25 was widely used to show that, upon intramuscular or subcutaneous injection, the toxin moves from the injection site via intra-axonal retrograde transport, reaching different areas of the CNS in an active form [43–45,47,48,50] even two synapses away from the injection site [46]. Therefore, we decided to test whether Ab-VAMP$_{77}$ can detect the cleavage of VAMP via TeNT in the CNS. We opted for a model of local tetanus generated by injecting a sub-lethal amount of TeNT at the level of the LAL muscles, thereby causing a spastic paralysis confined to the muscles of the ears [11]. Two days after injection, we collected the brain stem and made cryoslices of the facial nucleus. As shown in Figure 4A, Ab-VAMP$_{77}$ raised a very strong and bright, yet extremely confined staining for cleaved VAMP at the level of the seven dorsomedial and seven ventromedial subnuclei (7DM and 7VM) [82], the areas populated by the motor efferents innervating the LAL muscles. Of note, as shown by the magnification, in this case the signal also appeared as rounded varicosities, once again consistent with staining of presynaptic puncta. Moreover, it was restricted to areas deprived of the staining of intact VAMP-2 with little, if any, colocalization, again indicating that the two antibodies specifically recognize two distinct populations of VAMP. The same experiment performed in rats gave a similar result, although in this case the toxin was injected in the whisker pad and, accordingly, the signal appeared in a different area of the facial nucleus, i.e., the seven lateral and the seven dorsolateral subnuclei (7L and 7DL) [82], where the motor neurons commanding the muscles responsible for whiskers' movements reside. Notably, in this case the signal also appeared less intense (Figure 4B), probably due to an overall reduced activity of TeNT compared to mice.
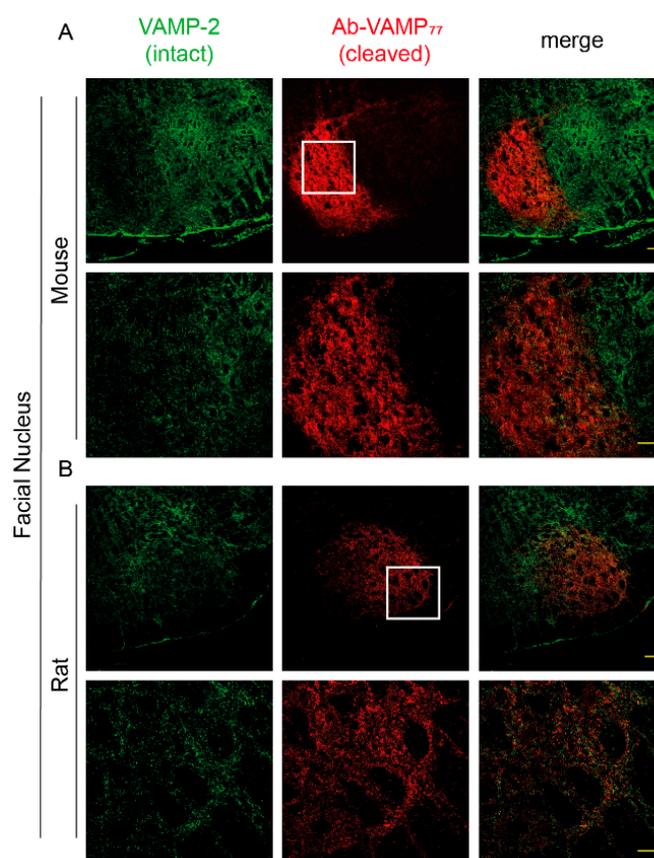
Figure 4. The Ab-VAMP$_{77}$ polyclonal antibody detects VAMP cleavage by TeNT in the brain stem. The TeNT was injected either at the level of the LAL in the mouse (**A**) or at the level of the whisker pad in rats (**B**) and then the cleavage of VAMP was evaluated in the brain stem with an antibody against intact VAMP-2 (green) and Ab-VAMP$_{77}$ (red). The bottom panels in (**A**,**B**) show a magnification of the white-squared area. Scale bar = 40 μm.

3. Conclusions

Clostridial neurotoxins are biochemical scalpels that surgically block neurotransmission at nerve terminals [8,83,84]. Not only the whole toxins, but also their isolated catalytic domains that are genetically expressed, transfected, or microinjected within target cells have been widely used to study the role of specific SNARE proteins in membrane fusion events, in neurons, in other cell types, and even in animal hosts naturally unsusceptible to their uptake [85–89]. Their use associated with modern biotechnologies still represents a reliable, efficient, and definitely convenient method to block neuroexocytosis in several biological systems [90,91]. Among them, TeNT and BoNT/B and their derivatives, which cleave the identical peptide bond in VAMP-1/2/3, are widely used. Here, we generated a polyclonal antibody recognizing the cleaved form of VAMP in a very specific and sensitive manner. This novel biochemical tool can be used both in Western blot and in immunofluorescence on cultured neurons, which we feel safe to extend to virtually any cell type TeNT or BoNT/B can be used on. This antibody can thus be used to image the in vivo proteolytic activity of TeNT and BoNT/B with high specificity using fluorescence microscopy. Compared to a recent report describing the properties of antibodies generated against the same linear epitope used here [64], Ab-VAMP$_{77}$ does not bind intact VAMP and recognizes, in a very selective manner, the cleaved VAMP generated by TeNT and BoNT/B, but not those generated by other VAMP-cleaving toxins. Such specificity was also reported with a monoclonal antibody used to develop in vitro cleavage-based immunoassays to detect CNT in biological isolates [35], but our work led to the development of an antibody suitable for the detection of VAMP cleavage by BoNT/B at the neuromuscular junction

and by TeNT in the central nervous system. This paves the way to future studies aimed at elucidating the action of these two toxins (or of their catalytic subunits) in vivo that was thus far not possible.

4. Materials and Methods

4.1. Antibodies, Toxins and Reagents

Botulinum Neurotoxins type B, D, and G were produced in *E. coli* (strain M15pREP4) as fusion proteins with a C-terminal StrepTag and purified on StrepTactin-Superflow matrix (IBA GmbH, Gottingen, Germany) as previously described [21,92]. Tetanus Neurotoxin was purified from C. tetani cultures [93]. Toxins were kept at -80 °C and diluted in complete culture medium for physiological solution plus 0.2% gelatin prior to use. Primary antibodies: anti-VAMP$_{77}$ was produced in rabbit in this study (see below); anti-VAMP-1 was produced in our laboratory as previously described [32,94]; anti-v-AChT (guinea pig polyclonal 139 105) and anti-VAMP-2 (mouse monoclonal 104 211) were from Synaptic System (Gottingen, Germany). Secondary antibodies for immunofluorescence (anti-mouse, antirabbit, anti-guinea pig) conjugated to Alexa fluorophores were from Thermo Fisher Scientific (Waltham, MA, USA). Secondary antibodies for Western blotting (anti-mouse, antirabbit) conjugated to HRP were from Calbiochem (San Diego, CA, USA). Where not indicated, reagents were purchased from Sigma Aldrich (St. Louis, MO, USA).

4.2. Anticleaved-VAMP Antibody Production and Purification

A New Zealand white rabbit was immunized by subcutaneous injection with the peptide FETSAAKLKRKYWC coupled to KLH [38]. This peptide corresponds to amino acids 77-89 of mouse VAMP-2 with an additional C-terminal cysteine to link the peptide to KLH. Following the primary subcutaneous immunization on day 0, booster intra-muscular injections were performed on days 32 and 60. For each injection, 500 µg of KLH-peptide conjugate were mixed with the non-mineral oil-based adjuvant Montanide^{TM} ISA 763 VG (Seppic, Cedex, France). Rabbit serum was collected on day 120, frozen in liquid nitrogen, and stored at -80 °C until antibody purification.

For purification, 5 mg of peptide FETSAAKLKRKYK-(biotin)-NH$_2$ (Caslo, Copenhagen, Denmark) was mixed with 500 µL of an agarose resin conjugated with Streptavidin (Thermo Fisher Scientific, cat. 20,359) and incubated into a disposable polypropylene column (cat. 29,922 from Pierce, Rockford, IL, USA) overnight at 4 °C in agitation for peptide–biotin–streptavidin coupling. The next day, the resin was extensively rinsed with PBS and then incubated (overnight at 4 °C) with the immune serum (previously ultracentrifuged for 15 min at 40,000 rpm at 4 °C to eliminate fat and blood cell debris). After overnight incubation, the resin was washed with 10 volumes of PBS. The antibodies were eventually eluted by the addition of 10 volumes (250 µL each) of glycine 0.1 M, pH 3.0. These fractions were collected in tubes containing 50 µL of Tris 1 M pH 7.4 to buffer the glycine solution. Protein concentration was assessed with Nanodrop (Thermo Fisher Scientific). Aliquots were then stored at -80 °C until use.

4.3. Cerebellar Granules Neurons Cultures

CGNs were prepared from 4–5-day-old rat pups as described in [68]. Cerebella were collected, mechanically disrupted, and enzymatically dissociated with trypsin in presence of DNase I. Cells were then plated in precoated (poly-l-lysine, 50 µg/mL) plastic 24 well plates or cover glasses at a cell density of 4×10^5 or 2×10^5 cells per well, respectively. Cultures were grown for at least 6 days at 37 °C, 5% CO$_2$, BME supplemented with 10% fetal bovine serum, 25 mM KCl, 2 mM glutamine, and 50 µg/mL gentamicin. To block the proliferation of non-neuronal cells, cytosine arabinoside (10 µM) was added to the culture medium 18–24 h after plating.

4.4. Intoxication of CGNs with CNT

Seven days after CGNs preparation, cells were treated with indicated doses of either BoNT/B, BoNT/D, BoNT/G, or TeNT for 12 h in a complete culture medium. Cells plated on plastic were then directly lysed on the wells with Laemmli Sample Buffer (LSB) (Hepes 10 mM, NaCl 150 mM, SDS 1%, EDTA 4 mM, protease and phosphatase inhibitors) supplemented with mercaptoethanol and bromophenol blue, and collected for Western Blot analysis. Cells lysed in LSB were loaded onto NuPage 4–12% Bis-Tris gels for SDS-PAGE electrophoresis in MOPS buffer (Thermo Fisher Scientific, B0001) and then proteins were transferred onto Protran nitrocellulose membranes and saturated for 1 h in PBS-T (PBS, 0.1% Tween 20) supplemented with 5% non-fat dried milk (PanReac Applichem GmbH, Darmstadt, Germany). Incubation with primary antibodies (intact VAMP-2 1:2000; Ab-VAMP$_{77}$ 1:2000) was performed overnight at 4 °C. Membranes were then washed with PBS-T and incubated at 4 °C with the appropriate HRP-conjugated secondary antibodies (1:5000) for 90 min. After extensive washings, signals were revealed with Luminata^{TM} using an Uvitec gel doc system (Uvitec, Cambridge, UK).

CGNs plated on cover glasses were washed with PBS and then fixed in 4% PFA in PBS for 15 min at room temperature for immunofluorescence analysis. PFA was quenched in 50 mM NH$_4$Cl PBS for 15 min. Neurons were then incubated for 3 min using 0.5% Triton X-100 in PBS for membrane permeabilization. Thereafter, cells were washed with PBS followed by 1 h of saturation (0.5% BSA in PBS) and incubated with primary antibodies (intact VAMP-2 1:200; VAMP$_{77}$ 1:200 diluted in PBS with 3% BSA) overnight at 4 °C. CGNs were then washed with PBS three times and incubated for 2 h at room temperature with appropriate secondary antibodies (1:200 diluted in PBS 3% BSA). After extensive washes with PBS, coverslips were finally mounted using Mounting Medium (Dako; Santa Clara, CA, USA) for fluorescence microscopy inspection.

4.5. Intramuscular Injection of BoNTs and TeNT

CD1 mice weighing 25–30 g were anesthetized with gaseous isoflurane and then injected with a sublethal dose of either BoNT/B (0.2 ng/kg) or BoNT/D (0.01 ng/kg) or BoNT/G (5 ng/kg) or TeNT (2 ng/kg), or vehicle (0.9% NaCl with 0.2% gelatin) at the level of the neck between the LAL muscles. Animals were then checked every 4 h. Mice treated with BoNTs were directly euthanized by cervical dislocation. The LAL muscles were directly collected and immediately fixed in 4% PFA for 30 min at room temperature. TeNT-treated mice were instead intracardiac perfused with PBS and immediately after with 4% PFA, and the brain stem was then collected and post-fixed for 1 h.

For rat experiments, male Wistar Han rats (University of Zagreb School of Medicine, Zagreb, Croatia), 3–4 months old, 350–450 g weights were anesthetized with ketamine/xylazine (70/7 mg·kg^{-1} i.p.), and then injected with a sublethal dose of BoNT/B (1 ng/kg) at the level of the gastrocnemius, or TeNT (0.1 ng/kg) in right whisker pad. The contralateral muscles were instead injected with vehicle (0.9% NaCl with saline 0.2% gelatin). After 48 h (BoNT/B) or 7 days (TeNT), rats were intracardiac perfused with PBS and immediately after with 4% PFA in PBS. Brain stems and solei were dissected and post-fixed for 1 h in 4% PFA in PBS.

LAL muscles from mice were used as a whole-mount preparation while the gastrocnemius from rats was separated in bundles of 10–20 myofibers under a dissection microscope.

For immunofluorescence staining, LAL and gastrocnemius muscle bundles were washed with PBS and quenched in 50 mM NH$_4$Cl in PBS for 20 min, then permeabilized and saturated in blocking solution (15% goat serum, 2% BSA, 0.25% gelatine, 0.20% glycine, 0.5% Triton X-100 in PBS) for 90 min. The muscles were then incubated with primary antibodies (v-AchT 1:500; intact VAMP-1 1:500; VAMP$_{77}$ 1:500) in blocking solution for 72 h at 4 °C, washed three times in PBS, and incubated with appropriate secondary antibodies (1:200 diluted in PBS 0.5% Triton X-100) for 2 h at room temperature. After extensive washes with PBS, the whole LAL and gastrocnemius bundles were mounted on coverslips using Mounting Medium (Dako) for fluorescence microscopy inspection.

Brain stems were frozen in OCT compound (Sakura Finetek, Torrance, CA, USA), cryosliced in 30 μm slices and left to dry at least for 12 h. Then, they were quenched in 50 mM NH_4Cl in PBS for 20 min, saturated and permeabilized for 1 h in blocking solution, and then added to primary antibodies (intact VAMP-2 1:500; $VAMP_{77}$ 1:500) in blocking solution overnight at 4 °C. Slices were then extensively washed and incubated with appropriate secondary antibodies (1:200 diluted in PBS 0.5% Triton X-100) for 90 min at room temperature. After extensive washes with PBS, slices were mounted on coverslips using Mounting Medium (Dako) for fluorescence microscopy inspection.

4.6. Microscopy

Samples from both neuronal culture and in vivo experiments were analyzed with a Leica SP5 Confocal microscope with a 40× HCX PL APO NA 1.4 oil immersion objective. Laser excitation line, power intensity, and emission range were chosen to minimize signal bleed-through. Laser excitation line, power intensity, and emission range were chosen according to each fluorophore in different samples to minimize bleed-through. Raw images were processed with ImageJ without altering the intensity of the signals.

Supplementary Materials: The following supporting information can be downloaded at: https://www.mdpi.com/article/10.3390/ijms23084355/s1.

Author Contributions: C.M., O.R. and M.P. conceived the project. F.F., P.Š. and I.M. performed and evaluated the experiments. T.B. produced and purified the recombinant toxins used in this study. A.T. immunized the rabbit and performed the blood sampling. M.P. and O.R. wrote the paper with contributions of C.M. and F.F. Conceptualization: C.M., O.R. and M.P.; methodology: F.F., P.Š., M.S. and I.M.; data curation: F.F., P.Š. and I.M.; original draft preparation: M.P. and O.R.; review and editing: C.M.; funding acquisition: C.M., O.R. and M.P. All authors have read and agreed to the published version of the manuscript.

Institutional Review Board Statement: Mice and Rabbits were handled by specialized personnel under the Veterinary Service of the Local Sanitary Service (ULSS 16-Padova) and the local officers of the Italian Ministry of Health. All experiments were performed in accordance with the Italian laws and policies (D.L. n° 26/2014 14 March 2014) and with the guidelines established by the European Community Council Directive n° 2010/63/UE and approved by the ethical committee and by the animal welfare coordinator of the OPBA, University of Padova and IZSV. All procedures are specified in the projects approved by the Italian Ministry of Health (authorization n° 81/2017, n°474/2019, and n° 265/2021). Rats were handled by specialized personnel and in accordance with international ethical directives for work on laboratory animals (Directive 2010/63/EU of the European Parliament and of the Council of 22 September 2010 on the protection of animals used for scientific purposes) and in accordance with the current Croatian Animal Protection Act (NN 102/17) and the Ordinance on the protection of animals used for scientific purposes (NN 55/13 with substitution 39/17 and 116/19).

Informed Consent Statement: Not applicable.

Data Availability Statement: All the data are contained in the article.

Conflicts of Interest: The authors declare no conflict of interest.

References

1. Rossetto, O.; Pirazzini, M.; Montecucco, C. Botulinum neurotoxins: Genetic, structural and mechanistic insights. *Nat. Rev. Microbiol.* **2014**, *12*, 535–549. [CrossRef] [PubMed]
2. Peck, M.W.; Smith, T.J.; Anniballi, F.; Austin, J.W.; Bano, L.; Bradshaw, M.; Cuervo, P.; Cheng, L.W.; Derman, Y.; Dorner, B.G.; et al. Historical Perspectives and Guidelines for Botulinum Neurotoxin Subtype Nomenclature. *Toxins* **2017**, *9*, 38. [CrossRef] [PubMed]
3. Smith, T.; Williamson, C.H.D.; Hill, K.; Sahl, J.; Keim, P.; Relman, D.A.; Collier, R.J. Botulinum Neurotoxin-Producing Bacteria. Isn't It Time that We Called a Species a Species? *mBio* **2018**, *9*, e01469-18. [CrossRef] [PubMed]
4. Rossetto, O.; Montecucco, C. Tables of Toxicity of Botulinum and Tetanus Neurotoxins. *Toxins* **2019**, *11*, 686. [CrossRef] [PubMed]

5. Sutton, R.B.; Fasshauer, D.; Jahn, R.; Brunger, A.T. Crystal structure of a SNARE complex involved in synaptic exocytosis at 2.4 A resolution. *Nature* **1998**, *395*, 347–353. [CrossRef]
6. Rizo, J. Molecular Mechanisms Underlying Neurotransmitter Release. *Annu. Rev. Biophys.* **2022**, *51*. [CrossRef]
7. Johnson, E.A.; Montecucco, C. Botulism. *Handb. Clin. Neurol.* **2008**, *91*, 333–368.
8. Pirazzini, M.; Rossetto, O.; Eleopra, R.; Montecucco, C. Botulinum Neurotoxins: Biology, Pharmacology, and Toxicology. *Pharmacol. Rev.* **2017**, *69*, 200–235. [CrossRef]
9. Yen, L.M.; Thwaites, C.L. Tetanus. *Lancet* **2019**, *393*, 1657–1668. [CrossRef]
10. Popoff, M.R. Tetanus in animals. *J. Vet. Diagn. Investig.* **2020**, *32*, 184–191. [CrossRef]
11. Megighian, A.; Pirazzini, M.; Fabris, F.; Rossetto, O.; Montecucco, C. Tetanus and tetanus neurotoxin: From peripheral uptake to central nervous tissue targets. *J. Neurochem.* **2021**, *158*, 1244–1253. [CrossRef] [PubMed]
12. Pirazzini, M.; Rossetto, O. Challenges in searching for therapeutics against Botulinum Neurotoxins. *Expert Opin. Drug Discov.* **2017**, *12*, 1–14. [CrossRef]
13. Rao, A.K.; Sobel, J.; Chatham-Stephens, K.; Luquez, C. Clinical Guidelines for Diagnosis and Treatment of Botulism, 2021. *MMWR Recomm. Rep.* **2021**, *70*, 1–30. [CrossRef] [PubMed]
14. Schiavo, G.; Benfenati, F.; Poulain, B.; Rossetto, O.; Polverino de Laureto, P.; DasGupta, B.R.; Montecucco, C. Tetanus and botulinum-B neurotoxins block neurotransmitter release by proteolytic cleavage of synaptobrevin. *Nature* **1992**, *359*, 832–835. [CrossRef]
15. Schiavo, G.; Santucci, A.; Dasgupta, B.R.; Mehta, P.P.; Jontes, J.; Benfenati, F.; Wilson, M.C.; Montecucco, C. Botulinum neurotoxins serotypes A and E cleave SNAP-25 at distinct COOH-terminal peptide bonds. *FEBS Lett.* **1993**, *335*, 99–103. [CrossRef]
16. Blasi, J.; Chapman, E.R.; Link, E.; Binz, T.; Yamasaki, S.; Camilli, P.D.; Sudhof, T.C.; Niemann, H.; Jahn, R. Botulinum neurotoxin A selectively cleaves the synaptic protein SNAP-25. *Nature* **1993**, *365*, 160–163. [CrossRef]
17. Schiavo, G.; Shone, C.C.; Rossetto, O.; Alexander, F.C.; Montecucco, C. Botulinum neurotoxin serotype F is a zinc endopeptidase specific for VAMP/synaptobrevin. *J. Biol. Chem.* **1993**, *268*, 11516–11519. [CrossRef]
18. Schiavo, G.; Rossetto, O.; Catsicas, S.; Polverino de Laureto, P.; DasGupta, B.R.; Benfenati, F.; Montecucco, C. Identification of the nerve terminal targets of botulinum neurotoxin serotypes A, D, and E. *J. Biol. Chem.* **1993**, *268*, 23784–23787. [CrossRef]
19. Schiavo, G.; Malizio, C.; Trimble, W.S.; Polverino de Laureto, P.; Milan, G.; Sugiyama, H.; Johnson, E.A.; Montecucco, C. Botulinum G neurotoxin cleaves VAMP/synaptobrevin at a single Ala-Ala peptide bond. *J. Biol. Chem.* **1994**, *269*, 20213–20216. [CrossRef]
20. Blasi, J.; Chapman, E.R.; Yamasaki, S.; Binz, T.; Niemann, H.; Jahn, R. Botulinum neurotoxin C1 blocks neurotransmitter release by means of cleaving HPC-1/syntaxin. *EMBO J.* **1993**, *12*, 4821–4828. [CrossRef]
21. Zanetti, G.; Sikorra, S.; Rummel, A.; Krez, N.; Duregotti, E.; Negro, S.; Henke, T.; Rossetto, O.; Binz, T.; Pirazzini, M. Botulinum neurotoxin C mutants reveal different effects of syntaxin or SNAP-25 proteolysis on neuromuscular transmission. *PLoS Pathog.* **2017**, *13*, e1006567. [CrossRef]
22. Neale, E.A.; Bowers, L.M.; Jia, M.; Bateman, K.E.; Williamson, L.C. Botulinum neurotoxin A blocks synaptic vesicle exocytosis but not endocytosis at the nerve terminal. *J. Cell Biol.* **1999**, *147*, 1249–1260. [CrossRef] [PubMed]
23. Wictome, M.; Newton, K.A.; Jameson, K.; Dunnigan, P.; Clarke, S.; Gaze, J.; Tauk, A.; Foster, K.A.; Shone, C.C. Development of in vitro assays for the detection of botulinum toxins in foods. *FEMS Immunol. Med. Microbiol.* **1999**, *24*, 319–323. [CrossRef] [PubMed]
24. Keller, J.E.; Cai, F.; Neale, E.A. Uptake of botulinum neurotoxin into cultured neurons. *Biochemistry* **2004**, *43*, 526–532. [CrossRef] [PubMed]
25. Dong, M.; Tepp, W.H.; Johnson, E.A.; Chapman, E.R. Using fluorescent sensors to detect botulinum neurotoxin activity in vitro and in living cells. *Proc. Natl. Acad. Sci. USA* **2004**, *101*, 14701–14706. [CrossRef]
26. Nuss, J.E.; Ruthel, G.; Tressler, L.E.; Wanner, L.M.; Torres-Melendez, E.; Hale, M.L.; Bavari, S. Development of cell-based assays to measure botulinum neurotoxin serotype A activity using cleavage-sensitive antibodies. *J. Biomol. Screen.* **2010**, *15*, 42–51. [CrossRef]
27. Kiris, E.; Nuss, J.E.; Burnett, J.C.; Kota, K.P.; Koh, D.C.; Wanner, L.M.; Torres-Melendez, E.; Gussio, R.; Tessarollo, L.; Bavari, S. Embryonic stem cell-derived motoneurons provide a highly sensitive cell culture model for botulinum neurotoxin studies, with implications for high-throughput drug discovery. *Stem Cell Res.* **2011**, *6*, 195–205. [CrossRef]
28. Restani, L.; Giribaldi, F.; Manich, M.; Bercsenyi, K.; Menendez, G.; Rossetto, O.; Caleo, M.; Schiavo, G. Botulinum neurotoxins A and E undergo retrograde axonal transport in primary motor neurons. *PLoS Pathog.* **2012**, *8*, e1003087. [CrossRef]
29. Pellett, S. Progress in cell based assays for botulinum neurotoxin detection. *Curr. Top. Microbiol. Immunol.* **2013**, *364*, 257–285. [CrossRef]
30. Rust, A.; Doran, C.; Hart, R.; Binz, T.; Stickings, P.; Sesardic, D.; Peden, A.A.; Davletov, B. A Cell Line for Detection of Botulinum Neurotoxin Type B. *Front. Pharmacol.* **2017**, *8*, 796. [CrossRef]
31. Meunier, F.r.A.; Lisk, G.; Sesardic, D.; Dolly, J.O. Dynamics of motor nerve terminal remodeling unveiled using SNARE-cleaving botulinum toxins: The extent and duration are dictated by the sites of SNAP-25 truncation. *Mol. Cell. Neurosci.* **2003**, *22*, 454–466. [CrossRef]
32. Duregotti, E.; Zanetti, G.; Scorzeto, M.; Megighian, A.; Montecucco, C.; Pirazzini, M.; Rigoni, M. Snake and Spider Toxins Induce a Rapid Recovery of Function of Botulinum Neurotoxin Paralysed Neuromuscular Junction. *Toxins* **2015**, *7*, 5322–5336. [CrossRef] [PubMed]

33. Barr, J.R.; Moura, H.; Boyer, A.E.; Woolfitt, A.R.; Kalb, S.R.; Pavlopoulos, A.; McWilliams, L.G.; Schmidt, J.G.; Martinez, R.A.; Ashley, D.L. Botulinum neurotoxin detection and differentiation by mass spectrometry. *Emerg. Infect. Dis.* **2005**, *11*, 1578–1583. [CrossRef]

34. Thirunavukkarasu, N.; Johnson, E.; Pillai, S.; Hodge, D.; Stanker, L.; Wentz, T.; Singh, B.; Venkateswaran, K.; McNutt, P.; Adler, M.; et al. Botulinum Neurotoxin Detection Methods for Public Health Response and Surveillance. *Front. Bioeng. Biotechnol.* **2018**, *6*, 80. [CrossRef] [PubMed]

35. von Berg, L.; Stern, D.; Pauly, D.; Mahrhold, S.; Weisemann, J.; Jentsch, L.; Hansbauer, E.-M.; Müller, C.; Avondet, M.A.; Rummel, A.; et al. Functional detection of botulinum neurotoxin serotypes A to F by monoclonal neoepitope-specific antibodies and suspension array technology. *Sci. Rep.* **2019**, *9*, 5531. [CrossRef] [PubMed]

36. Hobbs, R.J.; Thomas, C.A.; Halliwell, J.; Gwenin, C.D. Rapid Detection of Botulinum Neurotoxins-A Review. *Toxins* **2019**, *11*, 418. [CrossRef]

37. Caratelli, V.; Fillo, S.; D'Amore, N.; Rossetto, O.; Pirazzini, M.; Moccia, M.; Avitabile, C.; Moscone, D.; Lista, F.; Arduini, F. Paper-based electrochemical peptide sensor for on-site detection of botulinum neurotoxin serotype A and C. *Biosens. Bioelectron.* **2021**, *183*, 113210. [CrossRef]

38. Kegel, B.; Behrensdorf-Nicol, H.A.; Bonifas, U.; Silberbach, K.; Klimek, J.; Krämer, B.; Weisser, K. An in vitro assay for detection of tetanus neurotoxin activity: Using antibodies for recognizing the proteolytically generated cleavage product. *Toxicol. In Vitro* **2007**, *21*, 1641–1649. [CrossRef]

39. Whitemarsh, R.C.; Tepp, W.H.; Bradshaw, M.; Lin, G.; Pier, C.L.; Scherf, J.M.; Johnson, E.A.; Pellett, S. Characterization of botulinum neurotoxin a subtypes 1 through 5 by investigation of activities in mice, in neuronal cell cultures, and in vitro. *Infect. Immun.* **2013**, *81*, 3894–3902. [CrossRef]

40. Whitemarsh, R.C.; Tepp, W.H.; Johnson, E.A.; Pellett, S. Persistence of botulinum neurotoxin a subtypes 1-5 in primary rat spinal cord cells. *PLoS ONE* **2014**, *9*, e90252. [CrossRef]

41. Zanetti, G.; Azarnia Tehran, D.; Pirazzini, M.; Binz, T.; Shone, C.C.; Fillo, S.; Lista, F.; Rossetto, O.; Montecucco, C. Inhibition of botulinum neurotoxins interchain disulfide bond reduction prevents the peripheral neuroparalysis of botulism. *Biochem. Pharmacol.* **2015**, *98*, 522–530. [CrossRef] [PubMed]

42. Zanetti, G.; Mattarei, A.; Lista, F.; Rossetto, O.; Montecucco, C.; Pirazzini, M. Novel Small Molecule Inhibitors That Prevent the Neuroparalysis of Tetanus Neurotoxin. *Pharmaceuticals* **2021**, *14*, 1134. [CrossRef] [PubMed]

43. Antonucci, F.; Rossi, C.; Gianfranceschi, L.; Rossetto, O.; Caleo, M. Long-distance retrograde effects of botulinum neurotoxin A. *J. Neurosci.* **2008**, *28*, 3689–3696. [CrossRef] [PubMed]

44. Restani, L.; Antonucci, F.; Gianfranceschi, L.; Rossi, C.; Rossetto, O.; Caleo, M. Evidence for Anterograde Transport and Transcytosis of Botulinum Neurotoxin A (BoNT/A). *J. Neurosci.* **2011**, *31*, 15650–15659. [CrossRef]

45. Caleo, M.; Spinelli, M.; Colosimo, F.; Matak, I.; Rossetto, O.; Lackovic, Z.; Restani, L. Transynaptic Action of Botulinum Neurotoxin Type A at Central Cholinergic Boutons. *J. Neurosci.* **2018**, *38*, 10329–10337. [CrossRef]

46. Restani, L.; Novelli, E.; Bottari, D.; Leone, P.; Barone, I.; Galli-Resta, L.; Strettoi, E.; Caleo, M. Botulinum neurotoxin A impairs neurotransmission following retrograde transynaptic transport. *Traffic* **2012**, *13*, 1083–1089. [CrossRef]

47. Matak, I. Evidence for central antispastic effect of botulinum toxin type A. *Br. J. Pharmacol.* **2020**, *177*, 65–76. [CrossRef]

48. Matak, I.; Rossetto, O.; Lackovic, Z. Botulinum toxin type A selectivity for certain types of pain is associated with capsaicin-sensitive neurons. *Pain* **2014**, *155*, 1516–1526. [CrossRef]

49. Matak, I.; Riederer, P.; Lackovic, Z. Botulinum toxin's axonal transport from periphery to the spinal cord. *Neurochem. Int.* **2012**, *61*, 236–239. [CrossRef]

50. Matak, I.; Bach-Rojecky, L.; Filipović, B.; Lacković, Z. Behavioral and immunohistochemical evidence for central antinociceptive activity of botulinum toxin A. *Neuroscience* **2011**, *186*, 201–207. [CrossRef]

51. Cai, B.B.; Francis, J.; Brin, M.F.; Broide, R.S. Botulinum neurotoxin type A-cleaved SNAP25 is confined to primary motor neurons and localized on the plasma membrane following intramuscular toxin injection. *Neuroscience* **2017**, *352*, 155–169. [CrossRef] [PubMed]

52. Rhéaume, C.; Cai, B.B.; Wang, J.; Fernández-Salas, E.; Aoki, K.R.; Francis, J.; Broide, R.S. A Highly Specific Monoclonal Antibody for Botulinum Neurotoxin Type A-Cleaved SNAP25. *Toxins* **2015**, *7*, 2354–2370. [CrossRef] [PubMed]

53. Pirazzini, M.; Rossetto, O.; Bolognese, P.; Shone, C.C.; Montecucco, C. Double anchorage to the membrane and intact inter-chain disulfide bond are required for the low pH induced entry of tetanus and botulinum neurotoxins into neurons. *Cell Microbiol.* **2011**, *13*, 1731–1743. [CrossRef] [PubMed]

54. Sun, S.; Suresh, S.; Liu, H.; Tepp, W.H.; Johnson, E.A.; Edwardson, J.M.; Chapman, E.R. Receptor binding enables botulinum neurotoxin B to sense low pH for translocation channel assembly. *Cell Host Microbe* **2011**, *10*, 237–247. [CrossRef]

55. Peng, L.; Adler, M.; Demogines, A.; Borrell, A.; Liu, H.; Tao, L.; Tepp, W.H.; Zhang, S.-C.; Johnson, E.A.; Sawyer, S.L.; et al. Widespread Sequence Variations in VAMP1 across Vertebrates Suggest a Potential Selective Pressure from Botulinum Neurotoxins. *PLoS Pathog.* **2014**, *10*, e1004177. [CrossRef]

56. Keller, J.E.; Neale, E.A. The role of the synaptic protein snap-25 in the potency of botulinum neurotoxin type A. *J. Biol. Chem.* **2001**, *276*, 13476–13482. [CrossRef]

57. Keller, J.E.; Neale, E.A.; Oyler, G.; Adler, M. Persistence of botulinum neurotoxin action in cultured spinal cord cells. *FEBS Lett.* **1999**, *456*, 137–142. [CrossRef]

58. Fischer, A.; Mushrush, D.J.; Lacy, D.B.; Montal, M. Botulinum neurotoxin devoid of receptor binding domain translocates active protease. *PLoS Pathog.* **2008**, *4*, e1000245. [CrossRef]

59. Pellett, S.; Tepp, W.H.; Clancy, C.M.; Borodic, G.E.; Johnson, E.A. A neuronal cell-based botulinum neurotoxin assay for highly sensitive and specific detection of neutralizing serum antibodies. *FEBS Lett.* **2007**, *581*, 4803–4808. [CrossRef]

60. Wang, D.; Zhang, Z.; Dong, M.; Sun, S.; Chapman, E.R.; Jackson, M.B. Syntaxin requirement for Ca^{2+}-triggered exocytosis in neurons and endocrine cells demonstrated with an engineered neurotoxin. *Biochemistry* **2011**, *50*, 2711–2713. [CrossRef]

61. Pier, C.L.; Chen, C.; Tepp, W.H.; Lin, G.; Janda, K.D.; Barbieri, J.T.; Pellett, S.; Johnson, E.A. Botulinum neurotoxin subtype A2 enters neuronal cells faster than subtype A1. *FEBS Lett.* **2011**, *585*, 199–206. [CrossRef] [PubMed]

62. Jones, R.G.; Ochiai, M.; Liu, Y.; Ekong, T.; Sesardic, D. Development of improved SNAP25 endopeptidase immuno-assays for botulinum type A and E toxins. *J. Immunol. Methods* **2008**, *329*, 92–101. [CrossRef] [PubMed]

63. Wild, E.; Bonifas, U.; Klimek, J.; Trösemeier, J.H.; Krämer, B.; Kegel, B.; Behrensdorf-Nicol, H.A. In vitro potency determination of botulinum neurotoxin B based on its receptor-binding and proteolytic characteristics. *Toxicol. In Vitro* **2016**, *34*, 97–104. [CrossRef] [PubMed]

64. Gray, B.; Cadd, V.; Elliott, M.; Beard, M. The in vitro detection of botulinum neurotoxin-cleaved endogenous VAMP is epitope-dependent. *Toxicol. In Vitro* **2018**, *48*, 255–261. [CrossRef] [PubMed]

65. Mechaly, A.; Diamant, E.; Alcalay, R.; Ben David, A.; Dor, E.; Torgeman, A.; Barnea, A.; Girshengorn, M.; Levin, L.; Epstein, E.; et al. Highly Specific Monoclonal Antibody Targeting the Botulinum Neurotoxin Type E Exposed SNAP-25 Neoepitope. *Antibodies* **2022**, *11*, 21. [CrossRef]

66. Costantin, L.; Bozzi, Y.; Richichi, C.; Viegi, A.; Antonucci, F.; Funicello, M.; Gobbi, M.; Mennini, T.; Rossetto, O.; Montecucco, C.; et al. Antiepileptic Effects of Botulinum Neurotoxin E. *J. Neurosci.* **2005**, *25*, 1943. [CrossRef]

67. Coelho, A.; Oliveira, R.; Rossetto, O.; Cruz, C.D.; Cruz, F.; Avelino, A. Intrathecal administration of botulinum toxin type A improves urinary bladder function and reduces pain in rats with cystitis. *Eur. J. Pain* **2014**, *18*, 1480–1489. [CrossRef]

68. Azarnia Tehran, D.; Pirazzini, M. Preparation of Cerebellum Granule Neurons from Mouse or Rat Pups and Evaluation of Clostridial Neurotoxin Activity and Their Inhibitors by Western Blot and Immunohistochemistry. *Bio-Protocol* **2018**, *8*, e2918. [CrossRef]

69. Trimble, W.S.; Cowan, D.M.; Scheller, R.H. VAMP-1: A synaptic vesicle-associated integral membrane protein. *Proc. Natl. Acad. Sci. USA* **1988**, *85*, 4538–4542. [CrossRef]

70. Baumert, M.; Maycox, P.R.; Navone, F.; De Camilli, P.; Jahn, R. Synaptobrevin: An integral membrane protein of 18,000 daltons present in small synaptic vesicles of rat brain. *EMBO J.* **1989**, *8*, 379–384. [CrossRef]

71. Südhof, T.C.; Baumert, M.; Perin, M.S.; Jahn, R. A synaptic vesicle membrane protein is conserved from mammals to Drosophila. *Neuron* **1989**, *2*, 1475–1481. [CrossRef]

72. Patarnello, T.; Bargelloni, L.; Rossetto, O.; Schiavo, G.; Montecucco, C. Neurotransmission and secretion. *Nature* **1993**, *364*, 581–582. [CrossRef] [PubMed]

73. Rossetto, O.; Seveso, M.; Caccin, P.; Schiavo, G.; Montecucco, C. Tetanus and botulinum neurotoxins: Turning bad guys into good by research. *Toxicon* **2001**, *39*, 27–41. [CrossRef]

74. Mellanby, J.; Beaumont, M.A.; Thompson, P.A. The effect of lanthanum on nerve terminals in goldfish muscle after paralysis with tetanus toxin. *Neuroscience* **1988**, *25*, 1095–1106. [CrossRef]

75. Hunt, J.M.; Bommert, K.; Charlton, M.P.; Kistner, A.; Habermann, E.; Augustine, G.J.; Betzt, H. A post-docking role for synaptobrevin in synaptic vesicle fusion. *Neuron* **1994**, *12*, 1269–1279. [CrossRef]

76. Juzans, P.; Comella, J.X.; Molgo, J.; Faille, L.; Angaut-Petit, D. Nerve terminal sprouting in botulinum type-A treated mouse levator auris longus muscle. *Neuromuscul. Disord. NMD* **1996**, *6*, 177–185. [CrossRef]

77. Comella, J.X.; Molgo, J.; Faille, L. Sprouting of mammalian motor nerve terminals induced by in vivo injection of botulinum type-D toxin and the functional recovery of paralysed neuromuscular junctions. *Neurosci. Lett.* **1993**, *153*, 61–64. [CrossRef]

78. Negro, S.; Lessi, F.; Duregotti, E.; Aretini, P.; La Ferla, M.; Franceschi, S.; Menicagli, M.; Bergamin, E.; Radice, E.; Thelen, M.; et al. CXCL12alpha/SDF-1 from perisynaptic Schwann cells promotes regeneration of injured motor axon terminals. *EMBO Mol. Med.* **2017**. [CrossRef]

79. Mazzocchio, R.; Caleo, M. More than at the neuromuscular synapse: Actions of botulinum neurotoxin A in the central nervous system. *Neurosci. Rev. J. Bringing Neurobiol. Neurol. Psychiatry* **2015**, *21*, 44–61. [CrossRef]

80. Caleo, M.; Schiavo, G. Central effects of tetanus and botulinum neurotoxins. *Toxicon* **2009**, *54*, 593–599. [CrossRef]

81. Matak, I.; Lackovic, Z. Botulinum toxin A, brain and pain. *Prog. Neurobiol.* **2014**, *119-120*, 39–59. [CrossRef] [PubMed]

82. Paxinos, G.; Keith, B.J.; Franklin, M. *Paxinos and Franklin's the Mouse Brain in Stereotaxic Coordinates*; Elsevier Science: Amsterdam, The Netherlands, 2012.

83. Binz, T. Clostridial neurotoxin light chains: Devices for SNARE cleavage mediated blockade of neurotransmission. *Curr. Top. Microbiol. Immunol.* **2013**, *364*, 139–157. [CrossRef] [PubMed]

84. Schiavo, G.; Matteoli, M.; Montecucco, C. Neurotoxins affecting neuroexocytosis. *Physiol. Rev.* **2000**, *80*, 717–766. [CrossRef] [PubMed]

85. Lang, J.; Regazzi, R.; Wollheim, C.B. Clostridial Toxins and Endocrine Secretion: Their Use in Insulin-Secreting Cells. In *Bact. Toxins*; WILEY-VCH Verlag GmbH & Co: Weinheim, Germany, 1997; pp. 217–240.

86. Eisel, U.; Reynolds, K.; Riddick, M.; Zimmer, A.; Niemann, H.; Zimmer, A. Tetanus toxin light chain expression in Sertoli cells of transgenic mice causes alterations of the actin cytoskeleton and disrupts spermatogenesis. *EMBO J.* **1993**, *12*, 3365–3372. [CrossRef]

87. Sweeney, S.T.; Broadie, K.; Keane, J.; Niemann, H.; O'Kane, C.J. Targeted expression of tetanus toxin light chain in Drosophila specifically eliminates synaptic transmission and causes behavioral defects. *Neuron* **1995**, *14*, 341–351. [CrossRef]

88. Pasti, L.; Zonta, M.; Pozzan, T.; Vicini, S.; Carmignoto, G. Cytosolic calcium oscillations in astrocytes may regulate exocytotic release of glutamate. *J. Neurosci.* **2001**, *21*, 477–484. [CrossRef]

89. Yamamoto, M.; Wada, N.; Kitabatake, Y.; Watanabe, D.; Anzai, M.; Yokoyama, M.; Teranishi, Y.; Nakanishi, S. Reversible Suppression of glutamatergic neurotransmission of cerebellar granule cells in vivo by genetically manipulated expression of tetanus neurotoxin light chain. *J. Neurosci.* **2003**, *23*, 6759. [CrossRef]

90. Hilton, B.J.; Husch, A.; Schaffran, B.; Lin, T.-c.; Burnside, E.R.; Dupraz, S.; Schelski, M.; Kim, J.; Müller, J.A.; Schoch, S.; et al. An active vesicle priming machinery suppresses axon regeneration upon adult CNS injury. *Neuron* **2022**, *110*, 51–69.e57. [CrossRef]

91. Liu, Q.; Sinnen, B.L.; Boxer, E.E.; Schneider, M.W.; Grybko, M.J.; Buchta, W.C.; Gibson, E.S.; Wysoczynski, C.L.; Ford, C.P.; Gottschalk, A.; et al. A Photoactivatable Botulinum Neurotoxin for Inducible Control of Neurotransmission. *Neuron* **2019**, *101*, 863–875.e866. [CrossRef]

92. Rummel, A.; Mahrhold, S.; Bigalke, H.; Binz, T. The HCC-domain of botulinum neurotoxins A and B exhibits a singular ganglioside binding site displaying serotype specific carbohydrate interaction. *Mol. Microbiol.* **2004**, *51*, 631–643. [CrossRef]

93. Schiavo, G.; Montecucco, C. Tetanus and botulism neurotoxins: Isolation and assay. *Methods Enzym.* **1995**, *248*, 643–652.

94. Rossetto, O.; Gorza, L.; Schiavo, G.; Schiavo, N.; Scheller, R.H.; Montecucco, C. VAMP/synaptobrevin isoforms 1 and 2 are widely and differentially expressed in nonneuronal tissues. *J. Cell Biol.* **1996**, *132*, 167–179. [CrossRef] [PubMed]

Appendix IV

Fabris F, Varani S, Tonellato M, Matak I, Šoštarić P, Meglić P, Caleo M, Megighian A, Rossetto O, Montecucco C, Pirazzini M. **Facial neuromuscular junctions and brainstem nuclei are the target of tetanus neurotoxin in cephalic tetanus.** JCI Insight. 2023;8;8(11) (Q1)

Petra Šoštarić Mužić -acquisition, analysis, and interpretation of data for the work, reviewing, and editing the manuscriot for publication.

Fabris Federico - acquisition, analysis, and interpretation of data for the work, reviewing, and editing the manuscriot for publication.

Varani Stefano- acquisition, analysis, and interpretation of data for the work, reviewing, and editing the manuscriot for publication.

Tonellato Marika - acquisition, analysis, and interpretation of data for the work, reviewing, and editing the manuscriot for publication.

Matak Ivica- acquisition, analysis, and interpretation of data for the work, reviewing, and editing the manuscriot for publication.

Meglić Patrik- acquisition, analysis, and interpretation of data for the work, reviewing, and editing the manuscriot for publication.

Caleo Matteo- reviewing and editing the manuscriot for publication.

Megighian Aran- reviewing and editing the manuscriot for publication.

Rossetto Ornella- contributions to the conception and design of the work, writing, reviewing, and editing the manuscriot for publication.

Montecucco Cesare- contributions to the conception and design of the work, writing, reviewing, and editing the manuscriot for publication.

Pirazzini Marco- contributions to the conception and design of the work, writing, reviewing, and editing the manuscriot for publication.

Web link: https://insight.jci.org/articles/view/166978

JCI insight

Facial neuromuscular junctions and brainstem nuclei are the target of tetanus neurotoxin in cephalic tetanus

Federico Fabris,[1] Stefano Varani,[1] Marika Tonellato,[1] Ivica Matak,[2] Petra Šoštarić,[2] Patrik Meglić,[2] Matteo Caleo,[1] Aram Megighian,[1,3] Ornella Rossetto,[1,4,5] Cesare Montecucco,[1,4] and Marco Pirazzini[1,5]

[1]Department of Biomedical Sciences, University of Padua, Padua, Italy. [2]Department of Pharmacology, School of Medicine, University of Zagreb, Zagreb, Croatia. [3]Padua Neuroscience Center, University of Padua, Padua, Italy. [4]Institute of Neuroscience, National Research Council, Padua, Italy. [5]Interdepartmental Research Center of Myology (CIR-Myo), University of Padua, Padua, Italy.

Cephalic tetanus (CT) is a severe form of tetanus that follows head wounds and the intoxication of cranial nerves by tetanus neurotoxin (TeNT). Hallmarks of CT are cerebral palsy, which anticipates the spastic paralysis of tetanus, and rapid evolution of cardiorespiratory deficit even without generalized tetanus. How TeNT causes this unexpected flaccid paralysis, and how the canonical spasticity then rapidly evolves into cardiorespiratory defects, remain unresolved aspects of CT pathophysiology. Using electrophysiology and immunohistochemistry, we demonstrate that TeNT cleaves its substrate vesicle-associated membrane protein within facial neuromuscular junctions and causes a botulism-like paralysis overshadowing tetanus spasticity. Meanwhile, TeNT spreads among brainstem neuronal nuclei and, as shown by an assay measuring the ventilation ability of CT mice, harms essential functions like respiration. A partial axotomy of the facial nerve revealed a potentially new ability of TeNT to undergo intra-brainstem diffusion, which allows the toxin to spread to brainstem nuclei devoid of direct peripheral efferents. This mechanism is likely to be involved in the transition from local to generalized tetanus. Overall, the present findings suggest that patients with idiopathic facial nerve palsy should be immediately considered for CT and treated with antisera to block the potential progression to a life-threatening form of tetanus.

Introduction

Tetanus neurotoxin (TeNT) is a 150 kDa protein released by *Clostridium tetani* during infections of necrotic wounds, which causes a life-threatening neuroparalytic syndrome characterized by tonic muscle contractions and painful muscle spasticity (1–3).

Tetanus pathogenesis begins with the entry of TeNT into peripheral nerve terminals followed by retroaxonal transport and release into the spinal cord and brainstem (4–8). Therein, the toxin enters the synaptic terminals of inhibitory interneurons via synaptic vesicle endocytosis (9) and translocates its catalytic metalloprotease domain in the presynaptic cytosol (10), where it cleaves a single-peptide bond of vesicle-associated membrane protein (VAMP) (11). This biochemical lesion disrupts the molecular machinery responsible for synaptic vesicle fusion, with the presynaptic membrane inhibiting the release of inhibitory neurotransmitters, which in turn leads to motoneuron overexcitability and muscle spastic paralysis (5).

Tetanus can be effectively prevented via vaccination with a formalin-inactivated TeNT (tetanus toxoid) or by passive immunization with anti-TeNT immunoglobulins, which is the prophylactic therapy used with patients presenting in the emergency room with necrotic skin wounds and uncertain vaccination status (3, 8, 12, 13). Nonetheless, tetanus remains a major killer in low-income countries, where vaccination and antisera availability are limited, and where the disease affects particularly newborns in the tremendous form of *tetanus neonatorum* (12–15). Novel research for inexpensive chemical inhibitors of TeNT should be encouraged (16).

The spastic paralysis of tetanus starts from the face with lockjaw (trismus), distortion of mouth and eyes (risus sardonicus), followed by neck stiffness and trunk arching (opisthotonos). Spasticity progresses in a descending manner and eventually affects all muscles, causing body exhaustion and patient death

by a cardiorespiratory deficit (17). When a limited amount of TeNT is released in a confined anatomical area, a local form of tetanus develops with the involvement of regional muscles. This disease can then evolve into generalized tetanus depending on the further release of TeNT (2).

A rare (about 3% of cases), yet particularly dangerous, form of tetanus is cephalic tetanus (CT), which develops from infections of craniofacial wounds, of the inner ear, or of mouth gingivae with *C. tetani* spores. CT begins with a peculiar botulism-like cranial nerve palsy that generally precedes, or sometimes accompanies, trismus and risus sardonicus (17–19). This unusual manifestation complicates the diagnosis of tetanus, which often goes unsuspected for days, causing an unfavorable delay in the pharmacological intervention. For this reason, CT is a form of tetanus accompanied by a poor prognosis (17) because CT patients can rapidly develop cardiorespiratory deficits before, or even without, generalized spasticity (20–22).

How TeNT causes overlapping flaccid and spastic paralysis and how this can then rapidly evolve into cardiorespiratory defects remain unresolved aspects of CT pathophysiology.

Using a rodent model of CT based on the local injection of TeNT in the whisker pad and the use of an antibody that recognizes with high specificity TeNT-cleaved VAMP, but not intact VAMP (23), we show here that CT facial palsy is caused by the TeNT-mediated proteolysis of VAMP within the neuromuscular junctions (NMJs) of facial muscles. This action precedes and then overlaps with the canonical spastic paralysis ascribed to the TeNT activity within inhibitory interneurons of the spinal cord. We also report that specific nuclei of the brainstem are affected in CT and that TeNT can spread to other brainstem nuclei controlling critical functions, including mastication, deglutition, and respiration, via both peripheral diffusion and intraparenchymal dissemination of the toxin. These findings explain why CT can rapidly evolve into a life-threatening form of tetanus and suggest that patients presenting a facial nerve palsy of unknown origin should be immediately considered for CT and treated with the effective injection of human anti-TeNT immunoglobulins.

Results

TeNT local injection in the mouse whisker pad recapitulates human CT. To study CT pathophysiology, we established an experimental model in rodents based on the local injection of TeNT into the whisker pad (WP), the group of muscles responsible for vibrissa movement in whisking animals. The WP receives sensorimotor innervation from the facial nerve, and its neuromuscular activity can be recorded via live imaging of vibrissae in head-fixed animals (24) and by compound muscle action potential (CMAP) electromyography in anesthetized animals (25). Both techniques allow the monitoring of WP activity with time, which offers the advantage of evaluating TeNT effects in the same animal before and after toxin inoculation (Figure 1A). While naive mice freely moved their vibrissae, covering a wide angle depending on the whisking activity, TeNT-treated mice progressively lost the ability to move the ipsilateral WP, and vibrissae bent toward the jaw, appearing fully paralyzed after 1 day, a condition persisting also at days 3 and 5 (Figure 1B and Supplemental Videos 1–4; supplemental material available online with this article; https://doi.org/10.1172/jci.insight.166978DS1). Conversely, contralateral vibrissae were normal on day 1 but progressively stacked around their position, appearing paralyzed by day 5, though differently from ipsilateral ones. To characterize the 2 types of paralysis, we assessed neurotransmission at the NMJ by CMAP electromyography (Figure 1C). Facial nerve stimulation in naive mice elicited CMAP displaying a biphasic trace in both WPs, while TeNT provoked a marked reduction of maximal CMAP amplitude in the ipsilateral WPs at all time points, an indication of defective neurotransmitter release at the NMJ suggestive of flaccid paralysis (Figure 1C). To further test this possibility, we compared the TeNT-induced paralysis with that caused by botulinum neurotoxin type B (BoNT/B), another clostridial neurotoxin long known to cause flaccid paralysis by cleaving VAMP at the NMJ at the same peptide bond cleaved by TeNT (11, 23). In head-fixed mice, BoNT/B injection elicited a paralysis of the vibrissae that closely resembled the one caused by TeNT (Supplemental Video 5), and, consistently, the CMAP electromyography showed a strong decrease in amplitude (Supplemental Figure 1). Interestingly, the decrease in CMAP amplitude caused by TeNT recovered by day 5, indicating that this paralytic effect is rapidly reversible in mice. At the same time, contralateral WPs displayed no changes in CMAP traces and amplitude as occurred in naive mice, indicating that TeNT produces its local effect only in injected muscles.

Together, these results suggest that the action of TeNT at the NMJ is similar to the one of botulinum neurotoxins, does not cause degeneration of the motor axon terminals or the death of the motoneurons, and is rapidly reversed (8, 26, 27). This botulism-like paralysis in injected muscles is then followed, in a few hours, by the canonical spastic paralysis of other head muscles, found here in the contralateral WP muscle.
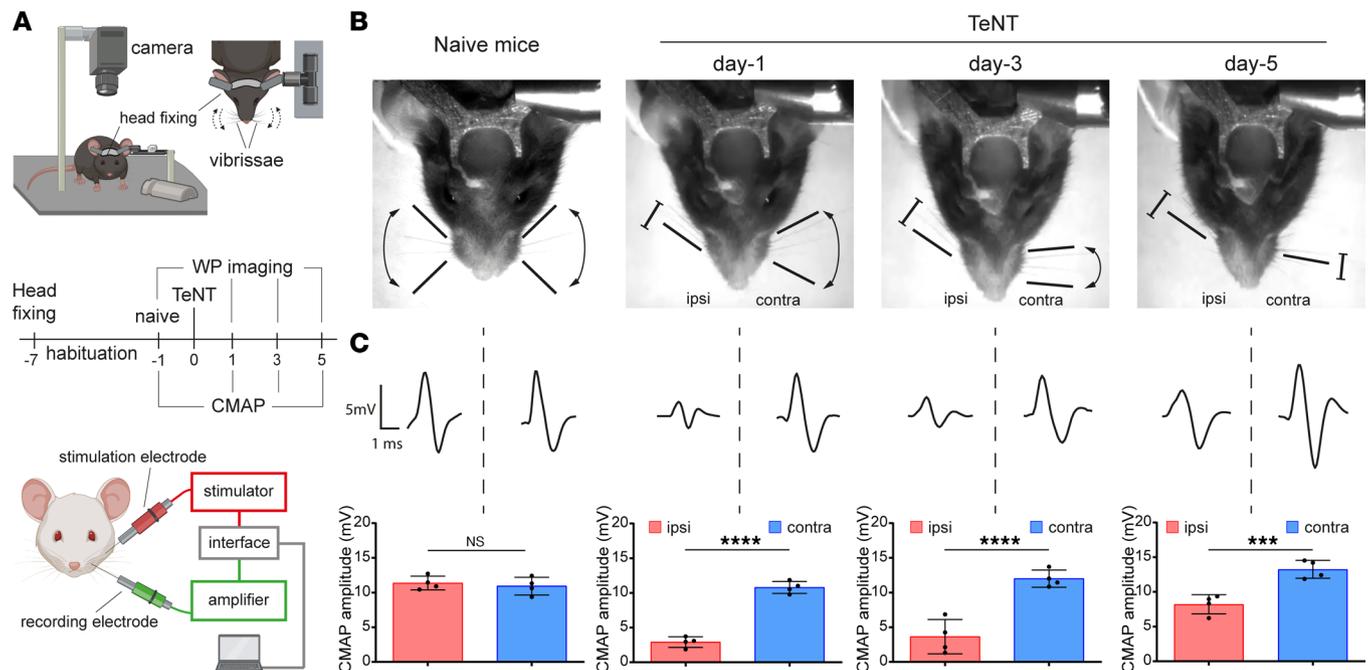
Figure 1. TeNT causes a botulinum neurotoxin–like flaccid paralysis upon injection in the WP in a model of CT. (A) The top panel illustrates the experimental setup to video record WP activity in head-fixed mice in a model of CT upon TeNT injection in the WP (1 ng/kg in a final volume of 1 μL) as a model of CT. Mice are held at the center of a mouse arena through a metal bar cemented to the skull; an infrared camera is positioned on top of the mouse snout to record the whisking activity. The bottom panel schematizes the apparatus to measure the compound muscle action potential (CMAP): the green electrode records WP myofibers' depolarization elicited by facial nerve stimulation through the red electrode; stimulation and signal amplification are controlled with a computer connected via an interface. The central panel shows the time course of a typical experiment for WP video recording and CMAP analysis across TeNT injection in the WP. **(B)** Representative video frames showing the whisking ability in naive mice and at indicated time points after TeNT inoculation in injected (ipsi) and noninjected (contra) WPs; black arrows and bars indicate the movement ability of the vibrissae as deduced from recorded videos; segments with blunt ends indicate full paralysis. **(C)** Representative traces of CMAP recordings in ipsi and contra WP (top) and their quantification (bottom) at indicated times after TeNT injection. Data are expressed as means ± SD; ***$P < 0.001$, ****$P < 0.0001$ assessed by Student's t test. Black circles indicate the number of animals used in the experiment.

These findings are reminiscent of what occurs in human CT in patients manifesting simultaneously a flaccid and spastic paralysis of facial muscles (please see ref. 19 for a direct comparison), thus qualifying this mouse model for the study of the molecular pathogenesis of CT.

CT flaccid paralysis is caused by the TeNT-mediated cleavage of VAMP within motor axon terminals of facial NMJs. Based on CMAP findings, we hypothesized that CT nerve palsy could derive from the direct activity of TeNT at the NMJs of the WP muscle. To test this possibility, we isolated the ipsilateral and contralateral WPs at different time points after TeNT injection and stained the muscles with an antibody that specifically recognizes VAMP only after TeNT proteolysis (hereafter indicated as cl-VAMP), not before cleavage (23). The postsynaptic membrane of the NMJs was stained with fluorescent α-bungarotoxin, which binds tightly to nicotinic acetylcholine receptors (AChRs). WPs injected with saline did not show cl-VAMP staining (Figure 2A), similarly to WPs contralateral to the injection side, throughout the entire course of TeNT intoxication (Figure 2B and Supplemental Figure 2A). Conversely, a clear staining of cl-VAMP appeared in the ipsilateral WPs (Figure 2C). This signal was localized within presynaptic terminals and associated with synaptic vesicles, as indicated by its colocalization with the vesicular acetylcholine transporter (VAChT), a protein marker of these organelles (Figure 2D). Consistent with the time course of CMAP amplitude, NMJ staining quantification showed that the number of cl-VAMP–positive synapses peaked at day 1 and then gradually decreased with time (Figure 2E).

To monitor the correlation between VAMP cleavage and flaccid paralysis, a dose dependence study was performed by injecting increasing doses of TeNT. A dose of 0.25 pg/g did not cause evident cleavage of VAMP at the NMJ (Supplemental Figure 2, B and C), and, consistently, CMAP amplitude was not altered (Supplemental Figure 2D), indicating that TeNT did not cause flaccid paralysis at this dosage. At the same time, injected animals developed spastic paralysis about 2 days after injection. At 0.5 pg/g, TeNT caused a VAMP cleavage lower than the one obtained with 1 pg/g. In parallel, CMAP showed an intermediate decrease in amplitude, indicating that there is a correlation between VAMP cleavage at the NMJ and
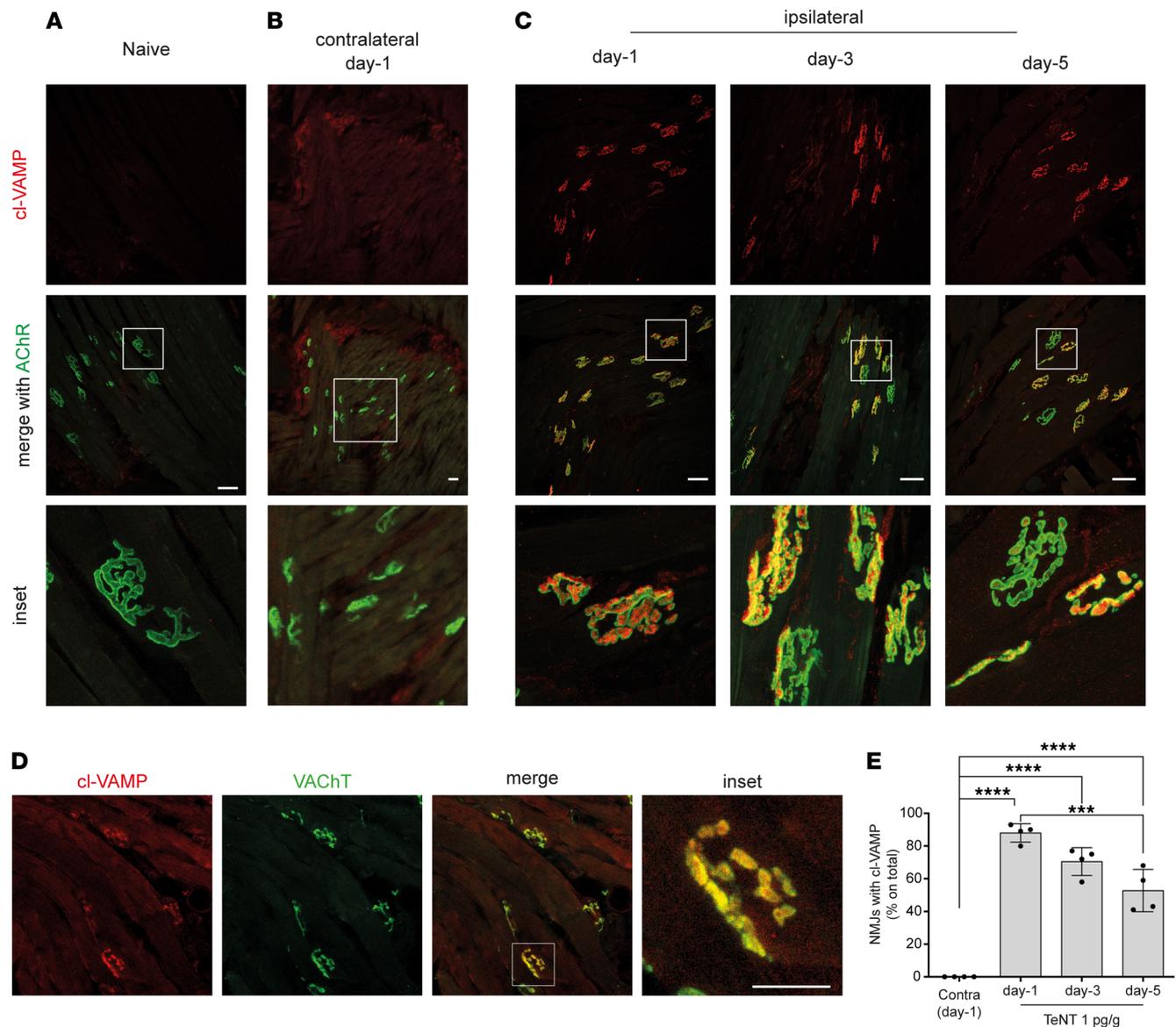
Figure 2. TeNT cleaves its target VAMP at motor axon terminals of the WP in mice. Confocal images of WP musculature from (**A**) naive and TeNT-treated mice (**B**) contralateral or (**C**) ipsilateral to injection at indicated times after injection; the red signal indicates the cleavage of VAMP at the NMJ identified through the labeling of nicotinic acetylcholine receptors (AChR, shown in green) with fluorescent α-bungarotoxin; insets show a 5× original magnification (**A** and **C**) and 3× original magnification in **B**. (**D**) Confocal images showing colocalization between cl-VAMP (red) and the vesicular transporter of acetylcholine (VAChT, green), a protein marker of synaptic vesicles, as expected from TeNT cleavage of VAMP on synaptic vesicles at the motor axon terminal; scale bar, 50 μm. (**E**) Quantification reporting the percentage of NMJs positive for the signal of cl-VAMP in the ipsilateral WP at indicated time points after TeNT injection compared with the contralateral at day 1. Data are expressed as means ± SD; ***$P < 0.001$; ****$P < 0.0001$ assessed by 1-way ANOVA with Bonferroni's test. Black circles indicate the number of animals used in the experiment.

TeNT-induced flaccid paralysis. Together with the progressive loss of cl-VAMP staining accompanying the functional recovery at day 5, these results also suggest that the reversible nature of TeNT paralysis at the NMJ depends on the degradation of the TeNT light chain within axon terminals and turnover of cl-VAMP, as reported for the other botulinum neurotoxins cleaving different soluble NSF attachment protein receptor (SNARE) proteins (27–29).

To provide further evidence that VAMP cleavage causes TeNT-induced flaccid paralysis, we extended the experiment to rats. This species carries a point mutation at the cleavage site of VAMP-1, rendering it resistant to TeNT proteolysis (Figure 3A). This is an effective biochemical knockin model (23, 30). Rats have long vibrissae whose movements can be simply and easily monitored via video recording with a high-speed camera (Supplemental Video 6). We examined their movements from proximal and distal positions with

respect to the caudal part of the body (cartoons of Figure 3B). These 2 positions were identified both in naive rats (Figure 3B) and in injected rats on day 1 (Figure 3C and Supplemental Video 7), suggesting that vibrissae movements did not display obvious alterations in both injected and noninjected WPs. At variance, ipsilateral whiskers began to remain stacked in between the distal and proximal positions on day 3 and appeared fully paralyzed by day 5 (Figure 3C and Supplemental Videos 8 and 9). To discriminate whether paralysis was flaccid or spastic, we performed a CMAP analysis. Both injected and contralateral WPs displayed a normal neuromuscular transmission, indicating a spastic paralysis (Figure 3, D and E). Consistently, we failed to detect the staining of cl-VAMP in the motor axon terminals of injected WPs (Figure 3F).

Together, these results show for the first time to our knowledge that TeNT can cleave VAMP in the cytosol of peripheral motor axon terminals, causing (in susceptible species) a reversible flaccid paralysis similar to that caused by botulinum neurotoxins.

The peripheral effect of TeNT at the NMJ is dominant on its central activity within inhibitory interneurons in the FN. The above results account for the molecular origin of CT facial palsy. Yet, the cardinal and most dangerous symptom of CT is the spastic paralysis of the head and facial muscles, rapidly followed by dysfunction of swallowing, respiration, and heart function (17, 18, 21). Accordingly, the brainstem areas corresponding to these essential physiological functions, suspected to be affected by TeNT proteolysis, were studied by monitoring VAMP cleavage as a function of time after TeNT inoculation in the WP (Figure 4A). As soon as 1 day after injection, a strong signal of cl-VAMP appeared at the level of the ipsilateral FN containing the motor efferents of the whisking musculature (Figure 4B) (31, 32). Consistent with a presynaptic action within inhibitory interneurons, we found the staining of GlyT2, the presynaptic plasma membrane transporter of glycine, around the cl-VAMP signal (Figure 4C), which appeared as puncta colocalizing with the signal of an antibody specific for VGAT, the vesicular transporter of GABA and glycine (Figure 4D). This staining suggests that VAMP cleavage occurred within the presynaptic space of axon terminals of inhibitory interneurons, where VAMP is localized on synaptic vesicles. The colocalization between cl-VAMP and VGAT was extensive but not complete (Figure 4E), yet some cl-VAMP puncta were not associated with this marker of inhibitory interneurons. This finding indicates that TeNT could also enter in the presynaptic space of non-glycinergic and non-GABAergic neurons, whose origin and contribution to the development of tetanus spasticity remain to be established.

With time, the intensity and occupancy of the cl-VAMP signal in the FN progressively increased, and some staining started to be visible by day 3 also in the contralateral FN. Of note, such a faint signal (compared with ipsilateral FN) was sufficient to cause muscle spasticity in the contralateral (noninjected) WP and, similarly, at day 5, suggesting that TeNT-induced muscle spasticity is determined by a comparatively limited amount of VAMP cleaved. Accordingly, considering the strong cl-VAMP signal in the ipsilateral FN, we postulated that the effect of TeNT at the NMJ causing the nerve palsy is dominant on the central activity on inhibitory interneurons associated with muscle spasticity.

TeNT central activity diffuses throughout brainstem nuclei, causing respiratory dysfunction before systemic spasticity. On day 1, VAMP cleavage was mainly confined in the ipsilateral FN, but Figure 5A shows a weak staining also in the paragigantocellular reticular nucleus (PGRN), a brainstem area located caudally just behind the FN containing neuronal nuclei involved in the control of respiration and autonomic cardiovascular functions (Figure 5A) (33, 34). Moreover, by day 3 VAMP cleavage was detected also in the trigeminal motor (TM), hypoglossal (HN), and ambiguus (NA) nuclei, i.e., brainstem areas controlling mastication, swallowing, and more broadly the activity of the upper respiratory tract (larynx and pharynx). Of note, cl-VAMP staining markedly increased at day 5 in all these nuclei, but not elsewhere, suggesting that TeNT diffusion within the brainstem remained localized and specific.

Given that the PGRN, the HN, and the NA are involved in the control of the upper airways' function and of respiration, we wondered whether TeNT action in these nuclei could cause any change in breathing. To answer this question, we took advantage of an electrophysiological assay that allows one to measure the intraesophageal pressure in living mice (Figure 5, B and C); this provides an accurate estimation of the intrapleural pressure, and thus, indirectly, of the air volume exchanged by the animal during the respiratory cycle. Of note, this technique is minimally invasive, allowing repeated measurements in the same animal, before and after toxin injection (35).

Figure 5C shows the normal respirogram of a mouse before toxin treatment. One day after TeNT injection in the WP, when the cleavage of VAMP is confined in the FN, we detected little, if any, change in the mouse respirogram. Conversely, when TeNT activity spread to PGRN, HA, and NA at day 3, the variations
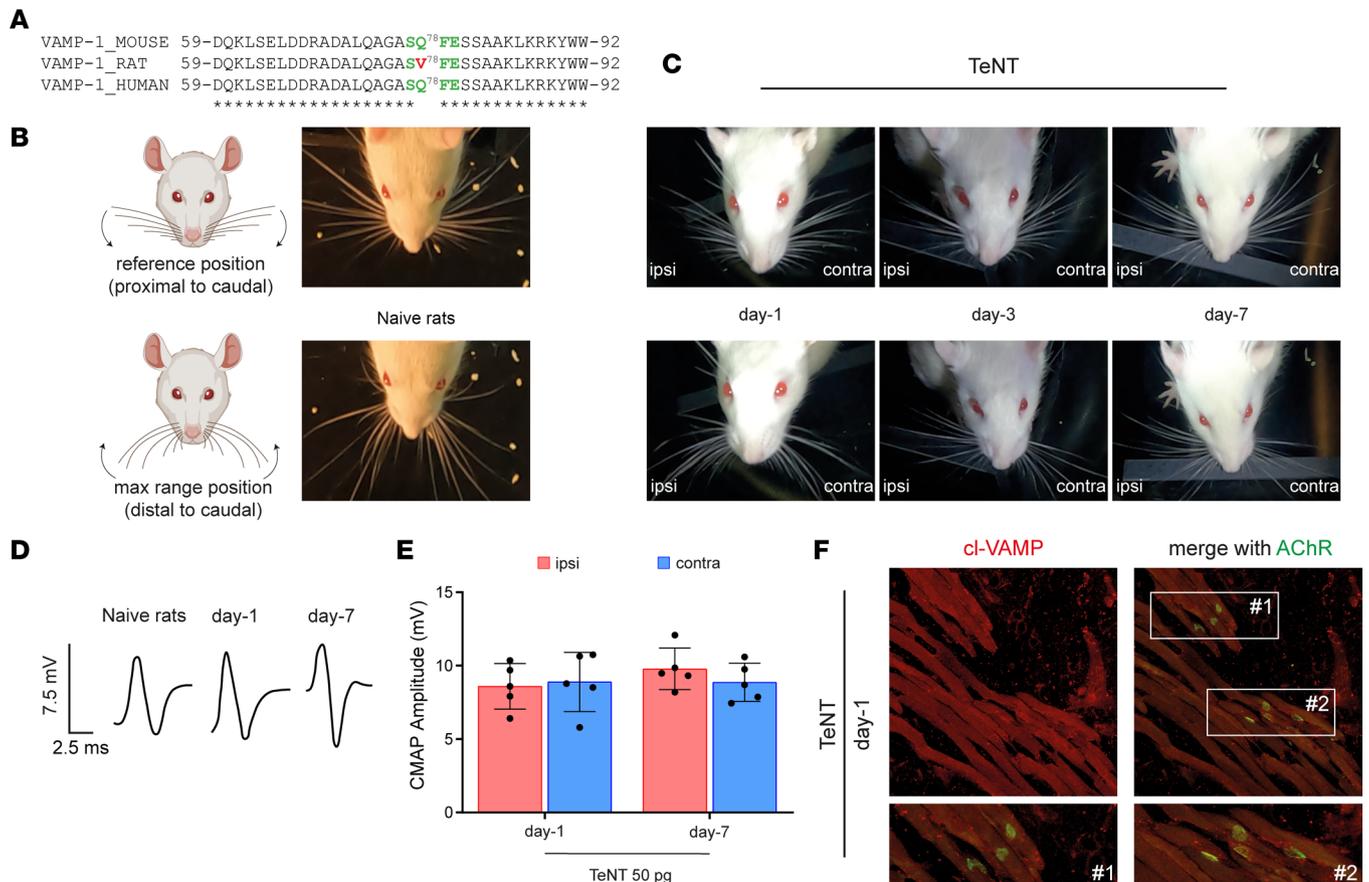
Figure 3. A point mutation in VAMP-1 renders rats resistant to TeNT peripheral neuroparalysis. (**A**) Alignment showing the peptide bond cleaved by TeNT (green) in mouse and human VAMP-1 that is mutated in rats, making the protein resistant to cleavage. (**B**) Scheme showing the extensions of vibrissae in rats used to evaluate their whisking behavior through video recording after unilateral TeNT injection; top and bottom panels show the maximum extensions proximally and distally from the rat snout; arrows indicate the direction of vibrissa movement. (**C**) Representative video frames from naive and TeNT-treated rats at the indicated time points after TeNT injection (50 pg in total in a final volume of 10 μL) in the ipsilateral WP; top and bottom panels show that at day 1 ipsilateral whisking is normal with no flaccid paralysis, while vibrissae are stacked around their position at day 3 and day 7, suggestive of WP spastic paralysis. (**D**) Representative traces of CMAP recordings at the indicated time points after the injection of TeNT in the WP and (**E**) their quantification. Data are expressed as means ± SD. Black circles indicate the number of animals used in the experiment. (**F**) Confocal images of the ipsilateral WP musculature 1 day after TeNT injection; the lack of cl-VAMP immunostaining indicates no TeNT activity at the NMJ identified through AChR labeling (green) with fluorescent α-bungarotoxin; insets show a 3× original magnification.

of intraesophageal pressure at each ventilation act were markedly reduced, consistent with a defect in the mouse's ability to breathe. To provide a quantitative estimation, we calculated an "inferred ventilation index" (IVI), i.e., a parameter indicative of the overall volume of air exchanged by the animals over 20 seconds. As shown in Figure 5D, at day 1 IVI was comparable to that of naive mice, while it decayed to about 40% at day 3, indicating a pronounced reduction in ventilation, though the animal had not yet developed evident symptoms of tetanus.

Together, these data suggest that when TeNT reaches the central nervous system, it first affects inhibitory interneurons impinging on the motor efferents responsible for its retroaxonal transport, but then it traffics trans-neuronally to adjacent areas involved in the control of mastication, swallowing, and respiration, causing a respiratory deficit without systemic spasticity, as occurs in human CT (17, 18, 20, 22).

TeNT spreading in the brainstem depends on both peripheral and brainstem intraparenchymal diffusion. Intrigued by the rapid spreading of the cl-VAMP signal in the brainstem, we wondered how TeNT can diffuse to several groups of neurons after having been taken up by neuronal efferents innervating head muscles.

The observation that TeNT injection in one WP causes VAMP cleavage in both ipsi- and contralateral brainstem areas indicates that the toxin partly diffuses at the level of peripheral tissues. On the other hand, the detection of VAMP cleavage within nuclei like the PGRN, which have no sensorimotor efferents projecting
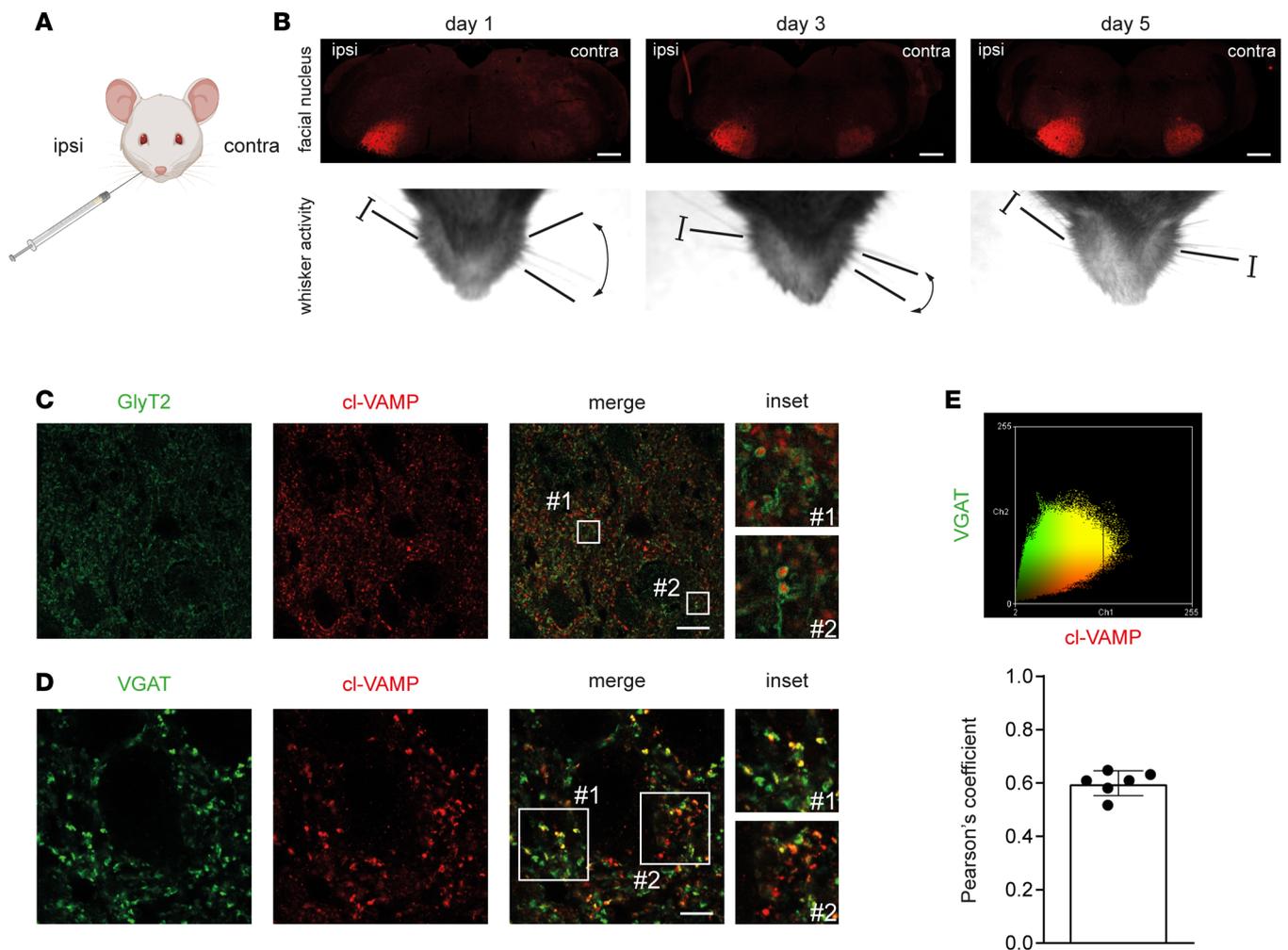
Figure 4. TeNT activity in the brainstem after injection in the WP is found at the level of inhibitory axon terminals. (**A**) Cartoon showing TeNT injection (1 ng/kg in a final volume of 1 μL) in the WP. (**B**) TeNT activity causes the appearance and progressive accumulation of cl-VAMP (red) in the facial nucleus (FN), which acts as a reporter to illuminate the brainstem areas reached by the toxin. As soon as 1 day after injection, the ipsilateral FN displays a strong signal of cl-VAMP (upper panels), which increases over time, though the mice still have flaccid paralysis (bottom panels). From day 3, a faint signal appears also in the contralateral side, when the noninjected WP starts to be spastic, and becomes clearly stained at day 5, when the spasticity of the noninjected WP is fully attained; scale bars, 500 μm. (**C**) The signal of cl-VAMP (red) is surrounded by the staining of GlyT2 (green), the plasma membrane transporter involved in the reuptake of glycine in the synaptic cleft, indicating that TeNT mainly acts within the presynaptic cytoplasm of inhibitory interneurons; scale bar, 25 μm. The insets show a 10× original magnification. (**D**) The signal of cl-VAMP (red) appears as puncta and colocalizes with the vesicular transporter of GABA and glycine (VGAT, green), indicating that TeNT activity occurs specifically at the level of synaptic vesicles within inhibitory axon terminals; scale bar, 10 μm. The insets show a 3× original magnification. (**E**) Pearson's colocalization analysis between cl-VAMP (red) and VGAT (green) signals shown as a scatterplot (top panel) and as a histogram of the correlation coefficient (bottom panel). Black circles indicate the number of brainstem slices used for the analysis.

to peripheral tissues, suggests that TeNT could undergo intraparenchymal dissemination after it arrives in the brainstem. To test this possibility, we exploited the particular anatomy of the 2 facial nuclei and set up an experiment on the levator auris longus (LAL) muscles, 2 muscles of the mouse pinna used to move the ears. As shown in Figure 6A, each of the 2 LALs is innervated by the posterior auricularis nerve, i.e., 1 out of the several branches of the FN (Figure 6B). Upon TeNT injection between the 2 LALs, we induced a bilateral intoxication of both muscles that was accompanied by a clear signal of cl-VAMP in their NMJs (Figure 6C). In addition to showing that TeNT peripheral effect was not limited to the WP, this procedure allowed TeNT retroaxonal transport to the brainstem via the 2 facial nerves and, as a result, elicited a simultaneous bilateral cleavage of VAMP in the 2 facial nuclei (Figure 6D). Also in this case, cl-VAMP initially (day 1) appeared in subnuclei of the FN populated by motoneuron efferents of the auricularis nerve (32) but then progressively spread and reached all the areas populated by motoneuron efferents of the entire mouse snout (Figure 6E) (32). Accordingly, we performed a partial transection to disconnect all FN efferents except those of the posterior auricularis (and digastric) subnuclei (Figure 6F), and then TeNT was injected between the LALs; its activity
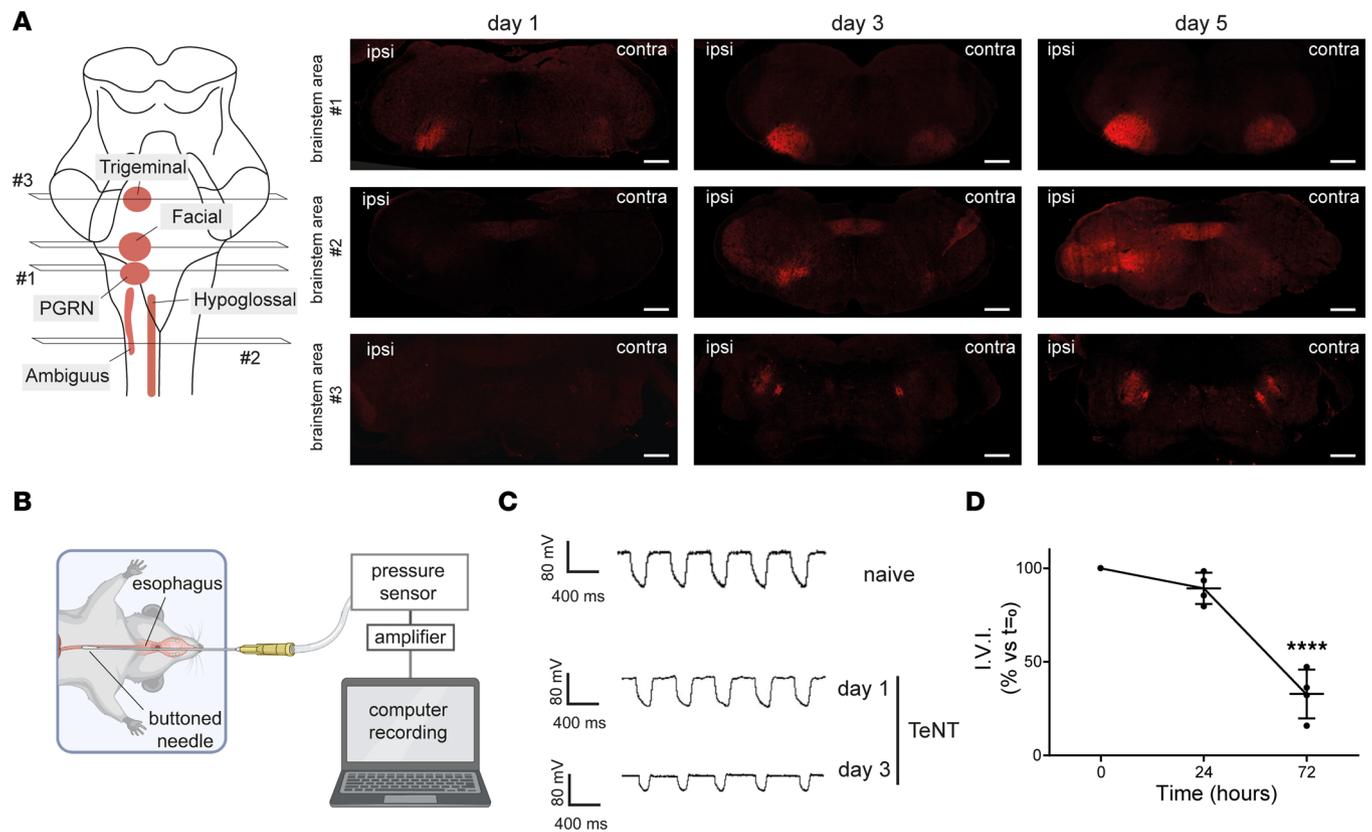
Figure 5. TeNT activity in the brainstem after injection in the WP rapidly spreads to nuclei controlling vital functions, including respiration. (**A**) TeNT was injected in the left WP (1 ng/kg in a final volume of 1 μL) that caused the appearance of cl-VAMP (red) at the level of different brainstem areas: by day 1 the paragigantocellular reticular nucleus (PGRN), involved in the regulation of respiratory and autonomic cardiovascular functions, and by day 3 trigeminal motor (TM), hypoglossal (HN), and ambiguus (NA) nuclei, controlling mastication, swallowing, and the upper airways (larynx and pharynx), respectively; scale bars, 500 μm. (**B**) Scheme illustrating the experimental setup used to measure the intraesophageal pressure in living mice, which provides an accurate air volume exchanged by the animal during the respiratory cycle: a buttoned needle connected to a pressure sensor is inserted in the mouse esophagus to measure the pressure; the signal is amplified and digitalized by computer. (**C**) Respirograms from naive (top trace) and TeNT-treated mice 1 day (central trace) and 3 days (bottom trace) after WP injection. Each trace deflection reports the pressure variations occurring during a single respiratory act, which highlight the progressive reduction in the air volume exchanged during CT; 1 day after TeNT, when VAMP cleavage is confined in the FN, few, if any, changes are present compared to naive respiration; at day 3 deflections at each respiratory act appeared markedly reduced, suggesting a deterioration in the ability of the mouse to breathe. (**D**) Quantification of the respiratory ability reported as "inferred ventilation index" (IVI), calculated as the overall volume of air exchanged by the animal over 20 seconds (see Methods); means ± SD; ****$P < 0.0001$ assessed by 1-way ANOVA with multiple comparisons and Bonferroni's test. The analysis was done with 4 animals per time point.

in the FN was monitored at day 5 via VAMP cleavage. As shown in Figure 6G, the axotomized FN displayed strong staining of cl-VAMP only in posterior auricularis and digastric subnuclei, while the FN with the intact nerve showed cl-VAMP appearance in the whole FN. However, a more careful inspection revealed cl-VAMP staining within axotomized subnuclei, though less intense compared with the contralateral nonaxotomized FN. In particular, the signal appeared more intense in proximal areas, especially at the level of platysmal subnuclei, and still detectable also in more distant subnuclei, where it appeared as discrete puncta around motoneuron soma. Intriguingly, we found a similar scenario also at the level of the PGRN, which showed a clear staining for cl-VAMP notwithstanding the partial axotomy of the facial nerve (Figure 6H). Considering that the PGRN does not have efferents reaching peripheral tissues but has internal connections with the FN (36), this result strongly suggests that the spread of TeNT activity into the brainstem, in addition to peripheral diffusion, also derives from intraparenchymal diffusion of the toxin.

Discussion

The present study unravels the pathogenesis and contrasting symptoms of CT and discloses potentially novel activities of TeNT within the central and peripheral nervous systems. These findings were made possible by developing a model of CT based on the local injection of TeNT in the mouse head muscles and by using an antibody that recognizes only VAMP cleaved by tetanus neurotoxin (23).
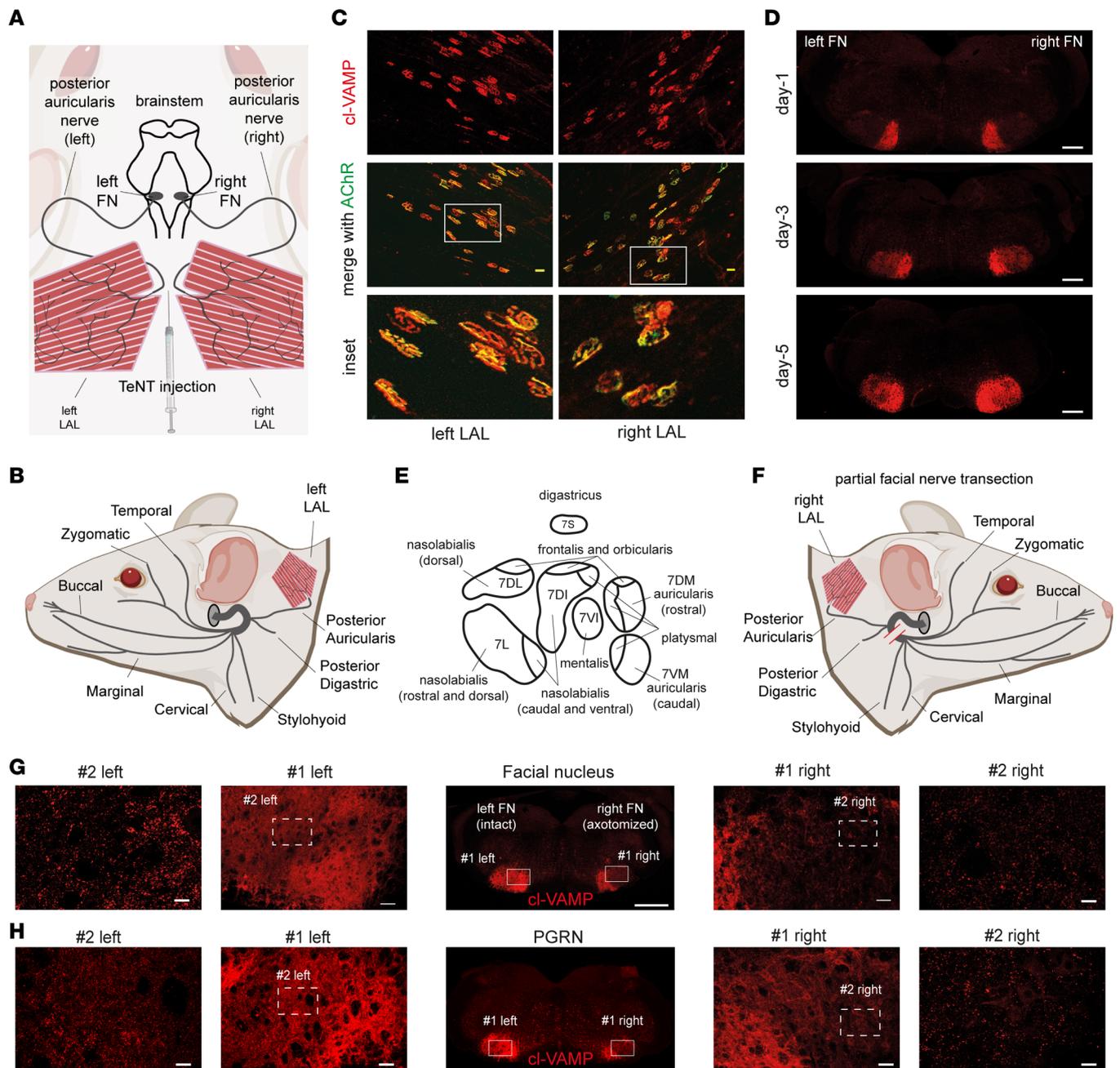
Figure 6. A combination of peripheral diffusion and intraparenchymal dissemination causes the rapid spreading of TeNT activity among brainstem neurons. (**A**) Scheme showing the bilateral innervation of LAL muscles by the posterior auricularis branch of the facial nerve connecting LAL NMJ motoneuron somas residing in the FN. (**B**) Scheme of facial nerve innervation of the dermomuscular system of the mouse head; each facial nerve exits at the level of the stylomastoid foramen (gray circle) and splits into distinct branches. (**C**) TeNT injection (1 ng/kg in 5 μL) between the 2 LAL muscles causes the appearance of cl-VAMP (red) in both left and right LALs; AChR labeling (green) with fluorescent α-bungarotoxin shows the NMJs. (**D**) TeNT injection between the 2 LAL muscles causes the bilateral appearance of cl-VAMP (red) in both FN; at day 1, the signal is restricted to the medial portions and then spreads distally, affecting the entire FN at day 5. (**E**) Scheme of facial motor subnuclei with efferent to specific muscles of the head. (**F**) Scheme of right facial nerve transection (red bars) showing the disconnection of all facial nerve branches except posterior auricular and digastric. (**G** and **H**) TeNT injection between the 2 LAL muscles with partial transection of the right facial nerve causes at day 5 a different distribution of cl-VAMP (red) in the FN (**G**) and PGRN (**H**) (central panels, scale bar: 500 μm): the nonaxotomized FN and PGRN display a signal diffused throughout the entire nucleus; cl-VAMP in the axotomized FN mainly affects the auricular and digastric subnuclei. Cl-VAMP also appears in distal FN subnuclei and PGRN like puncta around neuron somas, as shown via the progressive magnifications (scale bars: #1 = 50 μm; #2 = 20 μm). Images are representative of 1 of 3 animals.

The first major finding is the unexpected activity of TeNT at the NMJ of facial muscles. Together with the electrophysiological analyses showing impaired NMJ neurotransmission, which extend previous electromyographical findings in patients (37, 38), the demonstration of TeNT cleavage of VAMP

within facial NMJs, obtained here for the first time to our knowledge, discloses the molecular lesion at the basis of CT facial palsy. This symptom is a main confounding factor for CT diagnosis and is hardly associable with tetanus since TeNT toxic activity is traditionally considered to affect exclusively neurons of the spinal cord that lead to muscle contractures and spasms. Of note, TeNT local activity at the NMJ appears to be reversible. Although we did not investigate the molecular mechanism responsible for the functional recovery, it is likely that a major determinant of the persistence of TeNT paralytic action at the NMJ is the lifetime of its catalytic domain within the motor axon terminals, as is the case for botulinum neurotoxins (26, 27).

A second major finding is the rapidity of TeNT spreading within the brainstem as a result of both peripheral uptake and intraparenchymal dissemination. Notably, the combination of these 2 processes causes a broad and efficient intoxication of key neurons that control essential physiological functions, including breathing. This explains why a) TeNT displays its maximal toxicity in the brainstem (39), b) CT is a highly dangerous form of tetanus, and c) patients with CT suddenly and rapidly worsen after the onset of head muscle spasticity. In addition, these results clarify why CT can be very severe even without evolving into generalized tetanus (2, 40).

Whether the tropism for the brainstem derives from a particular affinity of TeNT for cranial nerve terminals remains to be established. Similarly, how TeNT intraparenchymal dissemination occurs, either via simple diffusion or via interneuronal consecutive cycles of retrograde transports as found for BoNT/A (41, 42), or their combination, remains unclear. Yet, connectome data show that the FN has inputs from the ipsilateral HN, input and output from the NA, and projections to PGRN and TM nucleus (36, 43). It is tempting to speculate that TeNT transneuronal trafficking privileges retroaxonal transport over the cytosolic entry also at central nerve terminals, thus supporting transnuclear spreading. Future investigations are necessary to reveal whether this mechanism contributes to the transition from local to generalized tetanus and to trismus being the initial symptom of tetanus (1–3, 15).

Another key observation of the present study is that the peripheral action of TeNT at the NMJ is dominant with respect to the activity of the toxin on inhibitory interneurons in the brainstem. This explains why nerve palsy in human CT can persist as a unique symptom for several days before head muscle spasticity, which then manifests suddenly and progresses to life-threatening symptoms in a short time (17, 20–22). Indeed, the peripheral effect first affects the muscles around the TeNT release site overshadowing the onset of spasticity; meanwhile, the toxin has the time to spread and intoxicate large portions of the brainstem. Arguably, this is the culprit factor responsible for the delay in CT diagnosis and the ensuing fast deterioration of patients' conditions requiring intensive care (20–22).

In conclusion, the findings of the present paper suggest that patients presenting with an idiopathic facial nerve palsy should be immediately considered for a diagnosis of CT and accordingly treated with anti-TeNT immunoglobulin, when skin, gingival, or inner ear lesions are present. This procedure is well established, innocuous, and inexpensive, yet it is capable of preventing the nefarious consequences of tetanus. In light of this, purified monoclonal antibodies with high neutralization activity injected intrathecally in the cerebrospinal fluid in the brainstem could represent a strategy with even better therapeutic outcomes than the intramuscular one (8, 44).

Methods

Antibodies, reagents, and toxins. TeNT was purified from *C. tetani* Harvard strain cultures and was kept at –80°C (45). When injected in vivo, the toxin was dissolved in physiological solution plus 0.2% gelatin (G2500, MilliporeSigma). An affinity-purified antiserum specific for TeNT-cleaved VAMP was obtained as recently described (23); anti-VAChT (1:500, 139 105), anti-intact VAMP-2 (1:500, 104 211), and anti-VGAT (1:500, 131 308) antibodies were purchased from Synaptic System; anti-GlyT2 (1:500, AB1773) was purchased from Chemicon; and α-bungarotoxin Alexa Fluor 488 conjugated (1:200, B13422) and anti–guinea pig Alexa Fluor 488 conjugated (1:200, A11073) were purchased from Thermo Fisher Scientific. Anti-rabbit Alexa Fluor 555 conjugated (1:200, A21428) was purchased from Life Technologies.

Ventilation recordings. Recordings were performed before and 24 and 72 hours after intoxication with 1 ng/kg of TeNT (diluted in 3 μL physiological solution containing 0.2% gelatin). Animals were anesthetized (xylazine/zoletil 48/16 mg/kg). A bottomed plastic feeding tube (20 ga × 38 mm, Instech Laboratories) was carefully introduced into the oral cavity and placed in the esophagus at the level of the mediastinum. Mice were laid on the left side on a prewarmed heat pad. Pressure variations were recorded via a pressure

sensor (Honeywell, 142PC01D) connected to an amplifier. Traces were digitized with WinEDR V3.4.6 software (Strathclyde University) and analyzed with Clampfit (Axon). We inferred the volume of exchanged air by measuring esophageal pressure variations, which reflect intrapleural pressure variations (46). At least 120 epochs were recorded, and at least 20 epochs were used for the analysis at each time point. The IVI parameter was calculated for each animal as the product of the mean area of the peaks multiplied by the number of peaks within 20 seconds. Data represent the percentage of t_0 taken in the same animal.

Whisking behavior. Whisking behavior in mice was recorded in awake individuals head-fixed with a custom-made head plate implanted onto the skull. Briefly, animals were anesthetized (isoflurane, Abbott Laboratories), then laid on a heating pad, and eye drying was avoided with an ophthalmic solution. The scalp was shaved, locally anesthetized with 2.5% lidocaine, and disinfected with betadine solution. An incision was made to expose the skull, and the head plate was fixed with dental cement. Baytril was administered to prevent infection, and the animal was allowed to recover in a warmed clean cage under monitoring to exclude signs of pain or distress. After animals recovered from the surgery (2–3 days), they were habituated to head restraint for 1 week by time-increased sessions each day (47) in the setup consisting of a high-speed camera (acA800-510um, Basler) and custom-made infrared illumination. Videos were recorded at 300 Hz for 2 minutes, taken before and at indicated times after TeNT injection.

For rat experiments, TeNT injections (50 pg in 0.9% NaCl 0.2% gelatin) in the WP were done under anesthesia with isoflurane. Whisking behavior was recorded with a GoPro 10 camera at 240 fps frame rate and 1,920/s shutter speed and evaluated by monitoring off-line the videos frame by frame to spot the points of maximum extension and retraction of vibrissae.

CMAP electromyography. Animals were injected in the WP with the indicated amount of TeNT (diluted in 0.9% NaCl, 0.2% gelatin, 1 μL of volume) or vehicle only. At indicated times, the animals were anesthetized (xylazine/zoletil 48/16 mg/kg), and CMAP was evoked by supramaximal stimulation with an S88 stimulator connected to needle electrodes (Grass) placed near the nerve. Recording and reference electrodes (Grass) were inserted into the WP and under the skin at the nose tip, respectively. The ground electrode was placed subcutaneously in the back lumbar area. Signals were digitized with an A/C interface (National Instruments) and then fed to a PC for online visualization (WinEDR) and software analysis (pClamp). CMAPs were determined as average peak-to-peak intensity (in mV) from 5 supramaximal rectangular stimulation pulses (200 μs) delivered from the isolated stimulator via a 2-channel amplifier (Npi Electronic). Stimulation and recording were controlled by a PC with Spike 2 software and a Micro1401-4 control panel (CED).

Immunofluorescence. WP and LAL muscles from CD1 mice or WPs from rats were dissected at indicated time points and fixed (4% paraformaldehyde, 30 minutes, room temperature [RT]). Brainstems were fixed by intracardial perfusion, collected, postfixed overnight (4% paraformaldehyde, 15% sucrose), and then left for at least 2 days in PBS 30% sucrose. Brainstem and WP slices of 30 μm of thickness were cut with a cryostat (Leica), while LALs were used for whole-mount staining. Tissues were quenched in PBS 0.25% NH_4Cl for 20 minutes, permeabilized, and saturated for 2 hours in blocking solution (15% goat serum, 2% BSA, 0.25% gelatin, 0.20% glycine, 0.5% Triton X-100 in PBS), then incubated with primary antibodies for 24 hours (slices) or 72 hours (LAL) in blocking solution at 4°C. Muscles were then washed 3 times in PBS and incubated with secondary antibodies for 2 hours at RT. Images were collected with a confocal microscope (Zeiss LSM900 Airyscan2) equipped with N-Achroplan (5×/0.15 Ph1 air), EC Plan-Neofluar (20×/0.5 air or 40×/0.45 oil) or Plan-Apochromat (100×/1.4 oil) objective. Laser excitation, power intensity, and emission range were kept constant and set to minimize bleed through.

The colocalization analysis was performed with ImageJ (plug-in colocalization analysis; NIH) on maximal projections of confocal images from at least 3 randomly chosen areas in at least 3 brainstem slices of the FN.

Statistics. Sample sizes were determined by analysis based on data collected by our laboratory in published studies. We used at least $n = 4$ mice/group for all experiments. We ensured the blinded conduct of experiments. Data were displayed as means ± SD, calculated with GraphPad Prism. Statistical significance was evaluated using unpaired 2-tailed Student's t test or by 1-way ANOVA. $P < 0.05$ was considered statistically significant.

Study approval. Our studies were carried out in accordance with the European Community Council Directive number 2010/63/UE and with national laws and policies after approval by the local authority veterinary services of the University of Padua and the University of Zagreb.

Mice were purchased from Charles River Laboratories Italia and maintained under 12-hour light/12-hour dark cycle in a controlled environment with water and food ad libitum. Rats (350–400 g) were

purchased from Inotiv and kept 2 to 3 per cage in a controlled environment with a 12-hour light/12-hour dark cycle at 21°C to 23°C and 40% to 70% humidity. Food pellets and water were available ad libitum.

Data availability. See Supporting Data Values.

Author contributions

CM, OR, and MP conceived the study; FF, SV, MT, PŠ, PM, and IM investigated; FF, SV, MT, PŠ, PM, IM, and AM curated data; CM, MP, AM, MC, and OR supervised; CM and MP wrote the original draft; and all authors reviewed and edited the manuscript.

Acknowledgments

Address correspondence to: Cesare Montecucco, Institute of Neuroscience, National Research Council, Via Ugo Bassi 58/B, Padova, 35131, Italy. Phone: 39.049.8276058; Email: cesare.montecucco@gmail.com. Or to: Marco Pirazzini, Department of Biomedical Sciences, University of Padova, Via Ugo Bassi 58/B, 35131 Padova, Italy. Phone 39.049.8276058; Email: marco.pirazzini@unipd.it.

1. Yen LM, Thwaites CL. Tetanus. *Lancet*. 2019;393(10181):1657–1668.
2. Megighian A, et al. Tetanus and tetanus neurotoxin: From peripheral uptake to central nervous tissue targets. *J Neurochem*. 2021;158(6):1244–1253.
3. Thwaites CL, Farrar JJ. Preventing and treating tetanus. *BMJ*. 2003;326(7381):117–118.
4. Brooks VB, et al. Mode of action of tetanus toxin. *Nature*. 1955;175(4446):120–121.
5. Brooks VB, et al. The action of tetanus toxin on the inhibition of motoneurones. *J Physiol*. 1957;135(3):655–672.
6. Schwab M, Thoenen H. Selective trans-synaptic migration of tetanus toxin after retrograde axonal transport in peripheral sympathetic nerves: a comparison with nerve growth factor. *Brain Res*. 1977;122(3):459–474.
7. Salinas S, et al. A hitchhiker's guide to the nervous system: the complex journey of viruses and toxins. *Nat Rev Microbiol*. 2010;8(9):645–655.
8. Pirazzini M, et al. Toxicology and pharmacology of botulinum and tetanus neurotoxins: an update. *Arch Toxicol*. 2022;96(6):1521–1539.
9. Matteoli M, et al. Synaptic vesicle endocytosis mediates the entry of tetanus neurotoxin into hippocampal neurons. *Proc Natl Acad Sci U S A*. 1996;93(23):13310–13315.
10. Pirazzini M, et al. On the translocation of botulinum and tetanus neurotoxins across the membrane of acidic intracellular compartments. *Biochim Biophys Acta*. 2016;1858(3):467–474.
11. Schiavo G, et al. Tetanus and botulinum-B neurotoxins block neurotransmitter release by proteolytic cleavage of synaptobrevin. *Nature*. 1992;359(6398):832–835.
12. WHO. Tetanus vaccines: WHO position paper – February 2017. *Wkly Epidemiol Rec*. 2017;92(6):53–76.
13. Kanu FA, et al. Progress toward achieving and sustaining maternal and neonatal tetanus elimination - worldwide, 2000-2020. *MMWR Morb Mortal Wkly Rep*. 2022;71(11):406–411.
14. Thwaites CL, Loan HT. Eradication of tetanus. *Br Med Bull*. 2015;116(1):69–77.
15. Thwaites CL, et al. Maternal and neonatal tetanus. *Lancet*. 2015;385(9965):362–370.
16. Rossetto O, et al. The role of the single interchains disulfide bond in tetanus and botulinum neurotoxins and the development of antitetanus and antibotulism drugs. *Cell Microbiol*. 2019;21(11):e13037.
17. Jagoda A, et al. Cephalic tetanus: a case report and review of the literature. *Am J Emerg Med*. 1988;6(2):128–130.
18. Kotani Y, et al. Cephalic tetanus as a differential diagnosis of facial nerve palsy. *BMJ Case Rep*. 2017;2017:bcr2016216440.
19. Nascimento FA, et al. Teaching video neuroimages: cephalic tetanus: not every facial weakness is Bell palsy. *Neurology*. 2019;93(21):e1995–e1996.
20. Guyennet E, et al. Cephalic tetanus from penetrating orbital wound. *Case Rep Med*. 2009;2009:548343.
21. Doshi A, et al. Just a graze? Cephalic tetanus presenting as a stroke mimic. *Pract Neurol*. 2014;14(1):39–41.
22. Seo DH, et al. A case of cephalic tetanus with unilateral ptosis and facial palsy. *Ann Rehabil Med*. 2012;36(1):167–170.
23. Fabris F, et al. Detection of VAMP proteolysis by tetanus and botulinum neurotoxin type B in vivo with a cleavage-specific antibody. *Int J Mol Sci*. 2022;23(8):4355.
24. Campagner D, et al. Prediction of primary somatosensory neuron activity during active tactile exploration. *Elife*. 2016;5:e10696.
25. Takeuchi Y, et al. A method package for electrophysiological evaluation of reconstructed or regenerated facial nerves in rodents. *MethodsX*. 2018;5:283–298.
26. Rossetto O, et al. Botulinum neurotoxins: genetic, structural and mechanistic insights. *Nat Rev Microbiol*. 2014;12(8):535–549.
27. Pirazzini M, et al. Botulinum neurotoxins: biology, pharmacology, and toxicology. *Pharmacol Rev*. 2017;69(2):200–235.
28. Zanetti G, et al. Botulinum neurotoxin C mutants reveal different effects of syntaxin or SNAP-25 proteolysis on neuromuscular transmission. *PLoS Pathog*. 2017;13(8):e1006567.
29. Duregotti E, et al. Snake and spider toxins induce a rapid recovery of function of botulinum neurotoxin paralysed neuromuscular junction. *Toxins (Basel)*. 2015;7(12):5322–5336.
30. Patarnello T, et al. Neurotransmission and secretion. *Nature*. 1993;364(6438):581–582.

31. Paxinos G, Franklin KBJ, eds. *Paxinos and Franklin's the Mouse Brain in Stereotaxic Coordinates*. 5th ed. Elsevier Science; 2019.

32. Komiyama M, et al. Somatotopic representation of facial muscles within the facial nucleus of the mouse. A study using the retrograde horseradish peroxidase and cell degeneration techniques. *Brain Behav Evol*. 1984;24(2–3):144–151.

33. Smith JC, et al. Structural and functional architecture of respiratory networks in the mammalian brainstem. *Philos Trans R Soc Lond B Biol Sci*. 2009;364(1529):2577–2587.

34. Machado BH, Brody MJ. Role of the nucleus ambiguus in the regulation of heart rate and arterial pressure. *Hypertension*. 1988;11(6 pt 2):602–607.

35. Stazi M, et al. An agonist of the CXCR4 receptor is therapeutic for the neuroparalysis induced by Bungarus snakes envenoming. *Clin Transl Med*. 2022;12(1):e651.

36. Isokawa-Akesson M, Komisaruk BR. Difference in projections to the lateral and medial facial nucleus: anatomically separate pathways for rhythmical vibrissa movement in rats. *Exp Brain Res*. 1987;65(2):385–398.

37. Garcia-Mullin R, Daroff RB. Electrophysiological investigations of cephalic tetanus. *J Neurol Neurosurg Psychiatry*. 1973;36(2):296–301.

38. Fernandez JM, et al. Cephalic tetanus studied with single fibre EMG. *J Neurol Neurosurg Psychiatry*. 1983;46(9):862–866.

39. Wright EA, et al. Tetanus intoxication of the brain stem in rabbits. *J Pathol Bacteriol*. 1950;62(4):569–583.

40. Rossetto O, Montecucco C. Tables of toxicity of botulinum and tetanus neurotoxins. *Toxins (Basel)*. 2019;11(12):686.

41. Restani L, et al. Evidence for anterograde transport and transcytosis of botulinum neurotoxin A (BoNT/A). *J Neurosci*. 2011;31(44):15650–15659.

42. Antonucci F, et al. Long-distance retrograde effects of botulinum neurotoxin A. *J Neurosci*. 2008;28(14):3689–3696.

43. Department of Anatomy - Neuroscience Group. University of Rostock. https://neuroviisas.med.uni-rostock.de/connectome/showRegion.php?id=4689. Accessed May 2, 2023.

44. Pirazzini M, et al. Exceptionally potent human monoclonal antibodies are effective for prophylaxis and therapy of tetanus in mice. *J Clin Invest*. 2021;131(22):e151676.

45. Schiavo G, Montecucco C. Tetanus and botulism neurotoxins: isolation and assay. *Methods Enzymol*. 1995;248:643–652.

46. Akoumianaki E, et al. The application of esophageal pressure measurement in patients with respiratory failure. *Am J Respir Crit Care Med*. 2014;189(5):520–531.

47. Gentet LJ, et al. Membrane potential dynamics of GABAergic neurons in the barrel cortex of behaving mice. *Neuron*. 2010;65(3):422–435.

12.   BRIEF CURRICULUM VITAE

Petra Šoštarić Mužić was born on 18th of June 1994, in Koprivnica, where she attended high school, specializing in pharmaceutical technology. In 2013, she enrolled in the Faculty of Veterinary Medicine at the University of Zagreb, where she obtained a Doctor of Veterinary Medicine degree. As a fifth-year student, she joined the work of the Laboratory for Bee Diseases (APISLAB) under the supervision of Prof. Ivana Tlak Gajger, where she also completed her master thesis. During her studies, she actively participated as a student demonstrator at the Department of Biology and Pathology of Fish and Bees, spent a short time on a CEEPUS exchange at a summer school on aquaculture in Sarajevo, and actively participated with award-winning presentations at domestic congresses and workshops. She was awarded the Rector's Prize for research on biomarkers of periodontal diseases isolated from dog saliva (2017). After completing her studies, she was employed as a pharmacovigilance expert at PrimeVigilance Ltd. Since September 2020, she has been employed as a PhD student/assistant at the Department of Pharmacology, School of Medicine, University of Zagreb, within the research project funded by HRZZ titled "Motor Effects of Clostridial Neurotoxins in the Central Nervous System (MEFCLO)," led by Dr.sc. Ivica Matak. As an author and co-author, she has published 6 internationally peer-reviewed scientific papers indexed in WoS, 4 of which are included in this PhD thesis. In 2022, she spent time at the Laboratory for Neurotoxins, Neurodegeneration, and Regeneration under the guidance of Assoc. Prof. Marco Pirazzini in Padua, Italy. During her studies, she actively participated in numerous domestic and international congresses, workshops, and summer schools, winning several awards for active participation. In 2023, her image depicting motor neurons in the rat spinal cord was selected as the best image captured by confocal microscopy by a jury of scientists and artists (Neuroart contest).

KRATKI ŽIVOTOPIS

Petra Šoštarić Mužić rođena je 18.6.1994. godine u Koprivnici gdje je pohađala srednju školu; smjer farmaceutski tehničar. 2013 godine upisuje Veterinarski fakultet Sveučilišta u Zagrebu na kojem stječe diplomu doktorice veterinarske medicine. Kao studentica pete godine priključuje se radu Laboratorija za bolesti pčela (APISLAB) prof.dr.sc. Ivane Tlak Gajger, u sklopu kojeg izrađuje i diplomski rad. Tijekom studija aktivno sudjeluje kao demonstratorica na Zavodu za biologiju i patologiju riba i pčela, boravi kratko vrijeme na CEEPUS razmjeni ljetne škole o akvakulturi u Sarajevu te aktivno sudjeluje s nagrađivanim sudjelovanjem na domaćim kongresima i radionicama. Nagrađena je Rektorovom nagradom za istraživanje biomarkera periodontalnih bolesti izdvojenih iz sline pasa (2017.). Po završetku studija zapošljava se na radnom mjestu stručnjaka za farmakovigilanciju u PrimeVigilance d.o.o. Od rujna 2020. zaposlena je kao doktorand/asistent na Zavodu za farmakologiju Medicinskog fakulteta Sveučilišta u Zagrebu u sklopu istraživačkog projekta HRZZ-a „ Motorički učinci klostridijskih neurotoksina u središnjem živčanom sustavu (MEFCLO), voditelja dr.sc. Ivice Mataka. Kao autor i ko-autor objavila je 6 međunarodno recenziranih znanstvenih radova indeksiranih u WOS-u, od kojih 4 iz rezultata disertacije. Tijekom 2022. godine boravi u Laboratoriju za neurotoksine, neurodegeneraciju i regeneraciju pod vodstvom izv. prof. Marca Pirazzinija u Padovi (Italija). Tijekom studija je aktivno sudjelovala na brojnim domaćim, ali i međunarodnim kongresima, radionicama i ljetnim školama. Osvojila je više nagrada za aktivno sudjelovanje na kongresima. 2023 je njezina slika prikaza motoričkih neurona u leđnoj moždini štakora odabrana kao najbolja slika uslikana konfokalnim mikroskopom od strane žirija znanstvenika i umjetnika (Neuroart natjecanje).